SUPERPLASTICISER FOR NAOH-ACTIVATED SLAG: COMPETITION AND INSTABILITY BETWEEN SUPERPLASTICISER AND ALKALI-ACTIVATOR

A thesis submitted to

University College London

for

The degree of Doctor of Philosophy (PhD)

by

Jun Ren

Department of Civil, Environmental and Geomatic Engineering

University College London

February 2016

I, Jun Ren, confirm that the work presented in this thesis is my own. Where information has been derived from other sources, I confirm that this has been indicated in the thesis.

MY PUBLICATION

REN, J., BAI, Y., EARLE, M. J. & YANG, C. H. Effect of Different Addition Methods of Lignosulfonate Admixture on the Adsorption, Zeta Potential and Fluidity of Alkali-activated Slag Binder. Young Researchers' Forum in Construction Materials, 2012 London. (**Best paper award**)

REN, J., BAI, Y., EARLE, M. J. & YANG, C. H. A preliminary study on the effect of separate addition of lignosulfonate superplasticiser and waterglass on the rheological behaviour of alkali-activated slags. Third International Conference on Sustainable Construction Materials & Technologies (SCMT3), 2013 Kyoto.

REN, J., SHENG, M. X., SHI, Y. C., ZHOU, Q. Z., BAI, Y., EARLE, M. J. & YANG, C. H. Effect of Different Addition Methods of Naphthalene Admixture on Rheology, Compressive Strength and Drying Shrinkage of NaOH-activated Slag Paste. Young Researchers' Forum II in Construction Materials, 2014 London.

REN, J., TALAFALA, I., KULASINGHAM, V., ZHOU, Q. Z., BAI, Y., EARLE, M. J. & YANG, C. H. Combined effect of Malic Acid Retarder and Naphthalene Superplasticiser on Rheological Properties and Compressive Strength of NaOH-activated Slag. 34th Cement and Concrete Science Conference, 2014 Sheffield,

REN, J., BAI, Y., ZHOU, J. Yang, C. H. & EARLE, M. J. 2016 Rheological Properties of Sodium Silicate Alkali-activated Slag in the Presence of Lignosulfonate Superplasticiser, ***in preparation.***

REN, J., BAI, Y., ZHOU, J. Yang, C. H. & EARLE, M. J. 2016 Effect of Different Addition Methods of Superplasticiser on the Properties of NaOH-activated Slag Paste- Part I: Effects on the Fresh Property, ***in preparation.***

REN, J., BAI, Y., ZHOU, J. Yang, C. H. & EARLE, M. J. 2016 Effect of Different Addition Methods of Superplasticiser on the Properties of NaOH-activated Slag Paste- Part II: Effects on the Hardened Property, ***in preparation.***

ACKNOWLEDGEMENTS

I would like to express my deepest gratitude to my supervisors, Dr Y. Bai and Dr Q. Z. Zhou, for their valuable advice and guidance through this research as well as their careful revision of the thesis. I would like to thank you for encouraging my research and for allowing me to grow as a researcher.

I would also like to extend my gratitude to my external supervisors, Professor C. H. Yang and Dr M. J. Earle, for their guidance and support from time to time throughout the project.

I am very thankful to Professor N. Tyler, Dr P. Domone, Professor D. Cleland and Professor X. G. Li for their valuable advice and support to this work.

My sincere thanks also go to Mr W. Gaynor (from Department of Civil, Environmental and Geomatic Engineering, University College London), Dr M. Russell (from School of Planning, Architecture and Civil Engineering at Queen's University, Belfast) and all the other technical staff from both universities for their assistance to me during my PhD.

I am greatly indebted to all the members of Advanced & Innovative Materials (AIM) Group in the Department of Civil, Environmental and Geomatic Engineering for their advice and support throughout this research.

My PhD was sponsored by the studentships from both University College London (2012-2015) and Queen's University, Belfast (2010-2012) due to my transfer from Queen's University, Belfast to University College London in 2012. The slag used was supplied by Hanson Heidelberg Cement Group, U.K. and the superplasticisers were supplied by Tianjin Jiangong Special Material Co. Ltd. China and Sika Group, UK. All the above organisations are grateful acknowledged.

I would also like to thank all of my friends who supported me in writing, and inspirited me to strive towards my goal.

Last, but not the least, I am extremely thankful to my beloved family. Words cannot express how grateful I am to my parents for all the sacrifices they did for me. Their love and constant inspiration have supported me through my whole PhD life.

ABSTRACT

Alkali-activated slag (AAS), consisting of slag and alkaline activator, is a novel low carbon cementitious material and has received increased attention worldwide. This is mainly due to its environmentally friendly nature and superior performance than Portland cement (PC) system. However, current commercially available superplasticisers (SPs) are generally developed based on the chemistry of PC system which has been found incompatible with AAS due to **1) competitive adsorption between SPs and activators**; and 2) **chemical instability of SPs in highly alkaline environment**. Two approaches, namely, ***separate SP addition methods*** (i.e. adding SP and activator separately) and ***synthesis of novel alkali-compatible superplasticiser***, offers the potentials to tackle the above two issues, respectively.

In this research, the effects of different addition methods of commercially available lignosulfonate and naphthalene superplasticisers on the properties of NaOH-activated slag paste, in particular the surface interaction among the SP, NaOH activator and slag particles (in terms of SP adsorption and zeta potential) and the fresh properties (such as minislump and rheology), were systematically investigated. The results demonstrated that, compared to the simultaneous addition, the separate addition methods improved the performance of lignosulfonate and naphthalene superplasticisers in NaOH-activated slag by avoiding the competitive adsorption between the SPs and the NaOH, which offers a chance to efficiently utilise the commercially available PC-based superplasticisers in AAS.

Moreover, a novel alkali-compatible polymer was also synthesised and its optimal synthesis conditions were obtained through response surface methodology. The results indicated that the synthesised polymer exhibited better chemical stability in highly alkaline media, which provides an opportunity to develop a tailored superplasticiser for the alkali-activated slag system.

However, the overall performance of the synthesised polymer in AAS under separate addition still needs to be improved by future research.

CONTENTS

LIST OF FIGURES

LIST OF TABLES

LIST OF ABBREVIATIONS

AA	Acrylic acid
AAS	Alkali-activated slag
AM	Acrylamide
AMPS	2-Acrylamido-2-methyl-1-propanesulfonic acid
AS	Amino sulfonate superplasticiser
BBD	Box-behnken design
CCD	Central composite design
CTA	Chain transfer agent
DF	Desirability function
DLVO	Derjaguin–Landau–Verway–Overbeek (theory)
DMC	Methacrylatoethyl trimethyl ammonium chloride
DMDAAC	Diallyldimethylammonium chloride
IC	Initiator concentration
LS	Lignosulfonate superplasticiser
MA	Maleic anhydride
MAA	Methacrylic acid
MAPTAC	[3-(Methacryloylamino) propyl] trimethyl ammonium chloride
MAPTMS	Trimethoxylsilyl proyl methacrylate
MAS	Sodium methylacryl sulfonate
MC	Monomer concentration
MEPG	Poly (ethylene glycol) acrylate
MEPGMA	Poly (ethylene glycol) methyl ether acrylate
MF	Melamine formaldehyde superplasticiser
MR	Monomer ratio
MW	Molecular weight
NaOH	Sodium hydroxide
NF	Naphthalene superplasticiser
NNDMA	N, N-dimethylacrylamide
MP	Modified polycarboxylate superplasticiser
PAA	Poly (acrylic acid)
PAM	Poly (acrylamide)

PAMPS	Poly (2-acrylamido-2-methyl-1-propanesulfonic acid)
PC	Portland cement
PCE	Polycarboxylate ether superplasticiser
PD	Polymer dosage
PDI	Polydisperse index
PDMDAAC	Poly (diallyldimethylammonium chloride)
PMA	Poly (maleic anhydride)
PMAA	Poly (methacrylic acid)
PSS	Poly (sodium-p-styrenesulfonate)
PVBS	Poly (sodium 4-vinylbenzenesulfonate)
RSM	Response surface method
SP	Superplasticiser
VBS	Sodium 4-vinylbenzenesulfonate (VBS)
VC	Vinyl copolymer superplasticiser
VP	2-Vinylpyridine
WG	Waterglass (Sodium silicate)

Chapter 1

Introduction

1.1 Research background

1.1.1 Superplasticiser

Superplasticiser (SP), also known as high range water reducer, is the most important chemical admixture used in concrete, which has been identified as the fifth component of concrete (El-Didamony *et al.*, 2012, Ouyang *et al.*, 2006, Aiad *et al.*, 2013). In 2012, the global consumption of the superplasticiser was 2,514 kilotons, with 72.7%.of share held by the region of Asia-Pacific and Middle East & Africa. With high expansion rate, the predicted global market of superplasticiser will reach 4.6 billion U.S. dollars by 2018 (MarketsandMarkets, 2014).

As one of the most important chemical admixture used in concrete, superplasticiser enhances the concrete properties through three ways: 1) reducing the water requirement for a given workability; 2) boosting the workability at a given water to cement ratio (w/c), and 3) decreasing the cement content in the concrete with given equivalent strength (Hewlett, 2004). Without the advent of SP, many advanced concrete technologies, such as high-strength concrete and self-compacting concrete, cannot be developed.

From the aspect of the history of development, the superplasticisers can be classified as first, second and third generations. The lignosulfonate (LS) based superplasticisers are the typical first generation superplasticiser; the naphthalene (NF) based SPs are the representative of the second generation superplasticiser; and the polycarboxylate ether (PCE) based SPs, so called next generation superplasticiser, are identified as the third generation superplasticisers (Büyükyağcı et al., 2009)

The superplasticisers are water soluble polymers with various chemical structures: i.e., linear polymer with the charged functional group on backbone for the first two generation SPs; and comb polymer which contains the positive/negative charged backbone and non-charged long side chain for the third generation SP. After it dissolves into water, the hydrolysed superplasticisers first adsorb on the particle surface, and then disperse the particles through **electrostatic repulsion** and **steric repulsion** (Ran et al., 2010, Ratinac et al., 2004). In the electrostatic repulsion, the negatively charged SPs are adsorbed to positively charged surface of cement

particles by electrostatic attraction. The residue negative charges contribute to the repulsion and dispersion of the cement particles by 'like poles' action. In steric repulsion (applied in the third generation superplasticiser), in addition to the electrostatic repulsion generated from the negative charges on the backbone of SPs, the non-charged long side chain physically keep the cement particles apart (Yamada et al., 2000, Pang et al., 2008, Ouyang et al., 2006).

The addition of superplasticiser not only improves the fresh properties of Portland cement system, but also affects its hardened properties. The superplasticiser provides better dispersion effect of cement particles in water, which leads to the refined pore structure through the development of hydration (Zhang and Kong, 2014). Consequently, the addition of SPs changes the hardened properties of cement system.

Much research has been conducted in depth to investigate the effects of chemical structure of superplasticiser, in particular, for the next generation superplasticiser, the comb shape of which provided lots of potential possibilities for generating a good superplasticiser (Yamada et al., 2000, Ran et al., 2009, Ferrari et al., 2000, Winnefeld et al., 2007, Zhang et al., 2008, Plank et al., 2008, Knaus and Bauer-Heim, 2003). In addition to the investigation on the chemical structure of SPs and the development of new type of SP, the compatibility with cementitious additives and other chemical admixture is also important, this is particularly with the novel cementitious system (Burgos-Montes et al., 2012, Jiang et al., 1999, Felekoğlu et al., 2011, Yamada et al., 2001, Alonso et al., 2007, Palacios and Puertas, 2005, Rashad, 2013).

1.1.2 Alkali-activated slag

The cement industry contributes to approximate 7% of total global carbon dioxide emissions, and accounts for 12-15% of the industrial energy consumption (Ali et al., 2011). Usually, 0.84 tonne of carbon dioxide per tonne of cement is emitted from the process of manufacturing Portland cement (PC), plus massive consumption of the large quantity of natural materials (Mehta and Monteiro, 2006). Therefore, how to solve the sustainability issue of cement industry becomes an urgent issue. During the last few decades, researchers have attempted to find and develop sustainable

cementitious materials, which could be used partly or fully to replace PC. They attempted to use various industrial by-products, such as ground granulated blastfurnace slag (GGBS), pulverised fuel ash (PFA) and metakaolin (MK) to replace PC as 'supplementary cementitious materials' (SCM). However, the by-products exhibit a pozzolanic reactivity and/or latent hydraulic reactivity, which require other chemicals to activate their potential reactivity. One of most commonly useful chemicals is the alkalies generated during the hydration of cement, which provides a possibility of SCM to partially replace PC. However, the development of the strength of this SCM partly replaced cement system is still low. Thus, new cementitious system with quick development of strength is needed.

One of the novel alternative cementitious systems, known as alkali activated cement, has received more attention worldwide (Shi et al., 2006, Pacheco-Torgal et al., 2008). It is defined as a clinker-free cementitious material mainly consisting of alkaline activators (such as sodium hydroxide and sodium silicate) and various SCMs. Among them, alkali-activated slag (AAS), which contains alkaline activator and ground granulated blastfurnace slag (slag for short here after), offers a better chance to replace PC (Shi et al., 2006). Compared to other SCMs, which are mainly composed of aluminium oxides and silicon oxides, slag is rich in calcium oxides, which offers quick hardening process and subsequent strength gain after activation by the alkaline activator. Such properties provided AAS potential to further industrial applications.

Since its invention in later 1957 by Glukhovsky, the AAS research has achieved significant development during recent years. The AAS has demonstrated many advantages over PC, i.e., rapid strength development, lower permeability, higher resistance to chemical attack, and lower heat of hydration (Rodriguez et al., 2008, Roy, 1999, Wang et al., 1994, Douglas et al., 1992, Douglas and Brandstetr, 1990, Wang et al., 1995). However, the further industrial application of AAS, i.e. to produce high-performance alkali-activated slag concrete, is still limited due to the lack of efficient chemical admixture, particularly superplasticisers. (Collins and Sanjayan, 1999).

1.1.3 Effects and issues of current superplasticisers on alkali-activated slag

It is widely accepted that adding superplasticisers could highly improve the workability of Portland cement, especially the delayed addition of SPs (Hsu et al., 1999, Aiad, 2003, Aiad et al., 2002, Hewlett, 2004). Although many investigations of SPs have been deeply carried out in Portland cement, limited research has been conducted in AAS with different activator (Isozaki, 1986, Douglas and Brandstetr, 1990, Gifford and Gillott, 1997, Bakharev et al., 2000, Collins and Sanjayan, 2001, Wang et al., 1994, Palacios and Puertas, 2005). Generally, based on those limited researches, it can be concluded that:

- The lignosulfonate (LS) and naphthalene (NF) based superplasticiser have some effects on the improvement of the workability of NaOH and solid waterglass activated slags;
- Other types of superplasticisers i.e., vinyl copolymer, polycarboxylate ether (PCE) SPs and melamine formaldehyde (MF) derivation SPs, have less effects in AAS systems.

From the review of the previous research, it can be concluded that, in general, the loss of the functionality of PC-based (from now onwards PC-based means PC compatible) SPs in AAS systems could be attributed to the following two reasons:

- The competitive adsorption between negatively charged alkaline activator and superplasticisers with negatively charged anchor groups reduces the adsorption of the PC-based SPs on the surface of slag grain, leading to a decrement of its efficiency.
- The change of chemical structure of PC-based SPs in highly alkaline environment, especially in the solution with pH above 13, leading to the loss of surface activity, which is the reason that conventional superplasticiser is not adaptable for alkali-activated slag.

These two issues mentioned above on the improper work of PC-based SPs in AAS are to be addressed in this research in order to improve the performance of superplasticiser in AAS.

1.2 Aim and objectives of the project

The overall aim of this project is to explore new approaches to improve the performance of superplasticiser in NaOH-activated slag. To achieve this, three main objectives have been identified:

1) To investigate the effect of different addition methods of current PC-based SP on the interaction between SP and activator and some fresh and hardened properties of NaOH-activated slag with an intention to identify a suitable approach to reduce the competitive adsorption between PC-based SP and NaOH-activator;
2) To synthesize the alkali-compatible superplasticiser and to obtain its optimal synthesis condition, which offers a chance to solve the chemical instability issue of current PC-based superplasticiser in highly alkaline media;
3) To examine the effects of different addition methods of synthesised polymer in NaOH-activated slag with an intention to combine the above two approaches to solve the current issues facing the application of superplasticiser in NaOH-activated slag.

1.3 Structure of thesis

Chapter 1 describes an overview background of the project.

Chapter 2 reviews superplasticisers and their effects in Portland cement. The review includes the type of superplasticiser, working mechanisms and interaction with cement particle, effect on both early age and hardened properties of cement, the addition method, especially compatibility with other admixtures.

Chapter 3 reviews the effects of current PC-based superplasticiser on the properties of NaOH-activated slag. Similar to previous chapter, the review includes background of alkali-activated slag cement with its composition and application, activation mechanism and hydration of NaOH-activated slag, working mechanism, effect on both early age and hardened properties of NaOH-activated slag. At the end, it

proposes the potential solution to solve the issues regarding the performance of current superplasticiser in NaOH-activated slag.

Chapter 4 describes the experimental programme for this research. The research rationale behind the project, details of materials, sample preparation, and test methods are given throughout this chapter.

Chapter 5 investigates the effects of different addition methods of lignosulfonate and naphthalene superplasticisers, reported to partly work in AAS, on the properties of NaOH-activated slag, including interaction with slag and activator, early age properties and hardened properties. The working mechanism of different addition methods in NaOH-activated slag system is also proposed. At the end of this chapter, the chemical stability of lignosulfonate and naphthalene superplasticisers is also determined.

Chapter 6 reports the synthesis of a modified polycarboxylate based polymer compatible with the highly alkaline environment. Its optimal synthesis condition is obtained through response surface method and the optimised conditions are verified by relative experiments.

Chapter 7 investigates the performance of the synthesised alkali-compatible polymer in NaOH-activated slag under different addition methods, followed by investigating its effects on the interaction with slag and activator, early age properties and hardened properties.

Chapter 8 concludes that two potential approaches both can be employed to improve the performance of superplasticiser in NaOH-activated slag as: separate SP addition methods reduced the competitive adsorption between PC-based superplasticiser and NaOH activator; and synthesised alkali-compatible polymer improved the chemical stability of superplasticiser in highly alkaline media. And then it presents recommendations for future work.

Chapter 2

Plasticiser/Superplasticiser Admixture and Its Effects on the Properties of Portland Cement

2.1 Introduction

Plasticiser/superplasticiser, also known as the water-reducing agent/high range water reducer, is one important category of chemical admixtures for concrete, which functions in concrete through the following three ways (Hewlett, 2004):

1) Reducing the water requirement at a given workability;
2) Boosting the workability at a given water to cement ratio (w/c);
3) Decreasing the cement content in concrete at given equivalent strength.

According to BS EN 934-2, conventional plasticisers (or water reducing agents) allow 5 to 15% decrease of water content; while superplasticisers, known as high range water reducers, provide higher water reduction from 12% to 25%, even up to 30% reduction of water requirement.

In the perspectives of chemistry, the superplasticisers are divided into five main categories:

- Modified lignosulfonate derivation;
- Hydroxycarboxylic acid (and hydroxylated polymer);
- Sulphated melamine formaldehyde polymers;
- Sulphated naphthalene formaldehyde polymers;
- Polycarboxylate polymer.

From the history of development, the superplasticisers can be classified as first, second and third generations. The lignosulfonate (LS) based superplasticisers are the representative of the first generation; the naphthalene- formaldehyde (NF) and melamine-formaldehyde (MF) based SPs are typical second generation and the polycarboxylate ether (PCE) based SPs, so called next generation of superplasticiser, are the third generation of superplasticisers (Büyükyağcı et al., 2009).

Due to the dominant position of Portland cement (PC), all the above superplasticisers have been developed to suit the chemistry of Portland cement. To appreciate the function of superplasticisers in alkali-activated slag system, a good understanding on the mechanisms and functions of the superplasticisers in PC system is essential.

Therefore, in this chapter, different generations of superplasticisers and their effects on Portland cement are reviewed. In section 2.2, each generation of superplasticiser is introduced, and the working mechanism of the superplasticisers is also described; In section 2.3, the effects of superplasticisers on both fresh and hardened properties of Portland cement are summarised; in section 2.4, the compatibility issue of superplasticisers with different Portland-composite cements and chemical admixtures are reviewed; and in section 2.5, the effects of addition methods of superplasticiser on the fresh and hardened properties of PC system are illustrated.

2.2 Type of superplasticiser and its working mechanism

In this section, the chemistry and working mechanism of lignosulfonate derivation (LS), naphthalene derivation (NF), and polycarboxylate ether derivation (PCE), which represent the 1st, 2nd and 3rd generations of superplasticiser respectively, are reviewed and compared.

2.2.1 The first-generation superplasticiser (lignosulfonate derivation)

Lignosulfonate is a by-product in the liquid waste from chemical pulp mills, which has been identified as the second most produced natural polymer (after cellulose) (Alonso *et al.*, 2001). The LS is one type of highly cross-linked polymer consisting of various phenyl-propanoid units with coniferyl alcohol, sinapyl alcohol and *p*-coumaryl identified as three main components (Pang *et al.*, 2008). As shown in ***Fig 2.1***, in addition to the hydrophobic carbon chains (C3 and C6 unit), there still exists a considerable number of hydrophilic groups, such as sulfonic, phenolic hydroxyl groups, carboxyl group and methoxyl group (Telysheva *et al.*, 2001). Such amphiphilic structures make LS a good surfactant which can exhibit wetting, adsorbing and dispersing abilities. Consequently, LS has been widely used in construction industry over the past 70 years (Nadif *et al.*, 2002, Aïtcin, 2000).

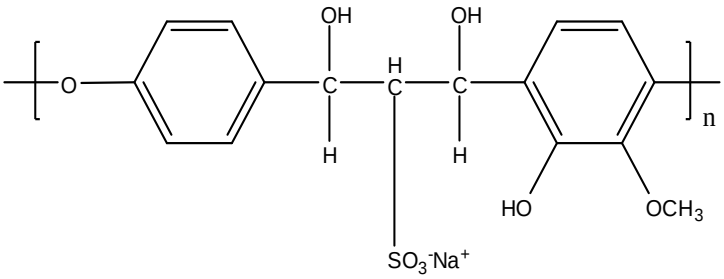

Fig 2.1 Schematic diagram of the repeat unit of sodium lignosulfonate superplasticiser (Yousuf *et al.*, 1995)

The LS contains many impurities such as pentose and hexose sugars in the raw form of LS. In order to be used as a superplasticiser, the impurities are removed by distilling and fertilising the raw materials. The sugar in the LS can retard the hydration of cement, which may have side effects on the properties of concrete. Thus, some simple chemicals such as calcium chloride or triethanolamine are often mixed as an accelerator in concrete (Singh *et al*., 2002).

The sodium and calcium salts of LS are the most commonly used forms. The formation of the salts depends on the chemicals used in neutralisation process. For example, sodium salts are formed by using sodium hydroxide as neutralizing agent, and calcium salts are produced by calcium hydroxide. Compared with two salts, the former is more soluble at a lower temperature; while the latter is much cheaper and less effective. Sodium salt of modified LS shows reduced fluid loss (i.e. good workability retention); while calcium salt can enhance the retarding effect of PC (Recalde Lummer and Plank, 2012).

The average molecular weight of the LS with the repeat unit as shown in ***Fig 2.1*** can vary from a few hundred to 100,000 (Rixom and Mailvaganam, 1999, Pang *et al.*, 2014, Ramachandran, 1996), which highly depends on the approaches and conditions under which refinement has been carried out, such as ultra-filtration, heat treatment at specified pH and fermentation. It was reported that the water-reducing ability of LS increased with increasing molecular weight and decreasing content of hydrophobic unit (Rixom and Waddicor, 1981).

Apart from the molecular weight, the molecular structure of LS, especially the content of hydrophilic groups, has been demonstrated to have great influence on the

surface physicochemical properties of cement particles (Ouyang *et al.*, 2006). For example, the more functional groups are attached onto the polymer, the better dispersion effects can be achieved. Usually, the performance of LS can be improved by chemical modification through three approaches, i.e. oxidation, hydroxymethylation and sulfomethylation by which the content of the hydrophilic group can be increased due to the increased hydroxyl group, carboxyl group and sulfonic group (Pang *et al.*, 2008, Ouyang *et al*., 2006, Alonso *et al*., 2005). The process of each chemical modification is presented in ***Figs 2.2 (a) – (c)***, respectively. In addition to the modification of LS, combining LS with other types of superplasticiser is another approach to enhance the performance of LS (Recalde Lummer and Plank, 2012).

It is generally agreed that, unlike many high molecular weight polymers, LS is not linearly flexible coiled polymers. The configuration of the LS is a polyelectrolyte spherical microgel with outside sphere and internal core (shown in ***Fig 2.3***). The outside sphere is electrolysed by carboxyl and sulfonate groups, with a higher degree of ionisation of sodium salts than that of calcium salts; while the hydrophilic groups in the inside core are non-ionised. Thus, the total degree of ionisation of LS is in the range of 20-30% (Hewlett, 2004).

The LS can be also considered as a typical anionic surfactant. The surface tension of LS (approximately 57×10^{-2} N/m) is lower than that of water (72×10^{-2} N/m). Furthermore, lower surface tension can be measured from the LS with higher molecular weight (Ouyang *et al*., 2006). Consequently, when mixing LS with concrete, a small portion (0.4 -2.7%) of air might be entrained into the concrete, which often becomes an undesired side effect. Usually, a small amount (less than 0.4%) of air-detraining agent such as tributylphosphate, dibutyl phthalate, water-insoluble alcohols borate ester or silicone derivatives can be added to overcome this side effect in order to improve the hardened properties of concrete (Rixom and Mailvaganam, 1999).

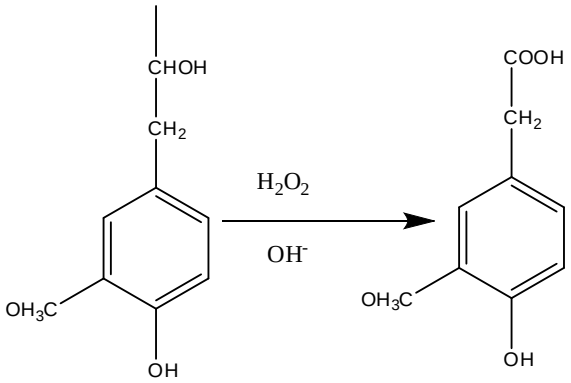

(a) Oxidation

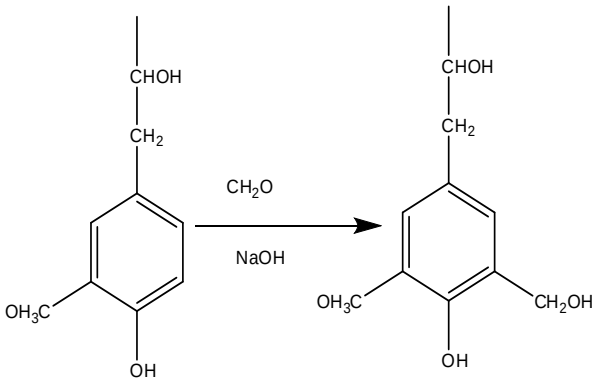

(b) Hydroxymethylation

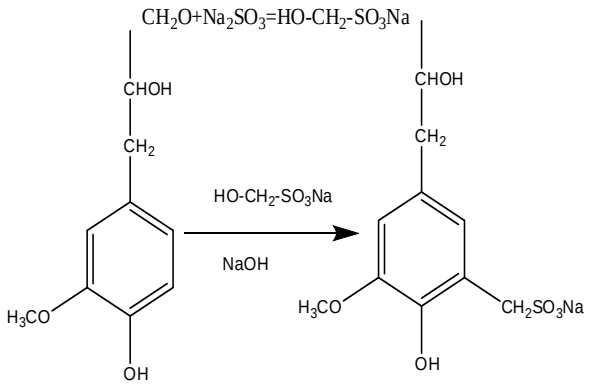

(c) Sulfomethylation

Fig 2.2 Chemical modification of the lignosulfonate superplasticiser (Ouyang et al., 2006)

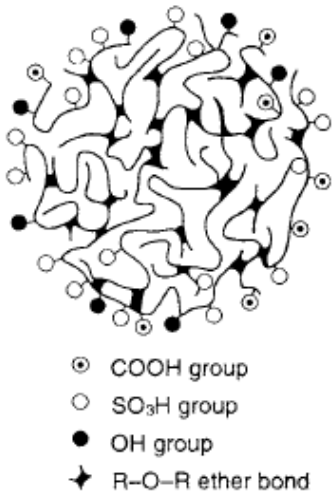

Fig 2.3 Schematic diagram of microgel of lignosulfonate (Hewlett, 2004)

Although LS has a spherical microgel structure, upon contacting with water, it can be dissociated to form organic macro-anions and cations. The organic macro anions adsorbs onto the surface of solid particles, introducing negative charges on the surface of the particles -- this leads to the electro-repulsion dispersion between solid particles (Li et al., 2012, Ratinac et al., 2004, Grigg and Bai, 2004). On the other hand, the reduction of the surface tension also means the LS can entrain some air bubbles which may improve the workability of the solid liquid dispersion system.

Although LS has demonstrated some success as a SP for PC-based system, it is manufactured from by-product and its quality is, thus, difficult to control. Moreover, the by-product contains some impurities of small molecule, which might reduce the effectiveness of LS. To overcome these issues, the second generation superplasticisers were developed which is reviewed in the next section.

2.2.2 The second generation superplasticiser (Naphthalene derivation)

Since being developed and marketed in 1960s in Japan, naphthalene derivation superplasticiser has become one of the most important types of superplasticiser in the chemical admixture market (Rixom and Mailvaganam, 1999, Pickelmann and Plank, 2012). In particular, sulfonated naphthalene-formaldehyde condensates (NF) has been identified as one of most widely used superplasticisers. As shown in ***Fig 2.4***, the NF is also an amphiphilic chemical containing naphthalene backbone as the

hydrophobic group and sulfonate group as hydrophilic group. The NF is an anionic water soluble synthetic polymer and the solubility depends on the presence of sulfonate groups attached to the main organic backbone. As it can be seen from ***Fig. 2.4***, one sulfonate group is anchored on each repeating unit, providing sufficient solubility. Similarly, other 2nd generation of superplasticisers, for example, sulfonated melamine-formaldehyde condensates (MS) are based on the same principle (Cunningham *et al*., 1989).

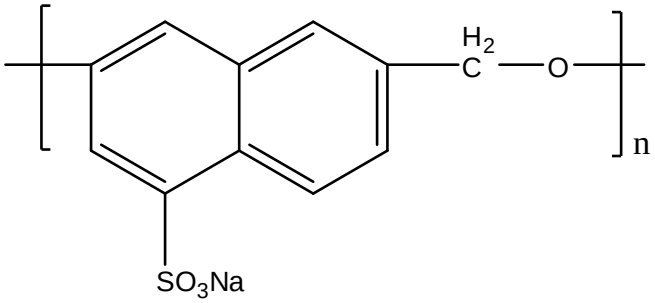

Fig 2.4 Schematic diagram of repeat unit of sodium sulfonated naphthalene formaldehyde superplasticiser (Bjornstrom and Chandra, 2003)

The raw naphthalene is usually obtained from the distillation of coal tar. Then the NFs are synthesised from naphthalene by oleum or sulphur trioxide through sulfonaion at 150-160 °C in which condition the β-sulfonate could be formed. Afterwards, the polymerisation occurs in the presence of formaldehyde, followed by neutralisation of sulfonic acid by sodium hydroxide or lime (Ramachandran, 1996). The condensation number (*n)* is normally low, which is typically 5-10, giving a molecular weight within the range of 1000-2000.

It has been confirmed by many researchers that the dispersing ability of NF is achieved after it is adsorbed on the surface, especially on the positively charged surface, of cement grains through the electrostatic adsorption (Plank and Hirsch, 2007, Yoshioka *et al*., 2002). Thus, similar to LS mentioned above, the adsorption of NF onto the surface of cement grains is important (Kim *et al*., 2000a). When NF dissolves in water, the hydrophilic groups are hydrolysed into Na^+ cations and anionic sulfonate group. The anionic sulfonate group is adsorbed onto the positively charged surface of cement grains through train mode and loop mode as shown in ***Fig 2.5***. The details will be discussed in section 2.2.4.

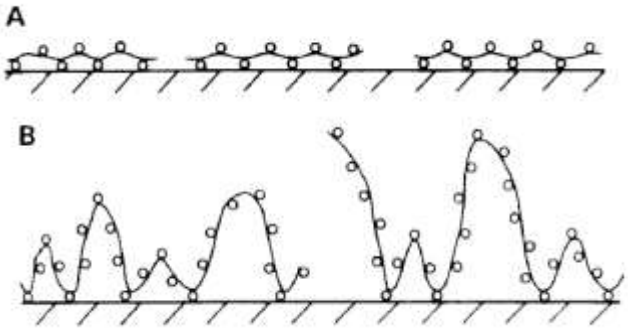

Fig 2.5 Possible mode of polyelectrolyte superplasticiser adsorbed on the surface of particles: (A - train mode; B - loop mode) (Taylor, 1997)

Generally, the NF exhibits a good dispersing effect in cement and concrete, and can reduce water demand up to 20% while still maintaining the flow characteristics of concrete (Pei *et al.*, 2000). However, there are still several limitations with NF, such as relatively high cost, large slump-loss (fluidity of concrete decreases over time), and toxicity of residue (from naphthalene).

2.2.3 The third generation superplasticiser (Polycarboxylate derivation)

Developed in 1980s, polycarboxylate ether (PCE) superplasticisers, also known as the third generation of superplasticiser, mark an important milestone in the cement and concrete industry (Okada and Sakagami, 1982, Gaidis and Rosenberg, 1984, Hirata *et al.*, 1989). The PCEs are grafted comb copolymers with anionic-ionised backbone and polyethylene glycol based side chains. Since it is manufactured by addition polymerisation from different types of vinyl monomer, the chemical structure varies significantly. Based on the chemical structure of PCE, generally, four types of PCEs are categorised (as shown in ***Fig 2.6***):

- Methacrylic acid and its ester based copolymer;
- Allyl ether based copolymer;
- Amide / imide based copolymer;
- Amphiphilic copolymer.

Based on the synthesis approach, the available monomers used for PCE are listed in ***Table 2.1***. Normally, almost all the PCEs are polymerised from negative monomers, particular acrylic based monomer. The positive or neutral monomers are seldom used. Only a few researchers tried to copolymerise them with positive polymer to enhance certain properties of SPs, such as adsorption in PC (Zhang *et al.*, 2015). In addition to the monomers used to form the backbone of PCEs, poly ethylene glycol macro monomers with different molecular weight range are also used to manufacture the side chain of SPs.

There are three synthesis approaches to manufacture PCE, which are summarised below (Büyükyağcı et al., 2009, Weng *et al.*, 2010, Liu *et al*., 2014, Ma *et al.*, 2013, Plank *et al*., 2008, Bouhamed *et al*., 2007, Cheng and Wang, 2010, Cho and Suh, 2005, Lim *et al*., 1999):

1) *'Graft from' method*: The concept of this method is to synthesis the comb polymer directly from the prepared monomer. The first and key step of this method is the preparation of macromonomers (normally methoxyl polyethylene glycol acrylate), which are used as the long side chain. Then the pre-synthesised macromonomers and other monomers are mixed and polymerised in solution. The procedure under this method is not too complex. However, the drawbacks of this approach are that the purification of the synthesised macromonomers is difficult to achieve and the cost is high.

2) *'Graft to' method*: The concept of this method is to anchor the side chains via esterification or other chemical reaction. In this method, the polycarboxylate polymers with controlled chemical structure (such as molecular weight, type and content of functional groups) are, firstly, prepared as backbone. Then the functionalised polyether chains of different length are grafted to the backbone via esterification. Applying this method could overcome the drawback of manufacturing the macromonomers mentioned in the previous method. However, the modification of the molecule and component of polymer is difficult to achieve, which limits the commercialisation of SP. Moreover, the esterification is not easy to control due to the poor compatibility between polycarboxylate and polyether.

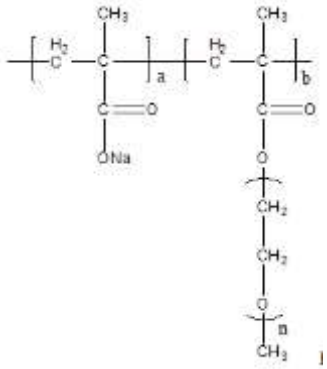

(a) Methacrylic acid based copolymer

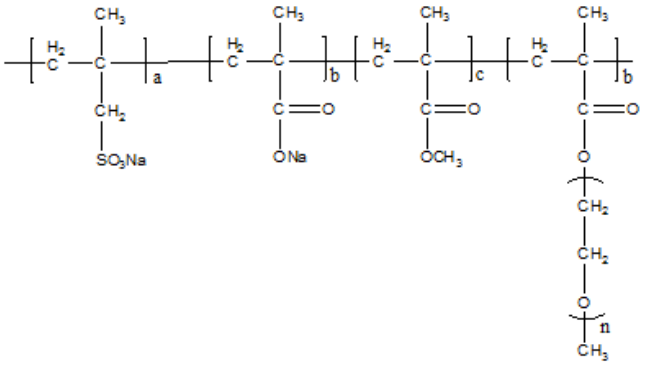

(b) Allyl ether based copolymer

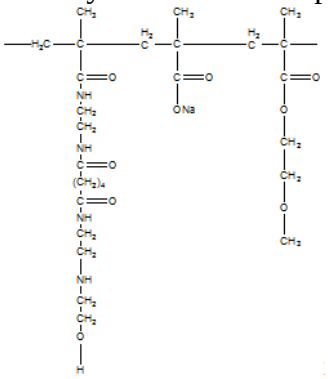

(c) Amide / imide based copolymer

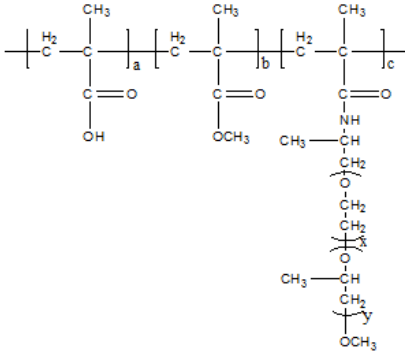

(d) Amphiphilic copolymer

Fig 2.6 Schematic diagram of four types of PCE superplasticiser (Habbaba and Plank, 2012, Plank et al., 2008, Lai et al., 2009, Winnefeld et al., 2007, Liu et al., 2014)

Table 2.1 Typical monomers used for polycarboxylate based polymer*

Chemicals	Abbr.	Chemical Structure	Charge	Anchor Groups
Diallyldimethylammonium chloride	DMDAAC	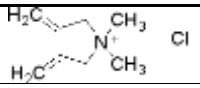	Positive	Ammonium
Methacrylatoethyl trimethyl ammonium chloride	DMC	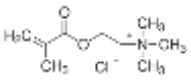	Positive	Ammonium
[3-(Methacryloylamino)propyl] trimethyl ammonium chloride	MAPTAC	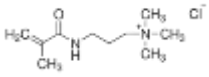	Positive	Ammonium
2-Vinylpyridine	VP	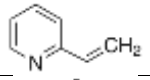	Positive	Pyridine
N,N-dimethyl acrylamide	NNDMA	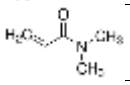	Neutral	Amide
Acrylamide	AM	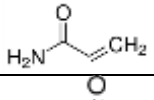	Neutral	Amide
Acrylic acid	AA	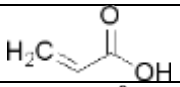	Negative	Mono-carboxyl
Sodium 4-vinylbenzenesulfonate	VBS	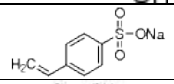	Negative	Sulfonic
2-Acrylamido-2-methyl-1-propanesulfonic acid	AMPS	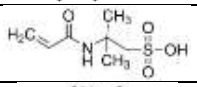	Negative	Sulfonic
Sodium methylacryl sulfonate	MAS	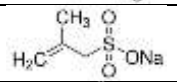	Negative	Sulfonic
Methacrylic acid	MAA	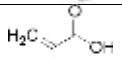	Negative	Mono-carboxyl
Maleic anhydride	MA	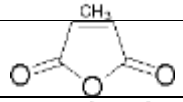	Negative	Bi-carboxyl
Poly (ethylene glycol) methyl ether acrylate	MEPGMA	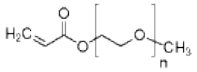	Neutral	Side Chain
Poly(ethylene glycol) acrylate	MEPG	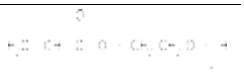	Neutral	Side Chain
Trimethoxylsilyl proyl methacrylate	MAPTMS	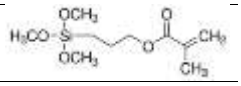	Neutral	Side Chain

* Summarised from the following literature: Ma et al., 2011, Peng et al., 2008, Liu et al., 2014, Ma et al., 2013, Plank and Yu, 2010, Plank et al., 2008, Plank et al., 2006, Fan et al., 2012, Habbaba and Plank, 2010, Felekoglu and SarIkahya, 2008, Puertas et al., 2005, Li et al., 2005, Yamada et al., 2000, Ohta et al., 2000, Zhang et al., 2015, Jiang et al., 2015, Plank and Gretz, 2008, Guo et al., 2012, Yuan et al., 2014, Habbaba and Plank, 2012, Cestari et al., 2013, Weng et al., 2010, Zhang et al., 2008

3) *'Living polymerisation' method*: The two approaches mentioned above are based on the free radical polymerisation, providing a wide molecular weight (MW) distribution. Through living polymerisation, such as **A**tom **T**ransfer **R**adical **P**olymerization (ATRP), and **R**eversible **A**ddition-**F**ragmentation Chain **T**ransfer Polymerization (RAFT), controlled MW with narrow MW distribution superplasticisers can be manufactured. Although living polymerisation can be employed to produce polymer with precise MW and configuration, its procedure is too complex and the reaction condition is restricted. Thus, this method mainly applies to the laboratory scale and aimed for research only.

To control the polymerisation, four factors have been identified as the most important for polymerisation (Liu *et al*., 2014, Guérandel *et al.*, 2011, Ferrari *et al*., 2012, Zhang *et al*., 2010, Zhang *et al*., 2008):

1) Generally, the copolymers consist of two or more types of monomers with different chemical structure and functional group. The various combinations of different monomers not only influence the chemical structure of the copolymer, but also affect its performance (Plank *et al*., 2008). Thus, the **monomer ratio**, which is related to the composition of the copolymer, is one of the important factors affecting its performance.

2) The **initiator** is considered as one of the keys to initiate the polymerisation process, the amount of which controls the rate of polymerisation and molecular weight. The initiator is the chemical containing a weak bond, which is easy to break down and, thus, to generate the free radicals to trigger the polymerisation. Theoretically, the lower molecular weight polymer is obtained with higher dosage of initiator (Zhang *et al*., 2008).

3) The **chain transfer agent** is the chemical with at least one weak chemical bond, which can facilitate the chain transfer reaction so that the molecular weight of polymer can be controlled. It has been widely used by polymer chemists to reduce the average molecular weight of the polymer (Benyahia *et al.*, 2010).

4) The **monomer concentration,** on the other hand, shows its influence on controlling the polymerisation process of free radical solution by affecting the chain propagation process (Simmons *et al.*, 2000). In addition, polymerisation time and temperature also shows some effects on the conversion rate and molecular weight of polymer (Stevens, 1999).

Differing from the first two generations of superplasticisers, the comb-like structure offers PCE better dispersion ability due to both ***electrostatic repulsion*** and ***steric repulsion*** (***Fig 2.7***) mechanisms. After being dissolved in water, the negatively charged backbones of SPs are adsorbed on the positively charged surface of cement grains through electrostatic and/or chemical attractions, generating electrostatic repulsion between them (Yoshioka *et al*., 2002, Ran *et al.*, 2010). Different from the 1st and 2nd generation SPs, which are mainly designed from sulfonic acid group, the functional groups of PCEs are carboxylic groups which can form Ca-ligands through the reaction between carboxylic groups and dissolved calcium ions from the dissolution process of cement (Winnefeld *et al*., 2007). In addition, the non-charged side chains can also physically hinder the aggregation of cement grains though steric repulsion.

The performance of PCE highly depends on its chemical structure, such as the applied monomers, the length of backbone, the length of the side chain, the density of the side chain, the electric density, and molecular weight & molecular weight distribution (Giraudeau et al., 2009, Guérandel et al., 2011, Liu et al., 2014, Marchon et al., 2013, Zingg et al., 2009). In the past three decades, various studies have been carried out on PCE. However, the effects of chemical structures on its performance are still not clearly understood. Yamada *et al.* (2000) proposed that the PCE with longer side chain, shorter backbone and higher density of sulfonic acid group have better performance. Ferrari *et al.* (2000) found that the key factor influencing the efficiency of PCE superplasticisers was the carboxylic acid to carboxylic ester ratio and the increase of this ratio could improve the adsorption of PCEs. On the other hand, Ohta's group (Ohta et al., 2000) observed that the comb-like copolymer displayed optimum dispersing ability when the degree of ethylene oxide addition on the side chain is 12. Later, Winnefeld *et al* (2007) recognized that the PCE with lower density of the side chain achieved better performance, while the effect of chain

length of backbone, chain length of side chain and molecular weight on workability of cementitious system was negligible. Though the effect of chemical structures on the performance of PCE is still not clear, it is generally agreed that the charge density of the comb copolymer could contribute to the performance of PCE due to its effects on the adsorption of superplasticiser.

Although the research on PCE has been very active in the past thirty years, the focus is mainly on its application in Portland-cement based cementitious system. As a result, the compatibility of PCE with different type of cement remains unclear, which still needs to be investigated (see detailed review in section 2.4).

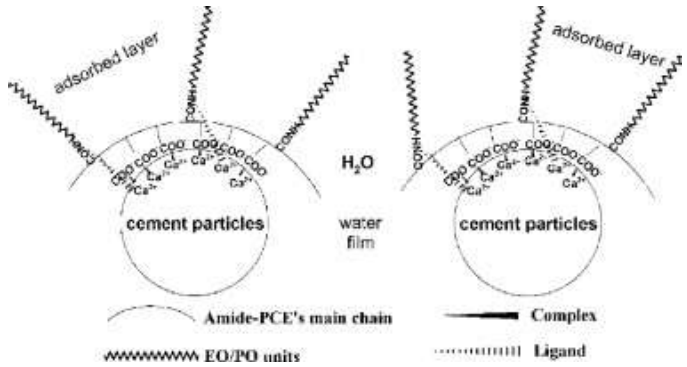

Fig 2.7 Schematic diagram of mechanism of polycarboxylate ether superplasticiser (Liu *et al*., 2014)

2.2.4 Working mechanism of SP

Regardless of the SP generations, the working mechanism of SP in Portland cement usually involves the following three steps: 1) **Adsorption** of SP on the surface of cement particles through electrostatic and/or chemical attraction; 2) **Dissolution** in the aqueous phase, which may play a part in dispersing cement particles and 3) **Intercalation, coprecipitation or micellisation** within the hydration product (for example, C-S-H gel), forming an organo−mineral phase. Among them, the adsorption of the superplasticiser on the surface of the cement particles is a crucial stage for the dispersion of cement particles through electrostatic repulsion and/or steric repulsion (Flatt and Houst, 2001).

Much research have been carried out to study the adsorption of SP and have proposed that the adsorption behaviour of superplasticiser follows Langmuir

adsorption (as illustrated in ***Fig 2.8***), which can be quantitatively expressed by ***Equation 2.1*** (Peng *et al.*, 2005). The ***Equation 2.2***, converted from ***Equation 2.1,*** is commonly used to quantitatively determine the characteristic plateau of SP adsorption behaviour (Morris *et al.*, 2002, Ran *et al.*, 2010). Moreover, the adsorption free energy ΔG_{ads} can be also calculated from ***Equation 2.3*** (Mpofu *et al.*, 2003).

$$\mathrm{A} = \mathrm{A}_s \frac{kc}{1+kc} \qquad \textbf{2.1}$$

$$\frac{c}{\mathrm{A}} = \frac{1}{\mathrm{A}_s k} + \frac{c}{\mathrm{A}_s} \qquad \textbf{2.2}$$

$$\Delta G_{ads} = -RTlnk \qquad \textbf{2.3}$$

Where, A stands for the adsorbed amount of SP (mg/g), A_s for the saturated amount of SP (mg/g), c for the equilibrium concentration of SP solution (g/L), k for adsorption constant, R for the gas constant (8.314 J/K·mol) and T for the absolute temperature. The adsorption constant k was obtained by $\frac{Slope}{Intercept}$ from regressed straight lines in the plot $\frac{1}{\mathrm{A}}$ versus c, the saturated amount of SP $\mathrm{A}_s$was calculated by $\frac{1}{Slope}$.

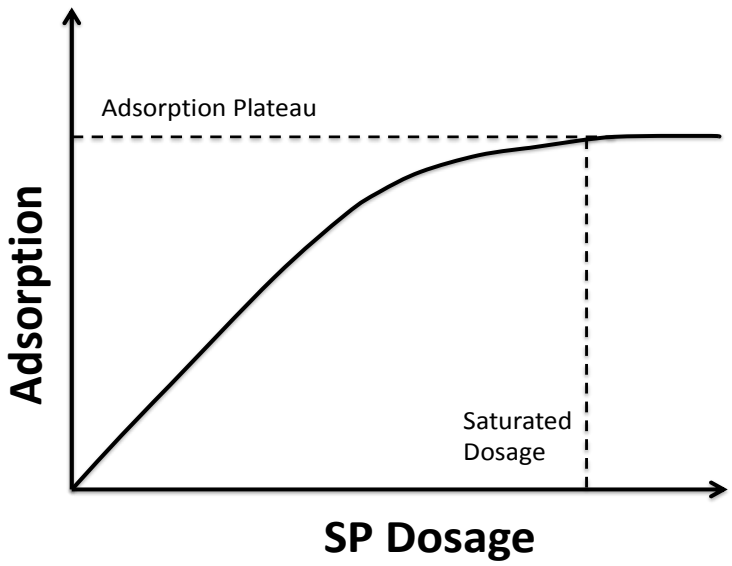

Fig 2.8 Schematic diagram of Langmuir isothermal adsorption of superplasticiser

It is widely accepted that the adsorption of superplasticiser is mainly driven by electrostatic interactions (Plank *et al.*, 2007, Zingg *et al.*, 2008) whilst the adsorption ability depends on the molecular structure of SPs, which is, in particular, the case for PCE. The surface charge of cement particles, on the other hand, also plays an important role (Yoshioka *et al.*, 2002).

In the case of LS, a lot of work suggested that the amount of LS adsorbed on the surface of cement particles increased with the increase of molecular weight of LS. It is concluded that the content of sulfonate groups, which provides the negative charge, increased with the increase of molecular weight and, therefore, can enhance the adsorption ability (Ouyang *et al.*, 2006, Pang *et al.*, 2014, Strán Ï and Sebök, 1999). However, for NF, due to the lower molecular weight (see section 2.2.2), there is no strong evidence to show the effect of molecular weight on the adsorption. But for most other 2nd generation SPs, higher adsorption has been observed for the SPs with higher molecular weight (Lou et al., 2012). Similar finding was also reported by Flatt *et al.* (1998) when they investigated PCE SP. In addition, an improved adsorption capacity was observed in PCE with shorter side chains and lower side chain density. This could be attributed to the charge density of polymer, which increased with decreasing both side chain length and side chain density (Winnefeld *et al*., 2007, Sakai *et al*., 2003).

As previously mentioned, the hydrophilic groups of superplasticiser are negatively charged. Therefore, higher adsorption can be achieved on a surface with positive charge. Among the four main phases in cement clinker, C_3A and C_4AF were observed as positively charged mineral phases whilst C_3S and C_2S negatively charged. In terms of the hydration products, ettringite and monosulfate are also reported as positively charged; while syngenite, portlandite and gypsum shows no charge or slightly negative charge. In general, the zeta potential of C-S-H is negative. However, it varies from negative to positive due to the adsorbed amount of cation, such as Ca^{2+} (Nonat, 2004, Viallis-Terrisse et al., 2001, Plank and Hirsch, 2007, Yoshioka et al., 2002, Zingg et al., 2008). As summarised in ***Table 2.2***, the superplasticisers preferentially adsorb on the positively charged phases.

Table 2.2 Effect of surface charge on the adsorption of superplasticiser

Category	Phases	Zeta potential/mV	Adsorption amount mg/g								
			NF	PCE (with sulfonic group)	PCE (lower ether chain)	PCE (long ether chain)	NF	MS SP	PCE (high charge density)	PCE (medium charge density)	PCE (low charge density)
Cement Clinker (Yoshioka et al., 2002)	C_3S	-2.78	18	35	68	88					
	C_2S	-7.59	20	38	54	142					
	C_3A	+13.04	220	60	435	680					
	C_3A+gypsum	+7.04	150	48	340	485					
	C_4AF	+5.68	225	66	315	595					
	C_4AF+gypsum	+4.46	48	40	200	375					
Hydration Product(Plank and Hirsch, 2007)	Ettringite	+4.15					113	111	28	27	17
	Monosulfate	+2.84					27	29	11	14	12
	Syngenite	+0.49					0.20	0.37	0.05	0.12	0.13
	Portlandite	-4.40					0	0	0	0	0
	Gypsum	-0.06					0	0	0	0	0

Zeta potential is known as the voltage difference between the surface of particles and the surrounding electrolyte solution (bulk of solution) (Srinivasan *et al.*, 2010a). As shown in ***Fig 2.9***, charged colloidal cement is surrounded by counter ions, forming a stern layer and a diffuse layer. When applied an electric field in the suspension, the colloidal particles with its surrounding ions (i.e. stern layer) move in the direction of the electric field, while the diffuse layer of particles is still stationary. Thus, the electric potential used to distinguish the firmly adsorbed ion layer and the diffuse layer is defined as zeta potential (Plank *et al.*, 2005). When considering the electrostatic repulsion, the zeta potential has generally been considered to be more significant than the surface potential. The DLVO theory (Derjaguin-Landau-Verwey-Overbeek) has been widely accepted to explain the stability of colloids by considering both van der Waals attraction and electrostatic repulsion (Neubauer *et al.*, 1998). In the system with SPs, the Van der Waals attractive forces generated between cement particles can be neutralised by adsorbing the anionic SPs. Then, the colloidal particles are dispersed by 'like poles' action. Therefore, based on DLVO theory, for colloidal system, the particles with higher zeta potential (either negative or positive) are electrically stabilized, while colloids with low zeta potentials tend to coagulate or flocculate (Kaszuba *et al.*, 2010).

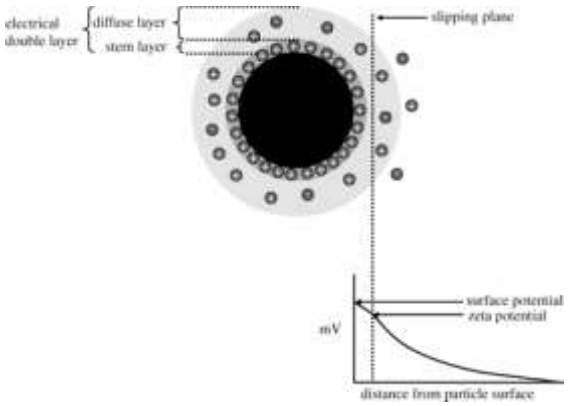

Fig 2.9 Schematic diagram of electrostatic potential surrounding a colloidal particle (Kaszuba et al., 2010)

Various researchers have attempted to explore the cement-superplasticiser interaction by studying the zeta potentials generated at the cement particle surface with adsorbed superplasticisers (Nägele and Schneider, 1989a, Neubauer et al., 1998, Elakneswaran et al., 2009, Zingg et al., 2008, Hodne and Saasen, 2000). The zeta

potential of cement paste was reported to be around -11 mV and even lower (Neubauer *et al.*, 1998, Zhang *et al.*, 2001). However, positive values of zeta potential (+8 mV) was also reported (Li *et al.*, 2005). As shown in ***Table 2.2***, due to the different surface charge of mineral phases of cement, the difference in the zeta potentials of cement could be attributed to the components of cement.

The relationship between adsorption and zeta potential has been studied by Much researchers (Kashani et al., 2014). Generally, the addition of superplasticiser induces negative charge on the surface of cement particles and, consequently, the zeta potential moves towards the negative direction. This, subsequently, increases the electrostatic repulsion between the particles. However, it should be noted that the value of zeta potential varies from sample to sample, depending on the type and chemical structure of superplasticiser (Fernández et al., 2013, Lv et al., 2012, Lei and Plank, 2012, Srinivasan et al., 2010b, Plank and Winter, 2008, Plank and Hirsch, 2007, Termkhajornkit and Nawa, 2004, Andersen et al., 1986, Srinivasan et al., 2010a). Among various research, regardless other factors (for example, the SP dosage), the type of superplasticisers plays an important role in the change of zeta potential.

Compared to all generations of superplasticisers, the lowest zeta potential reported in the cement suspension is from the second generation superplasticisers (below -20 mV), which was attributed to their higher adsorption capacity on the surface of cement particle; while the highest zeta potential observed is from the third-generation superplasticiser (above -10 mV), which was due to the steric repulsion effect caused by the non-ionised side chain of PCE (Srinivasan *et al*., 2010a, Li *et al.*, 2005, Uchikawa *et al*., 1997, Peng *et al.*, 2005). However, as discussed previously, instead of electrostatic repulsion, the non-ionised side chain also can provide physical steric repulsion. Therefore, although the reduction of zeta potential by adding PCE is insignificant, the dispersion effect of PCE is still good and usually much better than that of the other SPs.

In general, for the 1st and 2nd generation superplasticisers, it has been reported that a higher adsorption of SPs on the surface of cement leads to a lower zeta potential value, whilst for the 3rd generation SPs, there is no significant change in zeta potential with increasing or decreasing adsorption of SPs.

2.2.5 Summary

The chemistry, synthesis procedure and working mechanism of different generation of superplasticisers are reviewed in this section. The key points are summarised below (detailed information can be found in ***Table 2.3***):

- Generally, among the three types of SP, lowest efficiency is observed in the 1st generation superplasticiser (LS). Apart from the water-reducing effect, the addition of LS could also retard the hydration of cement and entrain air bubbles, which may further affect the quality of concrete. However, the cost of LS is low as it comes from the industrial waste and the quality of LS, which highly depends on the upstream industry, is also difficult to control.
- Compared to LS, the 2nd generation superplasticiser (NF) shows better performance in PC system as demonstrated by its better water-reducing effect, less retardation and less entrained air bubbles. However, the slump loss is still high and the environmental issue (toxicity from naphthalene) is still the drawback of this superplasticiser.
- The 3rd generation superplasticiser (PCE) shows the best performance in PC system in terms of higher water-reducing effect, less dosage required, and better slump retention. However, the cost of PCE is relatively high.

The working mechanism can be summarised as follows:

When dissolved in water, the superplasticisers are, firstly, hydrolysed to the negative hydrophilic groups, such as sulfonic, carboxyl and hydroxyl groups, and countering cations. The hydrolysed negatively charged groups of SPs are then adsorbed on the positively charged cement grains or hydration products (such as calcium ions dissolved from early hydration) near the surface of cement particles. This process makes the colloidal system negatively charged and, therefore, the zeta potential moves towards the more negative direction, resulting in the repulsion and dispersion of the colloidal cement particles by ‘like poles’ action. In the case of the third-generation SP (PCE), steric repulsion works in parallel with electrostatic repulsion. While the negative charges on the backbone of PCE SPs make SP adsorbed onto the cement particles and hence causes repulsion effect, the long side chain can

physically keep the cement particles apart. Therefore, the 3rd generation of SP shows superior performance than the 1st and 2nd generation of SPs.

Table 2.3 Comparison of different generations of superplasticiser

Generation	1st	2nd	3rd
Typical SP	Lignosulfonate	Naphthalene	Polycarboxylate Ether
Source	By-product Modification	Synthesis from Naphthalene and Formaldehyde	Synthesis from Vinyl Monomers and Macromonomers
Procedure	Sulphofication and Purification	Condensation Polymerisation and Sulphofication	Addition Polymerisation via "graft to", "graft from", and "living polymerisation
Configuration	Microgel with ionised out-sphere	Linear polymer	Comb polymer
Functional groups	• Sulfonic • Phenolic Hydroxyl • Carboxyl • Methoxyl	• Sulfonic	• Sulfonic • Carboxyl (main) • Hydroxyl • Non-charged chain
Working Mechanism	• Electrostatic Repulsion	• Electrostatic Repulsion	• Electrostatic Repulsion • Steric Repulsion
Advantage	• Some water reducing effect • Retardation effect	• Better water reducing effect • Low cost • Good compatibility with other admixture	• Best water reducing effect • Good workability retention
Disadvantage	• Lower water reducing effect • Air entraining • Difficult to control the quality	• Poor workability retention • Toxicity	• High cost • Low compatibility with cement type and working condition

The adsorption of SPs on the cement particles has been demonstrated to follow Langmuir adsorption, which could be expressed quantitatively. The terms from the Langmuir equation, A_s and k, could be employed to indicate the adsorbed amount and the adsorption energy of SPs on the surface of cement, respectively.

Once adsorbed on the surface of cement and lowered the zeta potential of cement particles, the SPs consequently repulse and disperse the cement particle, the process of which improves the workability and enhances the other properties of the cement system. Therefore, in the next section, the performance of SPs in PC cement system is discussed.

2.3 Effects of superplasticisers on the early age and hardened properties of Portland cement

2.3.1 Effects of SP on the early age properties of PC

The early age properties are important for cement and concrete in the mixing, placing, consolidating and finishing processes, which will, in turn, affect the other performance of cement and concrete. The addition of superplasticisers improves the fresh properties of cement and concrete, in terms of workability and rheological properties, which makes the superplasticiser the fifth components of concrete in addition to cement, fine aggregate, coarse aggregate and water (El-Didamony *et al*., 2012, Ouyang *et al.*, 2006, Aiad *et al*., 2013).

2.3.1.1 Workability and rheological properties

Rheological properties are essential for cement and concrete to achieve desirable mechanical and durable properties. Generally, the rheological behaviour of materials could be described by four models: Newtonian, Bingham, Shear-thinning and Shear-thickening (shown in ***Fig 2.10***). The rheological properties of Portland cement (PC) - based systems have been widely studied, and most of the results showed that fresh PC concrete is a thixotropic material which is featured by a decrease in viscosity when a certain amount of shear is applied and followed by a gradual recovery when the shear is removed (Fernàndez-Altable and Casanova, 2006). Although it is generally agreed that the down ramp of the hysteresis loop of the thixotropic materials can be well fitted by almost any rheological models, the most widely accepted for PC-based system is the Bingham model as expressed in ***Equation 2.4*** (Tattersall and Banfill, 1983, Banfill, 1994). The yield stress, which is the intercept

from the Bingham model, can be considered as the transition point below which the substance behaves as a solid and above which it becomes fluid (Lewis *et al*., 2000), resulting from the attractive interparticle forces responsible for the flocculation (Banfill, 1994, Barnes and Walters, 1985). When the applied shear stress (τ) is below the yield stress (τ_0), the material could support the shear stresses without flowing and vice versa. Thus, substance with a lower yield stress reflects a better dispersion and fluidity. On the other hand, the plastic viscosity, the slope from the Bingham equation, depends largely on the volume fraction of solid particles and the packed density (Struble and Lei, 1995). As a result, low plastic viscosity might cause the segregation (Feys *et al.*, 2008).

However, with the advent of self-compacting concrete (SCC), especially with the addition of superplasticisers, the yield stress of SCC is much lower than that of traditional concretes in order to achieve much-improved fluidity (Flatt, 2004, De Schutter *et al.*, 2008, Feys *et al.*, 2008). In some cases, in particular in the presence of thickeners and higher dosage of superplasticisers, the negative yield stress and a non-linear shear thickening (in which case the plastic viscosity increased with the increase of shear rate) have been identified (Larrard *et al*., 1998, Cyr *et al.*, 2000). It should be noted that the negative yield stress does not have any physical meaning. The occurrence of negative yield stress could be mainly attributed to the fact that the non-linear shear thickening flow pattern was fitted by the linear Bingham model. As a result, the modified Bingham model (***Equation 2.5***) and the Herschel-Bulkley model (***Equation 2.6***), which are both based on non-linear functions, are often used to describe this shear thickening rheological behaviour (Feys *et al*., 2008, Cyr *et al*., 2000, Nguyen *et al*., 2011). In this case, the negative yield stress could be avoided (Ren *et al.*, 2013).

$$\tau = \tau_0 + \mu \cdot \dot{\gamma} \qquad \textbf{2.4}$$

$$\tau = \tau_0 + \mu \cdot \dot{\gamma} + c \cdot \dot{\gamma}^2 \qquad \textbf{2.5}$$

$$\tau = \tau_0 + K \cdot \dot{\gamma}^n \qquad \textbf{2.6}$$

Where:τ stands for shear stress (Pa); τ_0 yield stress (Pa); μ plastic viscosity (Pa s); $\dot{\gamma}$ shear rate (s^{-1}); K consistency factor (Pa s^n); c second order parameter (Pa s^2), and n exponent (-).

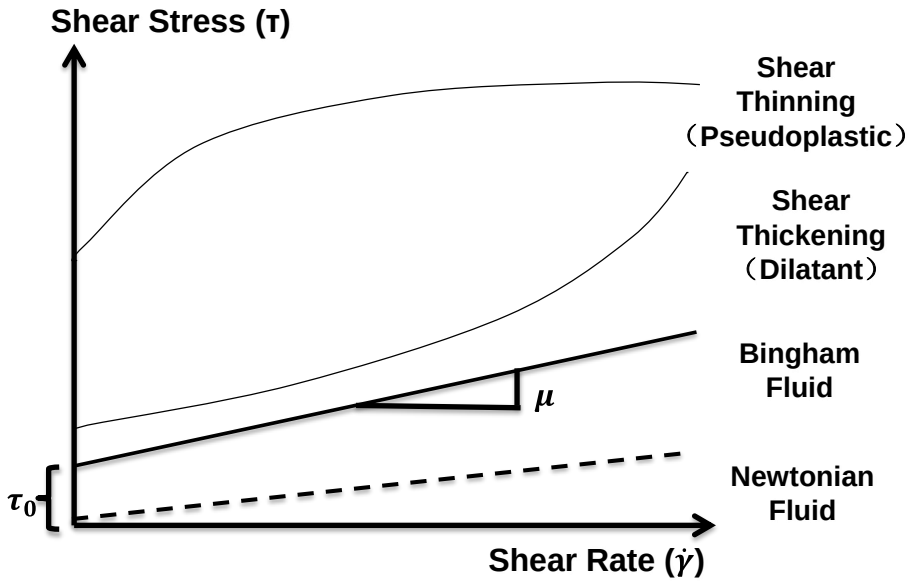

Fig 2.10 Rheological behaviours of materials (adapted from Barnes and Walters, 1985)

Apart from various tests conducted by the rheometer, many quantitative empirical measurements have been established to test the workability of cement and concrete, such as the slump test (minislump test is usually conducted for testing cement paste), vebe test, degree of compactability and flow table (BS EN 12350-2, BS EN 12350-3, BS EN 12350-4, BS EN 12350-5). With the advent of self-compacting concrete (SCC), which exhibits high flowability, high segregation resistance and good passing ability, new tests such as the slump-flow test, V-funnel test, L-box test, sieve segregation test and J ring test (BS EN 12350-8, BS EN 12350-9, BS EN 12350-10, BS EN 12350-11, BS EN12350-12) have also been developed.

Compared with '*two-point'* rheometer test (i.e. both yield stress and plastic viscosity can be measured), only one rheological property of cement and concrete (either of them) can be determined by the empirical workability measurement (*i.e. 'single-point'* test). Many studies have been carried out to establish the relationships between the rheological behaviour and empirical workability tests, which are summarised in ***Table 2.4***.

Table 2.4 Relationship between the rheological behaviour and empirical workability tests (summarised from Jau and Yang, 2010, De Larrard et al., 1997, Jin, 2002, Wallevik, 2006)

	Yield Stress	Plastic Viscosity	Slump or Spread	Slump Flow	V-funnel Time	U-box Time
Yield Stress						
Plastic Viscosity	X					
Slump or Spread	√(-)	X				
Slump Flow	√(-)	X	√(+)			
V-funnel Time	√(+)	√(+)	X	X		
U-box	√ (+)	√(+)	X	X	√(+)	

Note: √ indicates that there exists a relationship, X indicates that there is no relationship, (+) stands for positive correlation, (-) stands for negative correlation

The values of yield stress and plastic viscosity are quite different for cement paste, mortar and concrete. The typical ranges of yield stress and plastic viscosity are summarised in ***Table 2.5*** (Banfill, 2003). It can be concluded from Table 2.5 that the comparison crossing paste, mortar and concrete is infeasible.

Table2.5 Rheological properties of PC paste, mortar and concrete (Banfill, 2003)

	Material				
	Paste	**Mortar**	**Flowing concrete**	**Self-compacting concrete**	**concrete**
Yield Stress (Pa)	10-100	80-400	400	50-200	500-2000
Plastic Viscosity (Pa s)	0.01-1	1-3	20	20-100	50-100
Structural Breakdown	Significant	Slight	None	None	None

Generally, the effects of superplasticisers on paste, mortar and concrete are different. The vectorised-rheograph approach, which used plot of changes between yield stress (the y-axis) and plastic viscosity (the x-axis), was developed by Wallevik to describe the effects of material properties, time, additives on rheological properties (Wallevik, 2006). The effects of adding SP on the rheological behaviour of cement paste, mortar

and concrete are illustrated, respectively, in ***Fig 2.11***. It can be seen that the addition of SP in cement paste significantly reduces both yield stress and plastic viscosity of the paste, which is in a similar way as when water is added into the paste. However, it can be observed that the yield stress is highly reduced whilst the plastic viscosity is almost maintained constant when adding SP in concrete (Wallevik and Wallevik, 2011).

One of the most important factors affecting the rheological performance is the dosage of SP. Theoretically, the more SP added into the cementitious system, the better workability could be achieved. However, the adsorption of SPs normally reaches a plateau (see Section 2.3.2). After reaching the saturation point, the amount of SPs that can be adsorbed onto the cement grains could not increase even if extra SP has been added. Therefore, there exists a saturation dosage for SP, above which the workability cannot improve even with extra SP (Gołaszewski, 2012, Felekoğlu et al., 2011, Zhang et al., 2010).

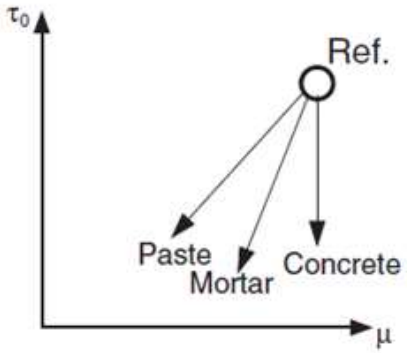

(Note: the direction of the arrow indicates the increase of SP dosage)

Fig 2.11 Effect of superplasticiser on the rheological behaviour of paste, mortar and concrete (Adapted from Wallevik, 2006)

Whilst the above discussion has been focused on the effect of superplasticiser on the improvement of the initial rheological properties of PC-based system, the importance of workability retention cannot be ignored. As highlighted in section 2.2.1, the SPs are consumed by intercalation, coprecipitation or micellisation within the hydration product. The chemical reactions during the formation of hydration product (such as ettringite and C-S-H) mean that the SP is no longer just performed as dispersion

admixture, but is also involved in the chemical reaction and consumed, causing the reduction of workability retention (e.g. slump loss). Compared with different types of SP, the superplasticisers based on the electrostatic repulsion, particularly those with linear structures (for example, NF) exhibits higher slump loss over time, which has limited its use (Kim *et al.*, 2000b, Chandra and Björnström, 2002). However, the addition of PCE showed better workability retention due to both electrostatic and steric repulsion mechanisms (Chandra and Björnström, 2002). Unlike LS and NF, PCE is a comb-shaped polymer grafted with non-ionic side chain, extending from the surface of cement particle in water, preventing coagulation between particles by physical steric hindrance (Weng *et al.*, 2010, Zhang *et al.*, 2007, Erdogdu, 2005). Therefore, it can be concluded that the slump loss of cement paste with SPs is mainly caused by the consumption of SP in early hydration, such as intercalation, coprecipitation and micellisation within the hydration product. Delayed addition of SP can reduce this consumption by avoiding trapping in the organo-mineral phase, which will be discussed in section 2.5.

2.3.1.2 Setting

The setting of cement has been defined as initial set and final set. The initial set starts at the time when the cement paste stiffens to an unworkable status without developing strength. And the final set is the time when the paste starts to harden with measurable strength. It has been established that the setting of cement, especially initial set of cement paste, is related to the hydration of cement. It is reported that the setting time is correlated with Ca^{2+} concentration in liquid phase and begins at the time when Ca^{2+} concentration reaches an equilibrium value (Uchikawa *et al.*, 1984). As discussed in section 2.3.1, the addition of superplasticiser can retard the hydration of cement. Although this depends on the mixture proportion and w/c ratio of the paste, the setting time of cement paste, commonly, is postponed when mixing with superplasticiser.

Zhang *et al.* (2010) used three methods to determine the initial set of cement pastes. These include measuring the time at the beginning of accelerating period, the time when yield stress increased significantly, and the time when Vicat needle penetrated to certain depth. They found that the initial setting time determined by the Vicat needle and at the beginning of accelerating were correlated with each other, but was

significantly longer than that obtained by the yield stress. It was also observed that the addition of all types of SP delayed the initial set of cement paste, with the longest being found from LS (shown in ***Table 2.6***).

Uchikawa *et al.* (1995) proposed that the setting was related to the Ca^{2+} concentration in the liquid phase. The retardation of hydration in cement by SP was attributed to the reduction of Ca^{2+} ions, which was consumed to form a complex by the reaction between hydrophilic groups of SP and the dissolved Ca^{2+} ions. Therefore, the lime saturation ratio was decreased and retardation of hydration of alite was observed. Much researchers (Collepardi, 1998, Felekoğlu et al., 2011, Zingg et al., 2009, Felekoglu and SarIkahya, 2008, Puertas and Vazquez, 2001, Yamada et al., 2000) reported similar results based on the superplasticisers commercially available on the market. Apart from the formation of a Ca-complex, the adsorption on the early hydration product was also proposed as the reason of delaying setting time of cement paste. Heikal *et al.* (2005) reported that the setting time of cement pastes was prolonged more at 35 ℃ than at 25 ℃, which was attributed to the increment of the adsorption capacity at higher temperature. Plank and Sachsenhauser (2009) also reported similar results.

Table 2.6 Initial setting time of cement pastes with superplasticiser measured by different test methods (Zhang *et al*., 2010)

Type of SP	w/c	Time at beginning of accelerate period / min	Time when yield stress increasing significantly /min	Time when Vicat needle penetrating to certain depth /min
No SP	0.26	60	n/a*	90
LS		1025	475	990
NF		175	75	230
PCE		260	110	300
No SP	0.32	60	n/a*	140
LS		1030	680	1105
NF		170	120	290
PCE		220	150	415

* No measurement due to high yield stress

2.3.1.3 Early hydration

Portland cement is a heterogeneous material comprising four major phases in the clicker and other admixtures, such as gypsum to regulate setting time. According to

BS EN 197, additional mineral additives, such as slag, fly ash, and silica fume, can be blended into cement. The reactions among the main phases are listed in ***Table 2.7***.

A series of reactions are triggered after Portland cement contacts with water, yielding a new dense and stable matrix. It has been agreed that solution processes, interface reactions and solid reactions are all involved in the hydration process, including the formation of hydration products and the development of the microstructure (Hewlett, 2004).

The hydration processes of Portland cement are divided into four periods: initial period (I), induction period (II), acceleration period (III) and deceleration period (IV) (Jansen *et al*., 2013, Hewlett, 2004, Bullard *et al*., 2011, Juilland *et al*., 2010). A typical heat evolution curve of PC is shown in ***Fig 2.12***.

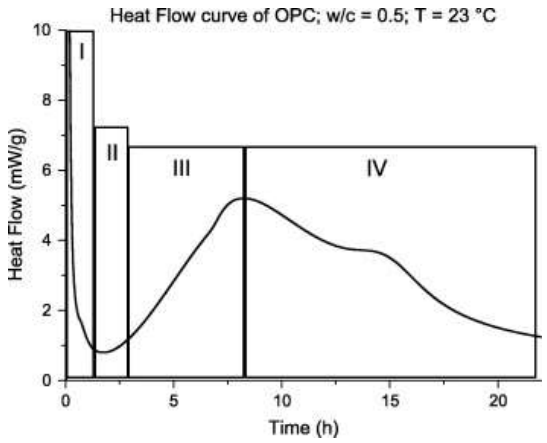

Fig 2.12 Schematic diagram of typical heat evolution of Portland cement (Jansen et al., 2013)

In general, addition of most superplasticisers retards the hydration of cement (Ramachandran, 1983, Jansen et al., 2012, Heikal et al., 2005, El-Gamal et al., 2012, Miyake et al., 1985). However, it was demonstrated by Lei and Plank (2012) that NF and synthesised cycloaliphatic superplasticiser showed less influence on the hydration of PC. But they also observed that the hydration of PC was obviously delayed by adding PCE. Winnefeld's group (Winnefeld *et al*., 2007) also confirmed that the PCE retarded the hydration of PC. As shown in ***Fig 2.13,*** the main hydration peak was delayed for several hours. Accordingly, the dormant period was also prolonged from 3 to 17 hours in the presence of PCE. The PCE with long side chain exhibited less ability on retarding the hydration of PC.

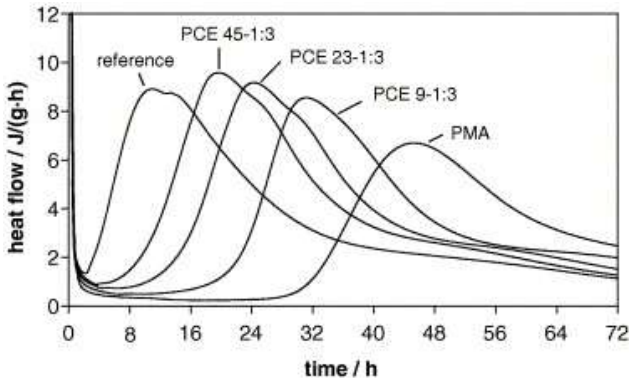

(Note: PCE 45-1:3 is a PCE SP with side chain of 45 ethylene oxide chain and the density of side chain is 1:3; PCE 23-1:3 for PCE SP with side chain of 23 Ethylene oxide chain and the density of side chain is 1:3; and PCE 9-1:3 for PCE SP with side chain of 9 Ethylene oxide chain and the density of side chain is 1:3)

Fig 2.13 Effect of PCEs with different chemical structures on hydration heat of Portland cement (Winnefeld *et al*., 2007)

The effect of chemical structure of SP, especially PCE, plays an important role on the effect of cement hydration. In the research led by Winnefeld, Yamada and Kirby (Winnefeld *et al.*, 2007, Yamada *et al.*, 2000, Lewis *et al*., 2000), PCEs with shorter side chain length and lower side chain density showed more retardation effect on the hydration of PC. However, the molecular weight of superplasticiser had little effect on the hydration of PC.

Three retardation mechanisms of superplasticisers on the hydration of cement were proposed by Mollah *et al.* (2001):

1) the diffusion of water and calcium ions on the surface of solid-liquid phase is hindered by a layer of adsorbed superplasticiser;
2) the nucleation and the precipitation of calcium ions is prevented by the formation of complexes between calcium ions and superplasticiser;
3) the growth kinetics and the morphology of hydration product is changed due to the dispersion effect of SP.

Table 2.7 Details of major mineral phases of Portland cement (Hewlett, 2004)

Type	Chemistry	Abbr.	Typical content	Reaction	Reaction speed	Main reaction product	Hydration heat/ J g
Alite	$3CaO \cdot SiO_2$	C_3S	55%	$2C_3S + 6H \rightarrow C_3S_2H_3 + 3CH$	Quick	C-S-H, CH	-517
Belite	$2CaO \cdot SiO_2$	C_2S	20%	$2C_2S + 4H \rightarrow C_3S_2H_3 + CH$	Slow	C-S-H, CH	-262
Aluminate	$3CaO \cdot Al_2O_3$	C_3A	6%	$2C_3A + 21H \rightarrow C_4A_2H_{13} + C_2AH_8$ $C_4SA_2H_{13} + C_2AH_8 \rightarrow 2C_3AH_6 + 9H$	Quick	C_3AH_6(without gypsum)	-910
				$C_3A + 3C\hat{S}H_2 + 26H \rightarrow C_6A\hat{S}_3H_{32}$		$C_6A\hat{S}_3H_{32}$ (Monosulfate)	-1144
				$2C_3A + C_6A\hat{S}_3H_{32} + 4H \rightarrow 3C_4A\hat{S}H_{12}$		$C_4A\hat{S}H_{12}$ (Ettringite)	-1672
Ferrite	$4CaO \cdot Al_2O_3 \cdot Fe_2O_3$	C_4AF	9%	$C_4AF + 3C\hat{S}H_2 + 29H \rightarrow C_6(A,F)\hat{S}_3H_{32} + (A,F)H_3$ $C_4AF + C_6(A,F)\hat{S}_3H_{32} + 7H \rightarrow 3C_4(A,F)\hat{S}H_{12} + (A,F)H_3$	Slow	$C_3(A,F)H_6$(without gypsum)	-418
						$C_6(A,F)\hat{S}_3H_{32}$ (Alumino-ferrite Monosulfate)	N/A
						$C_4(A,F)\hat{S}H_{12}$ (alumina-ferrite Ettringite)	N/A
Gypsum	$CaSO_4$		5%				

Abbreviation in reaction: C stands for CaO, S for SiO_2, A for Al_2O_3, F for Fe_2O_3, $\hat{S}$ for SO_3 and H for H_2O.

Based on the study of the combination between LS and PCE, Recalde and Plank (2012) concluded that the retardation of PC was due to the formation of complexes between calcium ion and LS，which associated into large agglomerates and then precipitated on the surface of cement grains to form a layer of polymer. This layer of polymer hindered the migration of water onto the un-hydrated cement particles. On the other hand, Jansen *et al.* (2012) proposed two mechanisms: 1) the complexation between SP and dissolved calcium ions depleted the Ca^{2+} in solution, leading to the retardation of both silicate and aluminate reaction; and 2) the adsorption of SP on the nuclei of early hydration product prevented the growth of hydration product.

Borget's and Fantinel's research (Fantinel *et al*., 2004, Borget *et al*., 2005) confirmed that the calcium-contained complexes were formed from reaction between Ca^{2+} and grafted-polyacrylates (PCE), binding reasonable amount of calcium ions. The binding capacity was depended on the amount of carboxylate groups. However, Lothenbach and Winnefeld (2007) examined the addition of PCE on the composition of pore solution of cement paste at different hydration ages (from 1 hour to 2 years), and found that the PCE showed no effects on the change of pore solution chemistry (for example, the calcium content). The results suggested that the interaction of SP with dissolved calcium ions could not be the reason of retardation.

Thus, the adsorption and the coverage by the SP on the surface of cement particles, which is highly related to the change of the SP density, could have played an important role on the retardation of PC.

2.3.2 Effects of SP on hardened properties of PC

The addition of SPs not only influences the fresh properties of cement pastes, but also affects the pore structure of hardened cement pastes. This section reviews the effect of SP on some properties of hardened PC systems, including compressive strength, drying shrinkage and porosity.

2.3.2.1 Compressive strength

One major advantage of concrete as a construction material is its good hardened properties such as high compressive strength and stiffness. Thus, the effect of different superplasticisers on the hardened properties is important.

Usually, the addition of superplasticisers will not have any adverse effect on the compressive strength of hardened cement paste or concrete. Water to cement ratio plays an important role in determining the compressive strength. As introduced in section 2.1, SP plays three roles in the enhancement of fresh properties of cement and concrete, namely, ***plasticiser***, ***water reducer*** and ***cement reducer.***

The basic concept of using superplasticiser as a cement reducer is to achieve the equivalent strength by using less cement and reduced free water content so that the free water to cement ratio is maintained. As a result, even though the cement content is reduced by adding SP, the strength of concrete is not affected (Hewlett, 2004).

When worked as a plasticiser, it is obvious from ***Table 2.8***, that, in most of the cases, the compressive strengths of the concretes with LS, MS and NF are higher than, or at least equal to, those of the control concrete mix without adding superplasticiser. In this case, the increase in compressive strength could be attributed to the improved dispersion of cement particles with the addition of superplasticisers, which increases the total surface area of cement exposed to water and, hence, better hydration could be achieved (Hewlett, 2004). However, in some cases, the reduction in compressive strength was observed. The unexpected results could be attributed to the increased air content introduced by the SPs (Büyükyağcı *et al.*, 2009).

Table 2.8 Effects of SPs on compressive strength (plasticising effect)

SP	Dosage of SP (% of cement)	Workability Improvement /%	Relative Compressive Strength/%				Reference
			7 days	28 days	56 days	90 days	
LS	0.50	23		99			(Matias et al., 2013)
	N/A	37.5		102	99		(Miyake et al., 1985)
MS	4.00	N/A		103			(Durekovic and Tkalcic-Ciboci, 1991)
NF	0.80	525	133	149			(Gao et al., 2001)
	1.00	650	137	147			
	1.20	800	134	140			
	1.40	1025	136	143			
	1.00	280	138	131	111	112	(Okafor, 1991)*
	2.00	550	175	138	117	118	
	2.50	750	188	145	124	125	
PCE	0.48	28		96			(Matias et al., 2013)
	0.40	11		95	105		(Felekoğlu et al., 2011)
	1.20	42		108	105		
	1.80	56		96	97		

When superplasticiser is used as a water reducer, the compressive strength of the concretes with superplasticiser is much higher than that of the corresponding concrete without superplasticiser (as shown in ***Table 2.9***) which could be attributed to the reduction in w/c ratios.

Table 2.9 Effects of SPs on compressive strength (water reducing effect)

SP	Dosage of SP (% of cement)	Water reduction/ %	Relative Compressive Strength/%				Reference
			7 days	28 days	56 days	91 days	
LS	N/A	18	135	130		132	(Rixom and Mailvaganam, 1999)
	0.20	1		119	118	119	(El Gamal and Bin Salman, 2012)
	0.40	6		138	136	136	
	0.60	11		146	144	143	
	0.15	1	107	108		108	(El-Gamal et al., 2012)
	0.30	3	115	124		110	
	0.50	5	120	129		114	
MS	N/A	18		125			(Grabiec, 1999)
	N/A	18	139	120		126	(Rixom and Mailvaganam, 1999)
	3.25	16	201	226		201	(Stuart et al., 1980)
	2.00	22		146	111	108	(Ray et al., 1996)
NF	N/A	18	132	135		128	(Rixom and Mailvaganam, 1999)
	2.20	19	212	186		160	(Stuart et al., 1980)
	0.15	2	120	122		108	(El-Gamal et al., 2012)
	0.30	4	128	126		111	
	0.50	5	129	133		116	
	2.00	20		154	113	110	(Ray et al., 1996)
PCE	0.35	24	146	133			(Meddah et al., 2010)
	0.70	24	171	172			
	0.15	11	108	110		121	(Çolak, 2005)
	0.31	17	149	130		138	
	0.46	19	175	156		147	
	0.62	22	194	161		153	

2.3.2.2 Drying shrinkage

When exposed to drying conditions, the moisture inside the hardened cement paste (HCP) evaporates, leading to a volume contraction, and this process is called drying shrinkage. The drying shrinkage is mainly attributed to the loss of adsorbed water in the small void in C-S-H gel, resulting in a shrinkage strain (Kawashima and Shah,

2011). The drying shrinkage induces tension and results in the initiation of cracks, causing durability problems. Various factors could affect the drying shrinkage of concrete, including mixing proportion, porosity, curing age and temperature, relative humidity, moisture content and addition of admixture (Barr *et al.*, 2003). As this thesis is mainly related to the application of superplasticiser in concrete, the effect of SP on the drying shrinkage is discussed in detail below.

As shown in ***Fig 2.14***, the drying shrinkage of mortar and concrete increases with the addition of superplasticiser, and increased with increasing dosage of superplasticisers (by plasticising effect). This was attributed to the refinement to the capillary pores in the presence of SPs (Ma *et al*., 2007). The later work conducted by Tam *et al.* (2012) also confirmed that the increase of the SP dosage would increase the drying shrinkage of concrete over all curing ages (shown in ***Fig 2.15***).

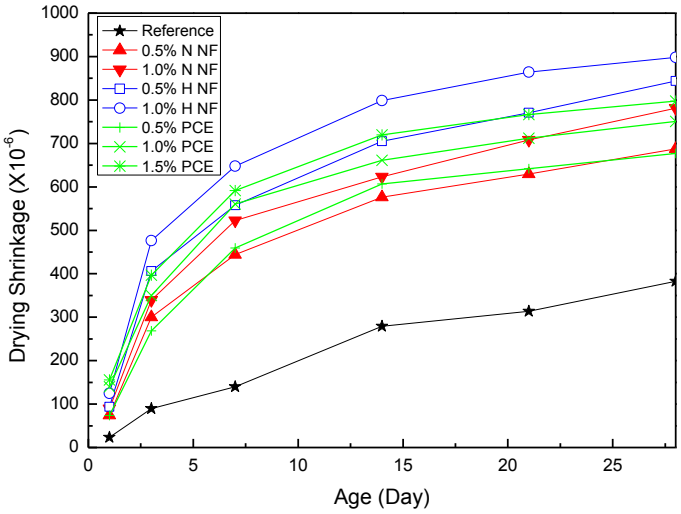

Fig 2.14 Effect of different type and dosage of superplasticiser on drying shrinkage of cement mortar at fixed W/C: N NF stands for Normal-thickness NF contained 16% sodium sulfate, H NF for High-thickness NF contained 0.5% sodium sulfate (Adapted from Ma *et al*., 2007)

Based on the water reducing effects, limited research has been conducted to investigate the effect of SP on drying shrinkage of concrete. Cartuxo *et al.* (2015) recently reported that the addition of SPs increased the 7 days' shrinkage of concrete (mixed with recycled aggregates), while it decreased 91 days' shrinkage. Tam *et al.* (2012) also reported that the decrease of the water-binder ratio decreased the drying shrinkage of superplasticised concrete (at fixed SP dosage) over all curing ages

The effects of superplasticiser on the drying shrinkage of cement and concrete are related to the change in the porosity, which will be discussed in the next section (section 2.3.2.3).

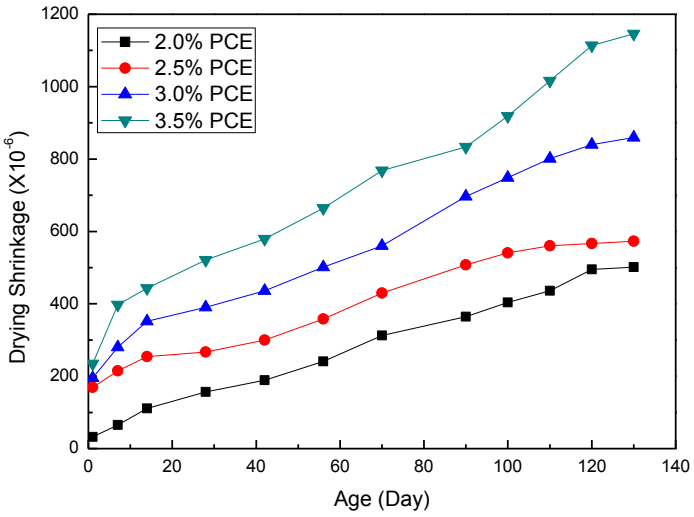

Fig 2.15 Effect of dosage of PCE on the drying shrinkage of concrete at fixed W/C (Adapted from Tam *et al.*, 2012)

2.3.2.3 Porosity

The adsorption of superplasticiser on the surface of cement particles can disperse the flocculates by introducing electrostatic and/or steric repulsion, leading to a better dispersion of cement particles (Ferrari *et al.*, 2010, Flatt and Houst, 2001), and refined pore structure of the hardened cement paste and concrete (Diamond, 2006, Zhang and Kong, 2014).

It was suggested that the pores with size larger than 50 nm, identified as *macropores*, affect the strength and permeability of hardened cement paste and concrete; whereas the pores with size smaller than 50 nm, referred to as *micropores*, can affect drying shrinkage and creep (Mehta and Monteiro, 2006). Later, some researchers used the scale as micropores (pore size less than 100 nm); mesopores (pore size between 100 nm and 600 nm); and macropores (pore size larger than 600 nm) to describe the pore structure (Ambroise et al., 2009). Moreover, the pore with size less than 10 nm, which is identified as the gel pores, has been reported to be linked to the hydration degree of cement (Zhang and Kong, 2014, Sakai *et al*., 2006). Generally, the well-dispersed cement particles in the fresh state lead to a finer pore structure in the hardened state of cement paste. It has been reported that the addition of superplasticiser decreased the pore volume of hardened cement (Khatib and Mangat, 1999, Singh *et al*., 1992). Based on the above theory, even though the refined pore structure might cause a problem to drying shrinkage and creep, it could be beneficial to the mechanical and durability properties of cement and concrete.

Under the concept of plasticising effect, Khatib and Mangat (1999) concluded that regardless of curing regime, the addition of SP refined the pore structure and reduced the total pore volume of cement paste. Similarly, Gao *et al.* (2008) demonstrated that the addition of SP reduced the pore volume of hardened paste. In Zhang and Kong's work (shown in ***Table 2.10***); it is clear that the pore volume, porosity and pore size of hardened cement paste was reduced over the hydration process. The addition of superplasticiser refined the pore structure of hardened cement paste, especially at the early age. Therefore, although the addition of superplasticiser can increase the compressive strength of hardened cement paste, the drying shrinkage could also be increased. Nowak-Michta (2015) also reported that the addition of SPs refined the pore structure of PC-based concrete.

It is well known that the reduction of w/c could reduce the capillary void of hardened sample(Mehta and Monteiro, 2006). Under a similar principle, the addition of SP based on water-reducing effect could also affect the microstructure of hardened sample. Garbalińska and Wygocka (2014) reported that the reduction of the w/c ratio by adding superplasticiser resulted in a decrease of bulk density and an increase of

macropores. However, the research on the effects of the addition of SPs (as water-reducer) on microstructure is limited. Further research need to be conducted.

Table 2.10 Effect of SP and curing age on the porosity of hardened cement paste (Zhang and Kong, 2014)

	Age(Day)	Total volume (ml/g)	Porosity (%)	Pore size distribution (%)			Average Pore Size (nm)
				<10 nm	10-100 nm	>100 nm	
Control	7	0.1299	25.50	6.74	76.69	16.57	25.6
0.1% PCE	7	0.1188	22.52	10.58	80.01	9.41	21.1
0.3% PCE	7	0.1177	22.35	12.43	83.75	3.82	18.1
0.5% PCE	7	0.1119	21.60	12.67	84.06	3.27	16.7
Control	28	0.0981	18.91	15.02	81.12	3.86	16.5
0.1% PCE	28	0.0957	18.34	15.11	80.89	4.00	16.3
0.3% PCE	28	0.0948	18.37	17.12	79.28	3.60	15.9
0.5% PCE	28	0.0931	18.16	16.67	80.18	3.15	15.4

2.4 Compatibility of superplasticiser

For environmental and economic reasons, various types of additives, such as limestone, pulverised fuel ash (PFA) and silica fume (SF), are added in Portland cement. According to BS EN 197-1, cements are divided into five categories: 1) CEM I: Portland cement; 2) CEM II: Portland-composite cement; 3) CEM III: Blastfurnace cement; 4) CEM IV: Pozzolanic cement and 5) CEM V: Composite cement. Moreover, the composites of cement are identified as main constituent, second main constituent, minor additional constituent, set regulator (calcium sulphate) and additives (grinding aids, pigments). The addition of various additives changes the properties of cement. Therefore, the compatibility of superplasticisers with different additives becomes an issue.

2.4.1 Effect of different type of cement/mineral additive

The effect of superplasticisers on the properties, especially fresh properties of concrete, varied from different types of cement. Uchikawa *et al* (1999) examined the compatibility of different Portland cements with two types of superplasticisers (LS and NF). As showed in ***Fig 2.16***, generally, NF exhibited better compatibility with various cements than LS. For the same type of SP, the improvement on fluidity varied, depending on the type of cement. In another study, Kim *et al* (2000) investigated the compatibility between NF and six types of cement, and identified three "compatible" cements (refer to ***Fig 2.16***).

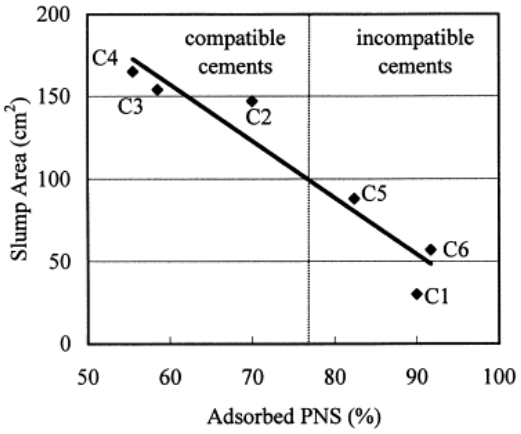

(a) **Relationship between the adsorbed PNS (NF) and minislump area**

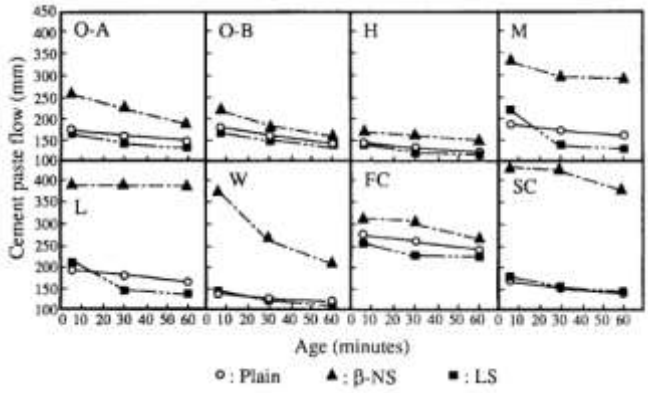

(b) Relationship between the adsorbed PNS (NF) and minislump area Effect of LS and NF on the fluidity of different types of cement (O-A stands for PC containing 0.3% free lime, O-B for PC containing 1.3% free lime, H for high early strength PC, M for moderate heat portland cement, W for white portland cement, L for low heat PC containing much belite, SC for blended cement with 50% of slag and FC for blended cement with 25% of fly ash)

Fig 2.16 Compatibility of SP with different types of cement (Kim et al., 2000b, Uchikawa et al., 1992)

All types of cement are mixed with mineral additives, which contain various percentages of natural and/or industry by-products. Therefore, the compatibility of superplasticisers with mineral additives needs to be understood which is summarised below:

- Cement blended with limestone: in general, the SPs are compatible with limestone particles. Various studies showed that the blending of limestone improved the affinity of superplasticiser, which allowed more SPs to adsorb on its particles. Therefore, the workability of cement increased with the addition of limestone (Şahmaran *et al.*, 2006, Artelt and Garcia, 2008, Mikanovic and Jolicoeur, 2008, Burgos-Montes *et al*., 2012, Adjoudj *et al.*, 2014, Alonso *et al.*, 2013).
- Cement blended with pulverised fuel ash (PFA): The workability of cement paste with SPs is enhanced with replacement of PFA. It was reported that blending PFA improved the affinity of all SPs (Artelt and Garcia, 2008, Erdoğdu et al., 2011, Burgos-Montes et al., 2012, Termkhajornkit and Nawa, 2004, Şahmaran et al., 2006, Alonso et al., 2007, Alonso et al., 2013, Ferraris et al., 2001). Compared with limestone blended cement, cement blended with PFA required lower dosage of superplasticisers due to the spherical shapes of PFA particles, which can reduce the friction through a ‘‘ball-bearing effect’’.
- Cement blended with silica fume (SF): The workability of cement paste with SPs is reduced by blending silica fume (Erdoğdu *et al.*, 2011, Vikan and Justnes, 2007, Plank *et al.*, 2009, Burgos-Montes *et al.*, 2012, Ferraris *et al.*, 2001). Erdoğdu *et al.* (2011) demonstrated that higher dosage of SP was required to improve the rheological properties of cement pastes due to the high specific surface of silica fume. Similarly, in Baghahra Al-Amoudi’s report, compared to plain concrete, more SP was required to retain the same workability of the concrete with silica fume (Baghabra Al-Amoudi *et al*., 2006). Moreover, when fixed the SP dosage, the addition of SF to the concrete increased the yield stress of concrete (Benaicha *et al.*, 2015).
- Cement blended with slag: The addition of slag could change the fresh properties of the cement (Adjoudj *et al.*, 2014, Park *et al*., 2005, Alonso *et al*., 2013). Adjoudj *et al.* (2014) proposed that the effects of slag depend on the relationship between specific surface area of cement and slag. Park et al.

(2005) found that the addition of slag can reduce both the yield stress and the viscosity of the cement paste. The workability of cement paste with SPs increased with replacement of slag and the dosage of SP to achieve required workability is reduced by increasing the quantity of slag (Palacios et al., 2009b). Gao's work demonstrated that the addition of slag could also improve the slump of concrete (Gao *et al.*, 2008, Gao *et al.*, 2001).

- Cement blended with kaolinite: The workability of cement paste with SPs is reduced by blending kaolinite. The possible reason could be due to the reduction of adsorption on the surface of Kaolinite (Şahmaran *et al.*, 2006, Lei and Plank, 2014).

Compared with different blended cements, Alonso *et al.* (2007) observed that the sequence of workability enhancement by PCE based SP was observed as: blended with slag > blended with PFA > blended with Limestone. Burgos *et al.* (2012) investigated the compatibility between LS, NF, and PCE with fresh CEM II paste containing limestone (CEM II/B-L), pulverised fuel ash (CEM II/B-V) and silica fume (CEM II/A-D). They concluded that NF is the most effective superplasticiser for all types of CEM II while LS exhibited the poorest effect on the rheological improvement of cement paste. Regarding the addition of PCE, lower yield stress was achieved with less adsorption of PCE.

2.4.2 Effect of other admixtures

Cement is not a homogeneous material, which contains various components. Moreover, there are also uncertainties with the hydration of cement due to different conditions. To control the quality of the cement system, many admixtures, particularly inorganic salts, such as $CaSO_4$, have to be employed. As demonstrated earlier in this chapter, the adsorption of SPs is based on the electrostatic attractions, and the process is sensitive to the environment of the solution. Therefore, the addition of admixture, as a consequence, changes the environment of solution and therefore, affects the performance of SPs.

In general, the presence of anions, for example, sulphate based salt, shows negative effects on the improvement of SPs. It has been reported that the sulphate concentration in aqueous phase of cement can affect the adsorption behaviour of SP on cement particles due to the competition between sulphate ion and superplasticiser. Yamada *et al.* (2001) used $CaCl_2$ and Na_2SO_4 to control the sulphate concentration (by forming $CaSO_4$) and determined its effects on the performance of PCE. They concluded that both adsorption and fluidity of cement paste decreased with the addition of sulphate (shown in ***Fig 2.17***). Moreover, Ferrari *et al.* (2010) investigated the effects of K_2SO_4 and KOH on the interaction between PCE and five different mineral particles representing both positively and negatively charged surface conditions. (The effects of four typical mineral particles on the adsorption of SP are re-plotted in ***Fig 2.18***). Their results confirmed that the addition of negative ions, such as SO_4^{2-} and OH^- , highly reduced the adsorption of SP due to the competition between these ions and the negatively charged groups on SPs in adsorbing to the surface of the grains. Pourchet *et al.* (2012) investigated the adsorption of PCE on the surface of calcite ($CaCO_3$), which is reactively inert with water (shown in ***Fig 2.19***). Their results indicated that the adsorption of PCE declined in the solution with higher sulphate concentration. The authors attributed this to the competitive adsorption between sulphate and SP on the particle surface. Correspondingly, the yield stress was also affected by adsorbed amount of PCE.

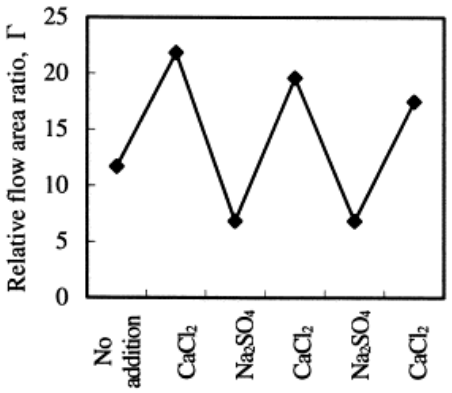

Fig 2.17 Effect of inorganic salt on the fluidity cement paste with SP (Yamada *et al.*, 2001)

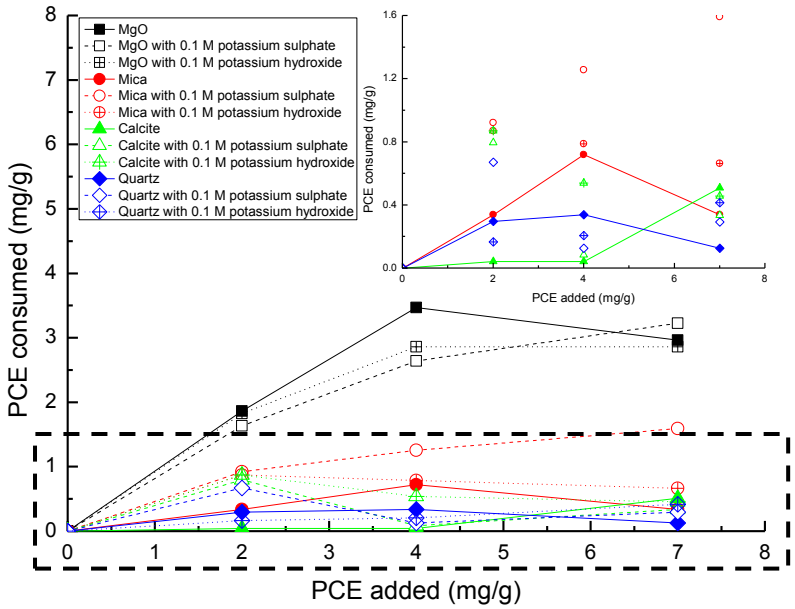

Fig 2.18 Effect of K_2SO_4 and KOH on the interaction between PCE and four types of mineral particle (MgO, Mica, Calcite and Quartz) (Adapted from *Ferrari et al.*, 2010b)

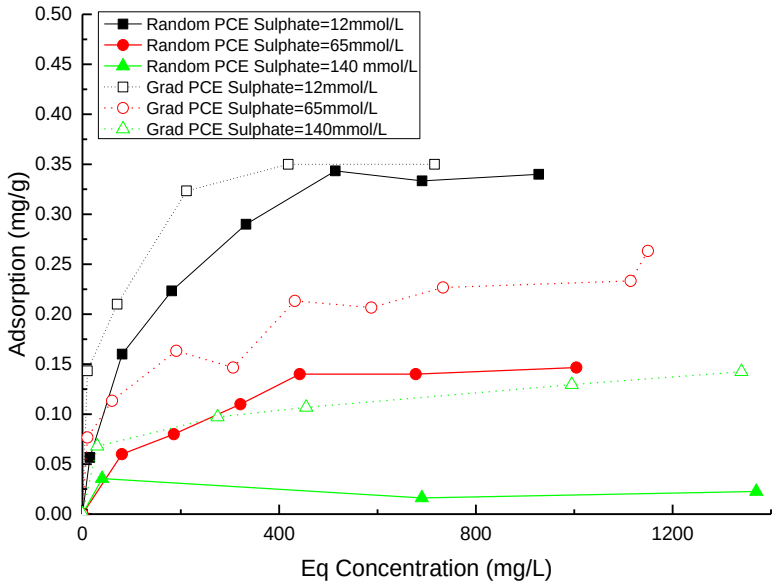

Fig 2.19 Effect of sulphate concentration on the adsorption of random and graduated PCE (Adapted from Pourchet *et al.*, 2012)

2.5 Effect of addition methods of superplasticiser on Portland cement

As discussed in section 2.3.1.3, the SP consumed during the intercalation, coprecipitation and micellisation within the hydration product is not available to contribute to the dispersion of cement particles, resulting in a reduction in the efficiency of SPs. On the other hand, this consumption also can lead to some adverse effects, for example, the slump loss, as discussed in section 2.3.2.1. The following section gives a detailed review on these issues.

It is widely agreed that, compared with the simultaneous addition of SP and cement, the delayed addition of SP can significantly enhance its efficiency in dispersing the cement particles, which, in turn, can modify the microstructure of hardened PC system (El-Didamony *et al.*, 2014). Chiocchio and Paolini (1985) investigated the delayed addition of NF and MS SP in PC paste and found that the maximum workability was obtained when adding SP at the beginning of the dormant period of cement (determined based on cement without superplasticiser). Hsu *et al.* (1999) indicated that the adsorption behaviour of NF on cement particles followed a Langmuir isothermal adsorption model. The optimum delayed time was about 10–15

minutes, which related to the beginning of the dormant period of cement paste. Aiad (2003) reported that the delayed addition of MS and NF could reduce the workability loss. These findings are in good agreement with his previous research (Aiad et al., 2002). The optimum delayed addition time from his work was observed as 15 minutes, which was corresponding to Hsu's work about 10-15 minutes (Aiad, 2003, Hsu et al., 1999). On the other hand, Flatt and Houst (2011) observed that delayed addition reduced the amount of SPs integrated into the hydration products which has caused a reduction in the SP efficiency in dispersing the cement particles. Moreover, as shown in ***Fig 2.20***, Uchikawa *et al.* (1995) identified that the setting time of cement paste with SP was prolonged by delayed addition of SP.

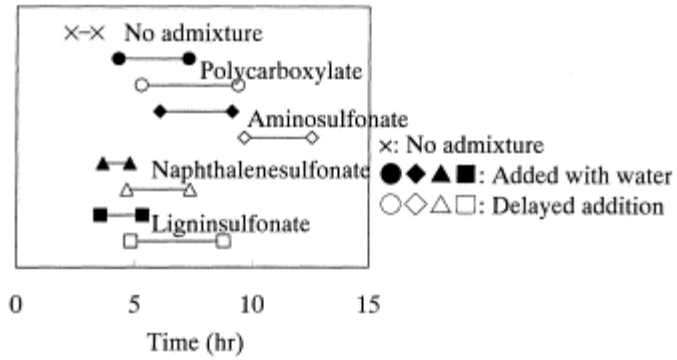

Fig 2.20 Effect of different types of SP and addition time on the setting time of cement paste (The X-axis is setting time) (Uchikawa *et al*., 1995)

As discussed in section 2.3.2, the superplasticiser is preferentially adsorbed on the surface of ettringite and monosulfate due to its positive surface charge. Based on this concept, two models regarding to linear (1st and 2nd generation SPs) and comb-shape (3rd generation SPs) SPs were proposed and demonstrated in ***Fig 2.21*** and ***Fig 2.22***. As it can be seen, the delayed addition of SP allowed the time for the reactions of gypsum and cement clinker to occur without competing with the superplasticiser. Only a few minutes' delay provided adequate time to form ettringite. Then the later added SP could be adsorbed on the newly formed early hydration product, such as ettringite. This could not only avoid the completion between SPs and gypsum, but also avoid the consumption by the intercalation, coprecipitation and micellisation.

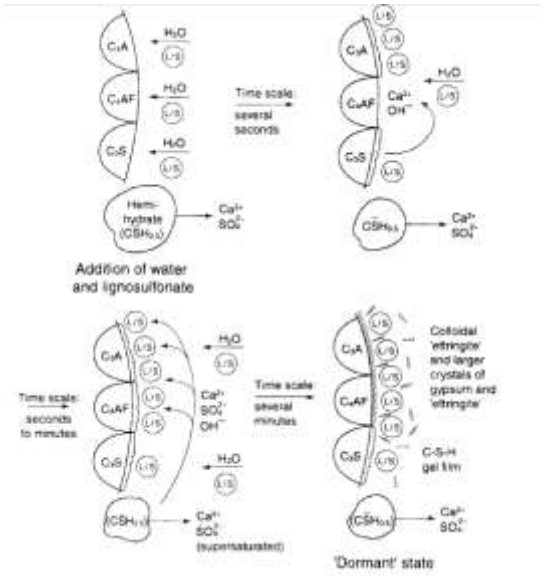

Fig 2.21 Schematic diagram showing the effect of delayed addition of LS on the early hydration of cement (Hewlett, 2004)

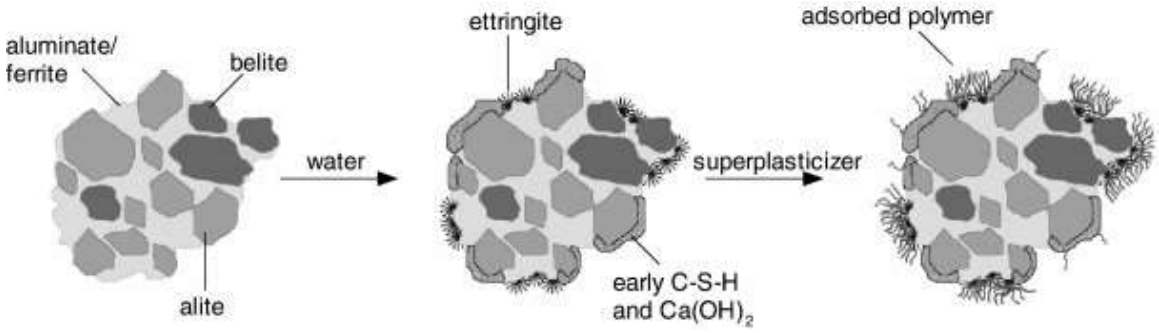

Fig 2.22 Schematic diagram showing the effect of delayed addition of PCE on the early hydration of cement (Plank and Hirsch, 2007)

2.6 Concluding Remarks

In this chapter, the superplasticisers employed in the Portland cement system have been reviewed and the following conclusion could be drawn:

- Plasticiser/superplasticiser is one of the most important chemical admixtures for cement and concrete, which plays three roles as **plasticiser**, **water reducer** and **cement reducer**. Superplasticisers provide 12-30% reduction of required water content, while plasticisers allow 5-15% decrease of water.

- Lignosulfonate (LS) and naphthalene (NF) derivation superplasticisers are the typical superplasticisers which represent the 1st and 2nd generation superplasticiser, respectively. They disperse the cement particles by electrostatic repulsion. Polycarboxylate ether (PCE) derivation is the representative of the 3rd generation superplasticiser, which is usually synthesised from vinyl monomers and ether macromonomers. In addition to electrostatic repulsion, the non-charged side chain of its comb-shape polymers provides steric repulsion to disperse the cement particles.
- The adsorption of superplasticiser plays the vital role in dispersing the cement particles. Regardless the type of SP, the adsorption behaviour of the SPs follows the Langmuir adsorption and is mainly controlled by the electrostatic interaction between the negative hydrophilic groups of SP and the positive charged cement surface. Consequently, the addition of superplasticisers reduces the zeta potential of cement particles.
- The addition of superplasticiser improves the workability of cement paste and concrete. However, its effects on rheology are varied among paste, mortar and concrete. The slump retention with the addition of SP is related to the early hydration of cement. The addition of superplasticisers can retard the hydration of cement. Correspondingly, it delays the setting of cement paste.
- The addition of SP not only affects the fresh properties, but also influences the hardened properties of cement and concrete. In general, the addition of superplasticisers slightly increases the compressive strength of cement and concrete when it is worked as a plasticiser and/or a cement reducer. However, the compressive strength is significantly increased when the SP is used as a water reducer. The drying shrinkage of hardened cement paste and concrete is also increased with the addition of superplasticiser due to the refined pore structure.
- The performance of superplasticisers varies depending on the type of cement and mineral additive as well as the chemicals. The sulphate ions reduce the adsorption of SP due to induced competition between the sulphate ions and superplasticisers. However, the addition of Ca^{2+} improves the effectiveness of SP through increasing the adsorption of SPs.

- Compared with simultaneous addition, the delayed addition of superplasticisers significantly enhances the efficiency of SP, delays the setting and further modified the microstructures of cement paste and concrete. The optimum time is related to the beginning of the dormant period of cement paste.

To sum up, the first important step towards the dispersion of cement particles by SP is the adsorption of SP on the cement surface. The negatively charged anchor groups of hydrolysed SPs are, firstly, adsorbed on the cement particles through the electrostatic attraction and the formation of Ca-complex (applicable for SPs with carboxyl groups). Then, the adsorbed SPs disperse the particles via electrostatic repulsion and steric repulsion (applicable for SPs with side chain).

The induced anions from other chemical admixtures reduce the performance of SPs due to the competitive adsorption between SPs and anions. Another key factor which influences the performance of SPs in PC system is the consumption of SPs in early hydration products, which could lead to the reduction in the efficiency of SPs in dispersing the cement particles. This issue can be solved by employing delayed addition of SP.

Chapter 3

Effect of Superplasticisers on the Properties of NaOH–activated Slag

3.1 Introduction

In addition to its advantages related to the economic and sustainable implications, the better overall performance of alkali-activated slag (AAS), such as rapid strength development, lower permeability, higher resistance to chemical attack, and lower heat of hydration, makes this low carbon cementitious material an attractive potential replacement for Portland cement in some applications.

As discussed in chapter 2, the addition of superplasticiser (SP) in Portland cement enhances various properties of PC-based system. However, the research on the performance of PC-based superplasticisers in alkali-activated slag is still very limited.

This chapter reviews the effect of current PC-based superplasticisers on the properties of NaOH activated AAS. Section 3.2 introduces the background of AAS cement including its composition and applications. Section 3.3 demonstrates the surface chemistry of NaOH-activated slag during the early activation stage and the working mechanism of current PC-based superplasticiser in AAS. Section 3.4 summarises the effects of current PC-based superplasticiser on both fresh and hardened properties of NaOH-activated slag. Section 3.5 discusses the chemical stability of PC-based SPs in highly alkaline media. Section 3.6 summarises the issues facing the application of the PC-based SPs in NaOH-activated slag and proposes potential solutions to solve these issues.

3.2 Background of alkali-activated slag

This section describes the composition of AAS including different types of activator and various nature of slag. The current application of AAS is also described in this section.

3.2.1 Alkali-activated slag and its composition

AAS cement is defined as a low carbon cementitious material, mainly consisting of alkaline activators and ground granulated blast furnace slag, a by-product from iron

and steel manufacture. Slag, the main cementing component, exhibits a good latent hydraulic cementing property. However, the reaction between slag and water is too slow to generate hydration product to develop sufficient strength for construction purpose, which makes no sense for practical use. Therefore, to stimulate this slow reaction, highly alkaline activators (for example, NaOH, sodium silicate, and sodium sulphate) are employed.

3.2.2 Alkaline activators

Usually, all the caustic alkalis or alkaline salts can be used as alkaline activator of AAS (Shi et al., 2006). According to the chemical composition, the various chemicals can be classified into six categories (Shi and Day, 1995):

- Caustic alkalis: NaOH, KOH;
- Non-silicate weak acid salts: Na_2CO_3, Na_2SO_3, Na_3PO_4;
- Non-silicate strong acid salts: Na_2SO_4, K_2SO_4
- Silicates: $Na_2O\ nSiO_2$
- Aluminates: $Na_2O\ nAl_2O_3$
- Aluminosilicates: $Na_2O \cdot Al_2O_3\ (2\text{-}6)SiO_2$

Due to the lower availability and high cost of potassium-based compounds, most activators are sodium-based compounds which provide similar properties to potassium-based compounds. Among these activators, NaOH, and $Na_2O\ nSiO_2$ have been reported as the most commonly used activators. Particularly, $Na_2O{\cdot}nSiO_2$ (waterglass) has been considered as the most effective one, primarily due to the much improved performance brought to the AAS system by the extra silicon component in waterglass. However, the exact reaction mechanism of waterglass activated AAS system is considerably complicated due to the increased complexity introduced by the silicon component (Fernandez-Jimenez and Puertas, 2003). Hence, NaOH activated slag could be used to investigate the fundamental mechanism involved in the alkaline activated slag system.

Apart from the type of activator, alkali concentration (calculated as Na_2O% by the mass of slag) shows a significant influence on the performance of NaOH-activated slag system, which is to be discussed in the following sections.

3.2.3 Type of slag

Ground granulated blast furnace slag has been identified as the most effective type of cementing component used in NaOH-activated slag cement (Shi et al., 2006). It is formed from the residue of iron ore after its reaction with coke, which may contain many remaining impurities such as silica (SiO_2), alumina (Al_2O_3), magnesia (MgO) and lime (CaO). Therefore, the chemical composition of slag varies from batch to batch, which highly depends on the manufacture process and the type of the iron ore. The composition of slag is usually illustrated in a CaO-SiO_2-Al_2O_3-MgO quaternary system.

The hydraulic reactivity of slag is affected by many factors including chemical composition, fineness and glass phase content. Among them, chemical composition plays an important role in evaluating its hydraulic reactivity. It is well accepted that there is a positive relationship between the hydraulic reactivity and CaO content of slag, which means higher reactivity is determined in the slag with a higher CaO content. To evaluate the hydraulic reactivity of slag, the degree of basicity (M_b) is introduced, which is defined in ***Equation 3.1***.

$$M_b = \frac{CaO\% + MgO\%}{SiO_2\% + Al_2O_3\%} \qquad \textbf{3.1}$$

Based on the degree of basicity, all the slag can be divided into three categories as following:

- Acid slag: $M_b < 1$
- Neutral slag: $M_b = 1$
- Basic slag: $M_b > 1$

Therefore, basic slag exhibits higher reactivity than acid and neutral slags.

The main chemical components of some typical commercial slags provided by worldwide suppliers are summarized in ***Table 3.1***. From this table, it can be seen clearly that the chemical compositions between slags supplied worldwide are various. Though basic slag provides higher reactivity, unfortunately, most of the slags available are acid slags, which are not favourable to produce AAS.

Table 3.1 Chemical composition and degree of basicity of typical slags

Category	Supplier	CaO%	MgO%	SiO_2%	Al_2O_3%	M_b
Basic slag	Poleks, **Ukraine**	47.46	5.64	39.36	6.75	1.15
	Long Steel Company, **China**	35.23	7.11	27.51	10.59	1.10
	Schwenk Cement **Germany**	42.80	6.44	35.90	11.40	1.04
	Eduardo Torroja Institute for Construction Sciences, **Spain**	40.21	7.44	34.11	12.38	1.02
	Acer ás Paz del R ó steelworks, **Colombia**	42.49	2.87	32.25	16.25	1.01
	Zeobond Pty Ltd, **Australia**	42.56	5.34	33.80	13.68	1.01
Basic Slag /neutral slag	Xiamen All Carbon, **China**	32-40	14.00	28-36	12-18	1.00-1.15
	M L Enterprises, **India**	32-40	10-14	28-36	12-18	1.00-1.05
	Holcim, Salzgitter Plant, **Germany**	36.40	11.50	36.30	11.50	1.00
Acid slag	Tongshun Industry and Trading Co., Ltd, **China**	38.60	9.22	34.48	14.49	0.98
	Tianjin Sheng Xing-Long Steel Industry & Trade Co., Ltd**, China**	38.88	9.23	33.42	15.80	0.98
	Profit Ocean Shipping Co., Ltd, **China**	35.22	9.02	31.43	14.63	0.96
	Civil & Marine, **UK**	39.40	8.00	34.30	15.00	0.96
	the Composite Materials Group, Universidad del Valle, **Colombia**	42.86	1.17	31.62	14.65	0.95
	Tangshan Guofeng Screws Co., Ltd**, China**	34.60	9.21	33.42	15.23	0.90
	Shafi, **Pakistan**	36-40	9.00	36-39	14-16	0.89-0.90
	Holcim, Hansa Bremen Plant, Bremen, **Germany**	38.60	6.40	38.60	12.40	0.88
	Iskenderun Iron-Steel Factory, **Turkey**	32.61	10.12	36.70	14.21	0.84
	Ereğli steel plant, **Turkey**	35.90	5.88	40.20	11.66	0.81
	Jenefa, **India**	30-35	8-10	32-37	15-18	0.81-0.82

Summarised from the following literatures: (Ma, 2013, Shi et al., 2006, Ismail et al., 2014, Bernal et al., 2014, Aydın and Baradan, 2014)

The chemical components of PC and slag are compared in ***Table 3.2***. It can be seen that the most distinctive difference between PC and slag is the content of CaO, which is linked to the reactivity. Since less content of CaO exists in the slag, the reactivity of slag in water is lower. Therefore, it is essential to employ alkaline activators to accelerate the hydration process of slag, which is to be discussed in the section below.

Table 3.2 Comparison of Portland cement and slag

Chemical Component	Typical Chemical Composition/%	
	Portland Cement	Slag
CaO	60-67	38-44
SiO_2	17-25	31-38
Al_2O_3	3-8	9-13
MgO	0.1-4	7-12

3.2.4 Application of alkali-activated slag

AAS was first invented in 1950s. In later years, AAS cements and concretes have been manufactured and used all over the world in both developed and developing countries from Australia, Far East, to Europe and North America. Some of its products have already been commercialised such as the Paramount cement (Pyrament Cement®) in U.S., "F-cement" in Poland and "E-Crete ™" in Australia (Shi et al., 2006, Wang et al., 1994, Douglas and Brandstetr, 1990). Some typical applications of AAS are summarized in ***Table 3.3***. However, most of the applications are still confined in small sales and some specific areas. Many factors still hinder its industrialisation, such as, the lack of efficient admixtures, the variability of raw cementing component and the lack of industrial standards, etc. Among these factors, the lack of efficient admixtures is one of the main barriers for its wider industrial applications. Thus, the research on developing compatible admixtures for AAS is essential.

Table 3.3 Summary of the current applications of AAS

Category	Construction	Non-construction
Agriculture	• Cast in situ and pre-cast concrete • Storage	
Hydraulic	• Irrigation systems • Break waters	• Linings
Industrial	• Acid-resistant buildings garages • Floor slabs • Foundations	• Bodies of machine tools
Mining	• Oil well grouts • Ties • Sealing • Prevent water • Penetrations	
Residential	• Pre-cast and in situ concrete buildings • Slabs • foundations	• Dies • Moulds
Transport	• Heavy-duty pavements cast in situ, pre-cast and reinforced	• Waste immobilization

Summarised from the following literature: (Roy, 1999, Shi et al., 2006, Qian et al., 2003)

3.3 Working mechanism of superplasticiser in NaOH-activated slag

The performance of superplasticiser is closely related to the surface condition of slag particles. This section firstly reviews the surface condition of NaOH-activated slag, and then the working mechanism of PC-based superplasticisers in NaOH-activated slag is summarised.

3.3.1 Surface condition of slag

Although slag shows latent hydraulic cementing properties, it is difficult to react and hydrate when mixed with water directly. To accelerate its reaction, highly alkaline chemicals have to be added. As a result, the surface condition of slag is different from that of PC.

When slag contacts with water, the ionic bonds, such as Ca-O and Mg-O on the surface of slag are prone to be cleaved, releasing Ca^{2+} and Mg^{2+} cations (Pu, 2010).

Under the polarisation effect of OH^-, some covalent bonds, such as Si-O and Al-O bonds, also break down. As shown in ***Table 3.4***, less bond dissociation energy of Ca-O and Mg-O bonds suggests that these bonds are weaker than Si-O and Al-O bonds. Therefore, more Ca^{2+} and Mg^{2+} are released into water, which determines the surface charge of slag (Shi et al., 2006).

Table 3.4 Typical bond dissociation energy (Luo and Kerr, 2007, Darwent, 1970)

Bond	Bond Dissociation Energy (kJ/mol)
C-H	473
C-O	402
C-C	618
C-N	335
C-S	97
Al-O	501
Si-O	799
Ca-O	383
Mg-O	358

However, as discussed in Section 3.2.3, due to the different manufacture processes and the type of the iron ore, the chemical composition of the slag varies from batch to batch. Therefore, the ions dissolved in water differ in different slags. As demonstrated in ***Table 3.5,*** the zeta potential of slag particles is dependent on the type of slag. It can be seen from the data that the initial zeta potential of slag in water varies from a negative value for acid slag (i.e. slag III) (-20.30 mV) to a positive value for basic slag (i.e. slag I) (+17.06 mV). This variation is illustrated in ***Fig 3.1***. It can be demonstrated from the figure that the basic slag, which consists of higher percent of CaO, exhibits positive initial zeta potential value, while the acid slag displays the negative value due to less cations adsorbed onto the slag surface. Correspondingly, higher cation concentration, particularly Ca^{2+}, can be observed in slag I suspension.

Along with the ongoing hydration of slag, more dissolution occurred in the slag. Therefore, as shown in ***Table 3.5***, more cations are dissolved into the water, which consequently increases the zeta potential of slag (Habbaba and Plank, 2010).

Table 3.5 Surface charge and ion concentration of different type of slag in Deionized (DI) water (Habbaba and Plank, 2010)

Slag	M_b	Time (min)	pH	Zeta potential (mV)	Ions Concentration (mg/L)		
					Ca^{2+}	K^+	Na^+
Type I	1.04	0	12.58	17.06	366.83	203.44	59.51
		20	12.66	22.43	342.79	227.50	61.96
		60	12.75	30.60	405.25	249.38	76.07
		120	12.79	32.40	480.52	288.75	93.87
Type II	1.00	0	12.50	1.00	214.20	54.69	12.88
		20	12.59	3.85	221.74	56.88	14.11
		60	12.68	5.62	252.62	65.63	20.86
		120	12.69	7.21	246.32	72.19	26.99
Type III	0.88	0	11.99	-20.30	90.52	13.03	3.07
		20	12.11	-17.42	108.58	13.13	5.52
		60	12.19	-15.08	110.50	13.35	7.36
		120	12.22	-14.14	104.22	13.63	11.66

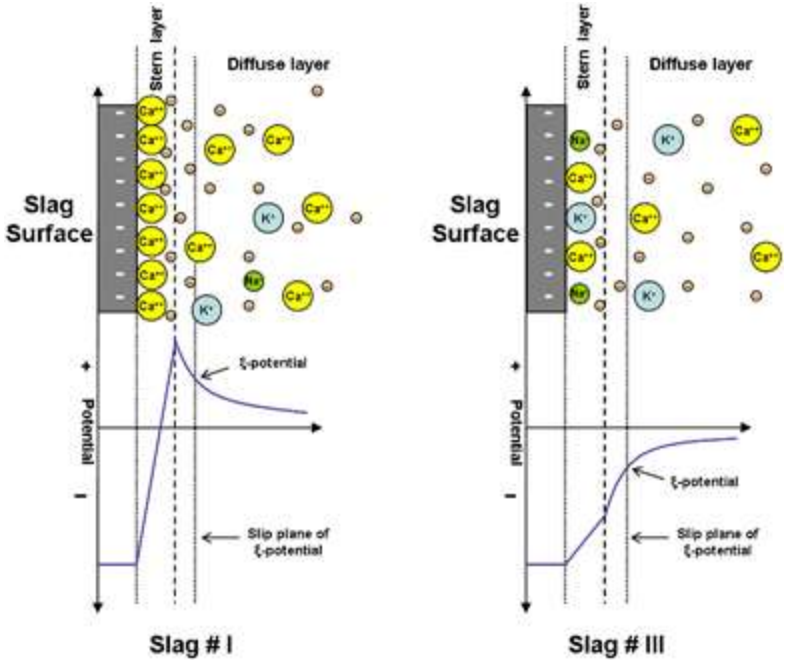

Fig 3.1 Schematic diagram of the surface charge of different slag dispersed in water: slags I (basic slag) and slag III (acid slag) (Habbaba and Plank, 2010)

Although slag exhibits hydraulic properties in water, this reaction is too slow (Rajaokarivony-Andriambololona et al., 1990). Since the alkaline activator can accelerate the hydration of slag, it is essential to be employed in slag in order to activate the hydration of slag. As a result, the hydration of AAS depends on the

nature of alkaline activator. However, the exact mechanism is not fully understood yet. Nonetheless, among different assumptions, it is generally accepted that the main activation process is composed of destruction–condensation process, which include the dissolution of raw material and the precipitation and polycondensation of the hydrates. The activation process can be identified in three steps described as following (Krivenko, 1992, Glukhovsky et al., 1980):

- The destruction of covalent bonds in the slag in highly alkaline media. The presence of high concentration of OH^- could not only break Ca-O and Mg-O bonds, but also cleave a significant amount of Si-O and Al-O bonds.
- Accumulation of the destroyed product, forming coagulated structures of slag. The broken groups of Si-O and Al-O bonds are transformed into colloid phase.
- Formation of new phases through condensation-crystallisation processes.

As illustrated in ***Fig 3.2,*** Duxson and Provis (2008) proposed one model of the dissolution mechanism of glass phase of slag with high calcium content and low Al content. It can be seen clearly that, compared with the site of Na^+, much greater extent of destruction in glass structure of slag is found by removing the divalent and monovalent cations through the ion exchange of H^+ for Na^+ or Ca^{2+}. Nonetheless, those three steps happened almost simultaneously, which is difficult to be identified as individual processes.

Based on the reports in literature, in the presence of NaOH activator, the initial zeta potentials of slag pastes are changed to negative value regardless of the type of slag (Yang et al., 2009, Kashani et al., 2014, Palacios et al., 2009a). The zeta potential of NaOH-activated slag decreases as the Na_2O% of NaOH is increased (Shown in ***Table 3.6***). However, Kashani (2014) reported that by increasing the Na_2O% of NaOH, the zeta potential of slag was increased and become to positive charge. The reason of these controversial results could be attributed to the greater amount of Ca^{2+} released from the slag particles at higher pH value.

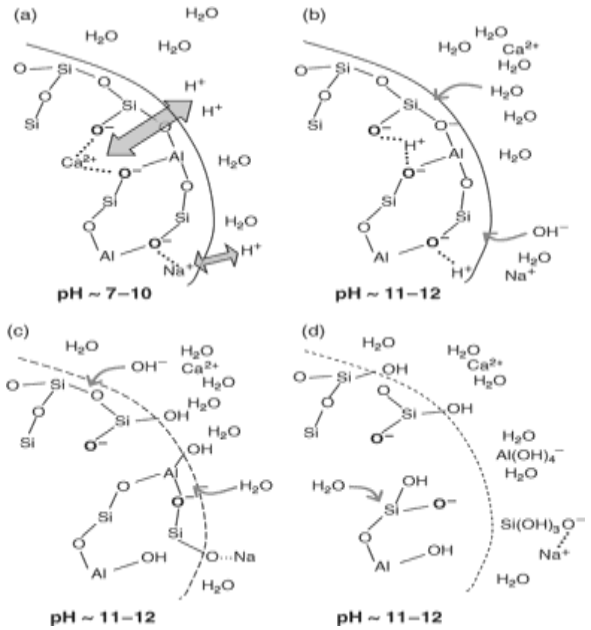

Fig 3.2 Dissolution mechanism of glass phase during the early stages of slag reaction: (a) exchange of H^+ for Ca^{2+} and Na^+, (b) hydrolysis of Al–O–Si bonds, (c) breakdown of the depolymerized glass network, and (d) release of Si and Al. (Duxson and Provis, 2008)

Table 3.6 Effect of dosages of NaOH activator on zeta potential of slag suspension

Yang's Work		Palacios' Work		Kashani's Work	
Na_2O%	Zeta Potential/ mV	pH	Zeta Potential/ mV	Na_2O% ($\times 10^4$ mol/g slag)	Zeta Potential/ mV
0%	-17.78	11.7	-2.00	0	-2.80
2%	-20.61	11.7	-2.98	2.2	-2.41
4%	-28.64	11.7	-2.89	4.4	+1.64
6%	-31.94			6.6	+3.96
				8.8	+5.31
				11.0	+6.86

Summarised from the following literature: (Yang et al., 2009, Kashani et al., 2014, Palacios et al., 2009a)

Only few studies can be found in the literature on the surface chemistry of slag in the presence of NaOH activator. Therefore, it is difficult to draw a conclusion about the effects of NaOH activator on the surface chemistry of slag. However, based on the

results obtained from the AAS activated by other activators, such as sodium silicate and sodium sulfate, it has been showed that the addition of alkaline activator reduced the zeta potential of the slag because the negatively charged anions could be adsorbed onto the surface of the slag (Habbaba and Plank, 2012, Kashani et al., 2014, Yang et al., 2013, Yang et al., 2009). Similar to ***Fig 3.3,*** generally, the more negatively charge SO_4^{2-} ion is added, the lower surface charge is observed. Therefore, when SP is added, the adsorbed negatively charged alkaline activator around the slag surface could occupy the positively charged site and cause the reduction of adsorption of SPs (as SP is usually also negatively charged).

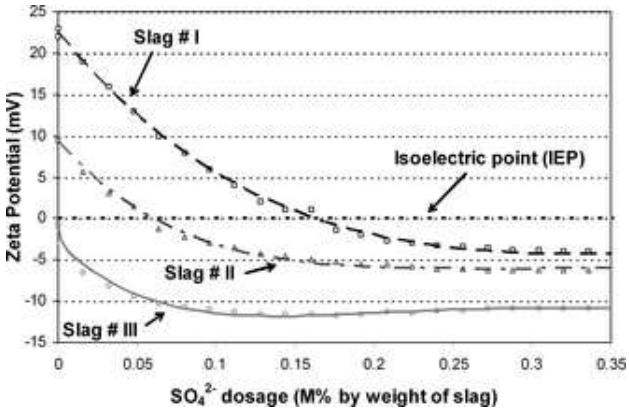

Fig 3.3 Zeta potential of slag dispersed in $CaCl_2$ solution as a function of SO_4^{2-} ion concentration (for the purpose of simulating the environment of cement pore solution) (Habbaba and Plank, 2012)

3.3.2 Isothermal adsorption

As discussed in Chapter 2, the adsorption of SPs on the surface of PC particles is a crucial stage for the dispersion of PC particles (Flatt and Houst, 2001). In a similar way, the adsorption of SPs on the surface of slag is also important for the dispersion of slag particles. However, only few researchers have been conducted on this topic and this has been summarised below.

The adsorption of polycarboxylate ether (PCE) SPs on the slag in pure water and synthetic pore solution of PC were investigated by Habbaba and Plank (Habbaba and Plank, 2012, Habbaba and Plank, 2010) (as shown in ***Fig 3.4 (a)*** and ***(b)***). Regardless of the type of SP and the dispersion media, the adsorption of PCE generally follows the Langmuir adsorption (as discussed in Section 2.3.4). However, the amount of

PCE adsorbed depends on, not only the nature of the slag (shown in ***Fig 3.4 (a)***), but also the dispersion media (illustrated in ***Fig 3.4 (b)***).As can be seen from Fig 3.4 (a), higher adsorption is identified in slag I, which consists of higher percentage of CaO. It is believed that the released Ca^{2+} can promote the adsorption of PCE due to the formation of a Ca-complex with carboxylic groups of PCE (Plank and Winter, 2008). The controversial trend of the effect of dispersion media on the adsorption of PCEs is observed with different type of slag, which is also attributed to the surface condition of the particles (Habbaba and Plank, 2010).

The adsorption behaviour of the current PC-based superplasticisers in NaOH-activated slag and PC was also studied by some researchers. Yang *et al.* (2009) reported that the adsorption of both Lignosulfonate (LS) and Naphthalene (NF) SP followed the Langmuir adsorption, which was consisted of two parts: the linear adsorption at lower dosage and the plateau in higher range of SP dosage (shown in in ***Fig 3.5***). Noticeably, it can be seen from the figure that the addition of NaOH activator reduced the adsorption of both LS and NF. With the increased dosage of NaOH, the adsorption of SPs was further decreased. The results suggest that there exists a competitive adsorption between the SPs and NaOH. Moreover, as shown in ***Fig 3.6***, Palacios *et al* (2009) also confirmed that the adsorption of both MF and NF were followed by Langmuir adsorption. However, for vinyl copolymer (VC), the plateau was not obvious, which might be due to the nature of the SPs.

It should be noted that the amount of SPs adsorbed in NaOH-activated slag was lower than that in PC. The reduced adsorption could be either due to the different surface condition between slag and PC cement, or, the competitive adsorption induced by the activator.

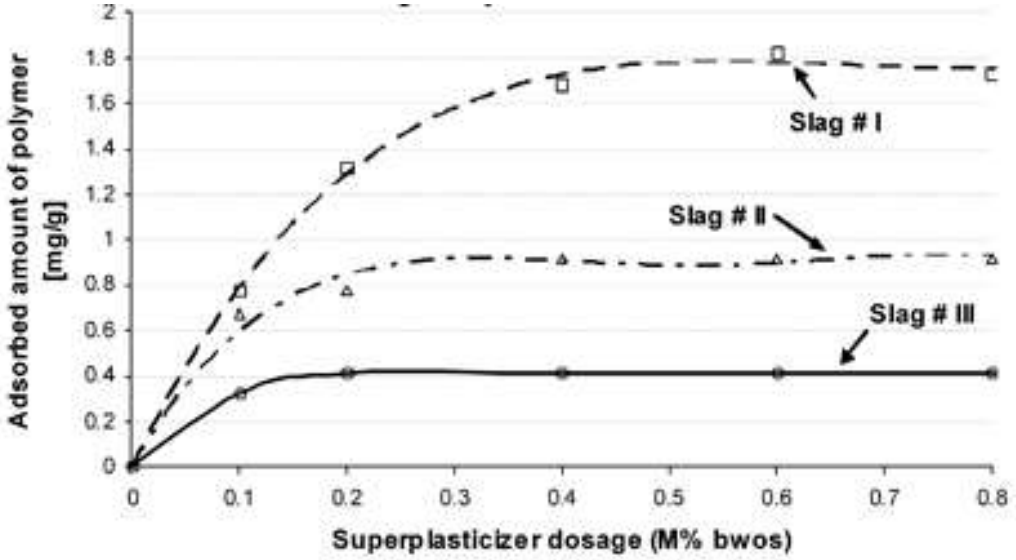

(a) In water

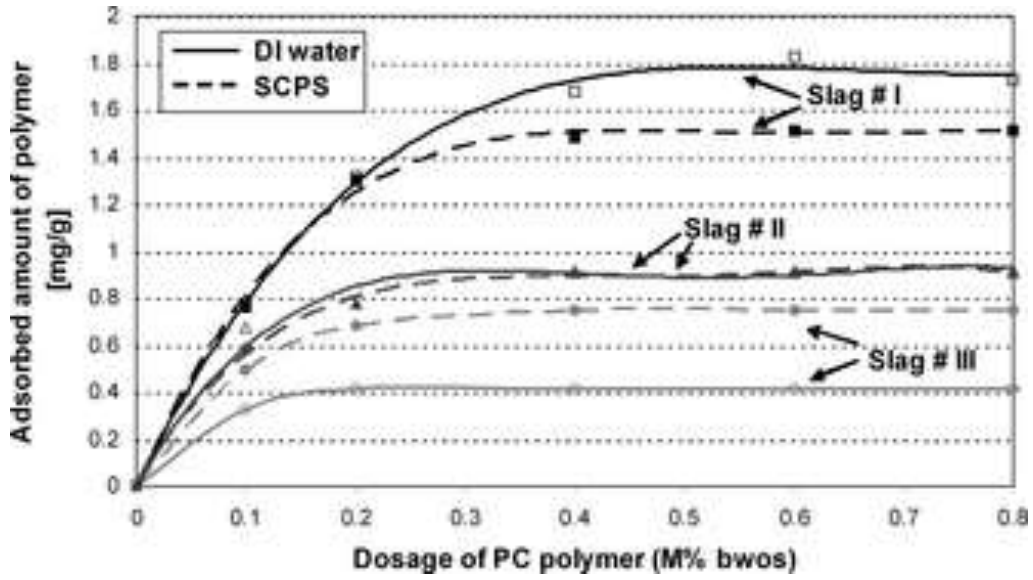

(b) In synthetic cement pore solution

Fig 3.4 Adsorption of PCE on the different type of slag: (a) in water and (b) in synthetic cement pore solution (Habbaba and Plank, 2012, Habbaba and Plank, 2010)

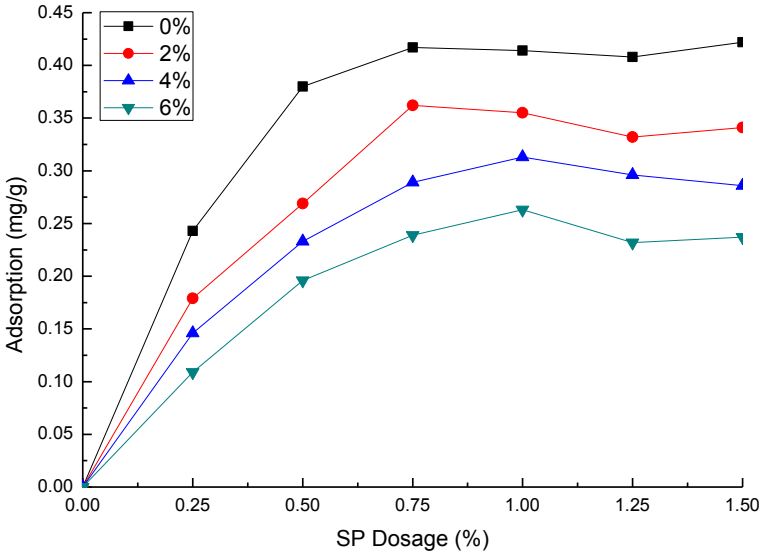

(a) LS

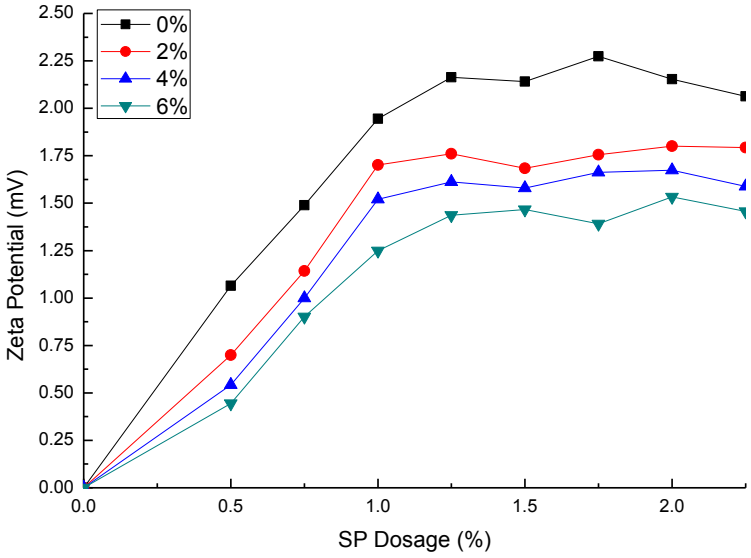

(b) NF

Fig 3.5 Effect of Na_2O% (0%, 2%, 4% and 6%) concentration on the adsorption behaviour of LS and NF in NaOH activated slag (Adapted from Yang et al., 2009)

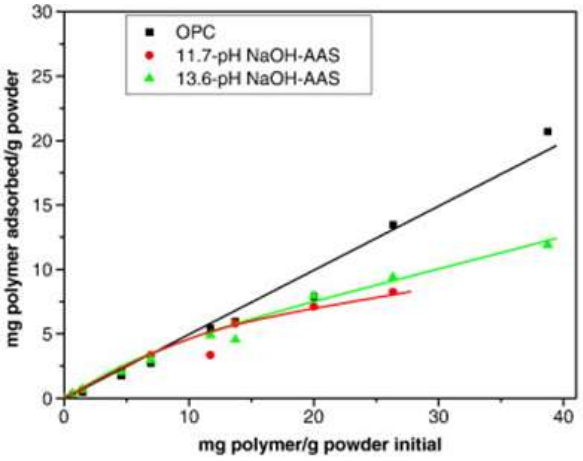

(a) MS SP

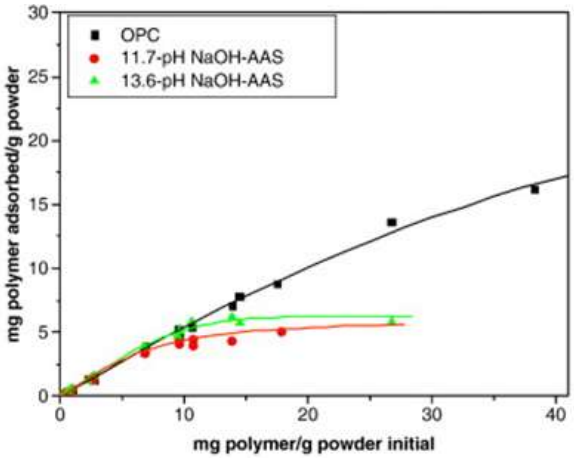

(b) NF

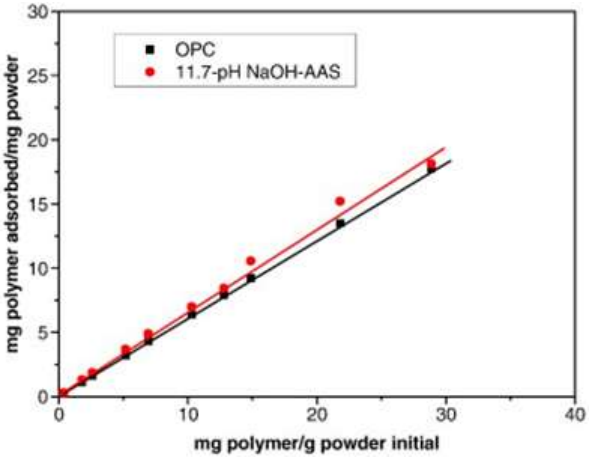

(c) VC SP

Fig 3.6 Adsorption of superplasticisers in NaOH-activated slag and PC: (a) MS SP, (b) NF and (c) VC SP (Palacios et al., 2009)

3.3.3 Surface charge

After being adsorbed by the SPs, the surface conditions of the PC or slag particles are changed due to the charges introduced by the SPs. Since SPs are usually anionic polymers, the zeta potential of slag particles is reduced after being adsorbed by the SPs.

However, the exact change in the surface charge also depends on the type of SPs. In the case of the slag suspension without adding the activator, as illustrated in ***Fig 3.7***, the addition of LS and NF, which are designed under electrostatic repulsion mechanism, decreases the zeta potential of slag particles (Yang et al., 2009). On the other hand, with the addition of PCEs, which is designed under both electrostatic repulsion and steric repulsion, the change of zeta potential varies (as shown in ***Fig 3.8***) (Habbaba and Plank, 2010). The change does not only depend on the type of slag, but also on the chemical structure of PCEs.

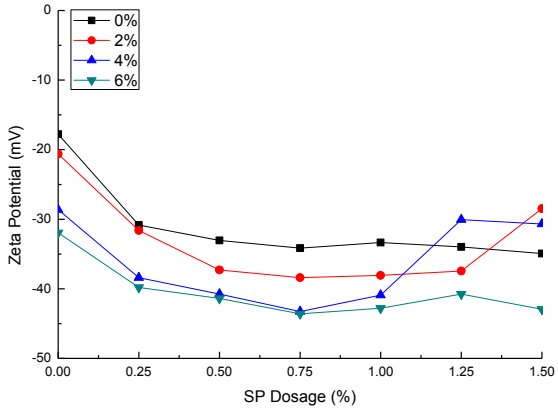

(a) Effect of LS with different Na_2O% as 0%, 2%, 4% and 6%

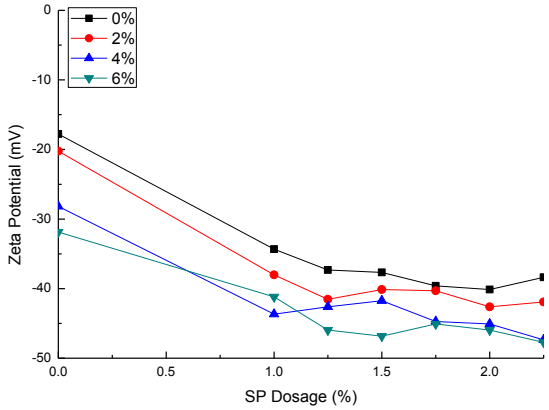

(b) Effect of NF with different Na_2O% as 0%, 2%, 4% and 6%

Fig 3.7 Effect of LS and NF on zeta potential of NaOH activated slag prepared by different Na_2O% (0%, 2%, 4% and 6%) (Adapted from Yang et al., 2009)

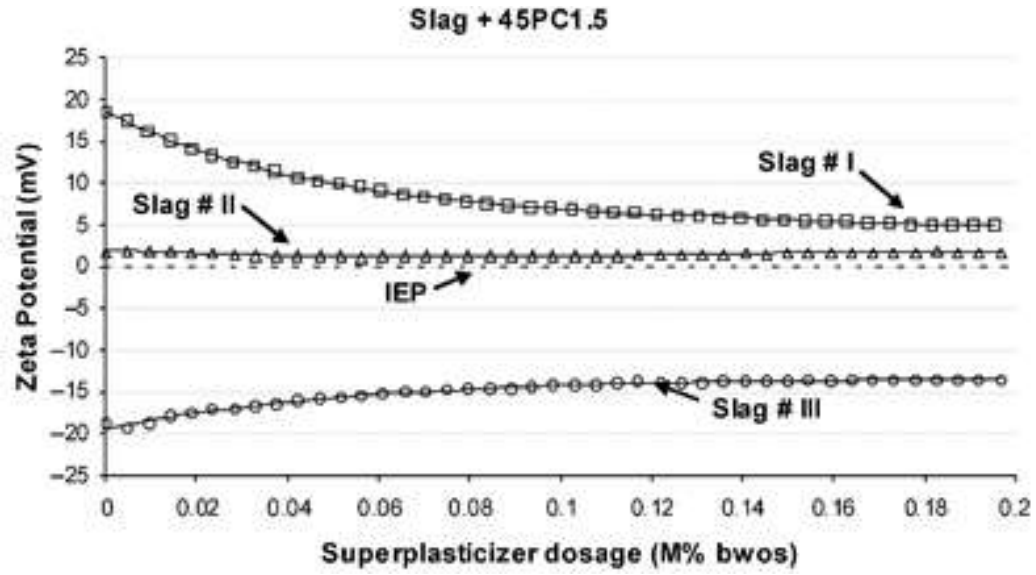

(a) Effect of PCE with molar ratio between methacrylic acid and side chain as 1.5:1

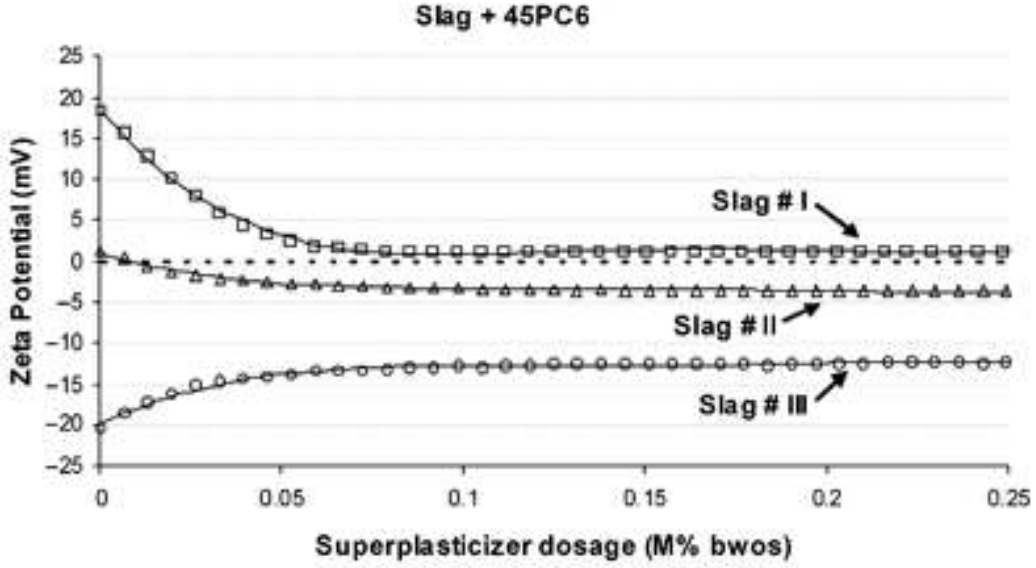

(b) Effect of PCE with molar ratio between methacrylic acid and side chain as 6:1

Fig 3.8 Effect of PCE on zeta potential of slag suspension (Habbaba and Plank, 2010)

However, over certain dosage, the addition of SP could not further decrease the zeta potential of NaOH-activated slag (Nägele and Schneider, 1989b, Yang et al., 2009). Similar results (shown in ***Fig 3.9***) were also obtained by Palacios *et al.* (2009). The results are consistent with the adsorption behaviour mentioned in the previous section.

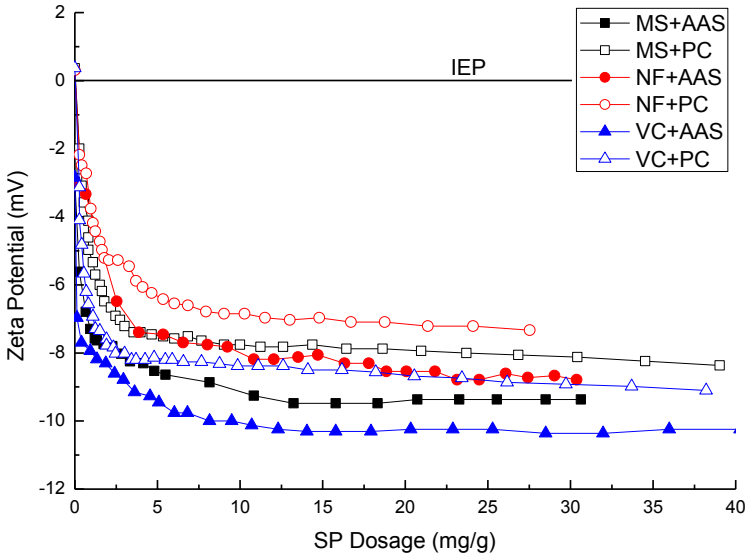

(Note: MS stands for melamine derivative, NF for naphthalene derivative, and VC for vinyl copolymer)

Fig 3.9 Effect of superplasticiser on zeta potential of NaOH-activated slag and PC (Adapted from Palacios et al., 2009)

3.3.4 Potential competition between superplasticiser and activator on the surface of slag particles in AAS

Although considerable investigations have been conducted on the adsorption behaviour of PC-based SPs in PC, the research on the adsorption of these SPs in NaOH-activated slag is still scarce (Yang et al., 2009, Pan et al., 2014, Yang et al., 2013, Palacios et al., 2009a). Based on these limited studies, it is clear that the addition of the alkali activator highly reduces the adsorption of SPs regardless of the type of SP and the nature of activator. As shown in ***Fig 3.7***, the adsorbed amounts of both LS and NF on slag surface are reduced in the presence of OH^-. Yang et al. (2009) concluded that the higher the OH^- concentration, the less the SP could be adsorbed on the surface of the slag. The reason for this reduced adsorption can be attributed to the competitive adsorption between the negative OH^- groups and the negatively charged SP on the surface of slag. As discussed in section 2.4.2, the addition of inorganic chemicals with negatively charged groups, such as K_2SO_4 and KOH, highly reduced the adsorption of SP on the surface Portland cement grain due to the competitive adsorption. In contrast, as shown in ***Fig 3.10***, the addition of YP-3

retarder which is positively charged (i.e. opposite to the charge of SPs), increases the adsorption of SPs in NaOH-activated slag. The results provide the evidence that the ions with the same type of charge can reduce the adsorption due to the competitive adsorption.

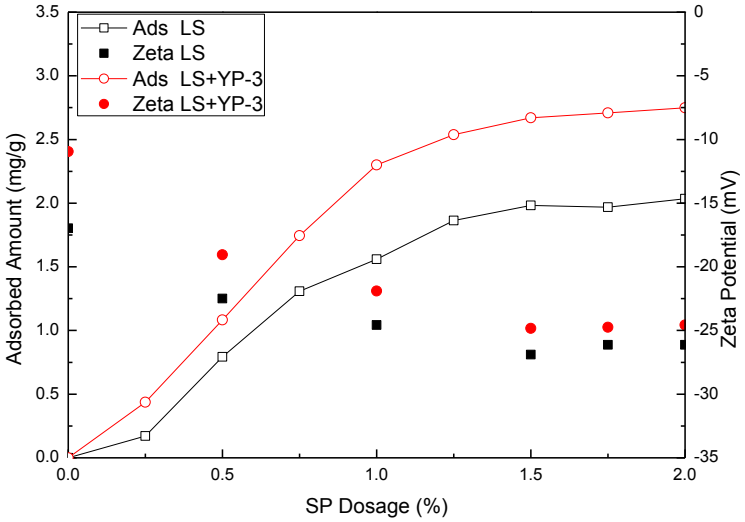

(a) In the presence of LS

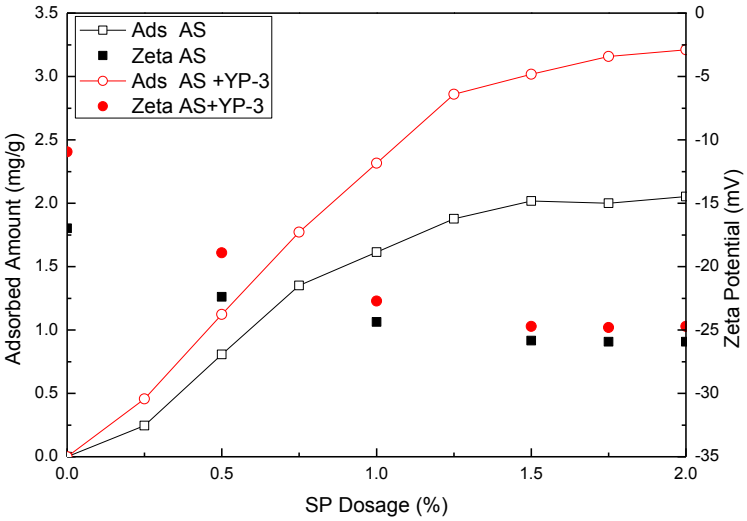

(b) In the presence of NF

Fig 3.10 Effect of YP-3 retarder on the adsorption and zeta potential of NaOH activated slag at 4% Na_2O concentration (Adapted from Pan et al. (2014) and Yang et al., (2013))

3.3.5 Summary

In this section, the surface condition of slag with/without NaOH activator is reviewed and the working mechanism of PC-based superplasticiser in NaOH-activated slag is also discussed. Similar to the interaction between PC-based SPs and PC particles, the adsorption of SPs on slag particles follows the Langmuir adsorption behaviour. However, since the surface condition of slag is changed by adding alkali activators, the adsorption behaviour of SPs is also changed accordingly. On the basis of the review in this section, it can be concluded that the addition of NaOH activators reduces the amount of PC-based SPs which can be adsorbed on the surface of the slag, leading to a reduction of the effectiveness of PC-based SPs in NaOH-activated slag.

3.4 Effect of superplasticiser on the properties of NaOH-activated slag

As discussed previously, the addition of NaOH activator introduces the competitive adsorption between SPs and NaOH, leading to a reduction of the effectiveness of PC-based SPs in NaOH-activated slag. Building upon the information and the knowledge developed on the surface condition and the competitive adsorption between the SP and the activator, this section reviews the effects of PC-based SPs on both early age and hardened properties of NaOH-activated slag which is considered as the most important information for the wider industrial application of AAS systems.

3.4.1 Effects of PC-based SPs on early age properties of NaOH-activated slag

3.4.1.1 Workability

Workability, defined as the quantity of mechanical work or energy required to compact concrete without segregation, is normally used as a general term to describe the fresh properties of cement paste and concrete (Shi et al., 2006). In this section, in order to distinguish from the rheological properties (will be discussed in next

section), the term "workability" is used to describe the flowability determined from *"single-point"* test (in terms of slump and/or minislump).

3.4.1.1.1 Workability of NaOH-activated slag

Many factors, including components of slag, nature of activator, water to slag ratio and addition of admixture etc., can affect the workability of NaOH-activated slag. Regardless of these factors, compared with PC, at a given water/slag ratio, NaOH-activated slag shows poor workability and quicker minislump loss (Jiang, 1997, Palacios and Puertas, 2005, Shi et al., 2006, Kashani et al., 2014, Jolicoeur et al., 1992). One typical example reported by Jolicoeur et al. (1992b) is shown in ***Fig 3.11***. They observed that when mixing slag with NaOH at lower w/c ratio (0.4), the concentration of NaOH activator showed less effect on the initial minislump. However, the 60-minute minislump reduced significantly regardless of the NaOH dosage; on the other hand, at the higher w/c ratio (0.5), the addition of NaOH in general increased the initial minislump area of slag paste (except the Na_2O 0.5%). However, the quick minislump loss of NaOH-activated slag was more obvious.

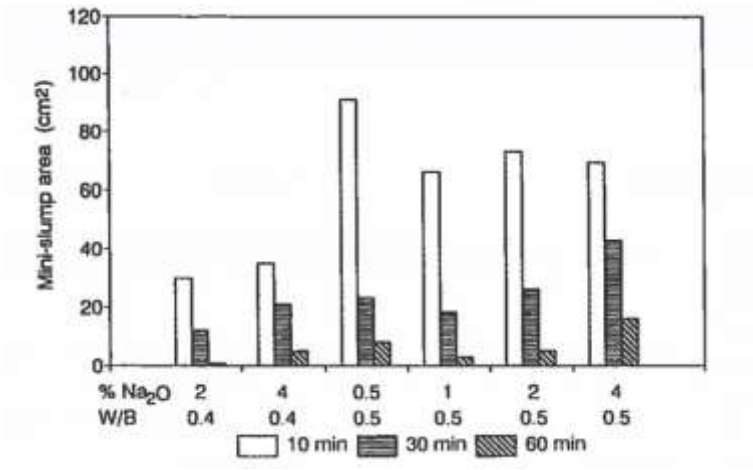

Note: the minislump area of the inactivated slag is 30 cm^2

Fig 3.11 Minislump area of NaOH activated slag at different Na_2O% (Jolicoeur et al., 1992)

3.4.1.1.2 Effect of superplasticiser

Previous results reported in the literature relevant to the superplasticiser in AAS are summarised in ***Table 3.7***. It can be seen that the effects of PC-based SP highly

depends on the nature of activators. In general, relatively better performance of PC-based SPs was identified in AAS formulated with NaOH and solid sodium silicate. However, in liquid sodium silicate solution, it was found that the SPs could not work properly.

It also can be noted from ***Table 3.7*** that compared with the relatively new generation of SPs, such as vinyl copolymer and polycarboxylate, it seems that the first and second generations of superplasticiser, such as lignosulfonate, naphthalene and melamine derivations, demonstrated some slight improvement on the workability of AAS. However, the workability retention of these SPs is considered to be insufficient (Palacios and Puertas, 2005). The reason was attributed to the change of the chemical structure of SP in highly alkaline media (Palacios and Puertas, 2004), which will be discussed in section 3.5.

Instead of adding one type of SP, it has been confirmed that the combined addition of two types of admixture can improve the workability of NaOH-activated slag, However, it was still not as good as in PC paste (Collins and Sanjayan, 2001).

In summary, the efficiency of the PC-based SPs in AAS system depends on the nature of the activator. However, even regardless of the activator nature, quick slump loss is a concern in most of the AAS systems. Although the addition of PC-based SPs can improve the workability of NaOH-activated slag, their performance in NaOH-activated slag is not as good as it is supposed to be. In addition to the reduced adsorption of PC-based SPs onto the surface of the slag due to the competitive adsorption mechanisms discussed in Section 3.3.4, the chemical instability of SPs in highly alkaline media could be another reason causing the dysfunction of the SPs in NaOH-activated slag.

Table 3.7 Summary of the effects of superplasticiser on the workability of alkali-activated slag

SP	Activator	Positive effect on workability	Negative effect on workability	Reference
LS	**NaOH**	**Improved**	**Quick slump loss**	Isozaki
	NaOH	**Slightly Improved**	**Quick slump loss**	Jolicoeur
	NaOH	**Improved**	**Medium slump loss**	Yang
	Waterglass (l)		No Effect	Douglas
	Waterglass (l)		No Effect	Gifford
	Waterglass (l)	Improved	Quick slump loss	Bakharev
	Waterglass (s)	Improved		Collins
	Na_2SO_4 & Na_2CO_3		No Effect	Gifford
	NaOH & Na_2CO_3	Improved	Quick slump loss	Bakharev
NF	**NaOH**		**No Effect**	Isozaki
	NaOH	**Improved**	**Quick slump loss**	Jolicoeur
	NaOH	**Improved**	**Medium slump loss**	Palacios
	Waterglass (l)		No Effect	Palacios
	Waterglass (s)	Improved		Collins
	NaOH+ Na_2CO_3	Improved	Quick slump loss	Bakharev
MS SP	**NaOH**	**Slightly improved**	**Quick slump loss**	Palacios
	Waterglass (l)		No Effect	Palacios
VS SP	**NaOH**		**Not obviously improved**	Puertas
	Waterglass (l)		No Effect	Puertas
	Waterglass (l)		No Effect	Palacios
AS SP	**NaOH**	**Slightly improved**	**Medium slump loss**	Pan
PCE	**NaOH**		**Not obviously improved**	Palacios
	Waterglass (l)		No effect	Puertas
	Waterglass (l)		No effect	Palacios
MS & Chromate	Waterglass (l)	Improved		Zhu
LS & NF	Waterglass (s)	Improved	Not good as in PC paste	Collins
LS & YP-3	**NaOH**	**Improved with less slump loss**		Yang
AS & YP-3	**NaOH**	**Slightly Improved with less slump loss**		Pan

Note: "*l"* means in liquid form; "*s"* means in solid form; "*&"* means combined addition with two and more types

Summarised from the following literature: (Gifford and Gillott, 1997, Isozaki, 1986, Palacios and Puertas, 2005, Puertas et al., 2003, Zhu et al., 2001, Pan et al., 2014, Yang et al., 2013, Douglas and Brandstetr, 1990, Shi et al., 2006, Bakharev et al., 2000, Palacios et al., 2009a, Jolicoeur et al., 1992)

3.4.1.2 Rheological properties

3.4.1.2.1 Rheological properties of NaOH-activated slag

Although various studies have been carried out on the rheological properties of PC-based system, as highlighted before, only a few studies have been reported on the rheology of AAS. It can be found from these studies that the rheology of AAS also depends on the nature of the activator. As shown in ***Fig 3.12***, NaOH-activated slag paste, which is similar to PC paste, behaves as Bingham fluids; while waterglass-activated slag pastes shows shear thickening behaviour with large hysteresis area. Similar rheological behaviours were observed in AAS mortar (The rheological behaviour of which is discussed in chapter 2). Compared to the cement paste, lower initial yield stress was observed in AAS, with NaOH-activated slag lower than waterglass-activated slag (Palacios et al., 2008). According to the study carried out by Kashani et al. (2014), waterglass activated slag showed lower plastic viscosity whilst higher plastic viscosity was identified in NaOH-activated slag. However, the increment of Na_2O% concentration of activator leads to a slight increase in both the plastic viscosity and the yield stress values (Puertas et al., 2014). This could be directly attributed to the increase of the concentration of OH^- ions, which favours the dissolution process of slag and consequently more reaction products are formed.

In addition to the effect of activators, w/s ratio is probably the most significant factor affecting the rheological properties of NaOH-activated slag. Compared with PC (w/c=0.50), only half value of the initial yield stress was observed in NaOH-activated slag (w/s=0.55) (Puertas et al., 2014). Similarly, the yield stress of PC with w/c=0.40, which reflected the normal water requirement of the materials, was double that of the corresponding NaOH-activated slag paste PC at 0.50 w/s (Palacios et al., 2008).

The addition of SPs also affects the rheological properties of NaOH-activated slag. However, the results reported by different researchers show some controversy, which will be discussed in next section.

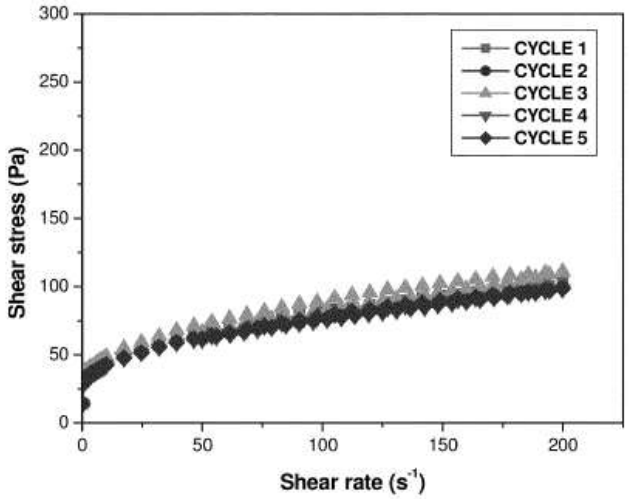

(a) PC paste

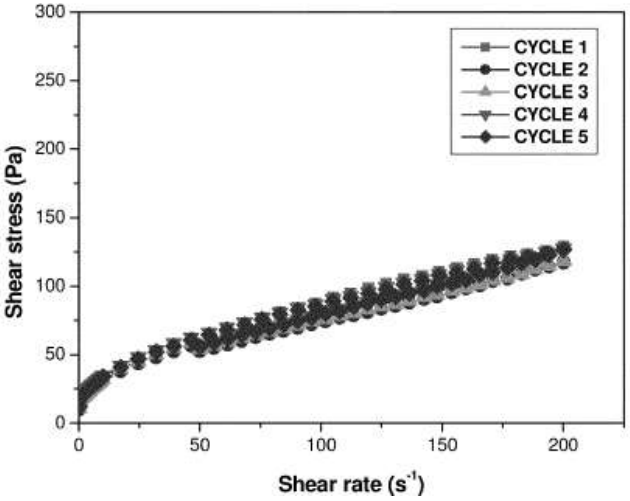

(b) NaOH-activated slag

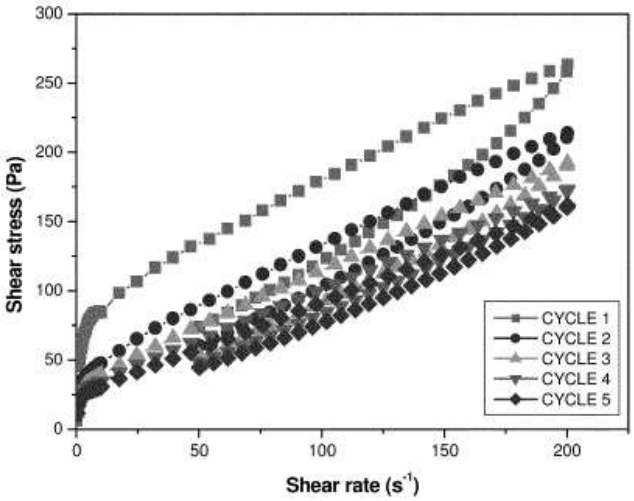

(c) Waterglass-activated slag

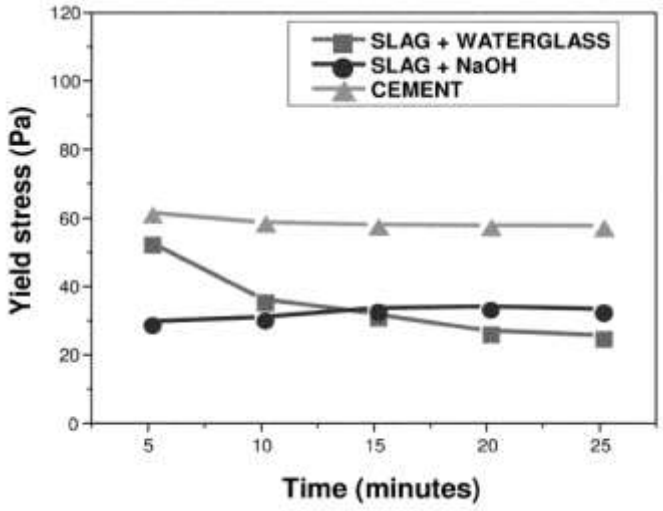

(d) Yield stress

Fig 3.12 Flow curve and yield stress of Portland cement, NaOH- and waterglass-activated slag pastes (Palacios et al., 2008)

3.4.1.2.2 Effect of superplasticiser

Among limited research, the effect of the addition of PC-based SPs on the rheological properties of NaOH-activated slag was observed by Palacios's group (Palacios et al., 2009a, Palacios et al., 2008). The effects of PC-based SPs on NaOH-activated slag paste and mortar are plotted in the rheographs (refer to section 2.3.1.1) in ***Fig 3.13 (a)*** and ***Fig 3.14 (a)*** respectively. They noticed that, regardless of the SP dosage, the addition of SPs highly reduced both yield stress (yield torque) and plastic viscosity of PC paste and mortar, which is in line with the discussion in Chapter 2. However, in NaOH-activated slag paste with SP, compared to reference sample (no SP), higher yield stress was observed at lower dosage of all SP excepting NF; while lower plastic viscosity was achieved in all mixes with SP. Additionally, the addition of SPs in NaOH reduced the initial yield torque with a slight change of the initial plastic viscosity. Among all the SPs studied, the NF enhanced the rheological properties of NaOH-activated slag pastes.

Palacios et al. (2009) also investigated the effects of pH on the performance of PC-based SPs on the rheological properties of NaOH-activated slag (summarised in ***Table 3.8***). In the paste with lower pH value, regardless of type of SP, the addition of SPs highly reduced both yield stress and plastic viscosity of NaOH-activated slag paste. However, with increased pH value of paste, the reduction ability of all SPs was

limited except NF, which might be due to the chemical instability of SPs in highly alkaline media. This will be discussed in detail in section 3.5.

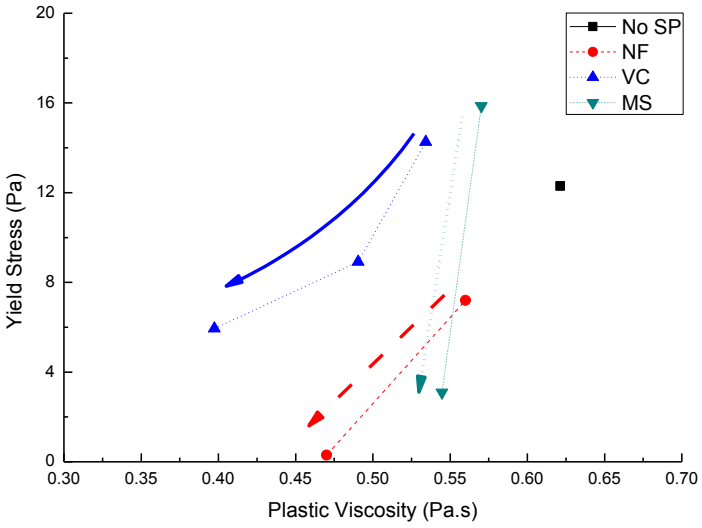

(a) NaOH-activated slag paste (w/s=0.50)

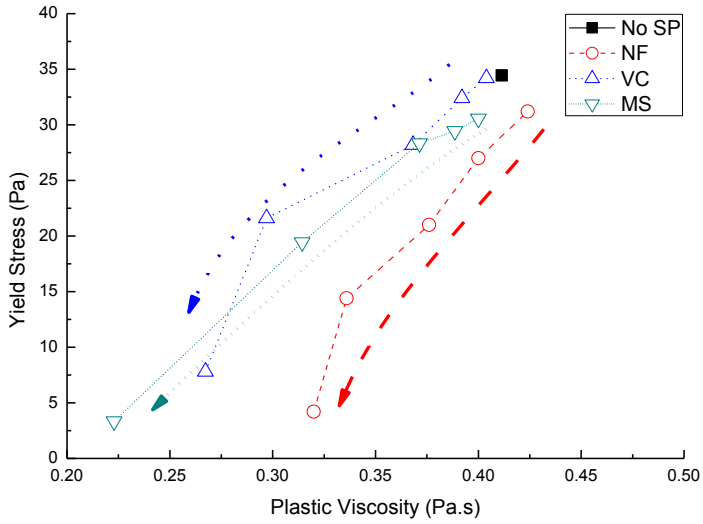

(b) PC paste (w/c=0.4)

Fig 3.13 Rheograph of NaOH-activated slag and PC paste with different type of superplasticisers measured at 5 minutes (The direction of arrow indicates the increment of SP dosage) (Adapted from Palacios et al., 2009)

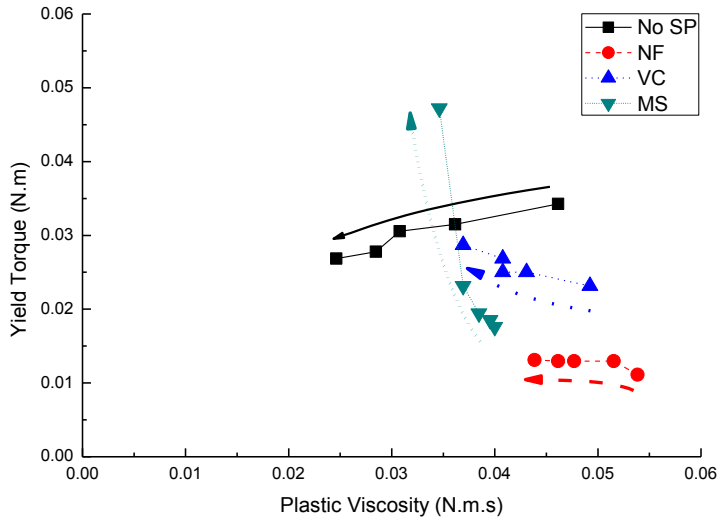

(a) NaOH-activated slag mortar (l/s=0.50)

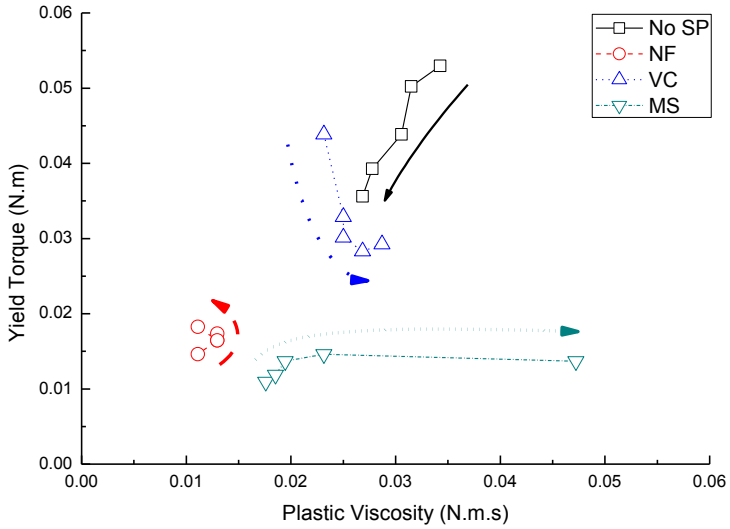

(b) PC mortar (l/s=0.42)

Fig 3.14 Rheograph of NaOH-activated slag and PC mortar with different type of superplasticisers at dosage of 1% with hydration time (The direction of arrow indicates the increment of hydration time from 5 minutes to 25 minutes with 5 minutes time intervals) (Adapted from Palacios et al., 2008)

Table 3.8 Effects of pH on the performance of SPs in NaOH-activated slag (NF=0.42 mg/g, VC SP=0.27 mg/g, and MS SP=0.38mg/g) (Palacios et al., 2009a)

pH	Reduction of yield stress (%)			Reduction of plastic viscosity (%)		
	NF	VC SP	MS SP	NF	VC SP	MS SP
11.7	96.07	91.17	93.13	22.85	31.43	21.42
13.6	41.44	-15.94	-28.99	9.86	14.01	8.22
Note: negative value means the yield stress is higher than reference.						

3.4.1.3 Setting

3.4.1.3.1 Setting of NaOH-activated slag

In general, compared with PC, both initial and final setting of NaOH-activated slag are much quicker, and the time interval between the initial setting and the final setting is shorter (Fernandez-Jimenez and Puertas, 2001, Duran Atiş et al., 2009, Palacios and Puertas, 2005, Bakharev et al., 1999). As shown in ***Table 3.9,*** compared to PC paste, the initial setting time less than 30 minutes and the final setting time less than 1 hour are reported for NaOH activated slag. Additionally, both initial setting time and final setting time are shortened by increasing the Na_2O% of NaOH (Duran Atiş et al., 2009). Similar results were reported by other authors (Palacios and Puertas, 2005, Bakharev et al., 1999, Zivica, 2007). The setting behaviour is linked to the rheological property during the hydration of NaOH-activated slag. Thus, the short setting time, which leads the paste to lose flowability in a short time and to set very fast, hinders the further industrialisation of NaOH-activated slag. Thus, the effect of superplasticiser on the setting is important, which will be discussed in next section.

Table 3.9 Setting time of PC and NaOH-activated slag mortar (Duran Atiş et al., 2009)

Type	w/c	Na_2O% (%)	Setting Time (min)		
			Initial Setting	Final Setting	Time Interval
Portland Cement	0.50	N/A	200	315	115
NaOH-activated slag	0.50	4	21	59	38
NaOH-activated slag	0.50	6	9	34	25
NaOH-activated slag	0.50	8	4	28	24

3.4.1.3.2 Effect of superplasticiser

As discussed in section 2.3.1.2, both initial and final setting time of PC are substantially retarded and become longer in the presence of superplasticiser. Similarly, it can be seen from ***Table 3.10*** that the addition of SPs also retards both initial and final setting times of NaOH-activated slag, with the best retardation effects being noticed from PCE. However, Puertas et al. (2003) reported that the superplasticiser shows no significant effect on the setting time of NaOH-activated slag paste except NF. In the case of NF, the addition of NF retarded the initial setting by 132 minutes and the final setting by 336 minutes. Although the effects of different SPs on the setting time of NaOH-activated slag have been investigated, the retardation mechanism of SPs in NaOH-activated slag is still not fully understood.

Table 3.10 Effect of superplasticisers on setting time of PC and NaOH-activated slag paste (w/s =0.50) (Puertas et al., 2003)

Type of SP	Binder	Setting Time (min)		
		Initial Setting	Final Setting	Time Interval
Ref	PC	211	336	125
	NaOH (4% Na_2O %)	60	84	24
	NaOH (5% Na_2O %)	51	85	34
MS SP	PC	393	441	48
	NaOH (4% Na_2O %)	62	95	33
	NaOH (5% Na_2O %)	49	75	26
NF	PC	606	741	135
	NaOH (4% Na_2O %)	192	320	128
	NaOH (5% Na_2O %)	109	145	36
VS SP	PC	733	763	30
	NaOH (4% Na_2O %)	74	128	54
	NaOH (5% Na_2O %)	57	80	23
PCE 1	PC	1062	1092	30
	NaOH (4% Na_2O %)	64	103	39
	NaOH (5% Na_2O %)	43	67	24
PCE 2	PC	733	763	30
	NaOH (4% Na_2O %)	63	111	48
	NaOH (5% Na_2O %)	51	81	30

3.4.1.4 Hydration and hydration product of NaOH-activated slag

3.4.1.4.1 Hydration and hydration product of NaOH-activated slag

As shown in ***Fig 3.15,*** it is seen clearly that, similar to PC, the hydration of NaOH-activated slag can be divided into five periods: initial period, induction period, acceleration period, deceleration period and diffusion period (Shi and Day, 1995, McCarter et al., 1999). From the typical heat evolution curve of NaOH-activated slag, two heat evolution peaks, initial and accelerated hydration peaks, are observed in the hydration of NaOH activated slag.

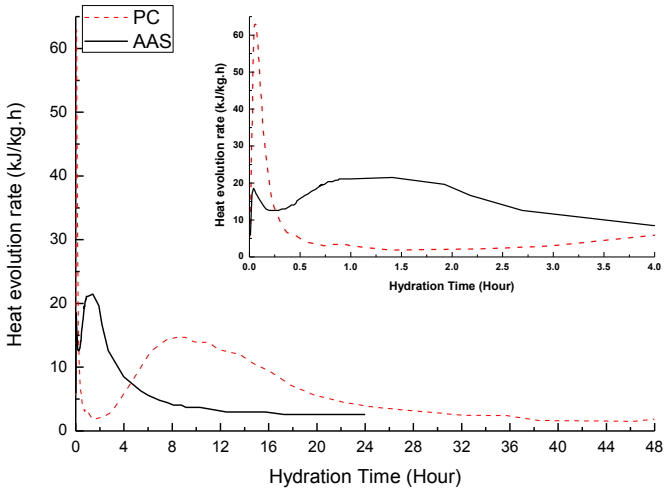

Fig 3.15 Heat evolution of early hydration of NaOH-activated slag (adapted from Shi and Day, 1995)

The activation process mentioned in section 3.3.1 occurs in the initial period (Shi and Day, 1995, Pu, 2010). During this period, the slag is firstly wetted and dissolved in the highly alkaline media with high concentration of OH^-. As demonstrated previously, the large amount of OH^- not only breaks the ionic bonds, i.e. Ca-O and Mg-O, but also cleaves covalent bonds, such as, Si-O and Al-O. Then, the early hydration products (for example, C-S-H gel) are formed and precipitated on to the surface of slag grain due to the different solubility of hydrates (shown in ***Table 3.11***). With the progress of precipitation, the hydration of slag comes into the induction period. Whereas obvious induction period is identified in PC, NaOH-activated slag does not show a noticeable induction period. This short induction period is attributed to the high initial rate of reaction which does not allow time for diffusion (Ben Haha et al., 2011, Kashani et al., 2014).

Along with the hydration process, when C-S-H concentration in the solution exceeds its saturation concentration, the secondary C-S-H gel is then formed due to the nucleation, growth and precipitation of C-S-H, leading to the acceleration period. Subsequently, a layer of hydration product is coated on the unhydrated slag grain, decreasing the reaction rate of NaOH-activated slag. Then the hydration process enters into the deceleration and diffusion period.

Table 3.11 Solubility of different hydrates (Shi and Day, 1996, Dean, 1999)

Hydrates	Solubility/K_{sp}
$Ca(OH)_2$	5.5×10^{-6}
C-S-H*	$1.0\times10^{-24\text{ to }-14}$
C_4AH_{13}	3.2×10^{-28}
C_2ASH_8	9.1×10^{-52}
$CaCO_3$	2.8×10^{-19}
$Ca_3(PO_4)_2$	$2.0\times10^{--29}$
CaF_2	2.7×10^{-11}
$CaHPO_4$	1.0×10^{-7}

*The solubility of C-S-H shows the negative relationship with the C/S ratio: the lower C/S, the higher solubility.

Generally, by increasing the activator concentration, the hydration of NaOH-activated slag is accelerated. The initial pH value is related to the NaOH concentration (Na_2O %). The activation of slag primarily depends on the initial pH value of activator solution. The degree of the hydration of slag is increased with the increment of pH in activator solution (Roy et al., 1992). Compared to other alkaline activators, NaOH shows the highest pH value at a given Na_2O %, which leads to the shortest induction period and fastest accelerated hydration (Song et al., 2000, Kashani et al., 2014). Song and Jennings (1999) suggested that the pH value higher than 11.5 can effectively accelerate the hydration of NaOH-activated slag. However, the research carried out by Shi and Day (1995) suggested that the hydration of AAS depends more upon the nature of the activator than the initial pH of the activator solution.

As discussed in the previous section, initial period of the hydration of NaOH activated slag is related to the destruction process of the slag grains. Thus, with the increase of Na_2O%, the alkalinity of the slag is increased, resulting in a stronger destruction of slag grains. The stronger destruction of the slag grains results in a

faster diffusion process. The higher pH value by large amount of OH^- in NaOH activator solution leads to serious destruction of slag grains. Therefore, it is difficult to find a noticeable induction period in NaOH-activated slag.

The acceleration period is attributed to the secondary formation of C-S-H gel, which is linked to the destroyed slag grain (Shi and Day, 1996). Therefore, the fact that heat evolution of the acceleration hydration peak increased with the increase of Na_2O% and pH could be due to the stronger destruction of the slag. Consequently, the cumulative heat of hydration of NaOH-activated slag increased with increasing Na_2O%.

The hydration products of NaOH-activated slag and PC are summarised and compared in ***Table 3.12***. In NaOH-activated slag, C-S-H (I) and hydrotalcite ($Mg_6Al_2CO_3(OH)_{16}\cdot 4H_2O$) are confirmed as the main hydration products of NaOH-activated slag. Moreover, C_4AH_{13}, C_2ASH_8 and AFm are also observed in the paste of NaOH-activated slag (Wang and Scrivener, 1995, Wang and Scrivener, 2003, Mozgawa and Deja, 2009, Puertas et al., 2004, Schilling et al., 1994, Hong et al., 1993, Escalante-Garcá et al., 2003).

Table 3.12 Hydration product of PC and NaOH-activated slag

	Portland cement	**NaOH-activated slag**
Hydration product	C-S-H (II) $Ca(OH)_2$ AFt/AFm	C-S-H (I) Hydrotalcite ($Mg_6Al_2CO_3(OH)_{16}\cdot 4(H_2O)$) C_4AH_{13} C_2ASH_8 AFm
Crystallinity of C-S-H	Low	High
Ca/Si ratio of C-S-H	High	Low
Morphology of C-S-H	Needle	Foil-like

3.4.1.4.2 Effect of superplasticiser

Lots of researches have been conducted on the effects of SPs in PC system. However, although few researches have been carried out to investigate the effects of PC-based SPs in NaOH-activated slag, they are mainly focused on the interactions between SPs and slag as well as the effects of SPs on workability and rheological properties. No

study has been reported on the effects of SPs on the early hydration of NaOH-activated slag.

3.4.2 Effects of PC-based SPs on hardened properties of NaOH-activated slag

3.4.2.1 Compressive strength

3.4.2.1.1 Compressive strength of NaOH-activated slag

Apart from water to slag ratio, for alkali-activated slag system, many other factors affect the strength, such as the composition of slag, the nature of activator(s), curing regime and the addition of both chemical and mineral additives.

Table 3.13 illustrates clearly that compared with the slag activated with other activators (Wang et al., 1994), NaOH-activated slag showed lowest compressive strength at a given equivalent Na_2O%. Similar results were also reported by other researchers (Krivenko, 1994, Fernandez-Jimenez and Puertas, 2003, Aydın and Baradan, 2012).

From ***Table 3.13***, higher compressive strength can be obviously identified from the pastes manufactured from basic slag, except in the presence of NaOH, which could be attributed to the higher reactivity of the basic slag as compared to the other slags stated in section 3.2.3.

The increase of the curing temperature could also increase the compressive strength regardless of the type of activator. And the effectiveness of increment curing temperature is more pronounced in less reactive conditions, such as in the acid and neutral slags or with weaker alkaline activator, such as Na_2CO_3, Na_2SO_3.

Overall, the compressive strength of NaOH-activated slag is lower than that of PC (Duran Atiş et al., 2009, Krivenko, 1994, Fernandez-Jimenez and Puertas, 2003, Aydın and Baradan, 2012, Aydın and Baradan, 2014). As shown in ***Fig 3.16***, the compressive strength of NaOH-activated slag increased with the increase of Na_2O% along with curing time. It should be noted that the advantage of higher Na_2O% on the compressive strength is not obvious at 7 days when Na_2O% is over 6%.

Table 3.13 Effects of activators and the type of slag on 28-days compressive strength of alkali-activated slag mortar (Wang et al., 1994)

Slag	Compressive strength/MPa				Compressive strength after curing at 80 ℃ for 16 hours/MPa			
	4M NaOH	2M Na_2SO_4	2M Na_2CO_3	2M Na_2SiO_3	4M NaOH	2M Na_2SO_4	2M Na_2CO_3	2M Na_2SiO_3
Acid slag	22	3	7	72	33	25	55	105
Neutral slag	23	20	41	98	34	34	64	117
Basic slag	20	30	53	110	31	47	70	113
Note: the dosage of activator is selected based on the same equivalent Na_2O%								

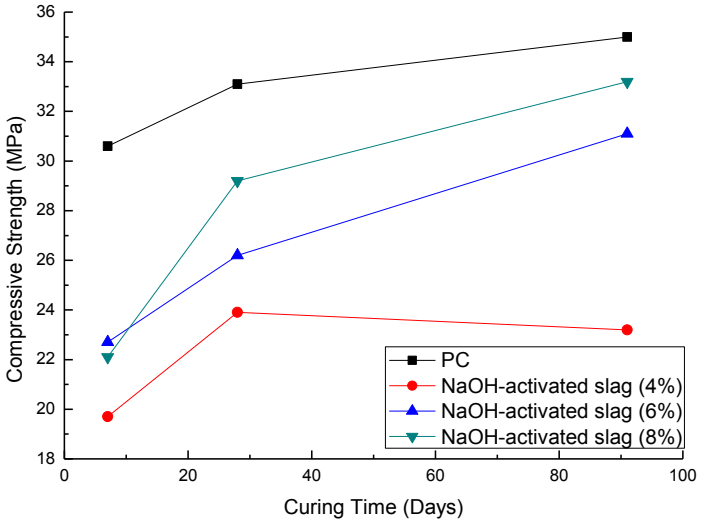

Fig 3.16 Effect of Na_2O% on compressive strength development of NaOH-activated slag and PC paste (adapted from Duran Atiş et al, 2009)

3.4.2.1.2 Effect of superplasticiser

The effects of superplasticiser on the compressive strength of NaOH-activated slag paste are illustrated in ***Table 3.14***. It can be seen that the addition of superplasticisers improved the compressive strength of NaOH-activated slag at 2 days, 7 days and 28 days. The increment of Na_2O% reduced the efficiency of the improvement that the SPs have on the compressive strength of NaOH-activated slag. NF and MS SPs showed significant improvement on the compressive strength, while PCE showed

less effect. These results are closely linked to its effects on minislump results as discussed in section 3.5.2. Higher strength could be attributed to improved dispersion of slag in the presence of SP.

Table 3.14 Effect of different type of superplasticiser on relative compressive strength of NaOH-activated slag (determined by water-reducing effect)(Palacios and Puertas, 2005)

SP	Relative compressive strength at 4% Na_2O% (%)			Relative compressive strength at 5% Na_2O% (%)			Relative compressive strength PC (%)		
	2 Days	7 Days	28 Days	2 Days	7 Days	28 Days	2 Days	7 Days	28 Days
NF	241	217	190	193	187	159	106	109	103
VC	150	151	126	150	157	137	124	128	104
MS	225	196	161	193	183	124	103	101	94
PCE 1	157	150	108	121	109	102	105	96	94
PCE 2	148	124	108	129	126	110	86	84	70

Note: the relative compressive is calculated based on the paste without SP at the same curing age.

3.4.2.2 Drying shrinkage

3.4.2.2.1 Drying shrinkage of NaOH-activated slag

Compared with PC, as shown in ***Fig 3.17***, NaOH-activated slag demonstrated higher drying shrinkage, the reason of which could probably be due to the lower porosity and higher portion of pores with r < 100 nm of NaOH-activated slag (as will be discussed in next section) (Shi et al., 2006). Severe drying shrinkage was observed in the paste formulated with higher Na_2O%. The reason could probably be due to the fact that higher Na_2O% promoted the hydration of NaOH-activated slag, increasing the surface area and the capillary tension by forming more hydration products , which is discussed in section 3.3.2 (Duran Atiş et al., 2009, Aydın and Baradan, 2014).

However, based on limited research, there is no evidence showing that the addition of superplasticiser affects the drying shrinkage of NaOH-activated slag. However, as discussed in chapter 2, the addition of SPs could increase the drying shrinkage.

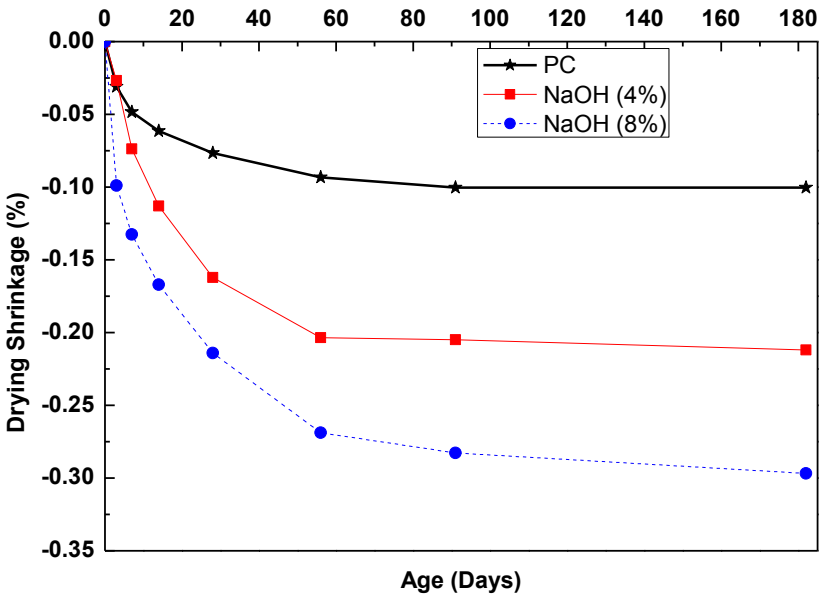

Fig 3.17 Drying shrinkage of NaOH-activated slag and PC paste (adapted from Duran Atiş et al, 2009)

3.4.2.2.2 Effect of superplasticiser

From the discussion in Section 2.3.2.2, the effects of SPs in Portland cement system have been widely investigated and it is accepted that the addition of SPs could increase the drying shrinkage of hardened cement paste. However, there is no research reported about the effects of PC-based SPs on drying shrinkage of NaOH-activated slag. The only study conducted by Bakharev reported that the addition of LS reduced the drying shrinkage of waterglass activated slag, whilst NF increased the drying shrinkage of waterglass activated slag (Bakharev et al., 2000).

3.4.2.3 Porosity

The cumulative pore volume of NaOH-activated slag and PC mortars is shown in ***Fig 3.18***. It can be seen that, compared with PC, the NaOH-activated slag showed higher porosity, which could be attributed to its lower compressive strength (refer to ***Fig 3.18(c)***). The uniformly distributed pores in NaOH-activated paste in the range of measured pore-size can also be observed. Additionally, Song *et al.* (2000) also found

that NaOH-activated slag paste exhibited a higher porosity with larger portion of capillary pores than PC paste.

Unfortunately, no evidence, among the limited literature, could be used to illustrate the effects of SP on the change in porosity of NaOH-activated slag.

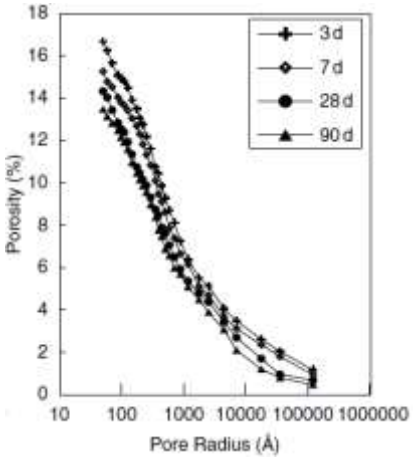

(a) Cumulative pore volume NaOH-activated slag mortar

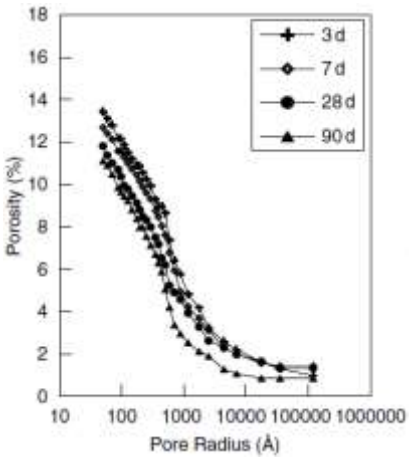

(b) Cumulative pore volume PC mortar

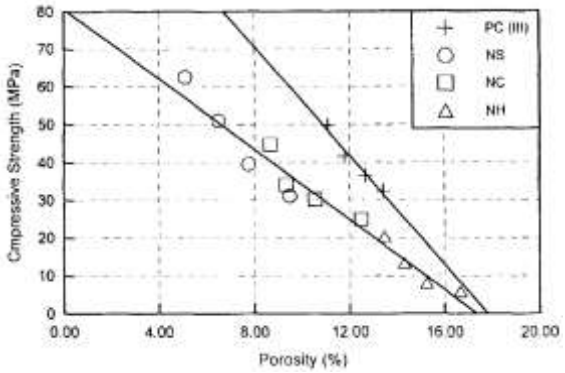

(c) Relationship between porosity and strength Note: PC stands for Portland cement, NS for NaSiO,-activated slag

Fig 3.18 Pore structure of alkali activated slag and PC mortars (Shi, 1996)

3.4.3 Summary

The current studies on the effects of PC-based SPs in NaOH-activated slag are reviewed in this section. Based on the information presented, the following could be summarised.

- Although the performance of PC-based superplasticisers varies in AAS, its improvement on workability of NaOH-activated slag is obvious. However,

the performance of the PC-based SPs in NaOH-activated slag is not as good as it is supposed to be. Regarding the type of SP, NF exhibits better performance than other types of SP. However, the loss of workability is unacceptable regardless of the types of SP used.

- The addition of SPs highly reduces both yield stress and plastic viscosity in NaOH-activated slag paste. The increment of Na_2O% shows strong effect on the performance of SPs. The higher Na_2O concentration, the less improvement on rheological properties. NF exhibits best performance on the improvement of rheological properties of NaOH-activated slag.
- Compared with its influence on the setting time of PC, the addition of superplasticisers could not retard both the initial and final setting of NaOH-activated slag. Its ability depends on the type of superplasticiser. NF highly retards the setting time of NaOH-activated slag, while other SPs do not show obvious retardation effect. The increment of Na_2O% reduces its ability to retard the setting of NaOH-activated slag.
- The compressive strength of NaOH-activated slag is improved by adding all types of superplasticisers. And higher improvement is found in the mix with NF. The increment of Na_2O% reduced the efficiency of SPs.
- The effects of superplasticiser on the other properties of NaOH-activated slag, such as drying shrinkage and porosity are not clear due to the shortage of relevant researches.

3.5 Chemical stability of current superplasticiser in highly alkaline environment

As mentioned in section 3.3, the initial pH value of NaOH-activated slag is much higher than that of PC. As a result, the stability of SPs in such a strong alkaline environment is a concern. From the view of chemistry, the stability of organic functional groups of SPs in alkaline media varies. For example, esters and amides tend to hydrolyse in highly alkaline solution while ethers and aromatic series are stable in high basic solution (Streitwieser et al., 1992).

The stabilities of four different types of superplasticiser in different alkaline media (which were used to simulate the liquid environment of the fresh AAS) are summarised in ***Table 3.15*** (Palacios et al., 2009a, Palacios and Puertas, 2005, Palacios and Puertas, 2004). It can be seen clearly that most of the SPs are stable in alkaline media with pH values up to 13. The chemical structural changes occur as the pH value increased above 13. Compared with different types of SPs, NF exhibits the best alkaline stability while melamine (MF), vinyl copolymer (VC) and polycarboxylate suffered more serious alkaline hydrolysis, which is also confirmed by other work (Ran et al., 2012, Yilmaz et al., 1993). The potential mechanisms of alkaline hydrolysis are illustrated in ***Fig 3.19.*** It can be clearly seen from the figure that the ester groups of PCE were hydrolysed to respective alcohol and carboxylate salts. Similarly, the amide groups of VC polymer were also hydrolysed to the chemical contains amine groups and corresponding carboxylate salts.

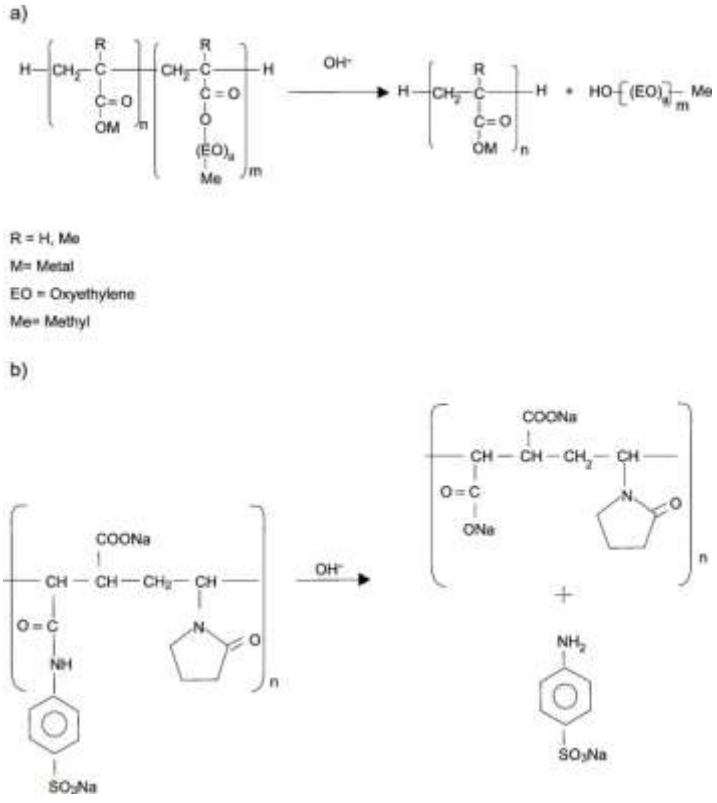

Fig 3.19 Degradation process of superplasticisers in highly alkaline media (Palacios and Puertas, 2005)

Table 3.15 Stability of superplasticiser in different alkaline solution (Palacios et al., 2009a, Palacios and Puertas, 2005, Palacios and Puertas, 2004)

	LS	MF SP	NF	VC	PCE
NaOH (pH=11.70)	N/A	Unstable	Stable	Stable	Not obvious
Ca $(OH)_2$ (pH=12.40)	N/A	Stable	Stable	Stable	Not obvious
Water Glass (pH=13.00)	N/A	Unstable	Unstable	Unstable	Unstable
NaOH (pH=13.60)	N/A	Unstable	Stable	Unstable	Unstable
decomposed products in NaOH	N/A	Amine	None	Amine, sulfonate carboxylate	Alcohol carboxylate
Groups detected in water glass solution	N/A	Sulfonate	Sulfonate	Sulfonate	Alcohol carboxylate

3.6 Discussion

The adsorption of SPs on the surface of cement particles is the most important stage for the dispersion of cement particles. It happens through the electrostatic attractive force between the negatively charged anchor groups of SPs and the positively charged sites on the particles surface, which is considerably sensitive to the environment of the solution. Unlike the PC system, in addition to water, NaOH activator is also involved in the hydration of NaOH-activated slag. The NaOH activator induces large amounts of negatively charged OH^- groups into the system, which is of the same charge as the SPs and, thus, changes the environment of the solution.

It has been demonstrated that, in the PC system, the addition of anionic chemicals, such as SO_4^{2-} and OH^- , highly reduces the adsorption of SP onto the surface of cement particles due to the competition between these ions and the negatively charged groups on SPs (Yamada et al., 2001). In a similar way, the addition of alkaline activator can reduce the adsorption of SPs due to the possible competitive adsorption between the negatively charged activator and the negatively charged SPs

(Yang et al., 2009). This reduced adsorption is one of the main reasons causing the poor performance of PC-based SPs in NaOH-activated slag.

In PC system, delayed addition of SP has been widely used to improve the performance of SPs. This can avoid the excessive consumption of the SP by early hydration products. Previous research reported in the literature has clearly demonstrated that the delayed addition can effectively improve the performance of SPs in PC system (Aiad et al., 2013). Based on a similar principle, it is anticipated that adding SPs and NaOH activator at different stages separately could possibly reduce the competitive adsorption between the activators and the SPs in NaOH-activated slag.

Three possible addition methods can, therefore, be potentially explored in this thesis, which include: 1) ***simultaneous addition (SA)****:* mixing slag with both SP and activator together – this method has been widely studied in the literature and will be used as a control; 2) ***delayed addition (DA)****:* mixing slag with activator first, then adding SP at certain time interval; and 3) ***prior addition (PA)****:* mixing slag with SP first, then adding activator at certain time interval.

In addition to the competitive adsorption, the change of the chemical structure of PC-based SPs in highly alkaline environment is considered as another reason that conventional PC-based SP demonstrated poor performance in AAS. From the Section 3.5, it can be seen that most of the SPs are hydrolysed in highly alkaline media, leading to the cleavage of the side chain. The amide and ester groups, which link the side chains to the backbone of SPs, are prone to be hydrolysed in a high pH media (Palacios and Puertas, 2005). In addition, in highly alkaline media, the anchor groups, for example, sulfonic groups, can de-graft from the backbone. Consequently, the overall efficiency of the SPs is reduced due to the change of chemical structure of SPs. Therefore, another approach to improve the performance of SPs is to remove the weak bonds by synthesizing novel alkali-compatible polymers.

In summary, based on the literature review, the **separate addition of SP and activator** and the **synthesis of alkali-compatible polymers** have been identified as two most possible approaches to address the SP issues in NaOH-activated slag

system. In this thesis, both approaches have been attempted and reported in the following chapters.

3.7 Concluding Remarks

In this chapter, the effect of current commercially available superplasticisers in the NaOH-activated slag has been reviewed and the following conclusion could be drawn:

- Alkali-activated slag has been identified as a low carbon cementitious material which is a potential replacement for Portland cement. It consists of alkaline activator and cementing component. Commonly, all the caustic alkalis or alkaline salts can be used as alkaline activator of AAS. In general, basic slag exhibits better reactivity than acid and neutral slags.
- In the presence of alkaline activator, not only the Ca-O and Mg-O bonds are cleaved, but also the Si-O and Al-O bonds are broken down.
- The adsorption of SPs on slag particles follows the Langmuir adsorption behaviour. However, since the surface condition of slag is changed by adding alkali activators, the adsorption behaviour of SPs is also changed accordingly. The addition of NaOH activators reduces the amount of PC-based SPs which can be adsorbed on the surface of the slag, leading to a reduction of the effectiveness of PC-based SPs in NaOH-activated slag.
- Although the performance of PC-based superplasticisers varies in AAS, its improvement on workability of NaOH-activated slag is obvious. However, the performance of the PC-based SPs in NaOH-activated slag is not as good as it is supposed to be. Regarding the type of SP, NF exhibits better performance than any other types of SP. However, the loss of workability is unacceptable regardless of the types of SP used.
- The addition of SPs highly reduces both yield stress and plastic viscosity in NaOH-activated slag paste. The concentration of Na_2O% shows a strong effect on the performance of SPs. The higher Na_2O concentration, the less improvement on rheological properties.

- NF highly retards the setting time of NaOH-activated slag, while other SPs do not show obvious retardation effect. The increase of Na_2O% reduces its ability to retard the setting of NaOH-activated slag.
- The compressive strength of NaOH-activated slag is improved by adding all types of superplasticisers. And higher improvement is found in the mix with NF. The increase of Na_2O% reduced the efficiency of SPs.
- The effects of superplasticiser on the other properties of NaOH-activated slag, such as drying shrinkage and porosity are not clear due to the shortage of relevant researches.
- The improper performance of PC-based superplasticisers in AAS could be attributed to the following reasons:1) the competitive adsorption between alkaline activator and the SPs and 2) the change of the chemical structure of the SPs in highly alkaline environment
- Two approaches can potentially resolve the reduced efficiency of PC-based SPs in NaOH-activated slag: 1) separate addition of SP and activator; and 2) synthesis of alkali-compatible polymers.

Chapter 4

Experimental Programme

4.1 Introduction

This chapter describes details of the experimental programme including the experimental methods and the analytical techniques employed. The overall experimental programme is described in Section 4.2, the materials are presented in Section 4.3, the mixing procedure and sample preparation of NaOH-activated slag are reported in Section 4.4, and the analysis and test methods are listed in Section 4.5.

4.2 Overall Experimental Programme

In this project, the effects of three generations of superplasticiser, i.e. lignosulfonate (LS), naphthalene (MF), and modified polycarboxylate (MP) derivation SP, on NaOH-activated slag have been investigated, respectively. The overall programme is shown in ***Fig 4.1***. Based on the literature review in Chapter 2 and Chapter 3, two reasons may potentially cause PC-based SP to malfunction in NaOH-activated slag. They are: a) the competitive adsorption between SP and activator, and b) the poor stability of superplasticiser in highly alkaline media.

In order to improve the performance of superplasticiser in NaOH-activated slag, two approaches have been carried out to tackle the issues highlighted above.

- **Separate addition methods:** Reducing competition between the SP and the activator by adding them at different mixing stages. The effects of these separate addition methods on the properties of NaOH-activated slag have been investigated.
- **Synthesis of alkali-compatible polymer:** To improve the alkali-stability of superplasticiser in highly alkaline media, PCE SP in particular, modified polycarboxylate (MP) polymer was synthesized. The optimal synthesis conditions were identified through an Experimental Design programme. The effects of optimised polymer in NaOH-activated slag were investigated.

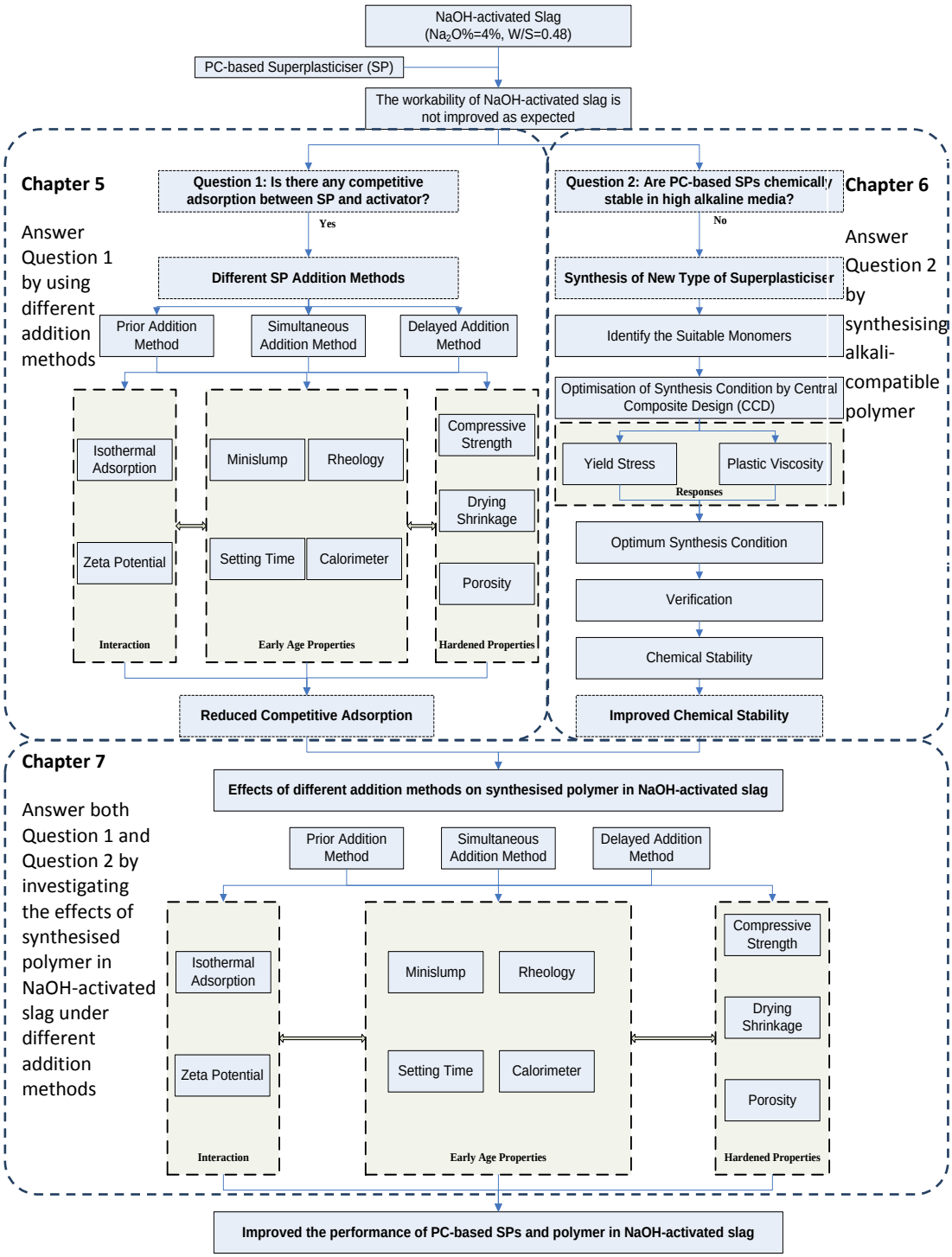

Fig 4.1 Diagrammatic experimental programme

The work in this thesis has been conducted in three stages:

1) Investigating different addition methods of applying PC-based SPs in NaOH-activated slag system. This offers a potential reduction of the competitive adsorption between the superplasticiser and the NaOH activator;

2) Synthesising the novel alkali-compatible polymer and optimising synthesis conditions. This offers a possibility to solve the chemical instability issue of PC-based SPs in highly alkaline media;
3) Examining the effects of different addition methods of synthesised polymer in NaOH-activated slag. This combines two proposed approaches to explore a new route of developing SPs for NaOH-activated slag system.

The tests conducted in this thesis can be summarised below, and a more detailed description can be found in Section 4.5:

- **Interactions among SP, activator and slag**

  When SP is added to the activated slag, it is firstly adsorbed on the surface of slag though electrostatic and/or chemical attraction. Therefore, the interaction between the SP and the slag is important. In addition, for NaOH-activated slag, the induced NaOH activator also affects the interaction. Therefore, it is important to examine the interaction among SP, activator and slag.

  Isothermal adsorption: This test is employed to reflect the amount of SP adsorbed on the surface of slag.

  Zeta potential: This test is used to detect the surface charge of slag particles, therefore, the interaction of SPs could be determined.

- **Effects on early age properties**

  The purpose of adding superplasticiser is mainly to improve the fresh properties of NaOH-activated slag, including workability and rheology. Moreover, the other properties in fresh state, such as the setting time and early hydration, are also affected by SPs. Therefore, the determination of early age properties is important.

  ***Minislump*:** This test is conducted to evaluate the dispersion of SP and change of workability.

  Rheological properties: The test is carried out by a rheometer to measure yield stress and plastic viscosity, thereby providing quantitative information of the workability.

  Setting time: The setting time is measured in correlation with workability performance to reflect the effects on setting.

***Isothermal Conduction Calorimetry (ICC)*:** The heat evolution of NaOH-activated slag is monitored by ICC to observe the effects on early hydration.

- **Effects on hardened properties of NaOH-activated slag**

  The addition of SPs not only changes the fresh properties of NaOH-activated slag, but also affects the hardened properties. Thus, its performance on hardened NaOH-activated slag is investigated.

  Compressive strength: The 1, 7, 28 and 56 day(s) compressive strength is determined.

  Drying shrinkage: Up to 180 days drying shrinkage of hardened paste is monitored.

  Porosity: The porosity of hardened paste is determined to understand the effect of SPs on porosity and pore structure of NaOH-activated slag.

- **Chemical stability of both PC-based SPs and synthesised polymers in alkaline media**

  As demonstrated previously, the SPs and polymers are not stable in highly alkaline media. Therefore, the chemical degradation of them has to be monitored.

  ***Fourier transform infrared spectroscopy (FTIR)**:* The FTIR is conducted to characterise the functional groups of the SPs and the polymers. The spectrum changes and/or peak shifts indicate possible change of chemical bonds.

  High Performance Size Exclusion Chromatography (HPSEC): The HPSEC is used to determine the molecular weight and weight distribution of the SPs and polymers. The results provide information on the length of chemical bond chain.

4.3 Materials

4.3.1 Ground Granulated Blast Furnace Slag (GGBS)

GGBS (short for slag hereafter), supplied by Hanson Heidelberg Cement Group; U.K. (Scunthorpe plant), has been used throughout the experiment programme. The

degree of the basicity (calculated from ***Equation 3.1***) of slag is 0.96. The details of the chemical composition and physical properties of slag are reported in ***Table 4.1*** and ***Table 4.2***.

Table 4.1 Chemical composition of slag

CaO	SiO_2	Al_2O_3	MgO	Sulfide	TiO_2
39.4%	34.30%	15%	8%	0.80%	0.70%
Mn_2O_3	Na_2O	Fe_2O_3	K_2O	LOI	
0.50%	0.45%	0.40%	0.38%	0.70%	

Table 4.2 Physical properties of slag

Fineness	450-550 m^2/kg （527 m^2/kg）
Bulk Density	1000-1100 kg/m^3 (Loose) 1200-1300 kg/m^3 (Vibrated)
Relative Density (Specific Gravity)	2.9
Color	Off White

4.3.2 Activator

Sodium hydroxide powder (industry grade) with a purity of 99% supplied by Tennants Distribution Ltd., U.K. was used as the activator of NaOH-activated slag paste.

4.3.3 Commercial Superplasticiser

Three types of superplasticisers, which represent the first, second and third generation of superplasticisers, were used in this project (Details are listed in ***Table 4.3***). Both lignosulfonate and naphthalene derivations of superplasticiser were dried powder and supplied by Tianjin Jiangong Special Material Co. Ltd, China. Sika ViscoCrete 10 was used as the polycarboxylate derivation superplasticiser, which represents the third generation of superplasticiser. Since the chemical structure is treated as confidential information by the manufacturer, the possible chemical structures of the commercial SPs can be referred to in Section 2.2.

Table 4.3 Details of commercial superplasticisers used in this project

Type	Origin	Physical appearance
Lignosulfonate derivation superplasticiser (LS)	Tianjin Jiangong Special Material Co. Ltd., China	Dark Brown Powder
Naphthalene derivation superplasticiser (NF)	Tianjin Jiangong Special Material Co. Ltd., China	Brown Powder
Polycarboxylate ester superplasticiser (PCE)	Sika ViscoCrete 10, U.K.	Straw Liquid (32-36% solid content)

4.3.4 Synthesis of polymer

4.3.4.1 Chemicals used in synthesis work

All the compounds used in the synthesis experiment are listed in ***Table 4.4***.

4.3.4.2 Synthesis equipment and procedure

The synthesis equipment includes 1 heater, 1 water bath, 1 flask with three necks (250 ml), 1 condenser, 1 separator and 1 thermometer. The schematic of the setup of synthesis equipment is shown in ***Fig 4.2***:

Table 4.4 Chemicals used in synthesis experiment

Name	Structure	Abbreviation	Purity/%	Manufacture
Acrylic Acid	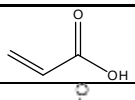	AA	99.0	Sigma-aldrich (UK)
Methacrylic acid	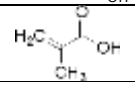	MAA	99.0	Sigma-aldrich (UK)
Acrylamide	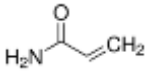	AM	99.0	Sigma-aldrich (UK)
Sodium 4-vinylbenzenesulfonate	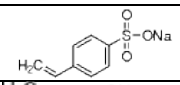	VBS	99.0	Sigma-aldrich (UK)
Diallyldimethylammonium chloride	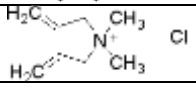	DMDAAC	99.0	Sigma-aldrich (UK)
2-Acrylamido-2-methyl-1-propanesulfonic acid	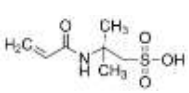	AMPS	99.0	Sigma-aldrich (UK)
Thioglycolic acid	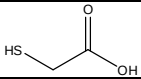	TA	≥98.0	Sigma-aldrich (UK)
Potassium persulfate	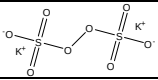	KPS	≥99.0	Sigma-aldrich (UK)
Maleic anhydride	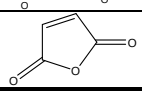	MA	95.0	Sigma-aldrich (UK)

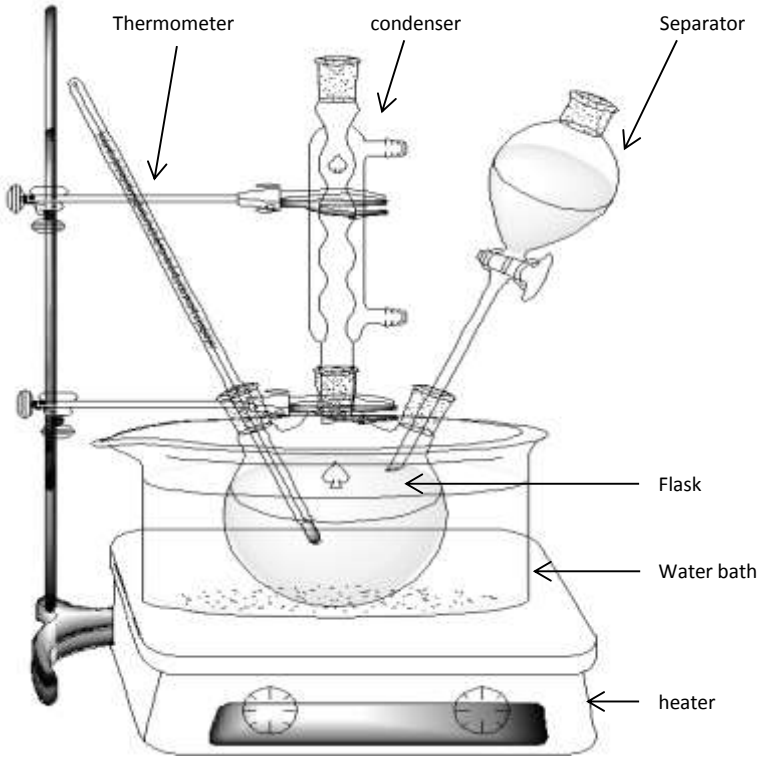

Fig 4.2 Schematic of synthesis experiment setup

Generally, the polymers were synthesised from selected monomers (detailed in Chapter 6) via free radical polymerisation in water media. The polymer was denoted as Poly-(A_x-B_y-C_z), where x is the degree of polymerisation of A unit, y is the degree of polymerisation of B unit (if applicable) and z is the degree of polymerisation of C unit (if applicable). In the synthesis work, potassium persulfate (KPS) was used as an initiator; thioglycolic acid (TA) was added as a chain transfer agent to control the molecular weight and weight distribution.

Before polymerisation, two solutions were prepared as follows:

i) The initiator solution was prepared by dissolving a calculated amount of KPS, in half of total ultrapure H_2O (electrical resistivity is 18 MΩ·cm);

ii) The monomer solution was prepared by mixing the correct amount of the monomers and a chain transfer agent in the remaining portion of ultrapure H_2O.

During the synthesis procedure, the initiator solution was firstly transferred into a 150ml three neck flask, connected by a thermometer and a condenser (***Fig 4.2***), and

was gradually heated under magnetic stirring to 80±5℃ through water bath. After reaching the designed temperature, the monomer solution was then added into the flask from the separator droplet by droplet in approximately 30 minutes. The reaction was let to proceed 3 hours under stirring. After polymerisation, the copolymer solution was immediately transferred into a glass bottle and stored in a fridge at 4 ℃ without any further purification.

4.4 Sample preparation and mixing procedure

4.4.1 Sample Preparation

In this project, twenty-eight slag pastes activated by NaOH, at a total alkali content of 4% Na_2O equivalent by mass of the slag, were investigated. Based on the results from some trial mixes, the water to slag ratio of all the mixes was fixed at 0.48, at which level the paste could offer sufficient fluidity to conduct the minislump test (80±5mm).

For each superplasticiser/polymer, three dosage levels were tested: the first level was selected in the range below the saturated point of SP; the second level was selected at the dosage around the saturated point; and the third level was selected at the range over the saturated point. Based on the preliminary trials (shown in ***Fig 4.3***), the dosages of lignosulfonate superplasticiser (LS) were selected at 0.500%, 0.750% and 1.000% (by mass of slag, hereafter); the dosages of naphthalene superplasticiser (NF) were controlled at 0.125%, 0.250% and 0.500%; and the dosages of modified polycarboxylate (MP) polymer were chosen at 0.125, 0.250 and 0.500%.

In order to obtain a full map of the effects of SP on NaOH-activated slag, for each mix, a total of five batches were conducted.

- Batch 1: NaOH-activated slag pastes for conducting minislump, zeta potential and rheology tests - the water to slag ratio was 0.48. The same pastes were also used to cast the cubes (25 × 25 × 25 mm) for compressive strength.

- Batch 2: NaOH-activated slag pastes for casting prisms (25 ×25 ×250 mm) for measuring the drying shrinkage - the water to slag ratio was 0.48.
- Batch 3: NaOH-activated slag pastes for determining setting time - the water to slag ratio was 0.48.
- Batch 4: NaOH-activated slag pastes for monitoring the heat of hydration - the water to slag ratio was 0.48.
- Batch 5: NaOH-activated slag suspensions for adsorption test - the water to slag ratio was 4.

In order to understand the effects of SP on hardened NaOH-activated slag, the porosity of hardened paste was measured. The samples for porosity test were prepared as follows: After the drying shrinkage reached to a constant, one of four prisms for drying shrinkage test (refer to section 4.5.3.2) was broken by a pincer into 1-2 cm^3 debris. The selected representative debris was soaked in acetone for three days in order to stop any further hydration. After three days, the debris was stored in a desiccator under vacuum for another three days. Before MIP test, the debris was thermal dried at 60 ℃ and then cooled to room temperature under vacuum.

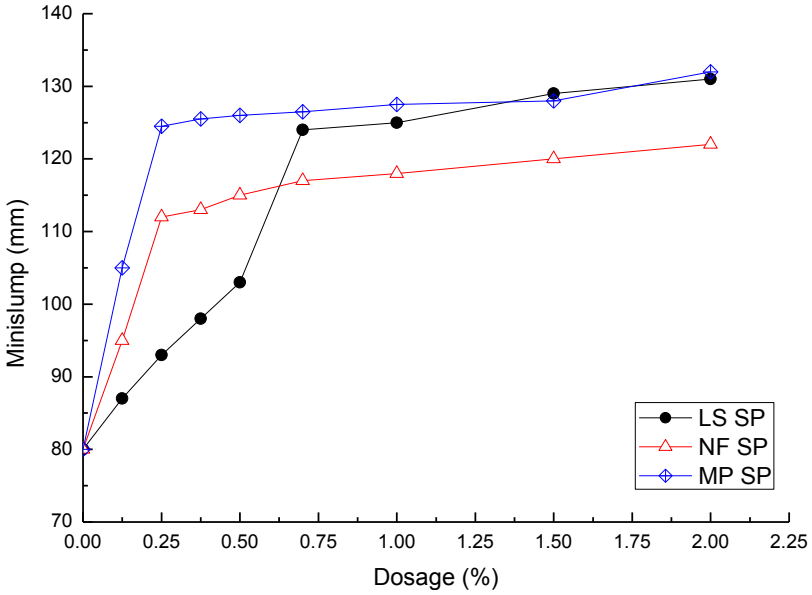

Fig 4.3 Effects of different dosage of three PC-based SPs on the initial (7 mins) minislump of NaOH-activated slag

4.4.2 Mixing procedure

In this project, in order to avoid the competitive adsorption and improve the performance of SP, three different addition methods, namely *simultaneous addition (SA), delayed addition (DA), and prior addition (PA),* were used. After a preliminary trial experiment, the time lag between the addition of SP and NaOH activator was set as 3 minutes. A total of 28 mixes were investigated in this project. The details are listed in ***Table 4.5***.

Addition Methods

- **Simultaneous addition**: Slag was mixed with both activator and SP solutions at the same time. (Only one component, including NaOH activator, SP and water, needed to be prepared during the mixing procedure.)
- **Delayed addition**: Slag was firstly mixed with activator solution (prepared by adding a certain amount of NaOH with 2/3 of the total mixing water), then mixed with SP solution (prepared by adding SP with the rest of the total mixing water) at 3 min intervals. (The first component was defined as activator solution and the second component was defined as SP solution.)
- **Prior addition**: Slag was firstly mixed with SP solution (prepared by adding a certain amount SP with 2/3 of the total mixing water), then mixed with activator solution (prepared by adding NaOH with the rest of the total mixing water) at 3 min intervals. (The first component was defined as SP solution and the second component was defined as activator solution.)

Mixing procedure

For producing NaOH activated slag paste, the activator solution was prepared by dissolving NaOH into mixing water one day before mixing, providing enough time to cool down to ambient temperature (20 ℃) . One hour before mixing, the required amount of SP was dissolved into the rest of the total mixing water. The materials were then mixed in a Hobart mixer (shown in ***Fig 4.4***).

The mixing procedure for the NaOH-activated slag is given as follows and the flow chart is shown in ***Fig 4.5***:

- The blade and bowl of the mixer were made slightly wet by using a damp tissue.
- For each addition method the first component was placed into the bowl before adding slag.
- In order to avoid loss of slag, the weighed slag was added into the bowl carefully. The addition time should be not more than 10 seconds.
- After adding slag, the mixer was immediately started at low mixing speed (140 ± 5 min^{-1}), whilst the time was started to be counted ("Zero" time).
- After mixing for a total of 90 seconds, the mixer was stopped for another 30 seconds. The materials adhering on the bottom and the wall of the bowls were removed by a scraper.
- The mixer was restarted for another 3 minutes.
- At 3 minutes (count from zero time), the second component was gently added into the bowl. The total addition time was no more than 10 seconds.
- At 4 minutes (count from zero time), the mixer was stopped for another 10 seconds to remove the adhered materials.
- The mixer was stopped at 5 minutes. All materials were transferred into the container for the tests of fresh properties.

Fig 4.4 Hobart mixer

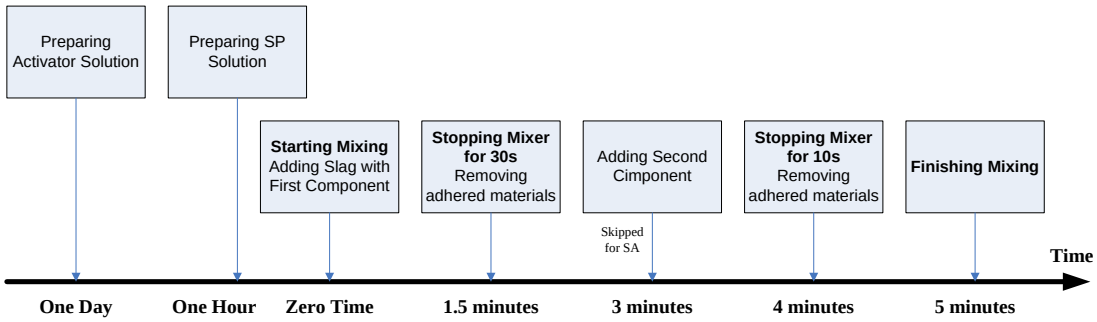

Fig 4.5 Flow chart of mixing procedure

Table 4.5 Details of mixing proportion

Sequence	Raw Materials	SP Type	SP Dosage (%)	Addition Method
1	Slag	None		N/A
2	Slag	LS	0.500	SA
3	Slag	LS	0.500	DA
4	Slag	LS	0.500	PA
5	Slag	LS	0.750	SA
6	Slag	LS	0.750	DA
7	Slag	LS	0.750	PA
8	Slag	LS	1.000	SA
9	Slag	LS	1.000	DA
10	Slag	LS	1.000	PA
11	Slag	NF	0.125	SA
12	Slag	NF	0.125	DA
13	Slag	NF	0.125	PA
14	Slag	NF	0.250	SA
15	Slag	NF	0.250	DA
16	Slag	NF	0.250	PA
17	Slag	NF	0.500	SA
18	Slag	NF	0.500	DA
19	Slag	NF	0.500	PA
20	Slag	MP	0.125	SA
21	Slag	MP	0.125	DA
22	Slag	MP	0.125	PA
23	Slag	MP	0.250	SA
24	Slag	MP	0.250	DA
25	Slag	MP	0.250	PA
26	Slag	MP	0.500	SA
27	Slag	MP	0.500	DA
28	Slag	MP	0.500	PA

4.5 Test Method

4.5.1 Test of interactions between SPs and particles

The SPs are added in cement to reduce water content or improve workability through the electrostatic (and steric) repulsion mechanisms. When dissolved in water, the negative charged superplasticisers are firstly adsorbed onto the surface of cement grains, which reduces the zeta potential value and results in the repulsion and dispersion of cement particles by 'like poles' action. Thus, the interactions between SPs and slag could be described by the adsorption amount of SPs and zeta potential of the slag particles.

4.5.1.1 Adsorption Test

Adsorption test was conducted to determine the interaction between the SP and the slag. The amount of SP in solution was determined by a UV-spectrophotometer (Camspec M550 Double Beam UV/Vis Spectrophotometer as shown in **Fig 4.6**) through Beer–Lambert law (***Equation 4.1***).

$$A = -\log T = -\log\left({}^{I}/_{I_0}\right) = \varepsilon \cdot b \cdot c \qquad \textbf{4.1}$$

Where A stands for measured absorbance, T for measured transmittance, I for intensity of the light passed through the sample, I_0 for initial intensity of the light, ε for wavelength-dependent absorptivity coefficient, b for path length, and c for analytic concentration.

Fig 4.6 Camspec M550 Double Beam UV/Vis Spectrophotometer

For each type of SP solution, the absorptivity coefficient and path length was fixed. As a result, the concentration was linear to the absorbance. The amount of SP was calculated from the concentration of the SP solution. Since ε was a wavelength-dependent coefficient, the best absorptivity wavelength for each superplasticiser was determined by a full wavelength scan. Based on the preliminary trial experiment (shown in ***Fig 4.7***), the wavelength used for adsorption test of LS, NF and MF polymer were set as 260 nm, 294 nm and 244 nm respectively.

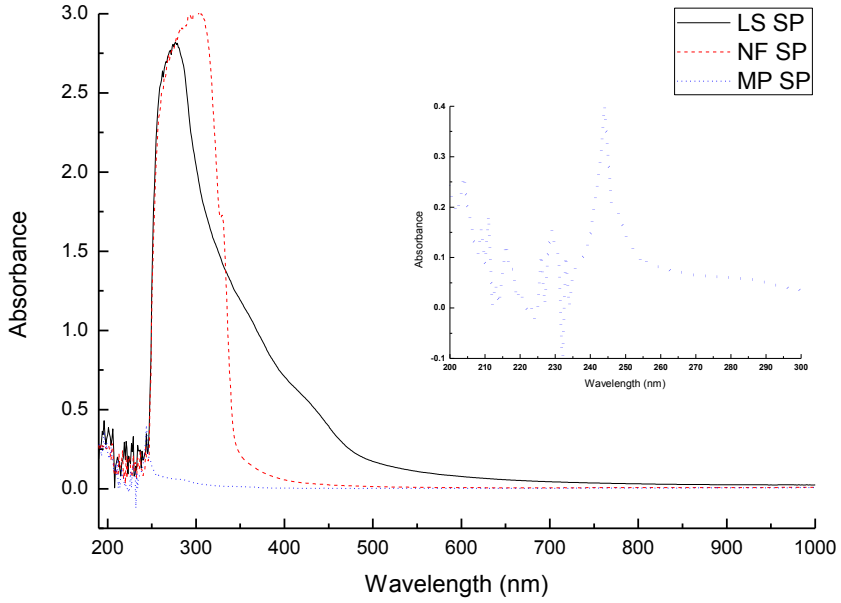

Fig 4.7 UV absorption of LS, NF SPs and MP polymer

The adsorption amount of superplasticiser was calculated from the difference of SP before and after it contacted with the slag. The calculation is expressed in ***Equation 4.2*** (Lou *et al*., 2012).

$$\Gamma(mg/g) = \frac{(C_0 - C_t) \times V}{m} \qquad \textbf{4.2}$$

Where Γ stands for adsorbed amount of SP per gram of slag, C_0 for initial concentration of SP solution (mg/ml), C_t for the concentration of SP solution after reaching adsorption equilibrium (mg/ml), V for total volume of solution (ml), and m for mass of slag (g).

Calibration procedure:

In the adsorption test, the NaOH solution amount was calculated as 4% Na_2O equivalent by the mass of slag, and water slag ratio was 4:1 (Yang *et al.*, 2013). The calibration procedures are illustrated as follows.

- Preparing NaOH solution by dissolving 2.58 g NaOH into 200g water one day before test.
- 20g slag was mixed with required NaOH solution and stirred for 1.5 minutes. Then the suspension containing slag and activator stayed still for 0.5 minutes and restarted to stir for another 3 minutes.
- The suspension was centrifuged at a speed of 3000 rpm for 10 min.
- The supernatant was collected by passing through a 0.45 μm filter membrane.
- The original SP solution was prepared by mixing 0.05 g (weight of solid) superplasticiser into 20.26 g NaOH solution.
- The original SP solution was diluted at 10, 20, 50 and 100 times by adding pure water to generate a calibration curve for determining the SP sample concentration.
- The absorbance of each solution was determined and the calibration curves between concentration and absorbance were plotted (the regression of LS, NF and MP polymer are shown in ***Fig 4.8***).

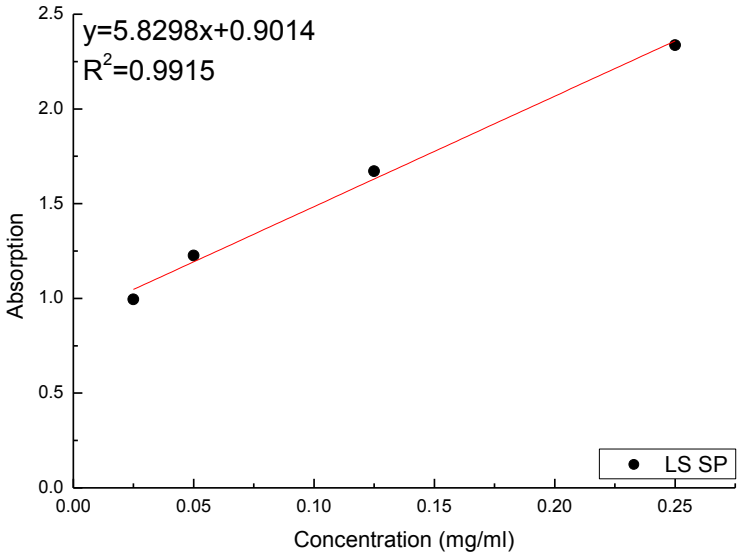

(a) LS SP

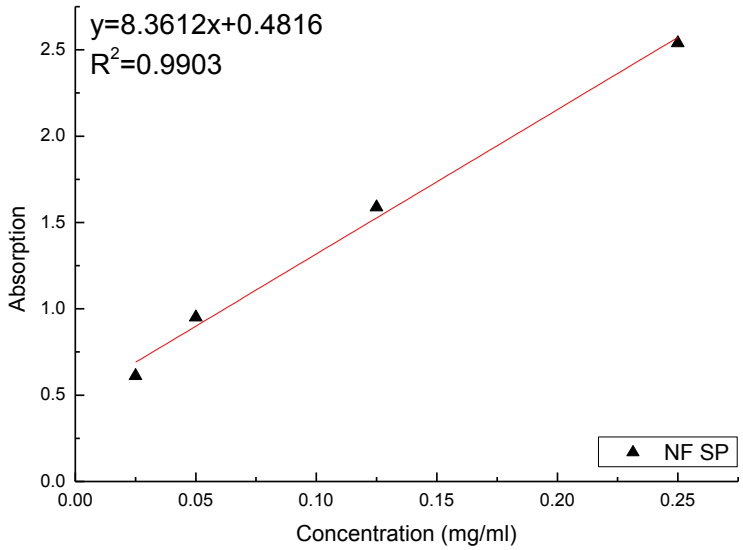

(b) NF SP

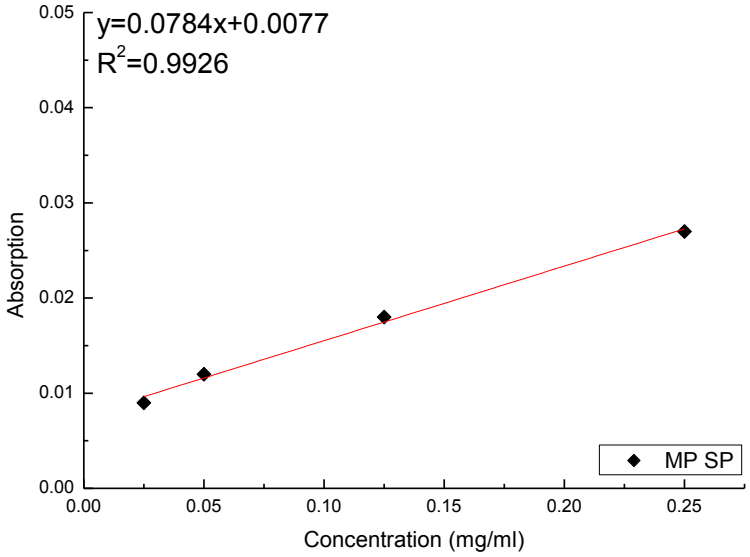

(c) MP SP

Fig 4.8 Calibration curve of LS, NF and MP polymer

Adsorption test procedure:

- **Simultaneous addition:** The slag suspensions were prepared by mixing 5g slag and relative NaOH solution with the required amount of SPs (refer to section 4.4.1) simultaneously. The total mixing time was 5 minutes. Immediately after adding slag, the suspension was stirred by magnetic stirrer for 1.5 minutes and then allowed to rest for 0.5 minutes. The suspension was then re-stirred for 3 minutes. After stirring, the suspension

was centrifuged at 3000 rpm and the supernatant was collected by passing through a 0.45 μm filter membrane. Then the supernatant was diluted in 10 times and examined by UV spectrometer.

- **Delayed addition:** The slag suspension was prepared by mixing 5g slag and relative NaOH solution. The SP solution was prepared by dissolving required amount of SPs into 5 g water. The total mixing time was 5 minutes. Immediately after adding slag, the suspension was stirred by a magnetic stirrer for 1.5 minutes and allowed to rest for 0.5 minutes. Following this, the stirrer was restarted to stir for 3 minutes. At 3 minutes from mixing, the previously prepared SP solution was added into the suspension. After stirring, the suspension was centrifuged at 3000 rpm and the supernatant was collected by passing through a 0.45 μm filter membrane. Then the supernatant was diluted in 10 times and examined by UV spectrometer.
- **Prior addition:** The slag suspensions were prepared by mixing 5 g slag, the required amount of SP and 15 g water. The NaOH solution was prepared by dissolving 0.26 g NaOH into 5 g water. The total mixing time was 5 minutes. Immediately after adding slag, the suspension was stirred by a magnetic stirrer for 1.5 minutes and allowed to rest for 0.5 minutes. Following this, the suspension was restarted to stir for 3 minutes. At 3 minutes from mixing, the previously prepared NaOH solution was added into the suspension. After stirring, the suspension was centrifuged at 3000 rpm and the supernatant was collected by passing through a 0.45 μm filter membrane. Then the supernatant was diluted in 10 times and examined by UV spectrometer.

4.5.1.2 Zeta potential Test

Zeta potential test was carried out to determine the effect of superplasticiser on the surface charge of slag, the value of which could indicate the interaction between the SP and the slag. The zeta potential of NaOH-activated slag was determined by Dispersion Technology Instruments DT-300 (Shown in ***Fig 4.9***). Compared with the traditional electrophoretic-based device, a paste with very high volume fraction could be directly measured by the DT-series instrument. The zeta potential of the slag grain

was calculated by the colloidal vibration current (CVI) measured by DT-300. The principle of the measurement is presented in ***Fig 4.9 (c)*.** Pulse-echo method, which means the signal sender and receiver are at the same side, is applied to the samples. The oscillating electroacoustic signal is generated by applying the RF-pulse to a piezo-transducer. The sound wave applied into the sample induces the relative movement of the solvent molecules to the suspended slag grains. From this, an electric current or field, which is generated from the movement, is detected from the receiver. The quantitative relationship between the zeta potential and CVI is expressed in ***Equation 4.3*** and ***4.4.***

For polar system:

$$CVI = A\phi \frac{\varepsilon_0 \varepsilon_m \zeta K_s}{\eta K_m} \frac{\rho_p - \rho_s}{\rho_s} \quad \textbf{4.3}$$

For non-polar system:

$$CVI = A \frac{\phi}{1-\phi} \frac{2\sigma a}{3\eta} \frac{\rho_p - \rho_s}{\rho_s} \quad \textbf{4.4}$$

Where CVI stands for colloidal vibration current, ε_0 for dielectric constant, ε_m for relative permittivity (liquid), ζ for zeta potential, η for dynamic viscosity (liquid), K_s for conductivity (dispersion), K_m for conductivity (liquid), ρ_p for particle density, ρ_s for solvent density, σ for surface charge density, a for particle radius and A for calibration constant.

After mixing (refer to section 4.4.2), the pastes (Referred in ***Table 4.5***) were placed in the sample cell and the zeta potential were measured at 7 minutes, which was corresponding to the measurement of initial minislump (refer to section 4.5.2.1). The sample to be tested was obtained from the same batch for minislump and rheology tests.

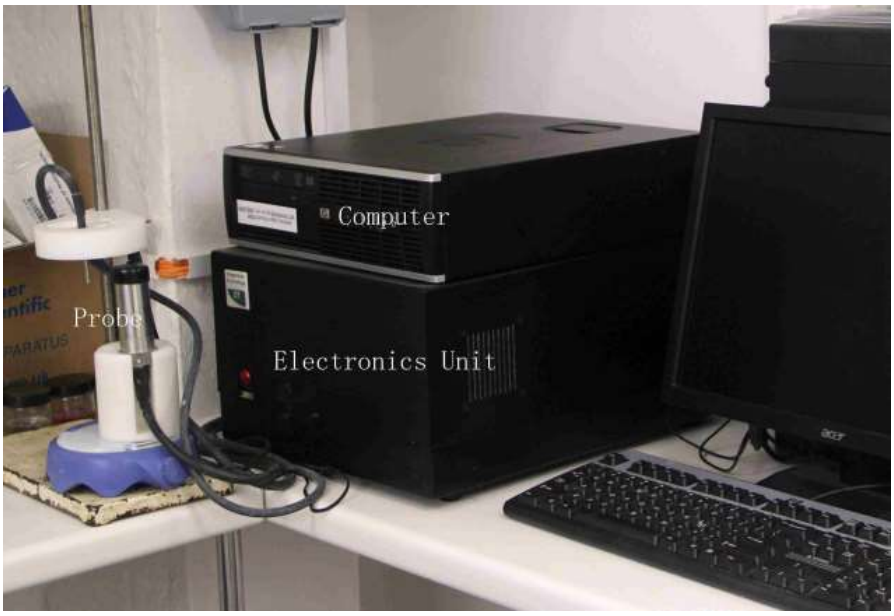

(a) Electronic Unit and PC

(b) Probes

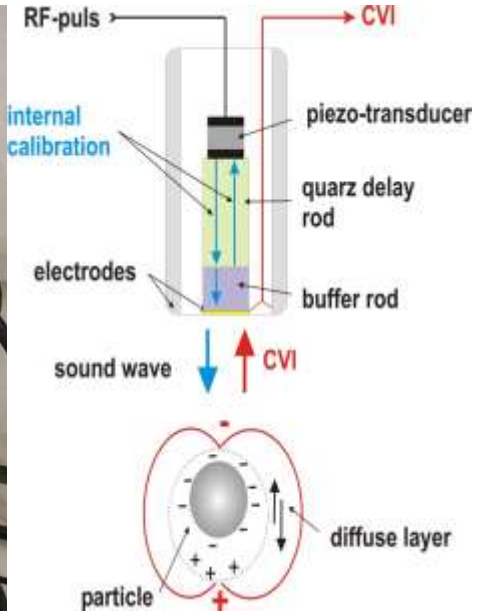

(c) Principle of Measurement

Fig 4.9 Dispersion Technology Instruments DT 300 and its working principle

4.5.2 Test of early age properties

The aim of the addition of superplasticiser is to improve the fresh properties, such as minislump and rheological properties. Minislump has been used as an empirical method to test the workability of NaOH-activated slag paste. However, the accuracy of minislump is not sufficiently high. Therefore, the two-point test was used to characterise the rheological properties of NaOH-activated slag. In addition to

workability and rheology, the setting time of NaOH-activated slag was determined and the early hydration of NaOH-activated slag was also monitored by ICC.

4.5.2.1 Workability Test (Minislump)

The minislump test was induced as a quick way to determine the effect of superplasticiser on the workability of NaOH-activated slag paste. The test was conducted based on the measurement of the spread of AAS paste placed into a conical mould (Palacios and Puertas, 2005). A PVC plate and a cone with a lower inner diameter of 38.1 mm, an upper inner diameter of 19 mm, and a height of 57.1 mm, were used to determine the spread (shown in ***Fig 4.10***,). During the test, the mould was placed in the centre of the plate and filled by the paste. Then the mould was vertically lifted up to let the paste flow freely. The diameter at two perpendicular directions was measured and recorded. The arithmetic mean of the two measurements was recorded as the result.

In order to test the minislump loss, the minislump measurement was conducted at different time intervals, namely 7, 15, 30, and 60 minutes after mixing (count from zero time). After mixing, the paste was moved into a 250ml plastic beaker and covered with damp tissue to minimise the evaporation of free water in the paste. In order to avoid segregation, before each testing time, the paste was remixed by hand for 30 seconds and filled into the conical mould for the test. The results were then recorded.

(a) Minislump Test

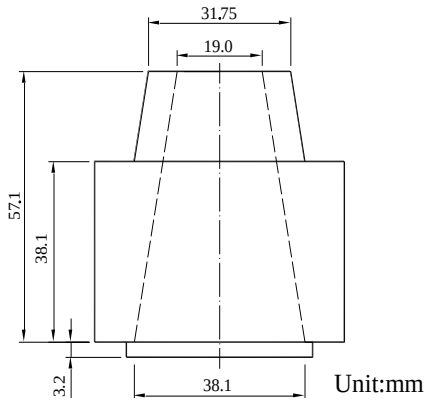

(b) Schematic diagram of minislump conical mould

Fig 4.10 Equipment for the minislump test

4.5.2.2 Rheology Test

The rheological properties of alkali-activated slag paste, with and without superplasticiser, were determined to understand the effects of different addition methods by using the two-point test. The NaOH-activated paste was from the same batch used to determine minislump and zeta potential. The mixing procedure was referred to in section 4.4.2. The rheometer was a modified Rheomat 115 viscometer with a Rheoscan 115 control Unit - originally it was a concentric cylinder viscometer for testing liquids (as shown in ***Fig 4.11***). It was then modified by replacing the concentric cylinder by a helical impeller to test paste and mortar samples (as shown in ***Fig 4.11 (b)***). The container with diameter of 92 mm was used. The modified Rheometer was calibrated and tested in UCL (Jin, 2002). The data was then recorded by a computer with the Instacal^{TM} logging programme installed.

The measurement of yield stress and plastic viscosity was conducted at 7, 15 and 30 minutes after mixing (count from zero time), and the results were linked with minislump results. To avoid damaging the equipment from quick-setting NaOH-activated slag paste, the measurement at 60 minutes was suspended. For each test, the sample was subject to one cycle with increasing and decreasing rotating speed between 0 and 112 revolutions per minute (rpm). The results were then recorded by the software and generated from the Bingham Model.

As discussed in section 2.3.1, the addition of superplasticiser could change the rheological behaviours of Portland cement from linear Newtonian to shear-thickening with a non-linear relationship between the shear stress and shear rate. However, in this thesis, in order to simplify the scenery and make it comparable, all the rheological properties of NaOH-activated slag pasted were calculated based on the Bingham model.

(a) Rheometer **(b) Schematic of helical impeller**

Fig 4.11 Rheometer Units

4.5.2.3 Setting time Test

NaOH activated slag has been identified as a quick-setting material. In the project, the setting time test followed BS EN 196-3:2005. The measurement was conducted by a Vicamatic apparatus from Controls (Shown in ***Fig 4.12***). The time interval between each drop was set to 10 minutes. The test finished when the final set was reached. The setting times were calculated by counting the number of lines on the recording paper plus the time lapse between zero time and the time at which the first penetration started.

- New batch of paste with 500 g of slag and required NaOH and superplasticiser was mixed following the procedure mentioned in section 4.4.2.
- After mixing, the paste was transferred into the mould (If the paste was so diluted to cause leakage from the mould, the paste was rested in the bowl and transferred until its minislump value was below 90 mm).
- After the paste-filled mould was placed inside the machine, the test was started.
- The initial setting time was defined as the time between zero time and the time at which the distance between the needle and the base-plate is 6 ± 3 mm.
- After the initial setting, the mould was taken out from machine, inverted, and placed back on the mould plate. Thus, the flat bottom surface faced

upward. The needle with a ring (final setting needle) was also changed to determine the final setting time.

- The final setting was determined as the time between zero time and the ring mark disappearing on the surface of specimen in the mould (which indicated the penetration was 0.5mm into the specimen).

Fig 4.12 Auto-Vicamatic

4.5.2.4 Isothermal conduction calorimeter (ICC)

The Isothermal Conduction Calorimetry (ICC) (TAM Air), as shown in ***Fig 4.13***, was used to measure the heat of NaOH-activated slag generated from early hydration and thereby following its initial reactions. Exactly 3 g of slag was weighed and placed in the glass sample bottle; the required activator and SP solution were filled into two separate syringes. The operation temperature was kept constant at 20 ℃. When thermal equilibrium was achieved, the slag, NaOH activator (4% Na_2O equivalent) and SP solution (the dosage of all types of superplasticiser was fixed at 0.5%) were mixed by injecting the solution according to the sequence of mixing procedure. The effects of all *SA*, *PA* and *DA* on heat evolution of NaOH-activated slag were conducted. The heat evolution was recorded and calibrated by software installed in a computer controlling the operation.

Fig 4.13 Isothermal Conduction Calorimetry (ICC) by TAM Air

4.5.3 Test of hardened properties

The addition of SP not only improves the fresh properties, but also affects the hardened properties of NaOH-activated slag by changing the pore size distribution and structure. Compressive strength, and drying shrinkage and porosity were tested to investigate the effects on hardened properties

4.5.3.1 Compressive Test

Sample preparation

Steel moulds with a size of 25mm × 25mm × 25mm (shown in ***Fig. 4.14***) were used to cast paste cubes for determining the compressive strength. Before casting, a layer of de-moulding oil was coated on the surface of the moulds.

The sample to be cast was from the same pastes which were used for zeta potential test. After zeta potential test (refer to section 4.5.1.2), the paste was filled into the prepared moulds and vibrated for 2 minutes. The cubes were de-moulded in 24 hours. The casting procedure was conducted before NaOH-activated slag hardening.

Curing Regime

The vibrated moulds were stored in an environmental box (100% RH and 20±2 ℃) for 24 hours before de-moulding, After de-moulding, the sample was wrapped in damp hessian, sealed within a sample bag, and stored at 20±2 ℃ with 100% RH.

Compressive Test

The compressive strength of the specimen was tested after curing at 1, 7, 28, and 56 days. At each test age, three specimens were tested with an Advantest 9 Flexural Frame from Controls (Shown in ***Fig 4.14***). The loading rate was controlled at 0.4 MPa/s and the peak sensitivity was 4 KN. The average value was recorded as the compressive strength at designed age.

(a) Advantest 9 Flexural Frame

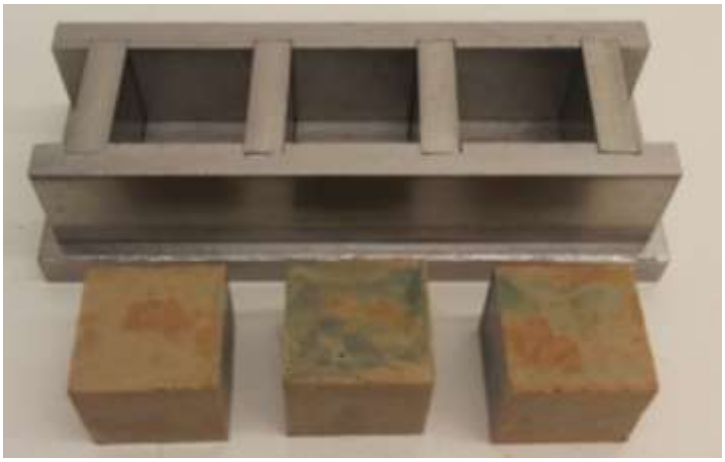

(b) Casting mould and specimens

Fig 4.14 Equipment for compressive strength

4.5.3.2 Drying shrinkage

Sample preparation

Steel moulds with a size of 25mm × 25mm × 250mm (shown in ***Fig. 4.15***) were used to cast the prism for determining the drying shrinkage. The method of measuring and calculating drying shrinkage is specified in ASTM C490. The change of length of prism was measured regularly by a model 63-L0035/A apparatus from Controls (Shown in ***Fig 4.15***).

A new batch of paste with 1000 g slag was mixed by following the procedure mentioned in section 4.4.2. Mixed paste was filled into the prepared moulds and vibrated for 2 minutes; the cast prisms were de-moulded in 24 hours.

Curing Regime

The vibrated moulds were stored in an environmental box (100% RH and 20±2 ℃) for 24 hours before de-moulding. After de-moulding, the sample was immersed

under water in a tank for another 72 hours. Then, the fully wet prism was cured under 50±5% relative humidity at 20±2 ℃.

Measurement

For each mix, four specimens were prepared and three of them were used for measurement. Two values of comparator from both sides of prism were recorded and the average value was recorded as the length of each specimen. The average value of three specimens was used to calculate the drying shrinkage of specimens.

(a) Model 63-L0035/A apparatus

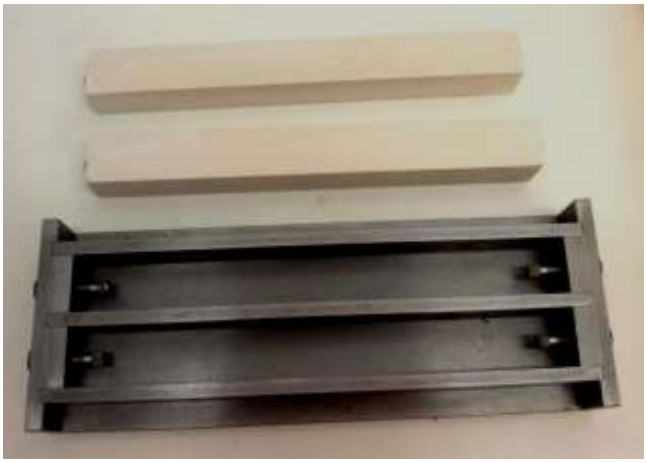

(b) Casting mould and specimens

Fig 4.15 Equipment for testing drying shrinkage

4.5.3.3 Mercury intrusion porosimetry (MIP)

The MIP was employed to determine the capillary pore distribution to illustrate the effect of different addition methods on drying shrinkage of NaOH-activated slag. The test was conducted by a Micromeritics AutoPore IV 9500 (***Fig 4.16***) with the pressure running from 0.0014 to 228 MPa. The surface tension of mercury is 485×10^{-3} N/m and its contact angle is 132 ℃(Wilkinson, 1972). Based on the calculation from the Washburn equation (Washburn, 1921), the pore size can be detected in the range from 360 to 0.005 μm.

The prepared samples (refer to section 4.4.1) were thermal dried at 60 ℃ and then cooled to room temperature under vacuum before testing. Then the samples were loaded into a penetrometer, filled with mercury, and evacuated to the required vacuum level. With the pressure increasing, the mercury was gradually forced to

enter into the pores of the specimens. Thus, the volume of the pores filled by mercury was linked with the volume of mercury induced in the penetrometer. Hence, the porosity and pore size distribution were deduced from the applied pressure.

In this thesis, the pore size is defined as: micropores pores with a pore size of less than 100 nm; and macropores with a pore size larger 100 nm (Ambroise *et al*., 2009).

Fig 4.16 Micromeritics AutoPore IV 9500

4.5.4 Characterisation of superplasticisers

The chemical stability of superplasticiser was evaluated by a Fourier Transform infrared (FTIR) and High performance size exclusion chromatography (HPSEC). By using FTIR, the change of structure (functional groups) in NaOH solution (from peak shift if applicable) can be detected. Possible polymer chain breaking can be identified by HPSEC.

4.5.4.1 Fourier Transform infrared (FTIR)

FTIR spectra over the wavenumber range of 400 cm^{-1} to 4000 cm^{-1} were obtained using a Nicolet 6700 Fourier transform infrared spectrophotometer from Thermo Scientific (***Fig 4.17)***.

All the materials were prepared as liquid form and tested in two solutions:

- Distilled water

- NaOH solution (10.75g NaOH/100g H_2O), which is used to simulate the activator solution for NaOH-activated slag.

The polymer/solution (w/w) ratio was set at 1:1. After setting for two hours, the sample was collected and tested.

A few droplets of the superplasticiser solution were dropped in a disk and mixed with KBr powder. Then, the mixed powder was crushed and cast to a thin film. The film was placed on a sample holder and scanned from 400 cm^{-1} to 4000 cm^{-1}.

Fig 4.17 Nicolet 6700 FTIR by Thermo Scientific

4.5.4.2 High performance size exclusion chromatography (HPSEC)

The HPSEC method is set up on the theory that small molecules diffuse easier into the pores of the column, thereby eluting out of the column later than large molecules (Liu, 2010). The HPSEC was conducted with a high performance liquid chromatography (HPLC) system (Perkin Elmer), series 200 with a UV detector. The column was a BIOSEP-SEC-S3000 from Phenomenex with size of 7.8 mm (ID) × 30 cm. The results were monitored and processed by the TotalChrom Navigator software. The result of chromatogram of UV absorbance vs. time was generated from software.

The measurement consists of two parts: the calibration process and test process, which were done separately according to as BS ISO 16014-2 (2009) and BS ISO 16014-3 (2009). The column was calibrated by using four Poly (sodium-p-styrenesulfonate) (PSS) -standards with MWs of 891, 6430, 15800 and 33500 Da. The examples of HPSEC chromatograms of all standards are presented in ***Fig 4.18***. Each PSS standard exhibited a single peak except the standard solution with MW of

891 Da, of which splitting peaks were observed in the chromatogram. To avoid the "splitting peak" effect, acetone (58 Da) was used to replace the standard with an MW of 891 (Liu, 2010).

Based on BS ISO 16014-2 (2009), the standards were dissolved into ultrapure water with a concentration of 0.4 mg/ml. According to BS ISO 16014-3 (2009), the superplasticiser solution was prepared at 5.0 mg/ml. The mobile phase used was 0.1M KCl/MeOH (80/20) (Pei et al., 2004). The UV detector was set at a wavelength of 254 nm (Hsu *et al*., 2000). The injection volume of the sample was set as 50 µl and the flow rate was 0.5 ml/min. The total running time was 40 min. The linear regression between the log peak MW and the retention time (t) (***Equation 4.5***), was used to calibrate the MW of superplasticiser.

$$Log\ (MW) = a + b\ (t) \qquad \textbf{4.5}$$

Where MW stands for molecular weight, a and b stand for coefficient of equation. An example of the calibration of standards is shown in ***Equation 4.6*** below.

$$log\ (MW) = 12.476 - 0.4994(t)\ \ (R^2 = 0.9735) \qquad \textbf{4.6}$$

The molecular weight and weight distribution were calculated with the following equations (Liu, 2010) (***Equation 4.7- 4.9***).

$$M_n = \frac{\sum_{i=1}^{n} h_i}{\sum_{i=1}^{n} \frac{h_i}{M_i}} \qquad \textbf{4.7}$$

$$M_w = \frac{\sum_{i=1}^{n} h_i M_i}{\sum_{i=1}^{n} h_i} \qquad \textbf{4.8}$$

$$PDI = \frac{M_w}{M_n} \qquad \textbf{4.9}$$

Where h_i stands for the height of the chromatogram curve; M_i for the molecular weight of chemicals at retention time t, which was determined according to the calibration results (***Equation 4.6*** in this project), M_n for number average molecular weight, which is calculated by arithmetic mean of the molecular weight of the individual polymers, M_w for weight average molecular weight, which is calculated by the average of the molecular weight of each weight percent, and PDI for

polydisperse index, which could be used to illustrate the molecular weight distribution.

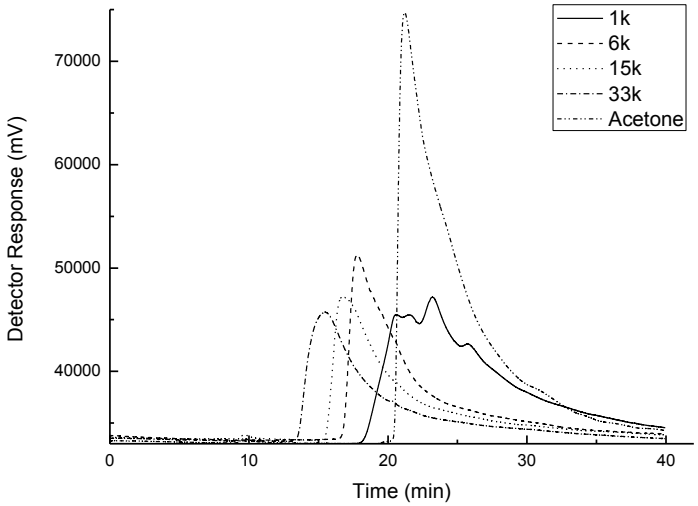

Fig 4.18 HPSEC chromatograms of all standards

Chapter 5

Effect of Different Addition Methods of PC-based Superplasticiser on the Properties of NaOH-activated Slag

5.1 Introduction

As discussed in section 3.4.1, two types of PC-based superplasticisers, namely, lignosulfonate superplasticiser (LS) and naphthalene superplasticiser (NF), showed some effects on increasing the workability of NaOH-activated slag. However, their performance in NaOH-activated slag is poorer than that in the PC system. Based on the literature review in chapter 3, one of the reasons causing this poorer performance has been identified as the **competitive adsorption** between the SPs and the activators. One possible solution to improve the performance of SP in AAS is, thus, to apply separate SP addition methods, which means adding SP and NaOH at different mixing stages.

Therefore, this chapter investigates the effects of the addition methods of these two SPs on various performance and properties of NaOH-activated slag in order to assess the potential of separate addition method for improving the efficiency of PC-based SPs in NaOH-activated slag system. Furthermore, the chemical stability of PC-based SPs under different addition method is also assessed in the chapter in order to achieve a better understanding of the mechanisms involved.

The objectives of this chapter are:

- To investigate the interaction and working mechanism of lignosulfonate and naphthalene superplasticisers in NaOH-activated slag under the different SP addition methods.
- To examine the effects of different SP addition methods of lignosulfonate and naphthalene superplasticisers on the early age properties of NaOH-activated slag including rheological properties, setting time and early hydration heat.
- To investigate the effects of different SP addition methods of lignosulfonate and naphthalene superplasticisers on the hardened properties of NaOH-activated slag in terms of compressive strength, drying shrinkage and porosity.

- To determine the chemical stability of PC-based SPs, namely lignosulfonate, naphthalene and polycarboxylate superplasticiser, in highly alkaline NaOH solution.

5.2 Experimental programme

To achieve the above objectives, the overall research programme was developed which is presented in ***Fig 5.1***. All the mixes for investigating the effects of different addition methods of LS and NF SPs in NaOH-activated slag are listed in ***Table 5.1***. The test details are described in Section 4.4.

Three aspects of the properties, namely, 1) interaction among SP, activator and slag; 2) early age and 3) hardened properties, of NaOH-activated slag were investigated by following the 4 stages as detailed below:

Stage 1: the adsorption behaviour of SPs on the surface of slag particles under different addition methods was investigated and its corresponding zeta potential value was measured in order to explore the working mechanism of SPs in NaOH-activated slag, especially the mechanisms of the competitive adsorption between SPs and activators.

Stage 2: the rheological properties under different SP addition methods were investigated to examine the effectiveness of SPs in fresh NaOH-activated slag. Then, the effects of different SP addition methods on the setting time and early age hydration (up to 48 hours) were monitored.

Stage 3: the hardened properties of NaOH-activated slag, in terms of compressive strength and drying shrinkage, were measured in order to investigate the effects of different SP addition methods on the long term properties of NaOH-activated slag. The porosity of the hardened pastes was also determined so that the possible mechanism related to the effect that the SPs have on the hardened properties of AAS could be identified.

In addition to the above three stages, the chemical structure of LS, NF and PCE in H_2O and NaOH solution (pH>14), respectively, were examined by Fourier

Transform Infrared Spectroscopy (FTIR) in **Stage 4**. And their molecular weight and weight distribution were also examined by High Performance Size Exclusion Chromatography (HPSEC).

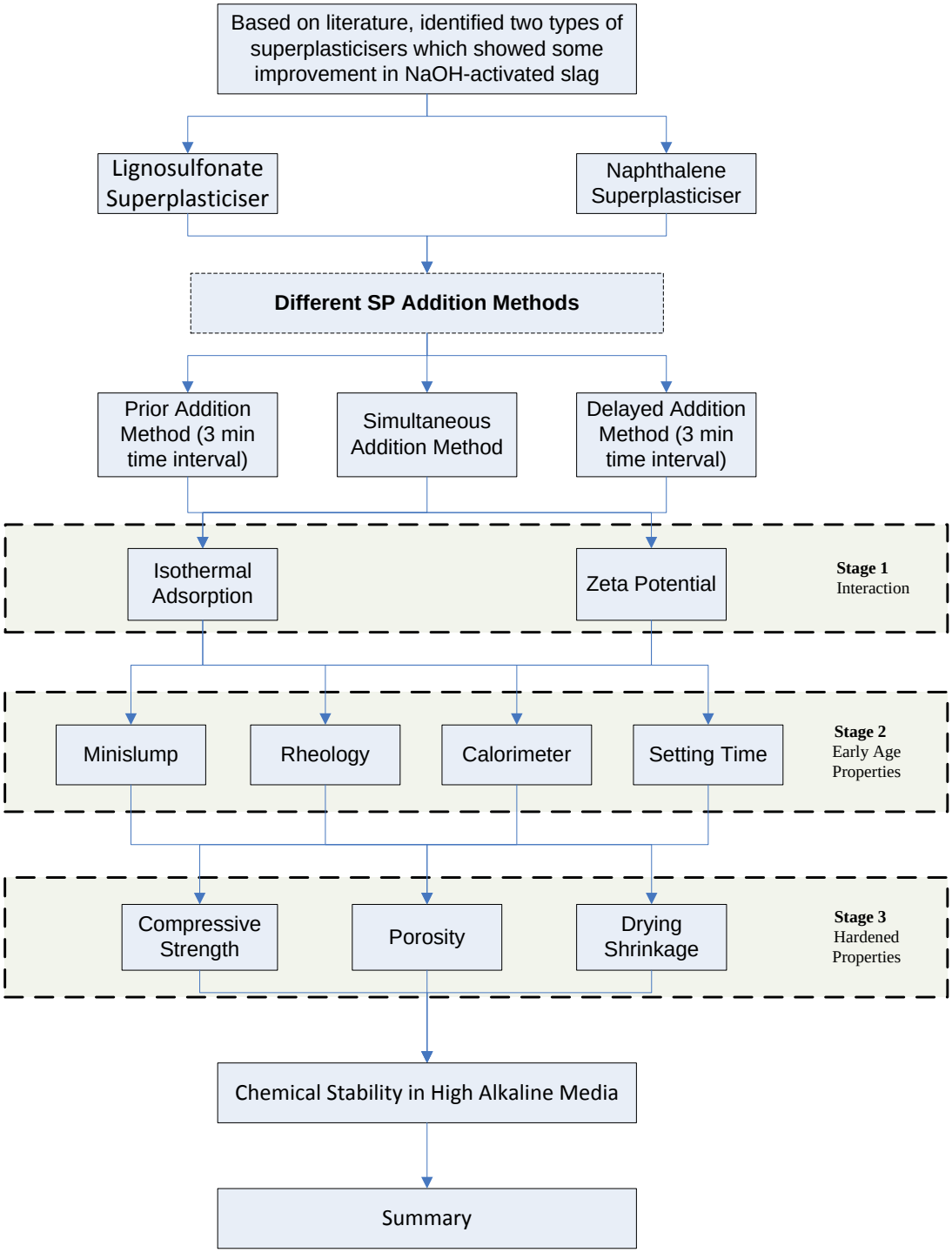

Fig 5.1 Flow chart of the overall research programme of Chapter 5

Table 5.1 Experimental details of PC-based SPs in NaOH-activated slag

No	Addition Method	Solution	SP Dosage (%)	No SP	Lignosulfonate Superplasticiser			Naphthalene Superplasticiser		
				Control	Interaction	Early Age	Hardened properties	Interaction	Early Age	Hardened properties
1	N/A	H_2O	0	Zeta						
2		NaOH	0	Zeta, MS, RM, ST,ICC,CS, DS ,MIP						
3	N/A	H_2O	0.125		Ads			Ads		
4		H_2O	0.250		Ads			Ads		
5		H_2O	0.500		Ads			Ads		
6		H_2O	0.750		Ads			Ads		
7		H_2O	1.000		Ads			Ads		
8	SA	NaOH	0.125		Ads			Ads, Zeta	MS, RM, ST,ICC	CS, DS,MIP
9		NaOH	0.250		Ads			Ads, Zeta	MSL, RM	CS
10		NaOH	0.500		Ads, Zeta	MS, RM, ST,ICC	CS, DS,MIP	Ads, Zeta	MSL, RM	CS
11		NaOH	0.750		Ads, Zeta	MSL, RM	CS	Ads		
12		NaOH	1.000		Ads, Zeta	MSL, RM	CS	Ads		
13	DA	NaOH	0.125		Ads			Ads, Zeta	MS, RM, ST,ICC	CS, DS,MIP
14		NaOH	0.250		Ads			Ads, Zeta	MSL, RM	CS
15		NaOH	0.500		Ads, Zeta	MSL, RM, ST,ICC	CS, DS,MIP	Ads, Zeta	MSL, RM	CS
16		NaOH	0.750		Ads, Zeta	MSL, RM	CS	Ads		
17		NaOH	1.000		Ads, Zeta	MSL, RM	CS	Ads		

18		NaOH	0.125	Ads			Ads, Zeta	MS, RM, ST,ICC	CS, DS,MIP
19		NaOH	0.250	Ads			Ads, Zeta	MSL, RM	CS
20	PA	NaOH	0.500	Ads, Zeta	MSL, RM, ST,ICC	CS, DS,MIP	Ads, Zeta	MSL, RM	CS
21		NaOH	0.750	Ads, Zeta	MSL, RM	CS	Ads		
22		NaOH	1.000	Ads, Zeta	MSL, RM	CS	Ads		

Note: **Ads** stands for adsorption; **Zeta** for zeta potential test; **MSL** for minislump test; **RM** for rheology test (by rheometer); **ST** for setting time; **CS** for compressive strength; **DS** for drying shrinkage; **ICC** for Isothermal conduction calorimeter; and **MIP** for Mercury intrusion porosimetry. (The mixing and testing procedures can be found in Chapter 4)

5.3 Interactions between PC-based superplasticisers and alkali activators

To understand the mechanisms of the different SP addition methods, the interactions between the two types of PC-based SPs and slag were determined by the amount of SPs adsorbed on the slag particles as well as the zeta potential of the slag particles in the presence of different SPs.

5.3.1 Isothermal Adsorption

The effects of LS and NF under different addition methods on the adsorption of NaOH-activated slag are shown in ***Fig 5.2 (a)*** and ***Fig 5.2 (b)*** respectively. It is clear that compared to the adsorption on pure slag, the adsorption of both types of SPs was significantly reduced in the presence of the NaOH activator.

In PC based system, the adsorption of superplasticisers on the surface of particles is strongly affected by two factors (Torn et al., 2003, Yan et al., 2010):
a) The nature of the surface of the adsorbing substrate, its surface charge and
b) The ionic conditions of the solution, such as pH and ionic strength.

However, the surface structure/charge and chemistry of slag are different from that of PC, which suggests that the performance of SPs in slag could be changed. Moreover, the previous research in the literature on adding SP together with activator showed that, in NaOH-activated slag, large amounts of OH^- are introduced into the NaOH-activated slag system, which increases the ionic strength in the solution significantly, leading to a reduction of the adsorption (Yang et al., 2009). In the current study, as shown in ***Fig 5.2 (a)***, when LS was added at a dosage of 1.000%, the adsorbed amount of LS on the slag surface was reduced from 2.35 mg/g in the absence of NaOH (i.e. slag mixed with water) to 1.32 mg/g in the presence of NaOH under SA method, which represents a 44% reduction in the LS adsorption. Similarly, at 1.000% dosage, the adsorption of NF in the presence of NaOH was less than 0.38 mg/g with SA method, which was approximately 60% of that in the mixture of slag and water. This clearly indicates that with SA method, there is a great competitive adsorption between the SP and the activator, which could lead to a decrease in the performance of PC-based SPs in NaOH-activated slag systems.

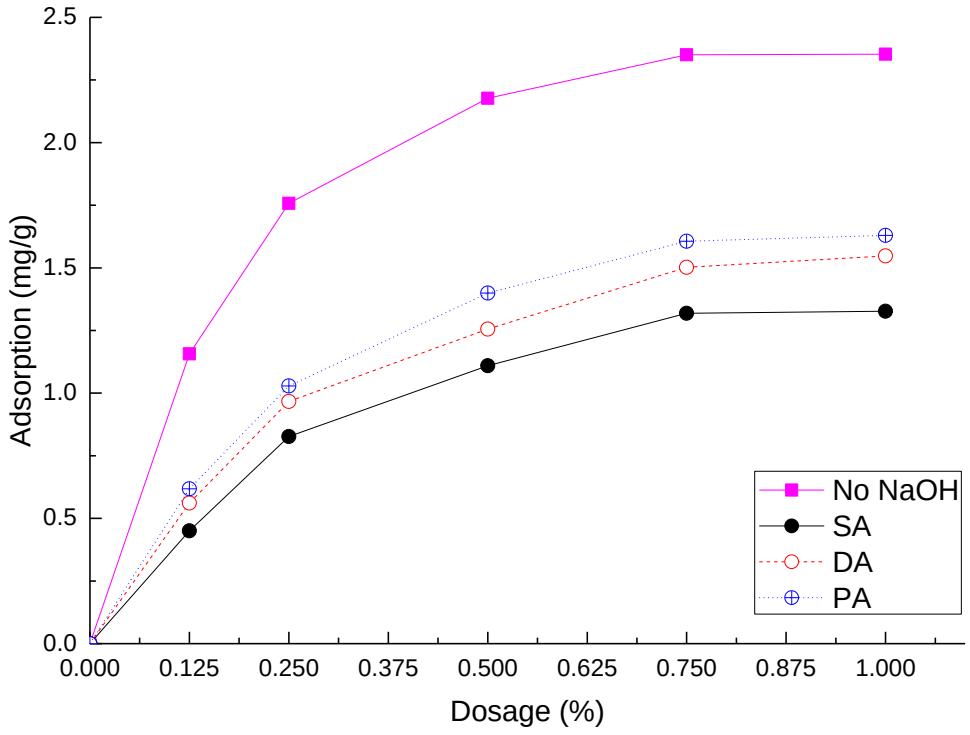

(a) LS

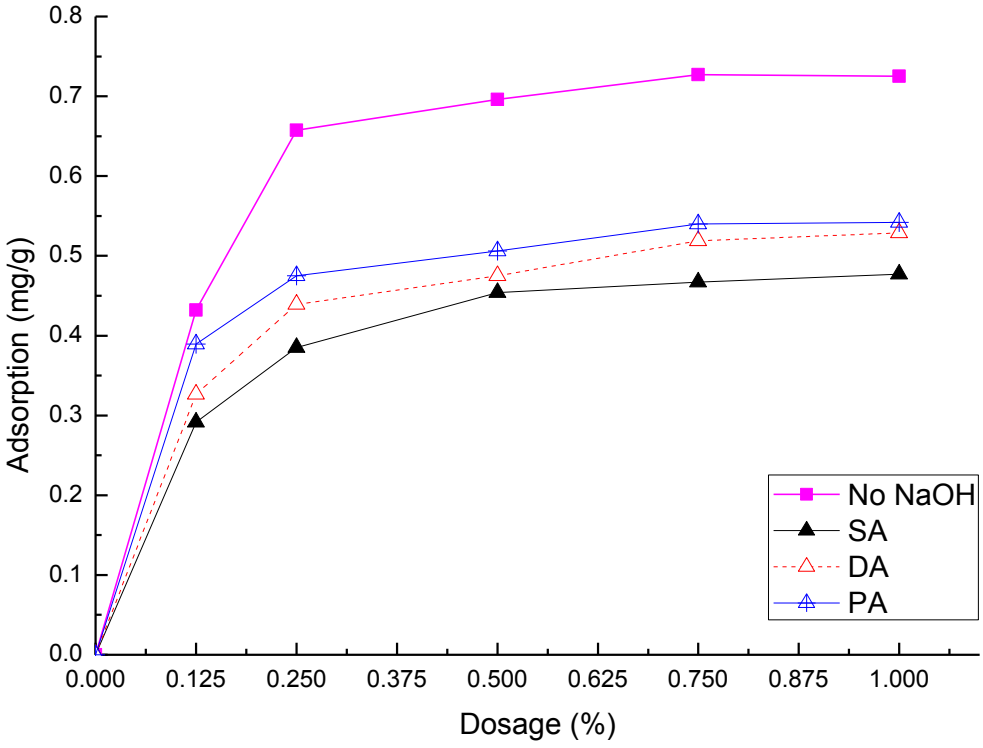

(b) NF

Fig 5.2 Effects of different addition methods of SPs on adsorption behaviour of NaOH-activated slag suspension: (a) LS and (b) NF

However, under the separate addition methods of LS, increased adsorption was observed in both the *Delayed Addition* and *Prior Addition* in ***Fig 5.2 (a)***. This indicates that adding SP and activator separately can reduce the competitive adsorption in the NaOH-activated slag. Similar trend can be observed from NF in ***Fig 5.2 (b)***. It can be seen that when the NF and NaOH activators were added separately, the adsorption of NF was increased. Therefore, the results from both the LS and NF SPs would suggest that the separate addition of SPs could be a promising approach to reduce the competitive adsorption between the SP and the NaOH activator on the surface of slag. Furthermore, regardless of the type of SPs, higher adsorbed SP was achieved from *PA* rather than *DA* and this was more pronounced in lower dosages (0.250% for LS and 0.125% for NF).

In addition, from ***Fig 5.2 (a)***, it can be seen that regardless of the addition methods, the adsorbed amount of LS increased rapidly with the increase of the SP dosage up to 0.750%. This could be due to the fact that sufficient amount of active sites are readily available on the surface of the slag grains from the beginning for the LS to occupy when the dosage of the SP is low (Zingg *et al.*, 2008). At a higher dosages (>0.750%), the adsorption increased slowly and gradually reached a saturated plateau. Similar result was also observed in NF. However the saturated dosage of NF was approximate 0.250%. This difference in the saturated SP dosage could be attributed to the nature of SPs, i.e., the chemical compound, the chemical structure and the configuration (Rixom and Mailvaganam, 1999).

It has been generally accepted that the adsorption of linear SPs follows the trend of Langmuir isothermal adsorption, with forming a monolayer of adsorbed SPs (Kong *et al.*, 2014, Ran *et al.*, 2010). Based on the Langmuir isothermal adsorption discussed in Chapter 2 (***Equation 2.1*** and ***2.2***), quantitative analysis of the adsorption behaviour of LS and NF was conducted and the results are shown in ***Fig 5.3 (a)*** and ***Fig 5.3 (b)*** respectively. The parameters used in the equation and the R^2 values from this analysis are summarised in ***Table 5.2***. The high value of R^2 (>0.96 in all cases) from this analysis suggests that the Langmuir adsorption equation can be used to describe the adsorption behaviour of both LS and NF in NaOH-activated slag. For both types of SPs, the values of the characteristic plateau (*As*) for both *PA* and *DA* were higher than those of *SA*, respectively. As the adsorption characteristic

plateau depends on the electrostatic force between the SP and slag, the higher value of *As* indicates that a stronger electrostatic attractive force exists between SP and slag (Ran *et al.*, 2010). Therefore, the above results suggest that when the SP and the NaOH were added separately, higher electrostatic attractive forces formed between the negatively charged LS/NF and the positively charged slag, and therefore, more SPs were adsorbed on the surface of slag particles. Between the two separate addition methods, *PA* exhibited a higher adsorption than that of the *DA.* The further explanation of this trend will be discussed in combination with zeta potential results in section 5.3.2.

Table 5.2 Parameters in Langmuir equation for PC-based SPs in NaOH-activated slag

SP	Activator	Addition method	R^2	Intercept	Slope	k/ L g^{-1}	As /mg g^{-1}	ΔG_{ads} /kJ mol^{-1}
LS	H_2O		0.9973	379.7	90.5	4.194	2.634	-3.658
	NaOH	SA	0.9708	635.9	241.4	2.634	1.573	-2.882
		DA	0.9677	555.8	195.5	2.842	1.799	-3.632
		PA	0.9821	548.3	137.8	3.978	1.824	-3.692
NF	H_2O		0.9965	1266.3	282.2	4.487	0.789	-3.494
	NaOH	SA	0.9960	1875.3	574.8	3.263	0.533	-2.360
		DA	0.9884	1727.1	389.0	4.440	0.579	-2.546
		PA	0.9944	1702.2	374.2	4.549	0.587	-3.365

The adsorption constant k was obtained by Slope/Intercept from regressed straight lines in the plot 1/A versus 1/c , and the saturated amount of SP (As) was calculated by 1/Slope

In addition to the As which can be used to indicate the affinity of the dispersant on the slag surface, the Langmuir adsorption constant *k* (in ***Equation 2.2***) can be used to calculate the adsorption free energy ΔG_{ads} (in ***Equation 2.3***) (Ran et al., 2010). As shown in ***Table 5.2***, based on the calculation from ***Equation 2.3***, the adsorption energy for both SPs on the surface of slag grain was negative, which indicates that the adsorption of both LS and NF on slag is favourable and the adsorption process is spontaneous (Ran *et al*., 2010, Bouhamed *et al*., 2007, Plank *et al*., 2010).

It is apparent from ***Table 5.2*** that the absolute values of adsorption free energy for both SPs are less than 5 kJ mol^{-1} regardless of the SP addition methods. As discussed in Chapter 2, the adsorption energy of electrostatic adsorption is approximately 10

kJ mol^{-1} or less (Ran *et al.*, 2010). Thus, the current results indicate that the interaction between the SP and the slag particle can be attributed to the electrostatic adsorption, which is similar to the mechanism identified in PC system (Ran *et al.*, 2010). Therefore, based on the above results, it can be concluded that the adsorption of PC-based SPs was reduced in NaOH-activated slag due to the competitive adsorption between the SP and the NaOH activator. The separate addition methods reduced this competition and, hence, increased the adsorption amount of PC-based SPs on the slag particles.

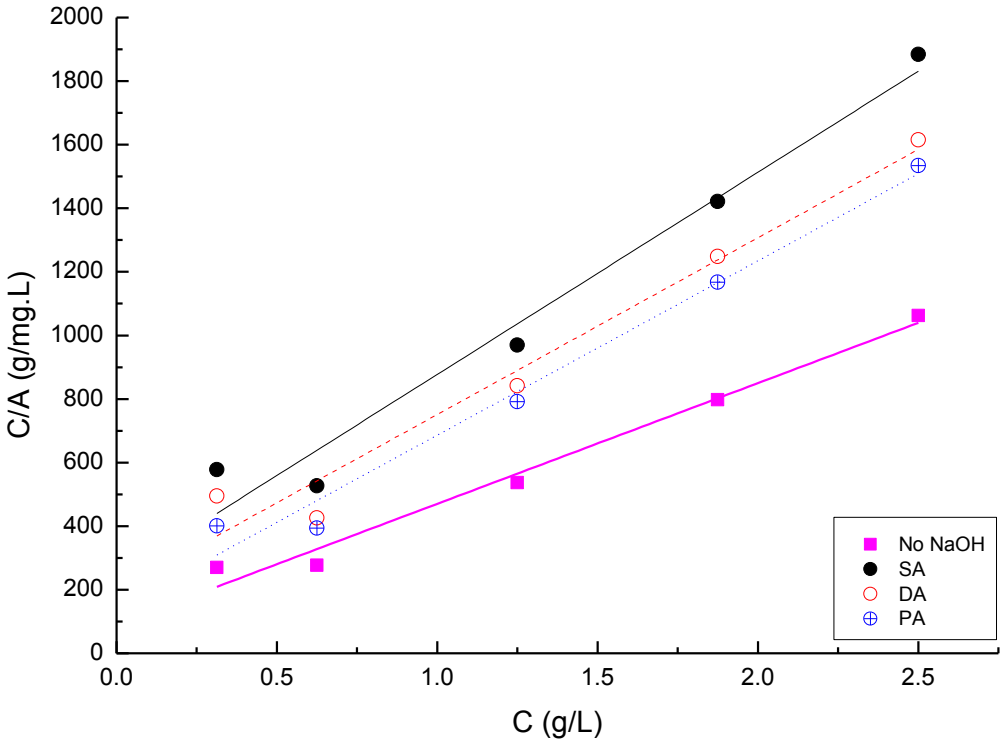

(a) LS

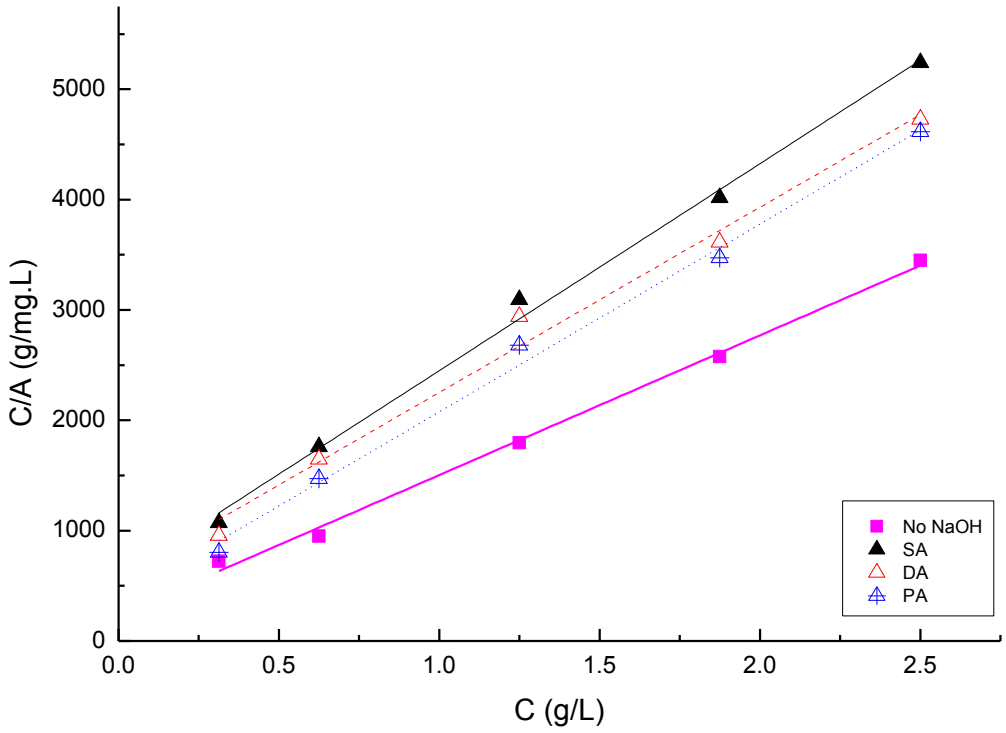

(b) NF

Fig 5.3 Re-plot of adsorption behaviour of PC-based SPs in NaOH-activated slag by following Langmuir adsorption behaviour model: (a) LS and (b) NF (where A stands for the adsorbed amount of SP (mg/g) and C for the equilibrium concentration of SP solution (g/L))

5.3.2 Zeta potential

The DLVO theory (Derjaguin-Landau-Verwey-Overbeek) has been widely used to explain the stability of colloids by considering both van der Waals attraction and electrostatic repulsion (Neubauer et al., 1998). The surface charge of the particles is important for the stability of colloidal particles. Zeta potential is the voltage between the surface and the surrounding solution, which is used to distinguish the firmly adsorbed ion layer (slipping layer) and the diffuse layer, indicating the magnitude of surface charge of the particles. Its magnitude depends on the degree of surface charge and the thickness of double layer. The DLVO theory has been employed to explain the performance of SPs, in particular, the SPs designed by electrostatic repulsion (refer to Section 2.2) (Neubauer et al., 1998, Termkhajornkit and Nawa, 2004a, Yoshioka et al., 2002). The adsorbed negatively charged SP forms an additional slipping layer, which affects the zeta potential. Therefore, the adsorption

of SPs can be reflected from the change of the zeta potential. Moreover, the zeta potential can also offer the information about the electrostatic repulsion force for dispersion of the particles (Ferrari et al., 2011). Based on the DLVO theory, to obtain a better dispersion effect, higher magnitude of zeta potential is preferred.

The effects of the different addition methods of LS and NF on the zeta potentials of NaOH-activated slag are illustrated in ***Figs 5.4 (a)*** and ***(b)***. The zeta potential of the slag (dispersed in pure water) was +0.49 mV, while the zeta potential of the NaOH-activated slag without SPs was -1.14 mV, which corresponds to other researchers' findings in alkali-activated slag paste (Palacios et al., 2009a). The significant reduction of the zeta potential value suggests that a considerable amount of negatively charged OH^- either surrounded the surface of the slag particles or even occupied the active sites on the slag surface.

From both figures, it can be seen that the addition of SPs further reduced the zeta potential of NaOH-activated slag. For LS, in the case of *SA*, the zeta potential of NaOH-activated slag with SP decreased from -1.14 mV (the zeta potential of NaOH-activated slag without SP) to less than -3.19 mV at 0.500% dosage, and was further decreased to approximately -4.62mV at a higher dosage of 1.000%. Similar to LS, under *SA*, the addition of NF reduced the zeta potential of NaOH-activated slag to -4.48 mV at 0.125% dosage, and further decreased to -5.68 mV by increasing the dosage of NF to 0.500%.

As demonstrated in Chapter 2, unlike the PCE, the LS and NF are designed mainly based on the electrostatic repulsion. Since they are both negatively charged polymers, the further reduction of the zeta potential indicates that the SPs were successfully adsorbed on the surface of slag. The higher magnitude of zeta potential would indicate that more SPs are adsorbed onto the surface, which would lead to a higher electrostatic repulsion between the slag particles. As a result, the dispersion of the slag particles was improved.

Compared with the *simultaneous addition (SA)*, lower zeta potential values were observed in the mixes prepared by separate addition methods at all SP dosages, with *PA* lower than *DA*. For example, in the case of LS, at 1.000% dosage, the zeta potential by *PA* and *DA* was -7.10 mV and -6.76 mV, respectively, which were lower

than that by *SA* (-4.62 mV). Similarly, when adding 0.500% NF by separate addition, the zeta potential was reduced from –5.63 (by *SA*) to -8.24 mV (by *PA*) and -7.19 mV (by *DA*).

As discussed in section 2.2.4, the LS and NF are negatively charged polymers, so are of the same type of charge as the NaOH-activated slag. Therefore, the electrostatic attraction between the SP and the slag surface is reduced and in some cases even disappeared. Hence, the adsorption ability of SP is reduced. As discussed, the adsorbed negatively charged SPs can form an additional slipping layer, which affects the zeta potential. The higher amount of negatively charged polymer adsorbed onto the slag surface lead to higher magnitude of zeta potential. As less LS and NF are adsorbed onto slag surface by *SA* (as shown in ***Fig 5.2***) lower magnitude of zeta potential is thus observed in *SA*.

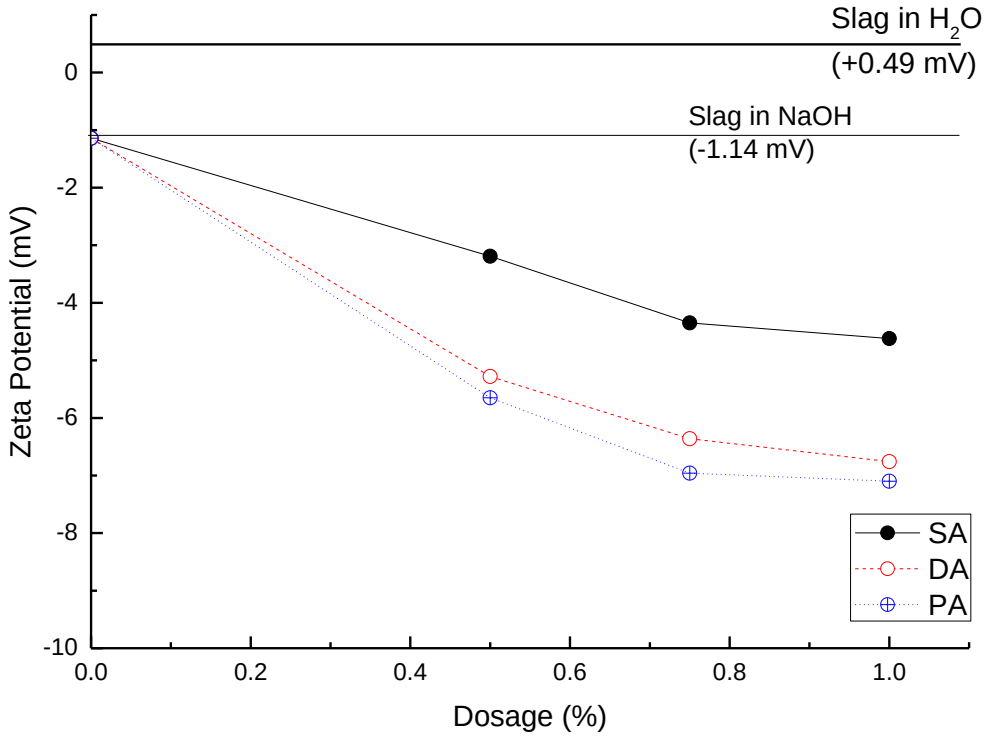

(a) LS

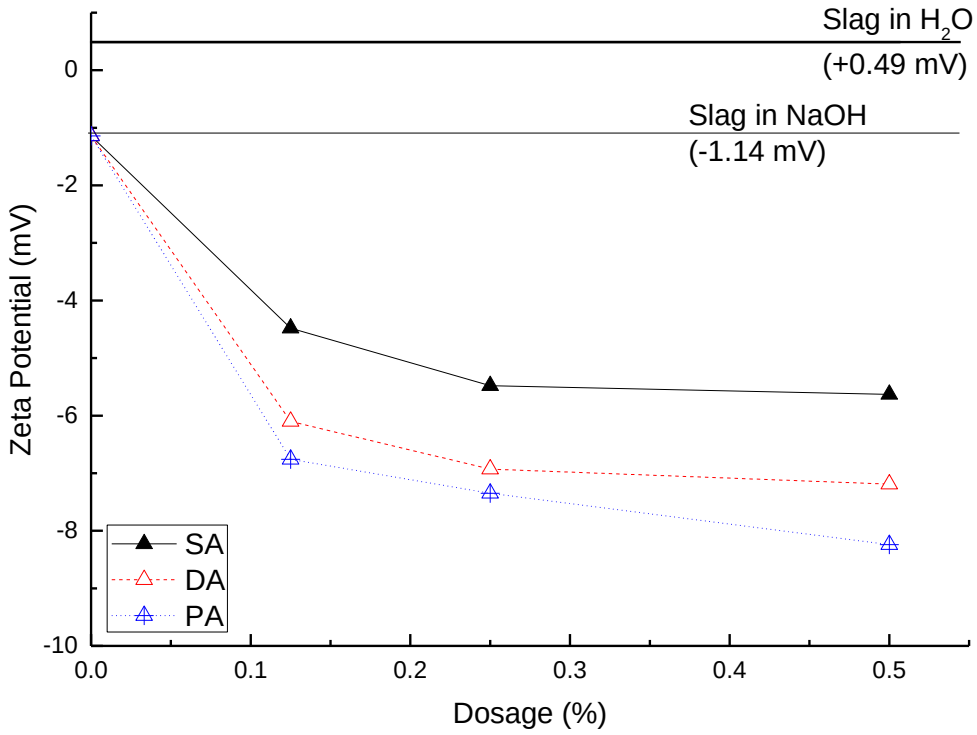

(b) NF

Fig 5.4 Effects of different addition methods of LS on zeta potential of NaOH-activated slag paste: (a) LS and (b) NF

As reported in the previous section, there exists a competitive adsorption between the SP and the activator. Previous research reported that the addition of an anionic polymer reduced the zeta potential of the slag suspension (Nägele and Schneider, 1989b). The results suggest that the negatively charged polymer could be adsorbed onto and occupy the active site on the surface of slag particles. Similarly, the addition of negatively charged NaOH activator also reduces the zeta potential of slag particles. Therefore, the results indicate that the OH^- hydrolysed from NaOH activator occupied the slag surface. Therefore, adding SP and NaOH simultaneously can also introduce the competition between negatively charged SP and OH^- ions.

Linking to the adsorption results described in the previous section, lower zeta potential was expected from the separate addition methods than that from the simultaneous addition, as the amount of SP adsorbed by the latter was lower. In both LS and NF, the highest adsorption amount of SP with the highest magnitude of zeta potential was observed in the paste by *PA*. It can therefore be predicted that the best dispersion could be observed in *PA*.

As discussed in Section 2.2.4 and 2.2.5, the more SPs are adsorbed, the lower the zeta potential. The separate addition methods increase the adsorption of SPs on the slag surface and subsequently reduce the zeta potential. Therefore, they could offer an opportunity to improve the workability of NaOH-activated slag.

5.3.3 Summary

The effects of different addition methods of both LS and NF on the adsorption and the zeta potential of NaOH-activated slag were investigated in this section. Based on the results, the following points can be summarised:

- The adsorption behaviour of both LS and NF on the slag surface can be characterised by Langmuir isothermal adsorption behaviour. The electrostatic attraction between the SP and the slag particles was identified as the main adsorption mechanism.
- The addition of NaOH activator reduced the adsorption of SPs on the slag surface, which could be attributed to the competition between the negatively charged SP and NaOH activators.
- The separate addition methods, in terms of *PA* and *DA*, increased the adsorption of SP on the slag surface by avoiding the competitive adsorption between the SP and the activator, with a higher adsorbed amount in *PA*.
- The addition of SP decreased the zeta potential of NaOH-activated slag paste. Lower zeta potential values were observed in the paste prepared by *DA* and *PA*, with PA even lower than DA.

5.4 Effects of different addition methods of PC-based SP on early age properties of NaOH-activated slag

The aim of the addition of superplasticiser is to improve the fresh properties, such as minislump and rheological properties. The influence of different SP addition methods on the fresh properties of NaOH-activated slag, in terms of minislump and rheological properties, linked with interaction of SPs (the relationship among them is illustrated in ***Table 5.3***), is reported in this section. In addition to workability and

rheology, the setting time of NaOH-activated slag is determined and the early hydration of NaOH-activated slag is also monitored by ICC.

Table 5.3 Relationship among adsorption, zeta potential, workability and rheological properties

	Adsorption	**Magnitude of Zeta Potential**	**Minislump**	**Yield Stress**	**Plastic Viscosity**
Adsorption					
Magnitude of Zeta Potential	+				
Minislump	+	+			
Yield Stress	-	-	-		
Plastic Viscosity	-*	-*	N/A	N/A	

Note: '+'stands for positive correlation, '-'for negative correlation, and N/A for not available.
* The effect on plastic viscosity varies among paste, mortar and concrete. The above relationship is established based on paste.

5.4.1 Workability (Minislump)

The initial minislump tests of NaOH-activated slag under the different addition methods of LS and NF are illustrated in ***Fig 5.5 (a)*** and ***(b)***. The addition of both SPs increased the minislump of NaOH-activated slag paste, which indicates that the addition of LS and NF SPs can improve the workability of NaOH-activated slag.

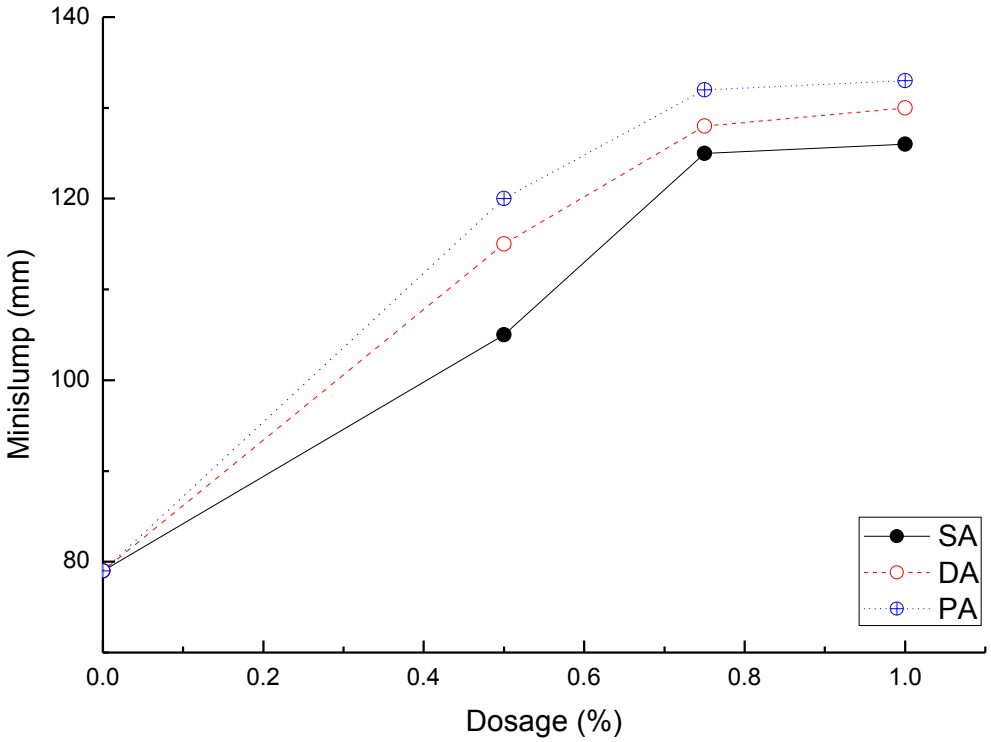

(a) LS

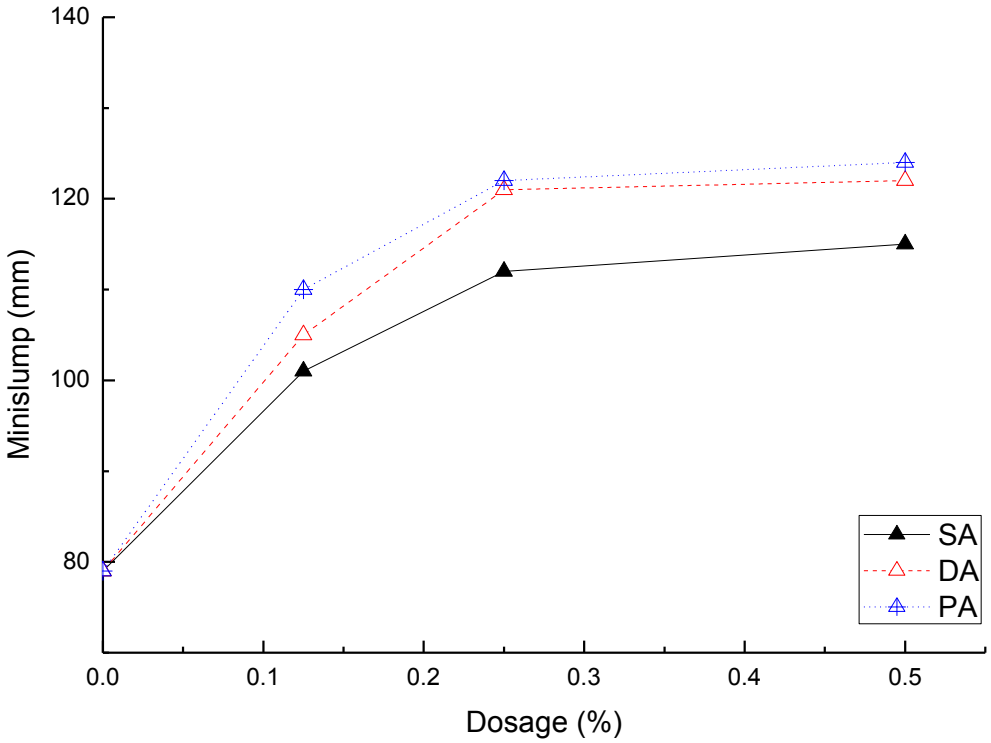

(b) NF

Fig 5.5 Effects of different addition methods of PC-based SPs on initial minislump of NaOH-activated slag paste: (a) LS and (b) NF

In the case of simultaneous addition (*SA*), the minislump of the NaOH-activated paste increased from 80mm (with LS dosage of 0%) to over 100mm at the LS dosage of 0.5%, and further increased to 120 mm after increasing the LS dosage to 0.750%. However, the increase was not significant for the LS dosages higher than 0.750%. On the other hand, the addition of NF increased the workability of NaOH-activated slag by enlarging the minislump spreads from 80mm (without SP) to more than 100mm at the NF dosage of 0.125%. It further reached a minislump spread of 112 mm when the NF dosage was increased to 0.500%. A plateau was also observed at a higher NF dosage (>0.250%), which indicates that the saturation dosage of NF is 0.250%. A similar saturation dosage can be identified at 0.750% for LS in Fig 5.5 (a). This correlated well with the saturation dosage of the adsorption test (***Fig 5.2***). It should be highlighted that after reaching the saturation dosage, no more SP could be adsorbed on the surface of slag, indicating that the effectiveness of SP was close to the maximal limitation (Yang *et al.*, 2013).

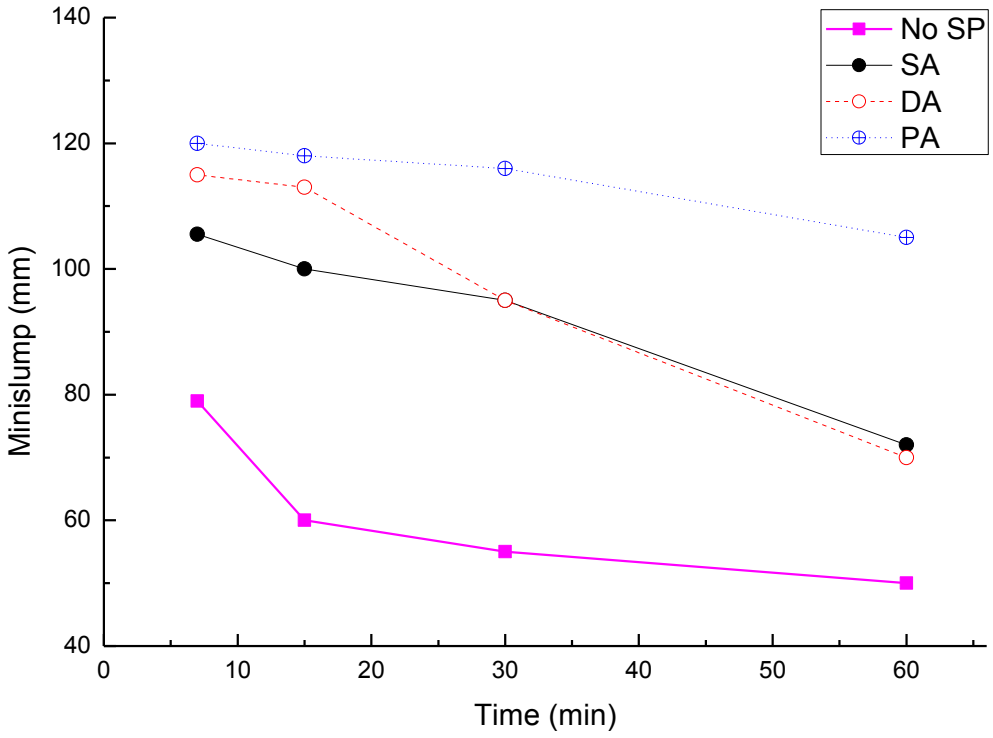

(a) 0.500% LS

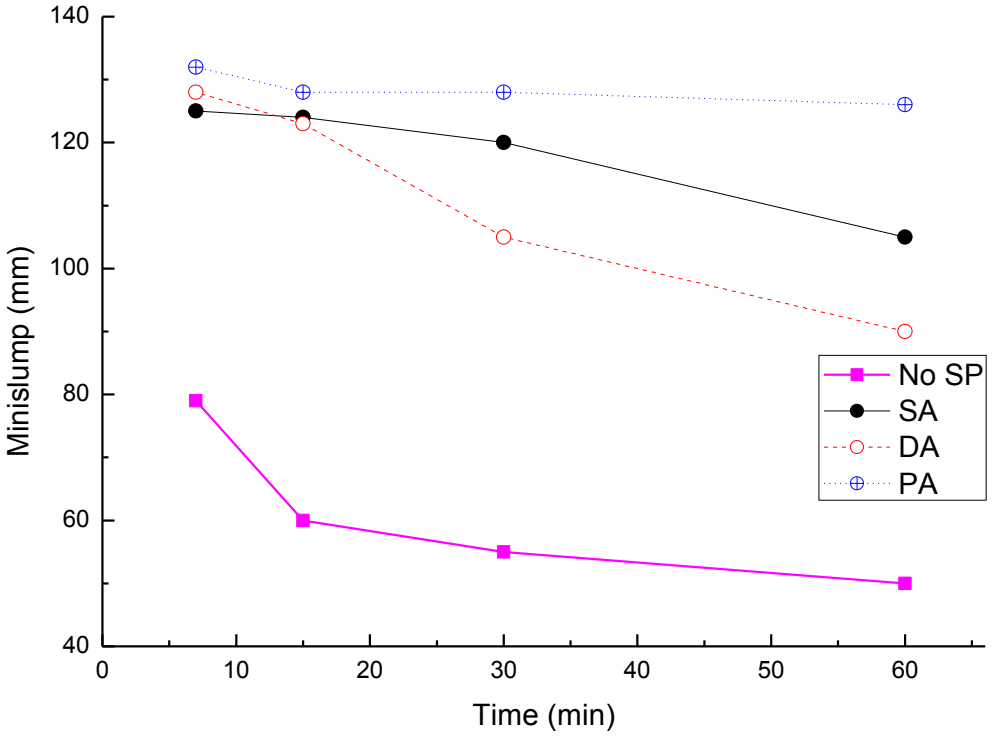

(b) 0.750% LS

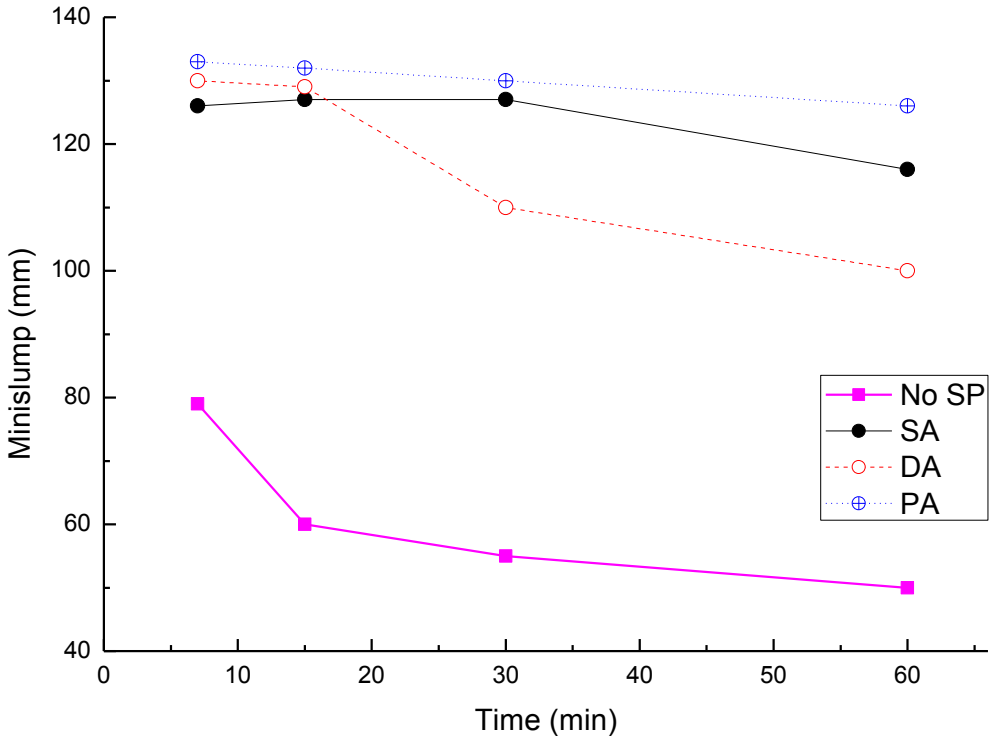

(c) 1.000% LS

Fig 5.6 Effects of LS on minislump loss of NaOH-activated slag paste under different addition methods

Compared to simultaneous addition, regardless of SP type, a further improvement of minislump can be observed from both *PA* and *DA*. The spread diameter of the minislump obtained from both *PA* and *DA* addition methods was at least 10 mm greater than that of the *SA* method (approximately 10% improvement), with *PA* higher than *DA* in all the cases. The results correlated well with the adsorption results presented in section 5.3.1 and the zeta potential results presented in 5.3.2. These results indicate that when the SPs and NaOH were added separately, due to the reduced competition, more SP can be adsorbed on the slag surface (particularly so in the case of *PA*), which further reduces the negative zeta potential and disperses the slag grains better, thus, improves the workability.

The change of the minislump was monitored over time in order to assess the effect of different addition methods on the workability retention of NaOH-activated slag. The results are shown in ***Fig 5.6 (a)*** to ***(c)*** for LS and ***Fig 5.7 (a)*** to ***(c)*** for NF. The three dosage levels were selected to represent the dosage below, around and over saturated point of SP (refer section 4.4.1) for each SP, respectively.

In the case of LS added by *SA*, despite the improved initial minislump, the minislump retention in the first 60 minutes was poor, especially at lower SP dosage. For example, when the dosage was 0.500%, the initial minislump reached a high value of 105mm. However, the minislump dropped to less than 72mm at 60min. Within 60 min, 33% minislump was lost. By increasing the LS dosage to 1.000%, an even higher initial minislump value of approximately 125 mm was obtained with less than 10 mm lost after 60 minutes, representing 8.00% minislump loss. Comparing the different addition methods, the best minislump retention was observed from *PA.* Moreover, it can be seen from ***Fig.5.6*** that both *SA* and *DA* experienced a quick minislump loss after 30 minutes at a lower LS dosage. When the dosage was increased to 1.000%, the quick minislump loss was still observed in *DA*.

In the case of NF-superplasticised NaOH-activated slag, it seems that at the lower SP dosage the NaOH-activated slag paste suffered more serious minislump loss. For example, at 0.125% of NF (by *SA*), the minislump decreased from 101 mm to less than 60 mm in the first 30 minutes and was gradually reduced to approximately 50 mm at 60 minutes, at which point the paste had almost lost the fluidity. However, the serious minislump loss was relieved by increasing the SP dosage. Comparing the SP

addition methods, a more serious minislump loss was observed in the paste prepared by the separate addition methods than SA at lower SP dosage, but at the higher dosage (>0.250%), the separate addition of NF and NaOH demonstrated better minislump retention of the NaOH-activated slag paste.

As discussed in Chapter 2, the SPs are consumed by the intercalation, coprecipitation or micellisation within the early hydration product which can reduce the efficiency of SPs and may lead to the slump loss of cement and concrete. This is particularly noticed from linear polymers, such as NF (Flatt and Houst, 2001). Comparing the two types of SPs investigated in the current study, LS provided better workability retention than NF. For example, under the *SA*, the minislump loss during the first 60 minutes was 27 mm with NF (0.500%), while only 10 mm minislump loss was observed in NaOH-activated slag with LS (1.000%). The reason could probably be due to the different configuration in water. As discussed in Section 2.2, after being dissolved in water, the LS is hydrolysed and manifests as an organic micro gel, while NF forms a linear loop (Hewlett, 2004, Kim et al., 2000a). The micro gel not only offers electrostatic repulsion effects, but also provides some steric repulsion (Matsushita and Yasuda, 2005). As discussed previously, the workability retention can be improved by introducing next generation SPs containing side chains, which provides steric repulsion effect (Winnefeld *et al.*, 2007). Unlike the linear polymer, the side chains can still physically prevent the aggregation between the particles even after being consumed by early hydration product.

The effects of different addition methods on the workability of NaOH-activated slag are also linked to the early hydration of NaOH-activated slag, which will be discussed in Section 5.4.4.

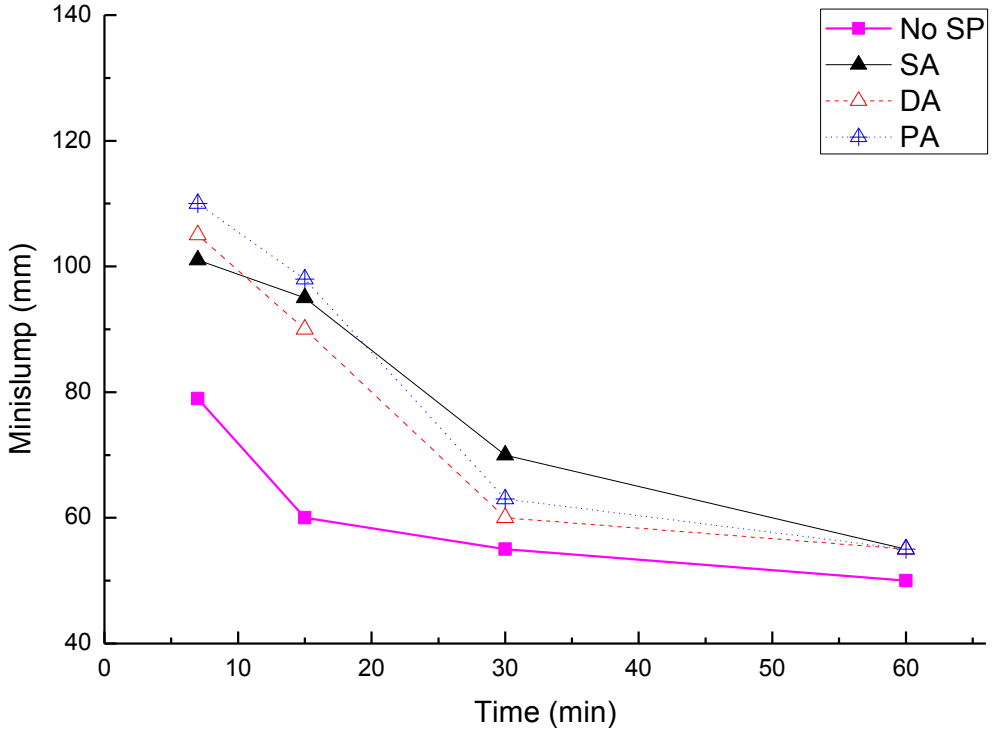

(a) 0.125% NF

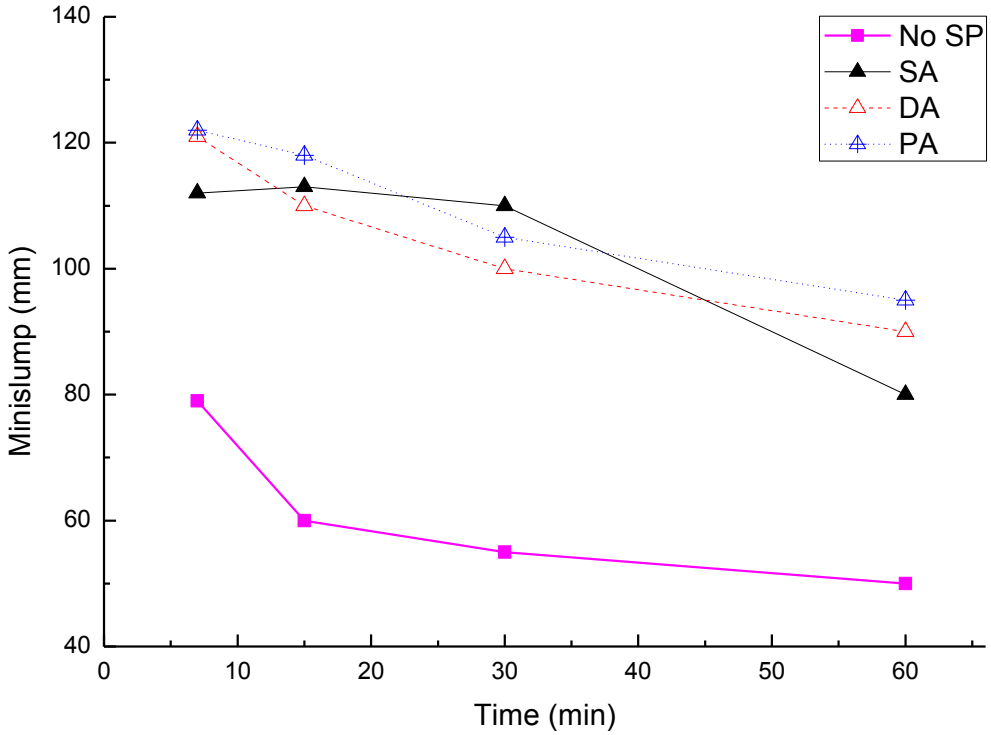

(b) 0.250% NF

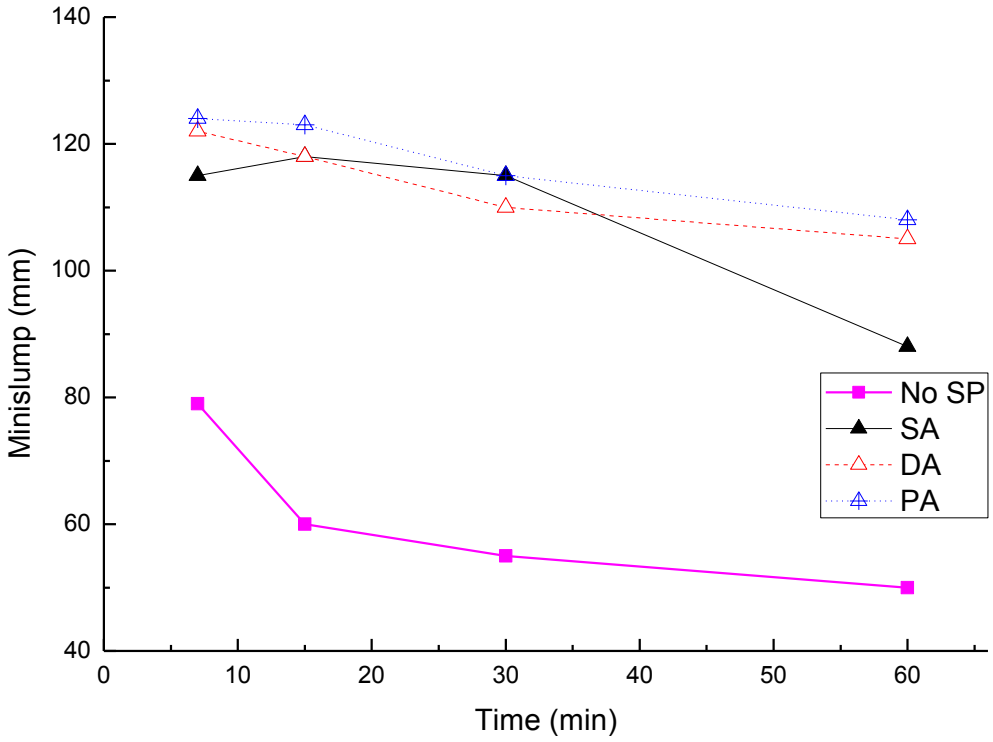

(c) 0.500% NF

Fig 5.7 Effects of NF on minislump loss of NaOH-activated slag paste under different addition methods

5.4.2 Rheological properties

The initial yield stress of NaOH-activated slag pastes based on the calculation from Bingham model is presented in ***Fig 5.8 (a)*** and ***(b)***. The yield stress, which is the intercept from the Bingham equation (Chapter 2, ***Equation 2.3***), can be considered as the transition point below which the substance behaves as a solid and above which it becomes fluid (Lewis *et al.*, 2000), resulting from the attractive interparticle forces responsible for the flocculation (Banfill, 1994, Barnes and Walters, 1985). Therefore, better workability is achieved with lower yield stress. Compared with that of the reference mixes (i.e. the mix with no SP), the yield stresses of NaOH-activated slag paste with SPs were significantly reduced, and the yield stress was also reduced with the increase of the SP dosage, especially so when adding SP and activator separately (both *PA* and *DA*), which corresponded well to the minislump results.

In the case of LS, the presence of LS highly reduced the yield stress from about 21 Pa to below 5 Pa under the SA method when the LS dosage was over 0.500%,

indicating that the addition of LS can improve the workability of NaOH-activated slag. In the case of NF, similarly, it is apparent that the yield stresses of the AAS pastes decreased from 21 Pa to below 6 Pa under the SA method when its dosage was 0.125%, and further reduced with increasing NF dosage. However, the further reduction of the yield stress by increasing SP dosage was not significant. Notably, negative yield stress was observed in the NaOH-activated slag, for example, in the case of PA, which cannot happen in reality and also conflicts with the common rheology science. The reason for the negative yield stress could be due to the change of the rheological properties from near Bingham to shear thickening. Such change of the rheological behaviour has been observed in Portland cement system in the presence of SPs (Feys et al., 2009, Cyr et al., 2000). In AAS, the addition of LS under different addition methods in waterglass activated slag was also found to be able to change the rheological behaviour from near Bingham to shear thickening (Ren et al., 2013). Although the rheological behaviour of NaOH-activated slag has been identified as near Bingham (Palacios et al., 2008), the addition of SPs could change its rheological behaviour. Therefore, negatively yield stress was generated from the regression of flow curve by using linear Bingham model (refer to ***Equation 2.4***). Thus, the advanced model, i.e. Herschel-Bulkley model, has to be employed to describe this rheological behaviour. However, in the thesis, as mentioned in section 2.3.1.1 and section 4.5.2.2, in order to simplify he scenery and make it consistent comparable, the yields stress regressed by the Bingham model is used. Nonetheless, the reduced yield stress could still indicate that lower interparticle force and better dispersion of slag grains were achieved.

From ***Fig. 5.8***, it also can be noticed that when the separate addition methods were employed, both the LS and NF modified NaOH-activated slag demonstrated lower yield stress than the corresponding SA method. In particular, it can be seen that the PA method showed the lowest yield stress, which correlates well with both the adsorption and zeta potential results. This, again, indicated that by avoiding the competitive adsorption through separate addition of SP and activator is an effective way to improve the workability of SP modified NaOH-activated slag system.

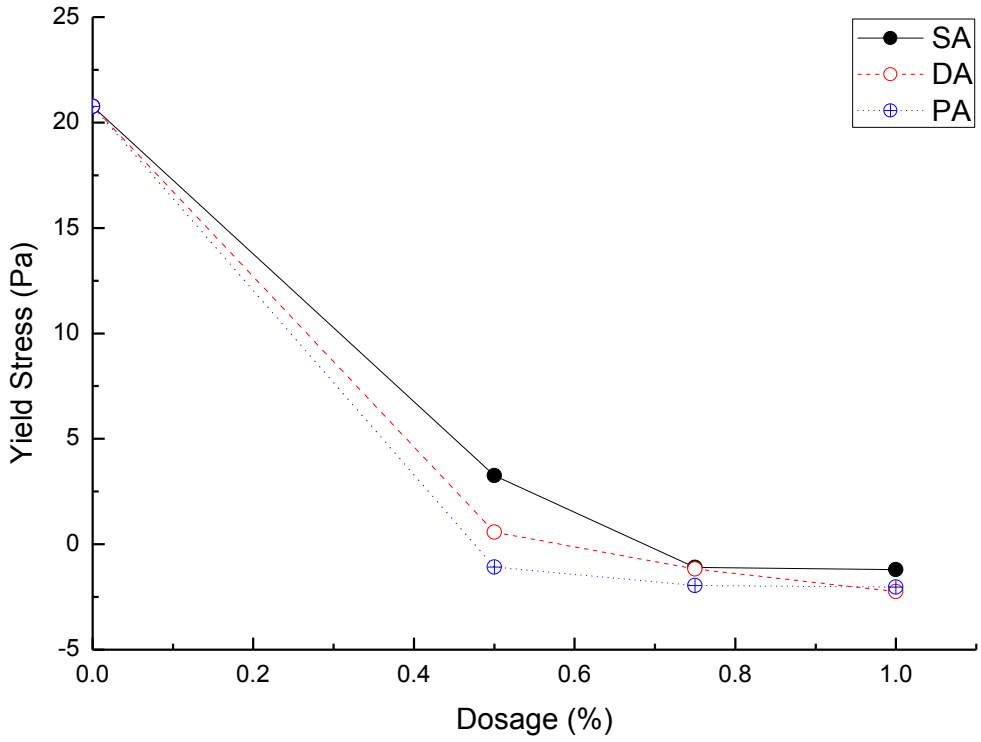

(a) LS

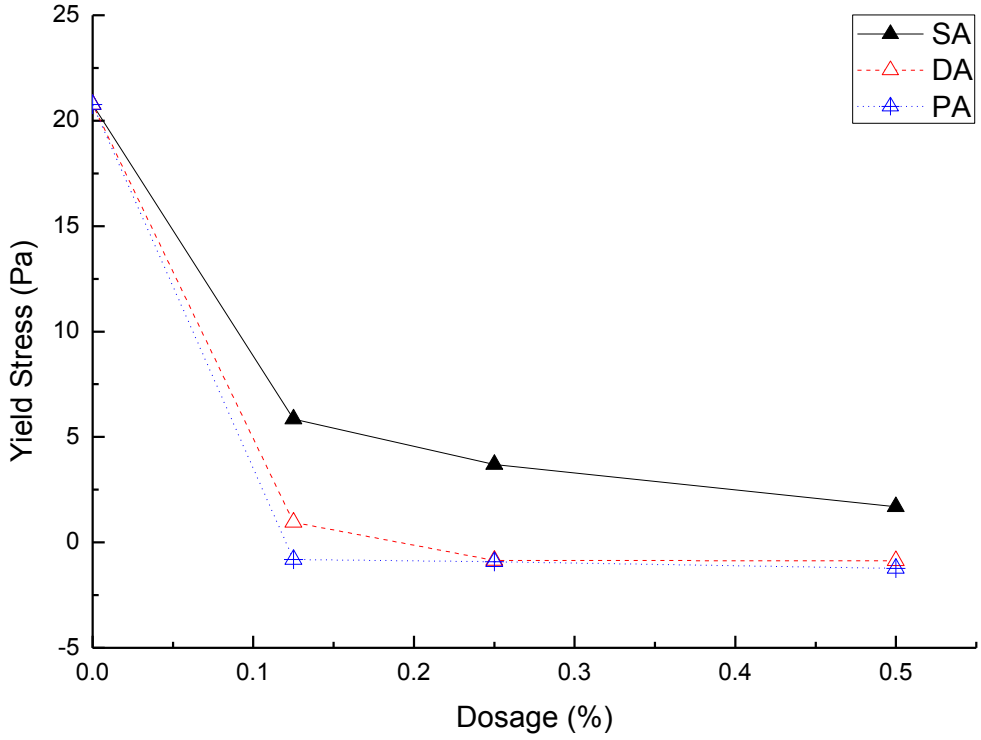

(b) NF

Fig 5.8 Effect of different addition methods of PC-based SPs on initial yield stress of NaOH-activated slag paste: (a) LS and (b) NF

The effects of different SP addition methods of LS and NF on the initial plastic viscosity of NaOH–activated slag pastes are plotted in ***Fig 5.9 (a)*** and ***(b)***, respectively. The plastic viscosity depends largely on the volume fraction of the solid particles and the packed density which could somehow reflect the flocculation state in the paste and the resistance of the flow (Struble and Lei, 1995). Similar to the effects on the yield stress, it is obvious from ***Fig 5.9*** that the addition of SP highly reduced the plastic viscosity of NaOH-activated slag paste. Similar finding has also been reported in the PC paste with SPs (Wallevik, 2006).

In the case of LS, the addition of LS under all the addition methods significantly reduced the plastic viscosity of NaOH-activated slag. However, with the increase of the LS dosage, less reduction on the plastic viscosity was observed. For example, under the *SA* method, the plastic viscosity of NaOH-activated slag with LS was decreased from 1.92 Pa s (no SP) to 0.54 Pa s at 0.500% dosage, and was further decreased to approximately 0.25 Pa s. Similarly, in the case of NF, the addition of NF under all the addition methods also reduced the plastic viscosity of NaOH-activated slag paste, with less further reduction observed by increasing the NF dosage. For instance, under the SA method, the addition of NF reduced the plastic viscosity of NaOH-activated slag from 1.92 Pa s to 0.87 Pa s at 0.125% dosage, and further decreased to 0.47 Pa s by increasing the dosage of NF to 0.500%.

When adding the SPs and the NaOH activator separately, particularly at the lower SP dosage, the plastic viscosity was even further reduced compared to the SA method, with *PA* always giving the lowest value in both the LS and NF systems. For example, at the LS dosage of 0.500%, the plastic viscosity of NaOH-activated slag by *DA* and *PA* were 0.22 Pa s and 0.20 Pa s, respectively, which is lower than the plastic viscosity under the *SA* method (0.54 Pa s). In a similar way, the plastic viscosity of the NF superplasticised NaOH-activated slag mixed by *DA* and *PA* were 0.28 Pa s and 0.26 Pa s, which is lower than that by *SA* (0.47 Pa s).

The decreased plastic viscosity could be due to the modification made to the flocculation, which changed the way that the shear concentrated in the media among the slag grains and/or flocs (Bey et al., 2014). As discussed previously, the separate addition provides a higher adsorption and a higher magnitude of zeta potential, which induces more electrostatic repulsion force. Consequently, better dispersion of

the slag particles is achieved and the flocculation is broken down. Therefore, lower plastic viscosity is identified from *DA* and *PA*.

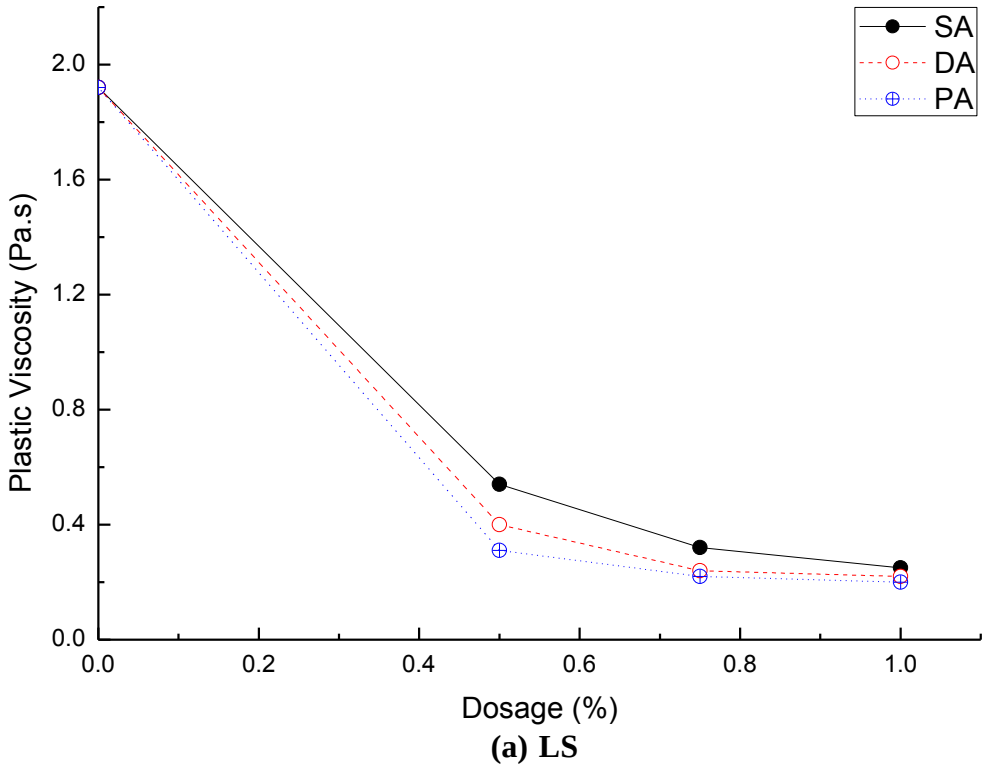

(a) LS

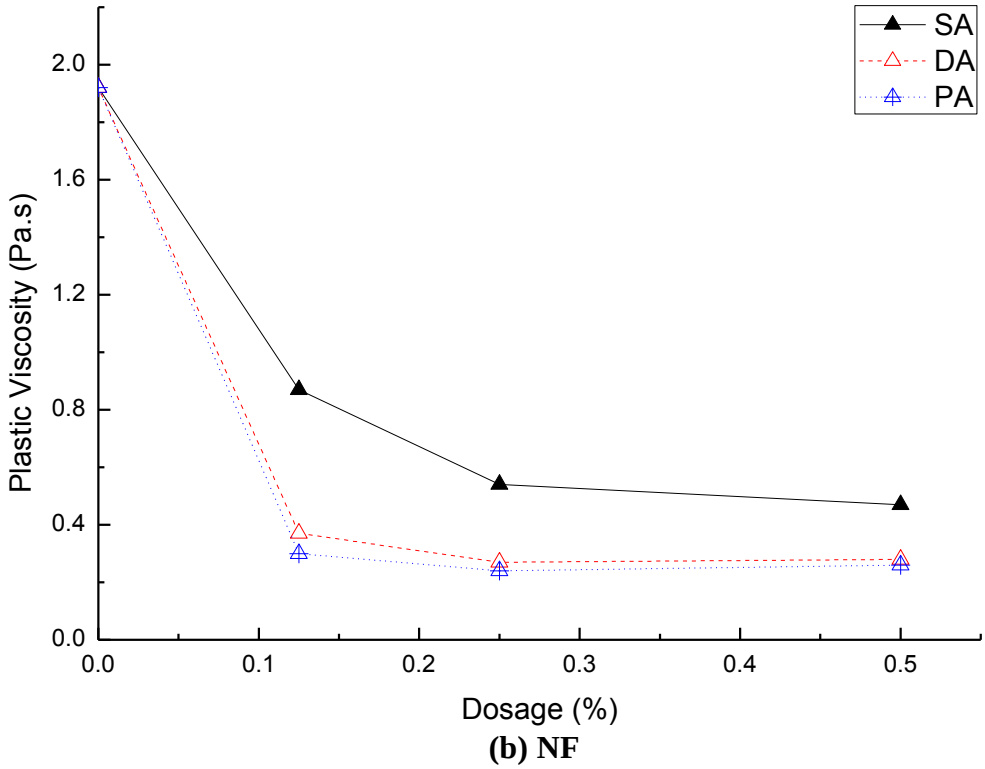

(b) NF

Fig 5.9 Effect of different addition methods of PC-based SPs on initial plastic viscosity of NaOH-activated slag paste: (a) LS and (b) NF

The effects of LS and NF dosages on the initial yield stress and the initial plastic viscosity under different addition methods are further presented by following the vectorised-rheograph approach as shown in ***Fig 5.10 (a)*** and ***(b)***, respectively. As discussed in section 2.3.3.1, the rheograph has been identified as a useful tool to analyse the change of the yield stress and plastic viscosity under the change of material properties, such as admixture, composition etc.

In the case of LS (***Fig 5.10 (a)***), with the increase of the LS dosage under all the addition methods, both initial yield stress and initial plastic viscosity of NaOH-activated slag paste moved toward the lower value, which results in the relocation of the data points to the bottom left of the rheograph. Similarly, the data points of NaOH-activated slag paste with NF were relocated to the bottom left of the rheograph (***Fig 5.10 (b)***). This change of the rheograph pattern reflected that the initial yield stress and the initial plastic viscosity of NaOH-activated slag were reduced by adding SPs under all the addition methods. The results are similar to the trend of SPs employed in PC paste (Wallevik and Wallevik, 2011).

It should be noted that negative yield stress was identified in both ***Figs 5.10 (a)*** and ***(b)***. As mentioned in Chapter 2, the negative yield stress does not have any physical meaning, and its occurrence is mainly due to the adoption of linear Bingham model to fit the non-linear shear-thickening flow curve, which could be avoided by fitting the shear-thickening flow curve with non-linear modified Bingham model and Herschel-Bulkley model (Ren *et al.,* 2013). However, due to the complex associated with non-linear models, in this thesis, it was decided to use the commonly accepted Bingham model with an attempt only to show the difference in the yield stress when different addition methods and superplasticisers were used.

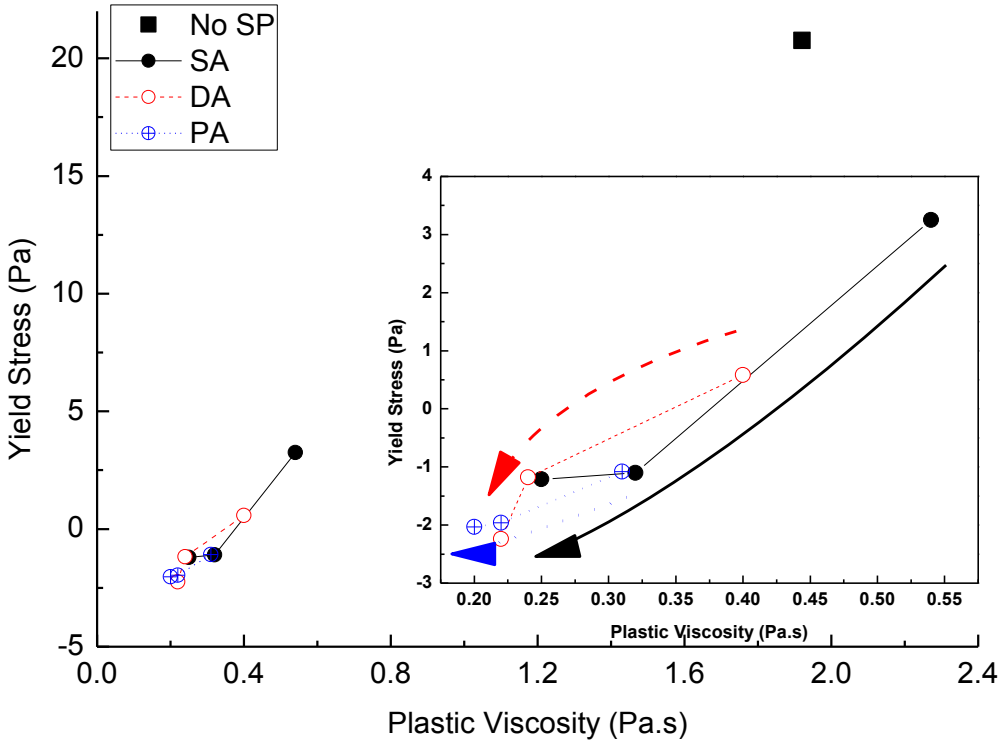

(a) LS

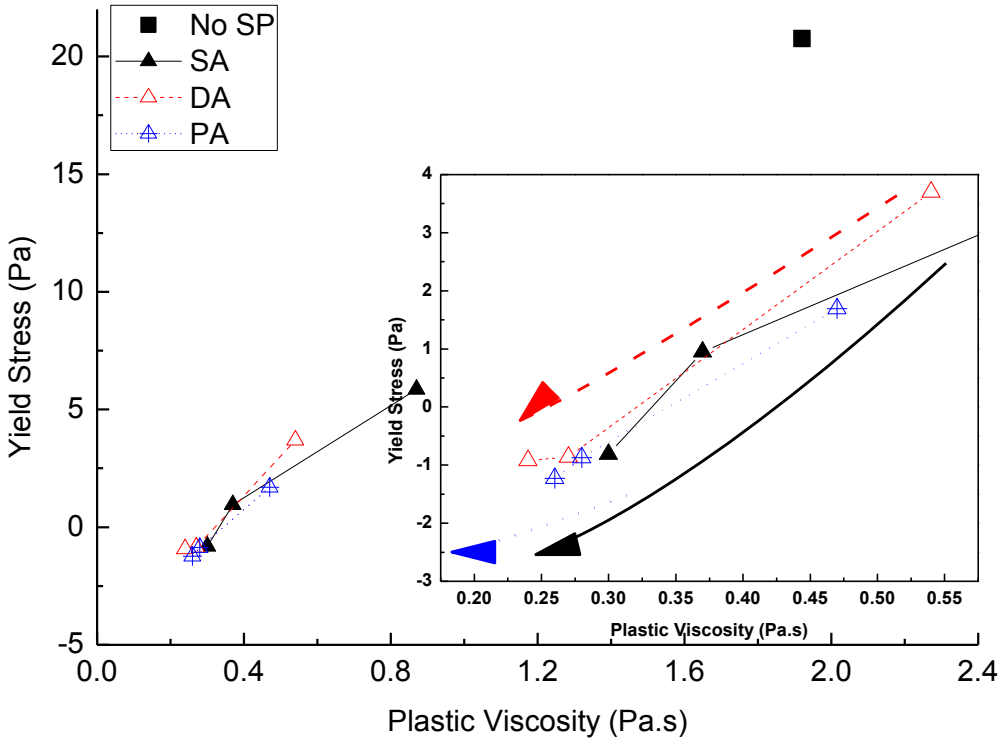

(b) NF

Fig 5.10 Rheograph of NaOH activated slag with SPs at 7 minute (The direction of arrow indicates the increase of SP dosage: (a) LS and (b) NF

When the separate addition methods were applied, both of the initial yield stress and the initial plastic viscosity have been further reduced compared with the SA. For LS, a lower plastic viscosity was observed from the *PA*, and a lower yield stress was obtained also from the *PA*, except at 1.000% dosage. However, compared the three addition methods used, for NF, a lower yield stress with a lower plastic viscosity were observed by *PA*.

As illustrated in ***Table 5.3***, there exist relationships among the adsorption, zeta potential and yield stress. The increasing adsorption of SPs on the slag surface results in a higher magnitude of zeta potential. Subsequently, the lower yield stress of the pastes can be observed. The results reported in this section reveal that, adding SP and activator separately, highly reduced yield stress and plastic viscosity of NaOH-activated slag can be achieved, which are in good agreement with the adsorption results presented in section 5.3.1. Moreover, as discussed previously, the minislump spread is linked to the yields stress, which reflects the flowability of the paste. To further corroborate the minislump results demonstrated in the previous section, the reduced yield stress of NaOH-activated slag by both separate addition methods suggests that the ease for NaOH-activated slag paste to start to flow was increased, which offers better consistency. Moreover, the reduced plastic viscosity by separate addition of SPs could also be attributed to the breakdown of the flocculation of the paste, releasing the entrained water, which then improves the dispersion of the NaOH-activated slag.

The effects of LS on the yield stress and the plastic viscosity of NaOH-activated slag at different time interval are presented in ***Fig 5.11*** and ***Fig 5.12***, respectively. Since the NaOH-activated slag has been identified as a quick-setting cementitious material (Rashad, 2013), to avoid the possible damage to the rheometer, the measurements were only conducted up to 30 minutes. Overall, both of the yield stress and the plastic viscosity of NaOH-activated slag were increased over time. The measurement of the reference NaOH-activated slag mix (i.e. the mix with no SP) at 30 minutes was not possible due to its quick setting. However, the addition of LS allowed the 30 minutes' measurement, which was due to the retardation effect of LS on the hydration of NaOH-activated slag. It can be seen from ***Figs 5.11*** and ***5.12*** that at a lower LS dosage, both the yield stress and the plastic viscosity were obviously

increased during the first 30 minutes under both *SA* and *DA*, while only slight changes were observed in the mixes under *PA*. However, at a higher dosage of 1.000%, both the yield stress and the plastic viscosity of NaOH-activated slag were not noticeably increased.

The effects of the different addition methods of NF on the yield stress and the plastic viscosity within the first 30 minutes of mixing are presented in ***Fig 5.13*** and ***Fig 5.14***, respectively. Both yield stress and plastic viscosity of NaOH-activated slag by *SA* were increased over time. Comparing different addition methods, regardless of the SP dosage, both yield stress and plastic viscosity obviously were increased during the first 30 minutes under *SA*, while only a slight change could be noticed in the mixes prepared by *PA* and *DA*. In particular, the yield stress and the plastic viscosity did not change much over time under *PA*. This could be attributed to the effects of the addition methods on the early hydration of NaOH-activated slag, which will be discussed in Section 5.4.4

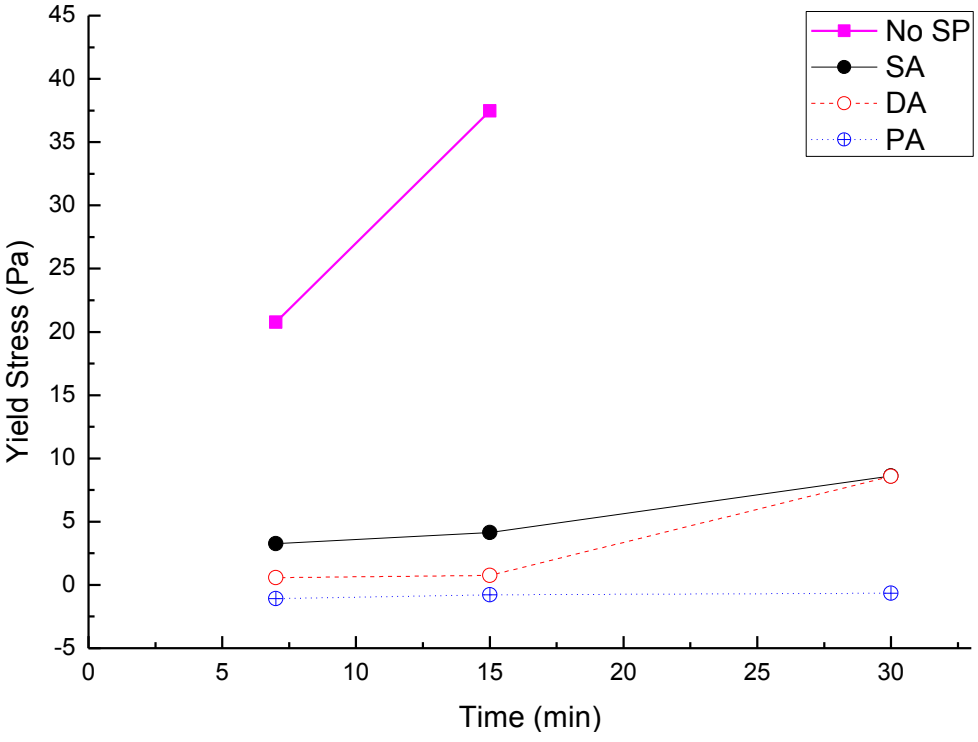

(a) 0.500% LS

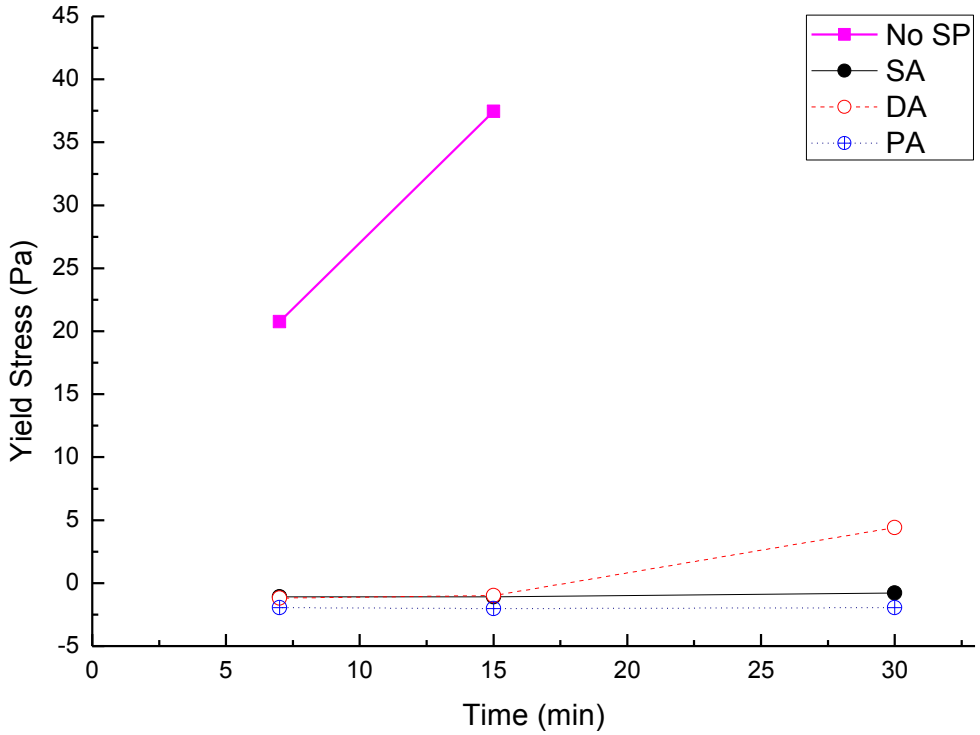

(b) 0.750% LS

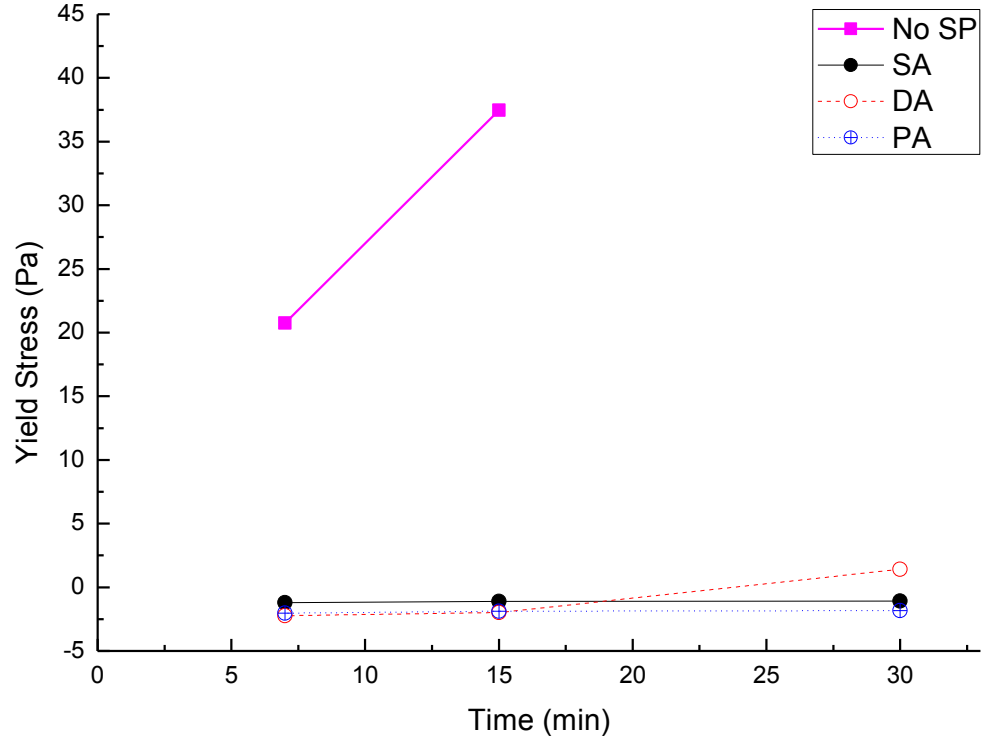

(c) 1.000% LS

Fig 5.11 Effects of LS on yield stress of NaOH-activated slag paste at different time interval under the different addition methods

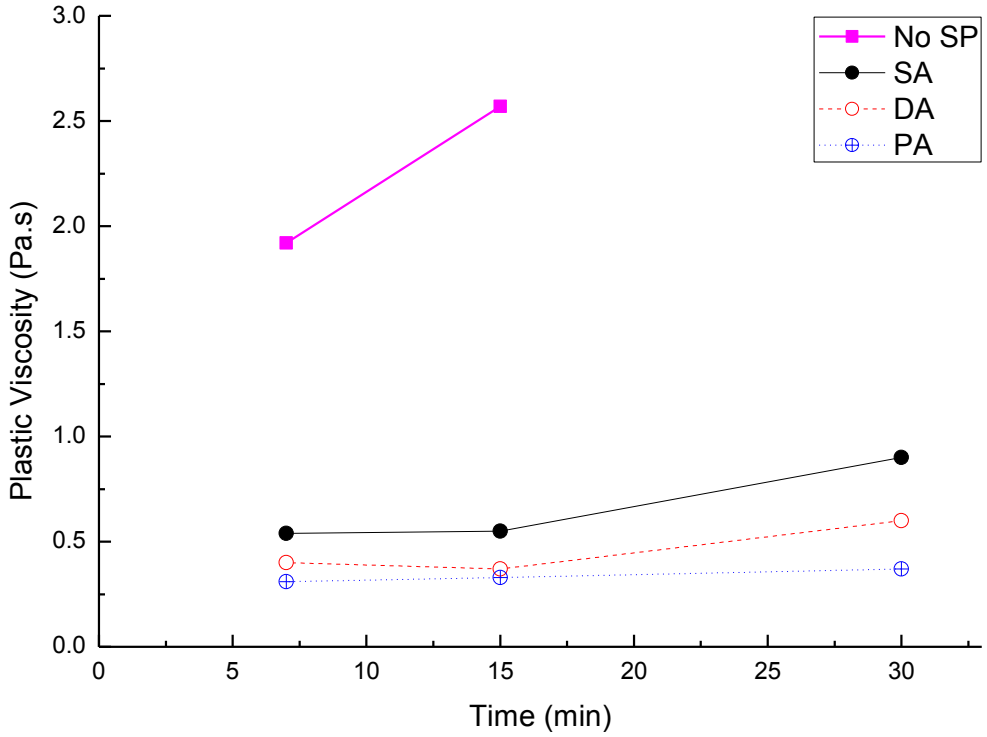

(a) 0.500% LS

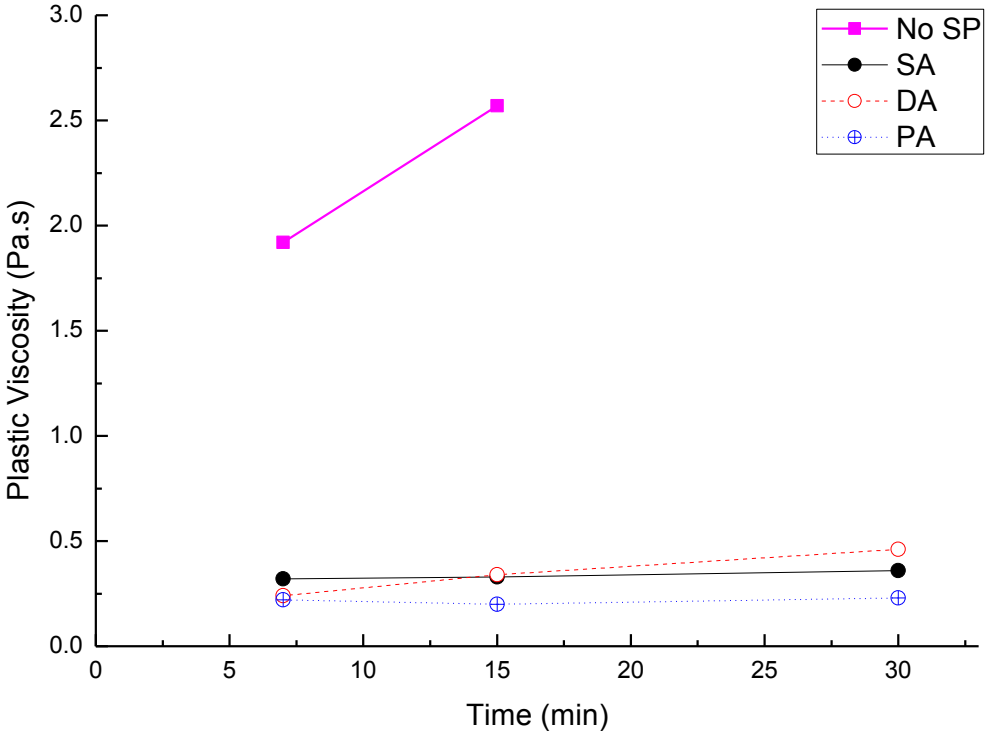

(b) 0.750% LS

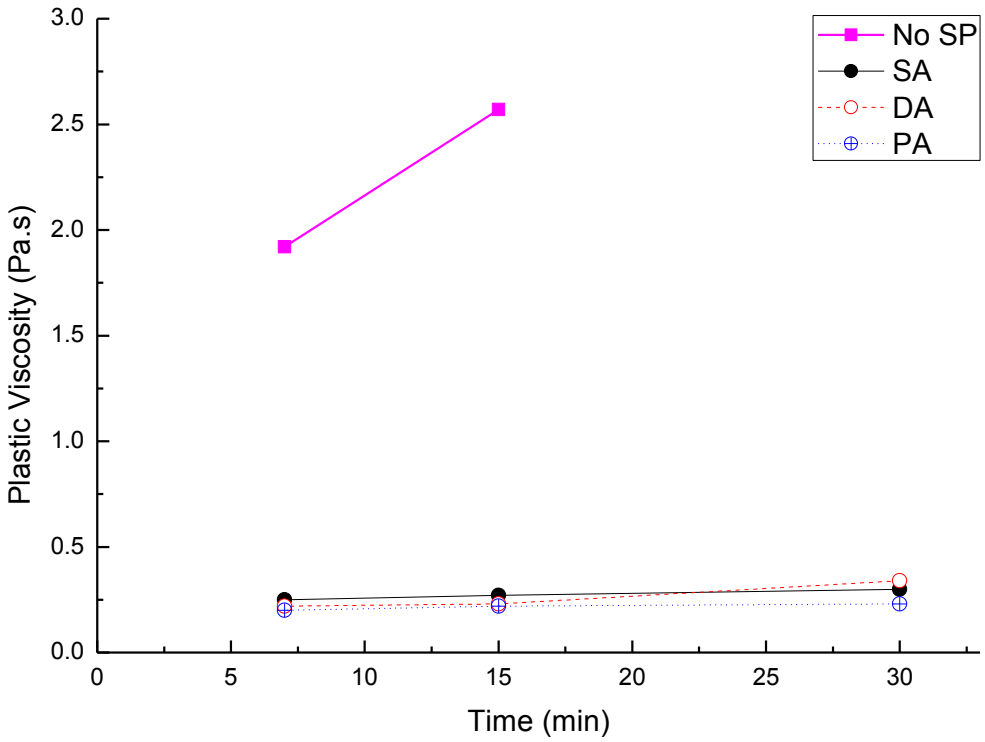

(c) 1.000% LS

Fig 5.12 Effects of LS on plastic viscosity of NaOH-activated slag paste at different time interval under different addition methods

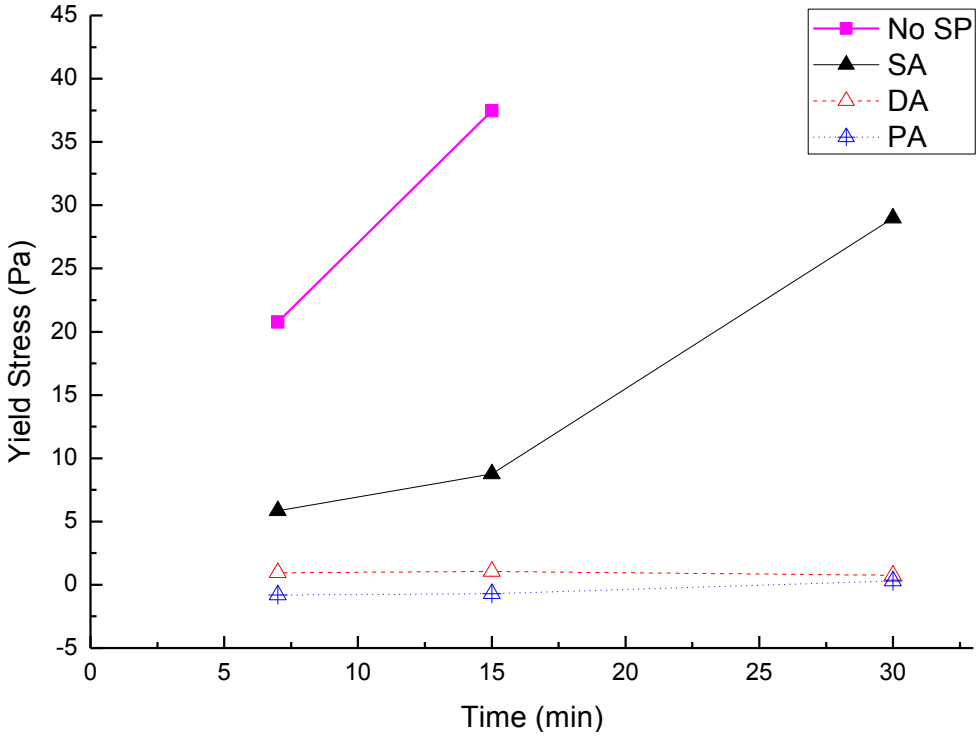

(a) 0.125% NF

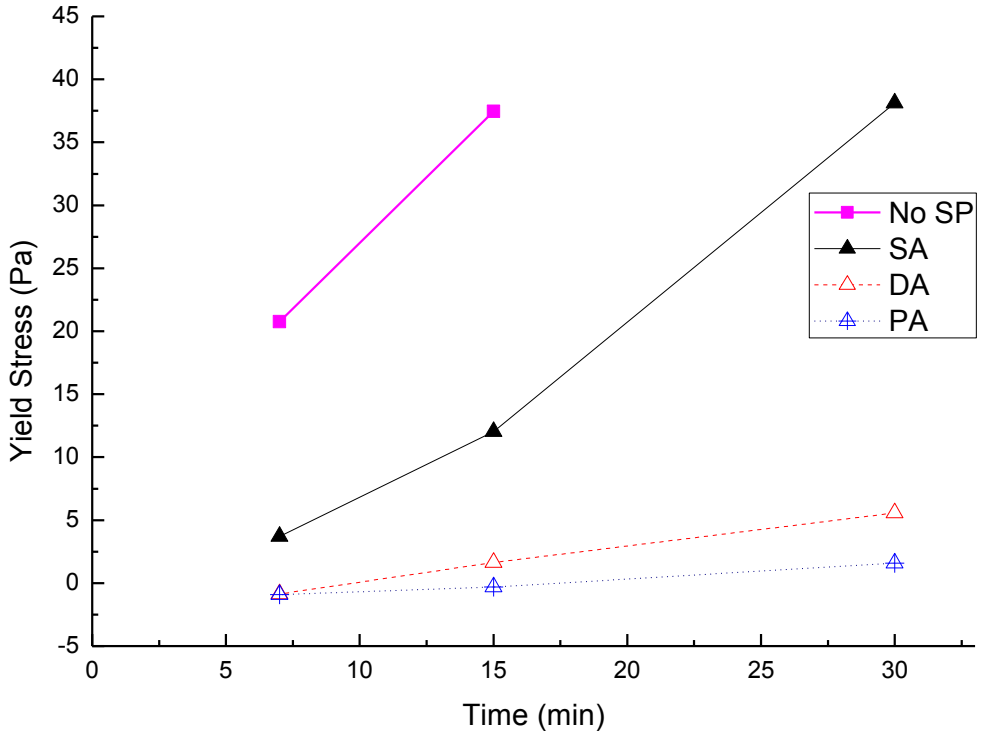

(b) 0.250% NF

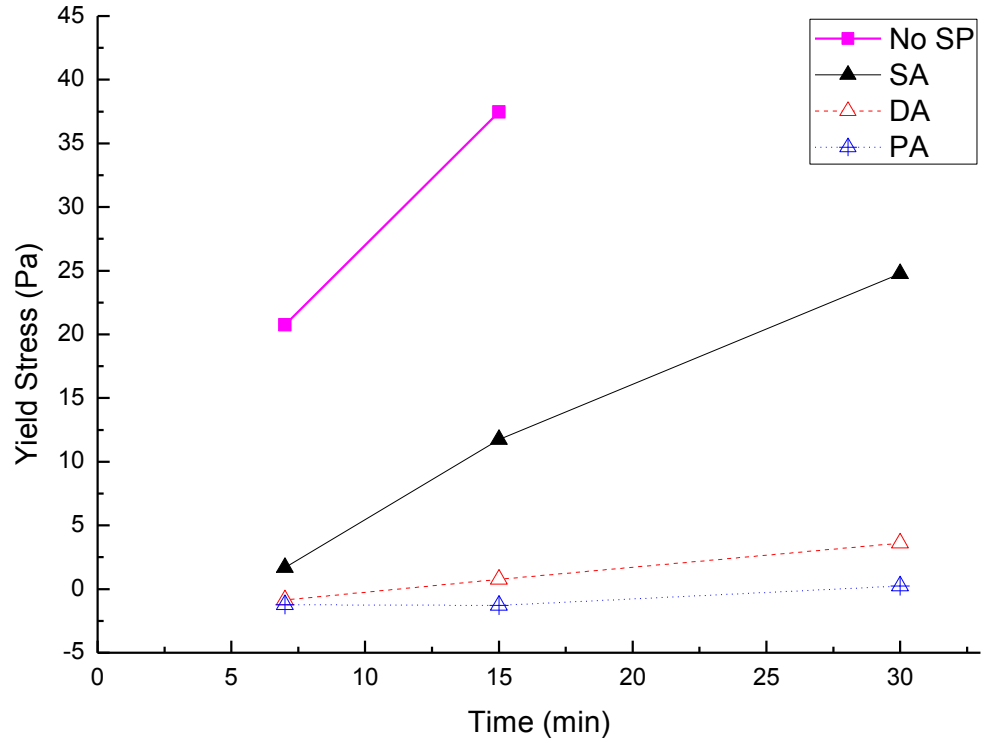

(c) 0.500% NF

Fig 5.13 Effects of NF on yield stress of NaOH-activated slag paste at different time interval under different addition methods

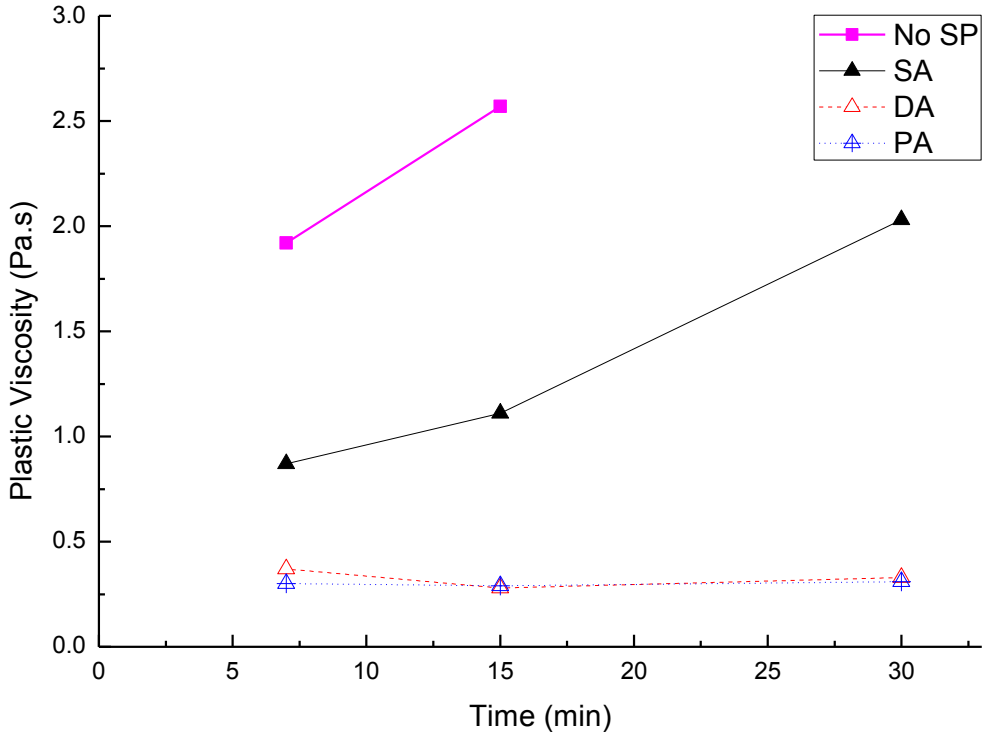

(a) 0.125% NF

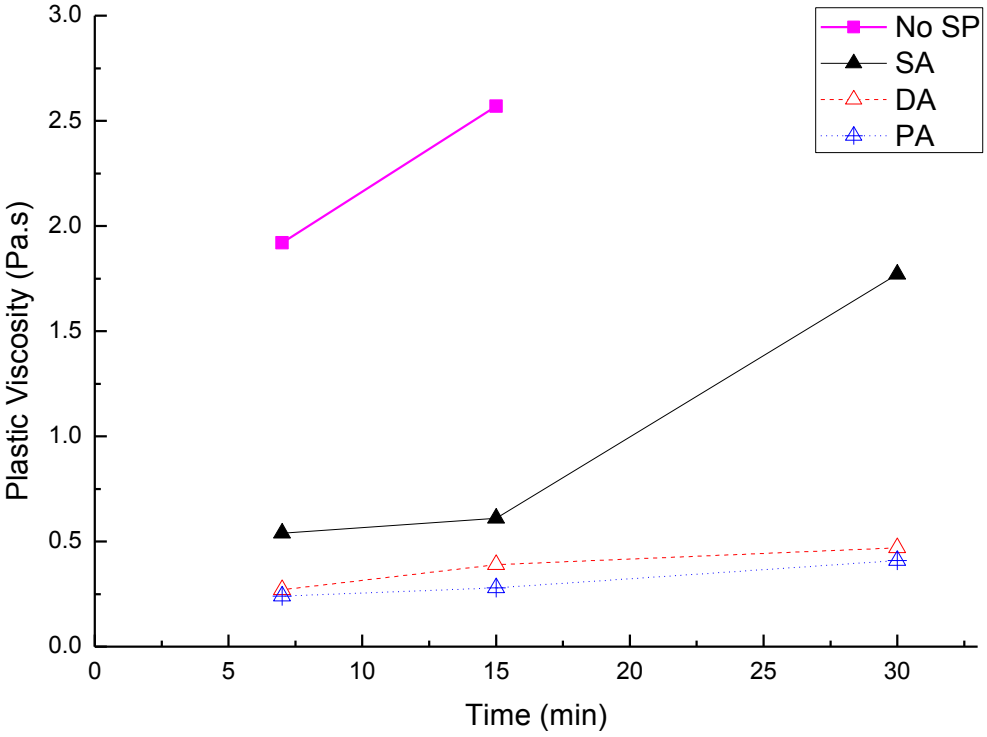

(b) 0.250% NF

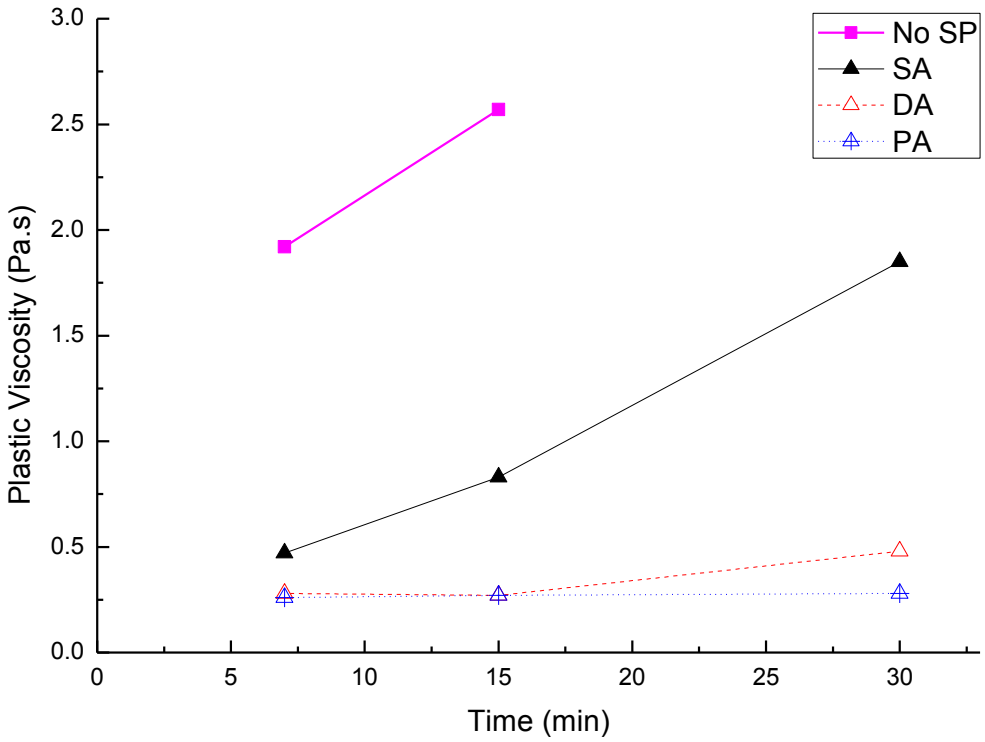

(c) 0.500% NF

Fig 5.14 Effects of NF on plastic viscosity of NaOH-activated slag paste at different time interval under different addition methods

As mentioned in Section 4.1, the minislump has been used as an empirical approach to describe the workability of cementitious pastes, which is very sensitive to the operator. Under this circumstance, minor variation could be induced during the test (Wallevik and Wallevik, 2011). Thus, to scientifically interpret the results obtained from this empirical approach, the relationship between the minislump and the rheology of materials needs to be studied. As discussed in section 2.3.3.1, various researchers have established correlation between slump and yield stress. It could be considered that the workability test is approximate to a special two-point test where the shear rate is zero or near zero, which will establish the theoretical basis where the slump result could be correlated with the yield stress (Wallevik, 2006, Murata and Kikukawa, 1992, Jin, 2002). Thus, based on the experimental results, the relationship between the minislump and the yield stress of NaOH-activated slag in the presence of LS and NF is plotted in ***Fig 5.15*** and the relationship between the minislump and the plastic viscosity is presented in ***Fig 5.16***.

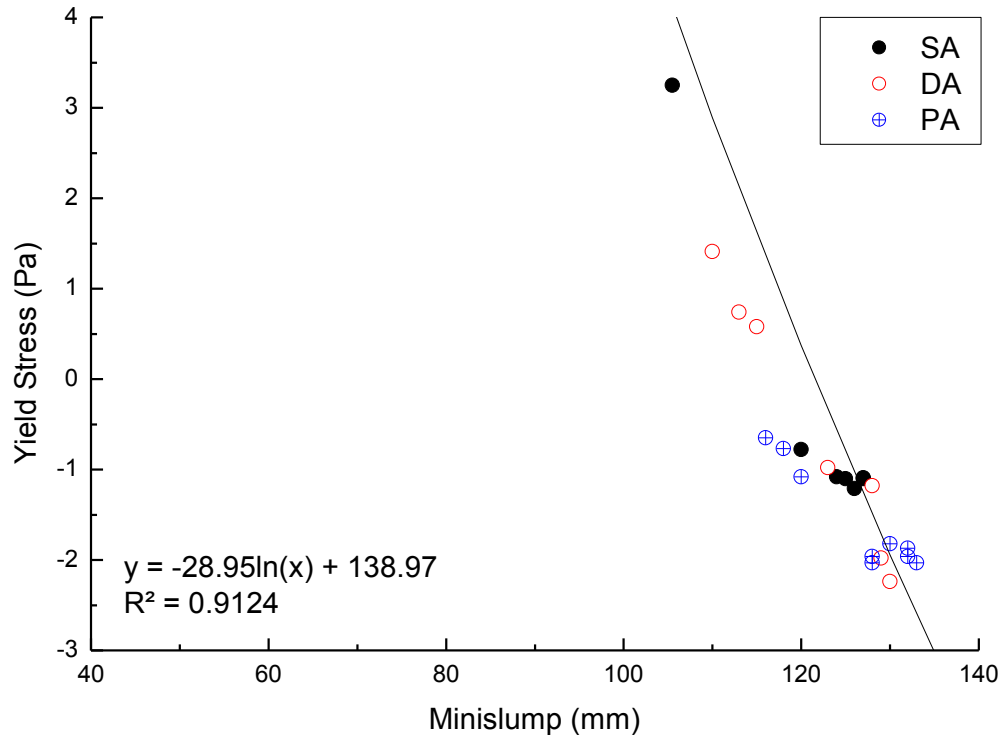

(a) LS

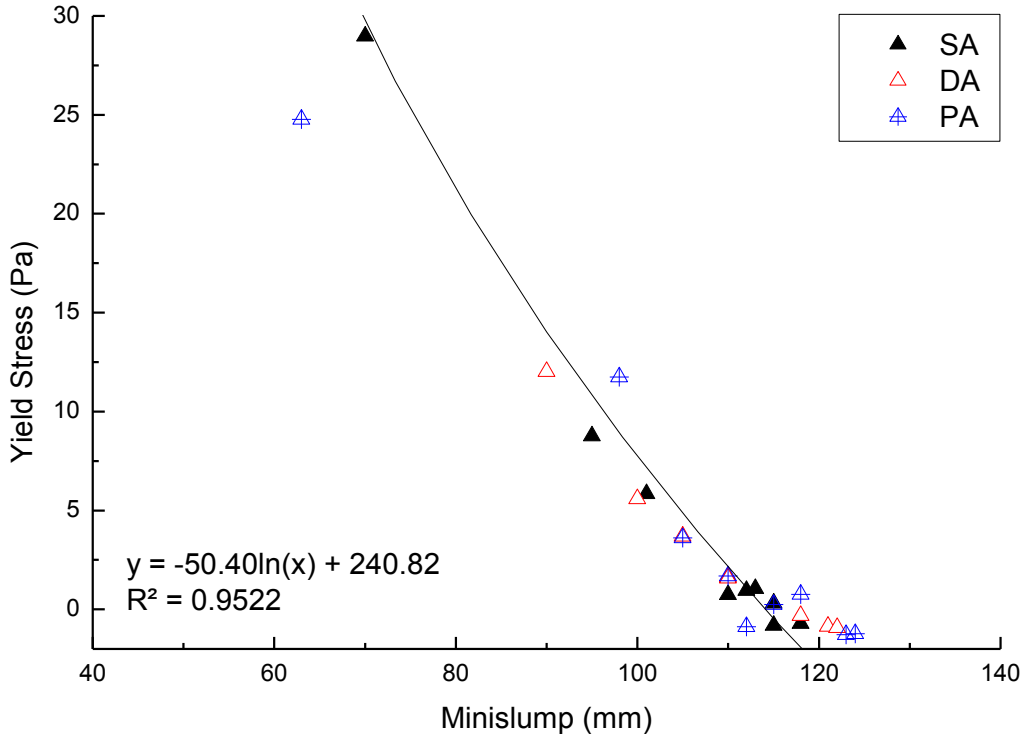

(b) NF

Fig 5.15 Relationship between the minislump and the yield stress of NaOH-activated slag pastes with SPs: (a) LS and (b) NF

In this study, a relationship between the yield stress and the minislump in the presence of LS under three different addition methods are shown in ***Fig 5.15 (a)***. An equation of $\tau = -28.95\ln(x) + 138.97$ with the coefficient (R^2) of 0.9124 was obtained. However, there is no relationship between the plastic viscosity and the minislump with the change of SP dosage (***Fig 5.16 (b)***).

Similarly, as shown in ***5.15 (b),*** a relationship between the yield stress and the minislump spread of NaOH-activated slag with NF is established and an equation of $\tau = -50.40\ln(x) + 240.82$ with the coefficient of 0.9522 was generated. Based on the results, it was again difficult to establish a relationship between the plastic viscosity and the minislump of NaOH-activated slag with NF (shown in ***Fig 5.16 (b)***).

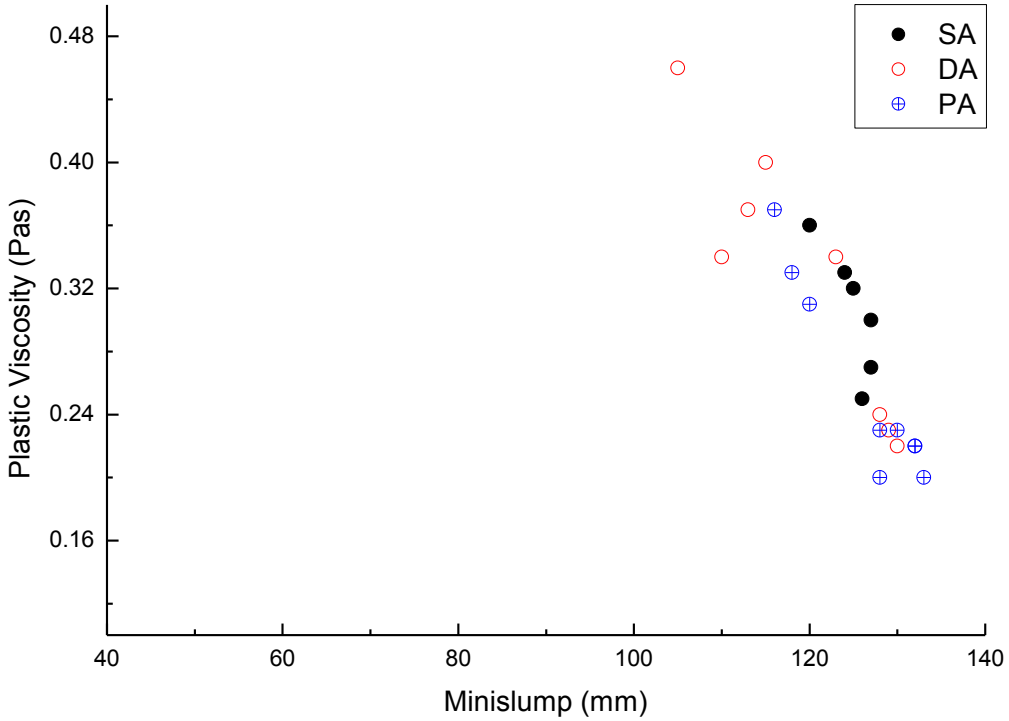

(a) LS

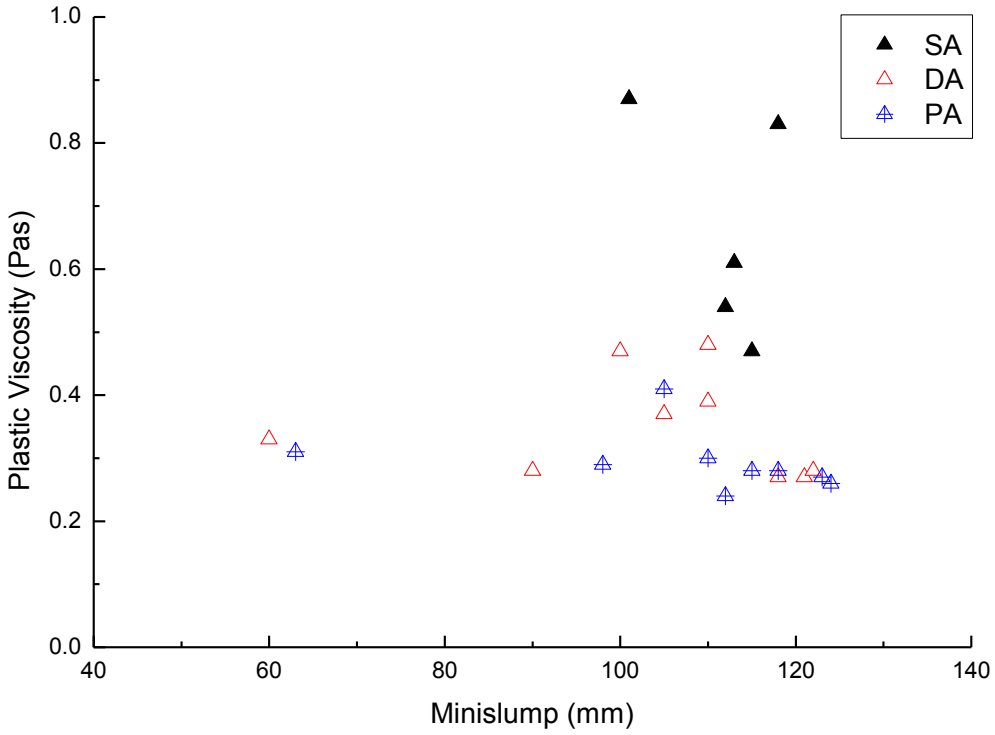

(b) NF

Fig 5.16 Relationship between the minislump and the plastic viscosity of NaOH-activated slag pastes with SPs: (a) LS and (b) NF

5.4.3 Setting time

The effect of LS (at the dosage of 1.000%) and NF (at the dosage of 0.500%) on the setting time of NaOH-activated slag are illustrated in ***Fig 5.17 (a)*** *and* ***(b)***, respectively. Generally, the addition of the PC-based SPs delayed both initial and final settings of NaOH-activated slag.

For LS, it can be found from ***Fig 5.17(a)*** that both the initial and final setting time of the reference NaOH-activated slag (No SP) were less than 120 minutes, and the interval between initial and final setting was 10 minutes. However, by adding LS, regardless of the addition methods, both initial and final setting time were prolonged, and the time interval was extended as well. Compared with the simultaneous addition, *DA* slightly delayed the initial setting time of the NaOH-activated slag, while PA further prolonged the initial setting to approximately 300 minutes. Overall, the separate addition methods increased the time interval between the initial and final setting.

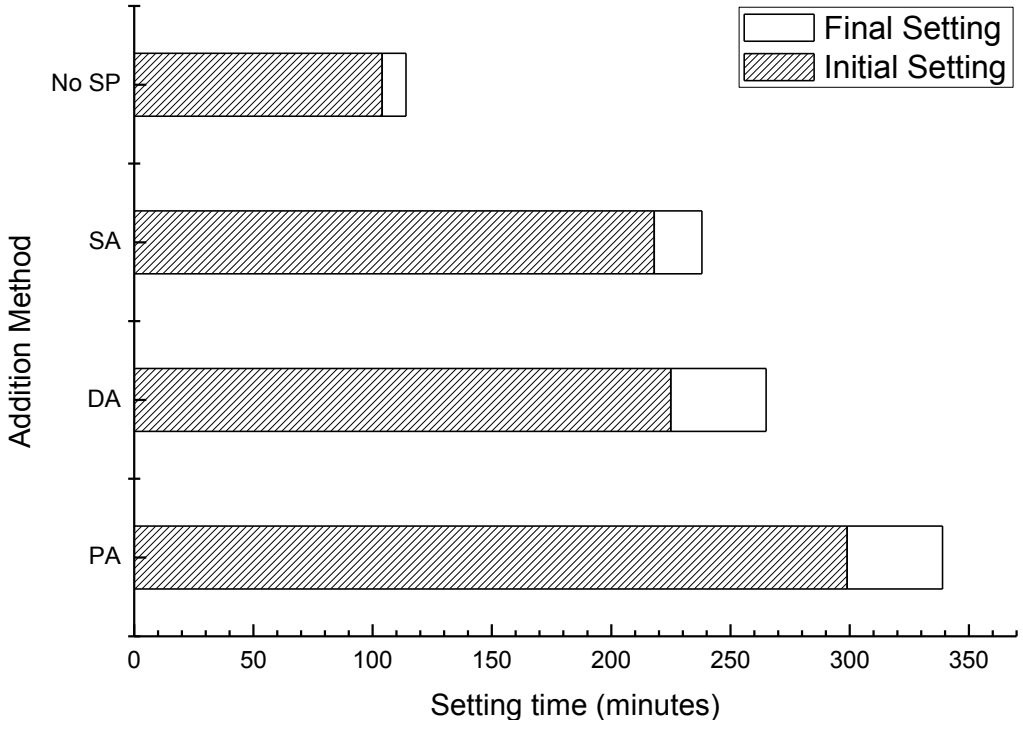

(a) LS

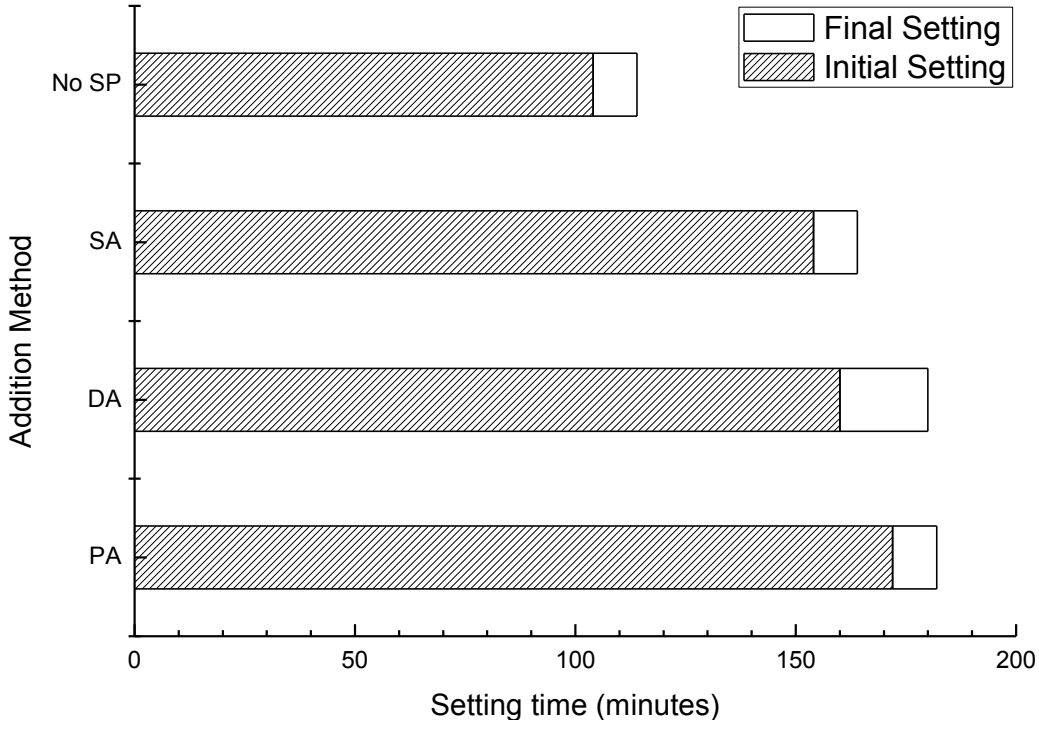

(b) NF

Fig 5.17 Effects of different addition methods of PC-based SPs on the setting time of NaOH-activated slag paste: (a) LS (1.000% dosage)and (b) NF(0.500% dosage)

For NF, the addition of NF delayed the initial setting of the NaOH-activated slag for more than 50 minutes under SA. Comparing the different addition methods, *SA* showed least retardation effect, whilst the longest initial setting was observed from *PA*. However, the interval between the initial and final setting was not prolonged except in the case of *DA*.

Comparing the ***Fig 5.17 (a)*** and ***Fig 5.17 (b)***, it can be concluded that similar trend of the effect of addition methods on the initial setting time by LS and NF can be observed. With both SPs, the longest setting time was observed in the NaOH-activated slag paste prepared by *PA*. As presented in the previous section, *PA* provided better workability retention at all SP dosages, which could be attributed to its enhanced retardation effect. It is accepted that the retardation of the SPs in PC is due to the adsorption of the polymer onto the surface of cement particles, which forms a barrier to the cement hydration and inhibits the nucleation and growth of the crystalline of hydration product (Zhor et al., 1999). For *PA*, the SPs were firstly adsorbed on the surface of the slag particles, forming a layer of negatively charged polymer, which not only provided the negative charge to generate electrostatic repulsion among the slag particles, but also physically hindered the hydration between the slag and the NaOH activator. As a consequence, this could explain why *PA s*howed the best workability and workability retention of NaOH-activated slag paste.

5.4.4 Early hydration

The effect of both SPs at the highest dosage, i.e. LS at the dosage of 1.000% and NF at the dosage of 0.500%, on the heat flow of NaOH-activated slag paste are presented in ***Fig 5.18 (a)*** *and* ***(b)***, respectively. Similar to the previous studies reported in the literature, two heat evolution peaks, initial and accelerated hydration peaks were observed during the hydration of NaOH-activated slag (Shi and Day, 1995, McCarter et al., 1999).

In the case of LS, it can be concluded from ***Fig 5.18 (a)*** that adding LS under the different addition methods did not change the overall hydration mechanism of NaOH-activated slag because the general shape of the NaOH-activated slag remained the same. However, the peak time and the intensity of the peak were

changed. Obviously, the addition of LS delayed the hydration of the NaOH-activated slag and the accelerating peak has been shifted to longer time. Compared with the other addition methods, *DA* showed less effect on the retardation of the hydration of NaOH-activated slag, while apparent retardation were observed from the other two methods, especially by *PA*, which is corresponding to the results of setting time presented in 5.4.1. Moreover, as shown in the inset in ***Fig 5.18 (a)***, the addition of LS increased the height of initial peak of NaOH-activated slag, with the highest peak being observed by PA, indicating stronger surface interaction and enhanced initial hydration occurred in the presence of LS SP.

Similar findings can be identified from the NF modified NaOH-activated slag. Again, the addition of NF did not change the general shape of the heat flow of NaOH-activated slag, which indicates that the presence of NF did not change the overall hydration mechanism of NaOH-activated slag. However, the addition of NF also delayed the appearance of both initial and accelerating peaks. Comparing the different SP addition methods, longest apparent time of the accelerating peaks was observed from *PA*, while *DA* showed less retardation effect. Noticeably, the addition of NF increased the height of initial peak of NaOH-activated slag and the highest initial peak of NaOH-activated slag was observed from *PA*. This is again possibly due to the better dispersion provided by *PA*.

While limited research have been reported on the effect of SP on the hydration of alkali-activated slag, the studies on the PC based materials have revealed that the addition of PC-based SP delays the hydration (Lei and Plank, 2012, Winnefeld et al., 2007). Moreover, the addition method of SP is also found to be able to affect the early hydration. It has been reported that the delayed addition of SPs prolongs the appearance of the second peak, which is related to the setting of cement paste (Uchikawa et al., 1995). Although it is not well explained, the reason that a layer of adsorbed superplasticiser hinders the diffusion of water and calcium ions and dispersion effect of SP changes the growth kinetics and the morphology of hydration product could be employed to explain the retardation effect of SPs (Mollah et al., 2000).

As displayed in ***Fig 5.18***, two heat evolution peaks, namely, initial and accelerated hydration peaks, were observed during the hydration of NaOH activated slag.

Regardless of SP type, the height of initial peaks was increased with the addition of SP. Among the addition methods, separate addition was higher than simultaneous addition (*SA*). The initial peaks have been identified to be related to the breakdown of the chemical bonds (such as Ca-O, Mg-O, Si-O, and Al-O) on the surface slag in the presence of OH^- (Shi and Day, 1995). Thus, the addition of SPs dispersed the slag grains and broke the agglomerates, which increased the total surface area of slag, and increased the heat flow of NaOH-activated slag. For *PA*, in order to prepare the activator solution, the same amount of NaOH dissolved in less water (1/3 of which compared to *SA*). Therefore, the activator solution with higher concentration of OH^- was prepared. Consequently, highest heat flow was observed by *PA*.

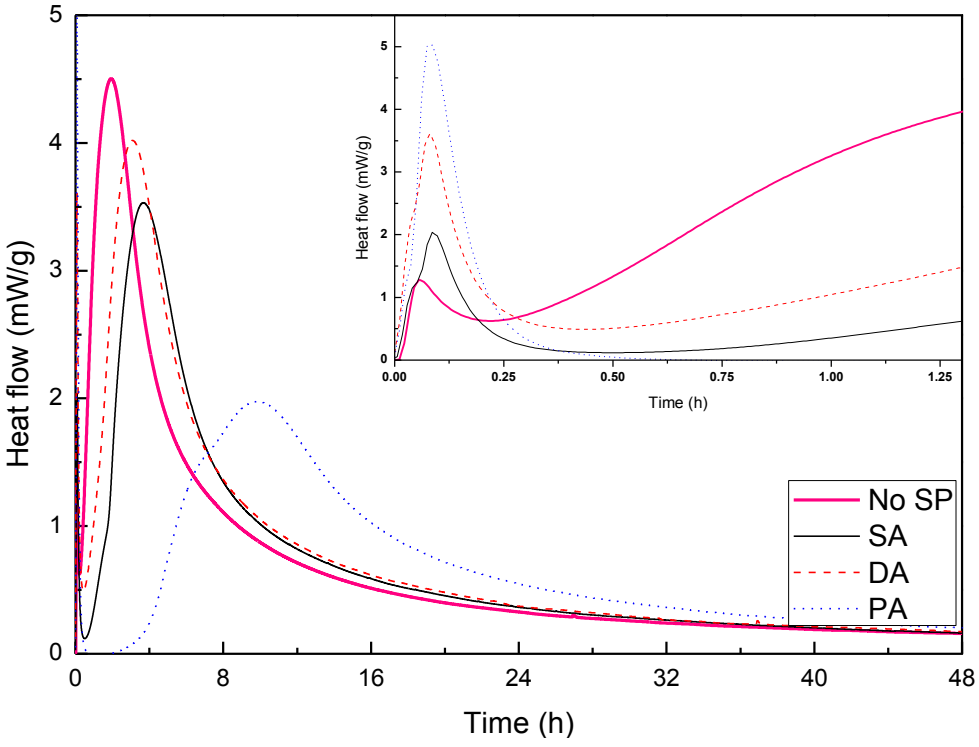

(a) LS

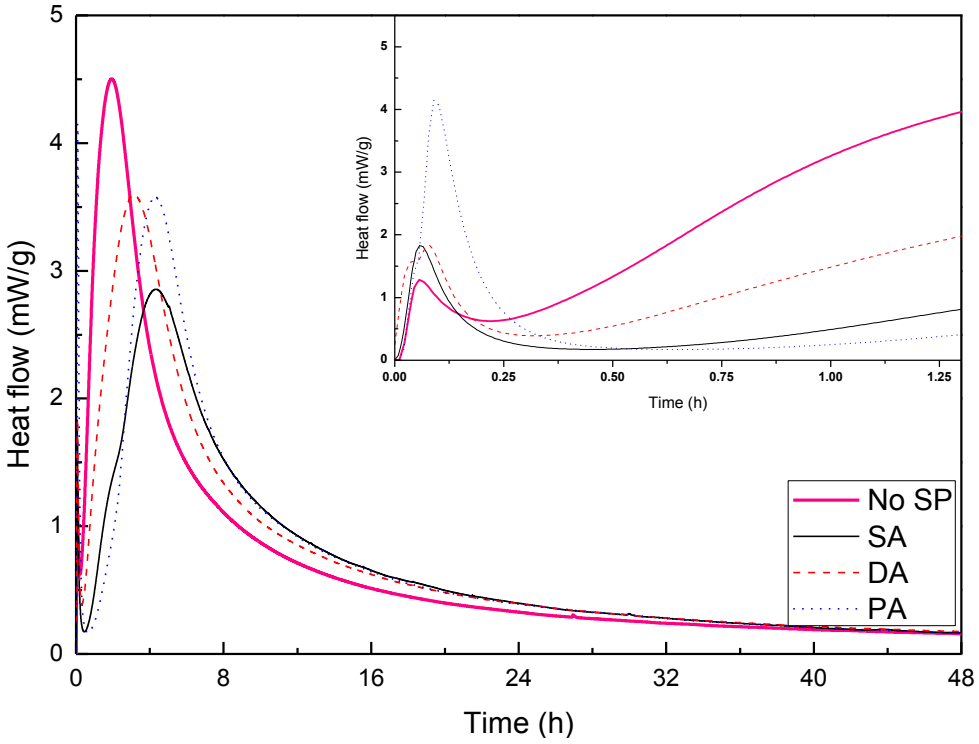

(b) NF

Fig 5.18 Effect of different addition methods of SP on heat flow of NaOH-activated slag paste: (a) LS (1.000% dosage)and (b) NF(0.500% dosage)

5.4.5 Summary

The effects of LS and NF on the early age properties of NaOH-activated slag were investigated. Based on the results obtained, the following conclusion could be drawn:

- The initial minislump obtained by the separate addition methods, namely *DA* and *PA*, was higher than that by simultaneous addition method (*SA*), with *PA* better than *DA*.
- The addition of both LS and NF reduced the minislump loss of NaOH-activated slag paste during the first one hour, this is especially significant at the higher SP dosages. Comparing different addition methods, regardless of the type and dosage of SP, *SA* and *DA* showed quick minislump loss whilst *PA* provided better ability to retain the minislump.
- The effects of different addition methods of LS and NF on initial rheological properties of NaOH-activated slag were analysed on a rheograph plotting by yield stress vs. plastic viscosity. Both the yield stress and the plastic viscosity of NaOH-activated slag pastes were reduced by adding the SPs and the activator separately.
- Regardless of the type of SPs, both the yield stress and the plastic viscosity of NaOH-activated slag paste under different addition methods were increased over time.
- The addition of LS and NF delayed the setting time of NaOH-activated slag. *SA* showed least retardation effect on the setting time of NaOH-activated slag, while *PA* demonstrated the longest setting time.
- The addition of SP did not change the overall shape of the hydration heat flow, which suggests that the hydration mechanism was not altered. However, the addition of SPs delayed the accelerating peaks of NaOH-activated slag.

5.5 Effects of different addition methods of superplasticiser on hardened properties of NaOH-activated slag

The different SP addition methods can not only improve the fresh properties, but also can affect the long-term properties of NaOH-activated slag by changing the pore size

distribution and structure. Therefore, in this section, the compressive strength, drying shrinkage and porosity were tested to investigate the effects on different addition methods of SP on the hardened properties of NaOH-activated slag.

5.5.1 Compressive strength

The effects of LS on the compressive strength of NaOH-activated slag under different addition methods are shown in ***Fig 5.19 (a)*** *to* ***(c)***. Compared to the reference (No SP), the compressive strengths of NaOH-activated slag pastes at all curing ages were increased with the addition of LS at all three SP dosages, except at the dosage of 0.500% at 1 day. Furthermore, in general, the compressive strengths of NaOH-activated slag increased with the increase of the LS dosage. When SP is used as a water-reducer, it is expected that the compressive strength should increase due to the reduced water/cement ratio. However, in the current study, both LS and NF were used as a superplasticiser. The increased compressive strength is, thus, presumably attributed to the change of the microstructure of hardened paste through breaking the flocculation and increasing the surface area of the slag, leading to much improved hydration.

Comparing different addition methods, it was found that the difference among addition methods is not obvious at early ages (e.g. 1 day). However, with the development of compressive strength, *DA* showed the lowest compressive strength, while *PA* provided the highest compressive strength. For example, at the age of 56 days, the compressive strengths of *DA* and *PA* at 1.000% LS dosage were 22.54MPa and 31.15MPa respectively. The change of the compressive strengths of NaOH-activated slag pastes under different addition methods could be related to the modification of the microstructure of hardened paste, which will be discussed in the next section.

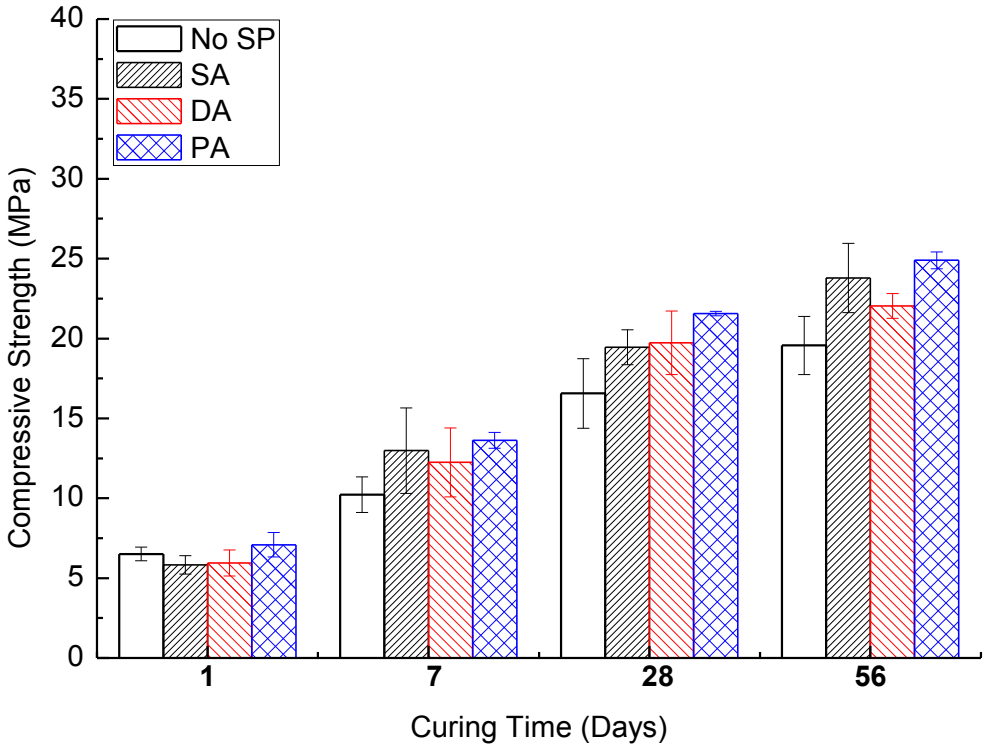

(a) 0.500% LS

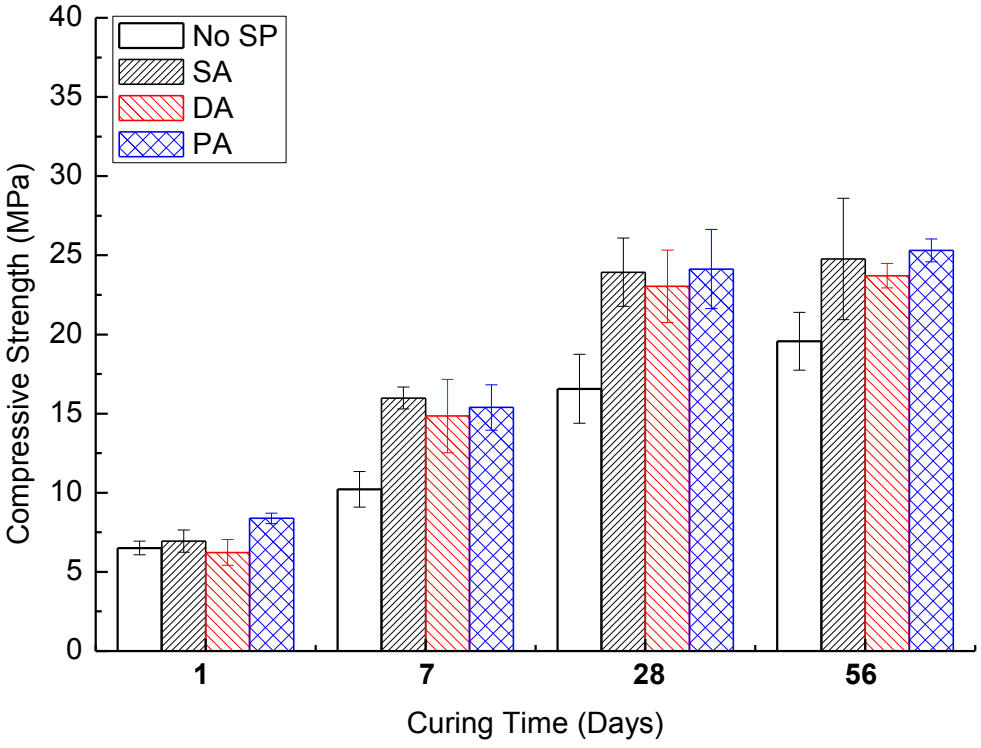

(b) 0.750% LS

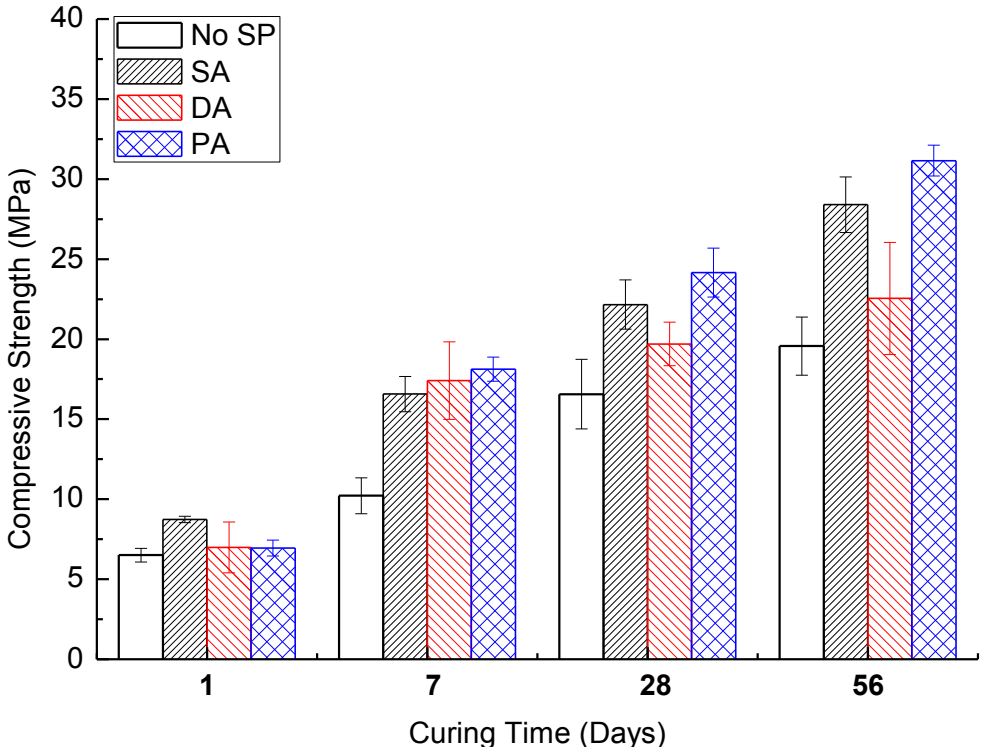

(c) 1.000% LS

Fig 5.19 Effects of different addition methods of LS on compressive strength of NaOH-activated slag paste

The effects of different addition methods of NF on the compressive strengths of NaOH-activated slag are illustrated in ***Fig 5.20 (a)*** *to* ***(c)***. It is apparent that the addition of NF increased the compressive strengths of NaOH-activated slag at the ages of 7, 28 and 56 days. However, the 1-day compressive strength of NaOH-activated slag was reduced in the presence of NF at the dosages of 0.125% and 0.25%. The reason for the reduction of early compressive strength could be due to the retardation effect of NF, which was discussed in section 5.4.3 and reported by other researchers as well (Puertas et al., 2003). However, at the NF dosage of 0.5%, the compressive strengths with the DA and PA were higher than that of the reference (No SP). Comparing different addition methods, there is a trend that the *SA* provided highest compressive strength at all curing age excepting one day, whilst the lowest compressive strength was observed in the pastes by *DA*. Such changes of compressive strengths of NaOH-activated slag pastes are again related to the microstructure of hardened paste, which will be discussed in next section.

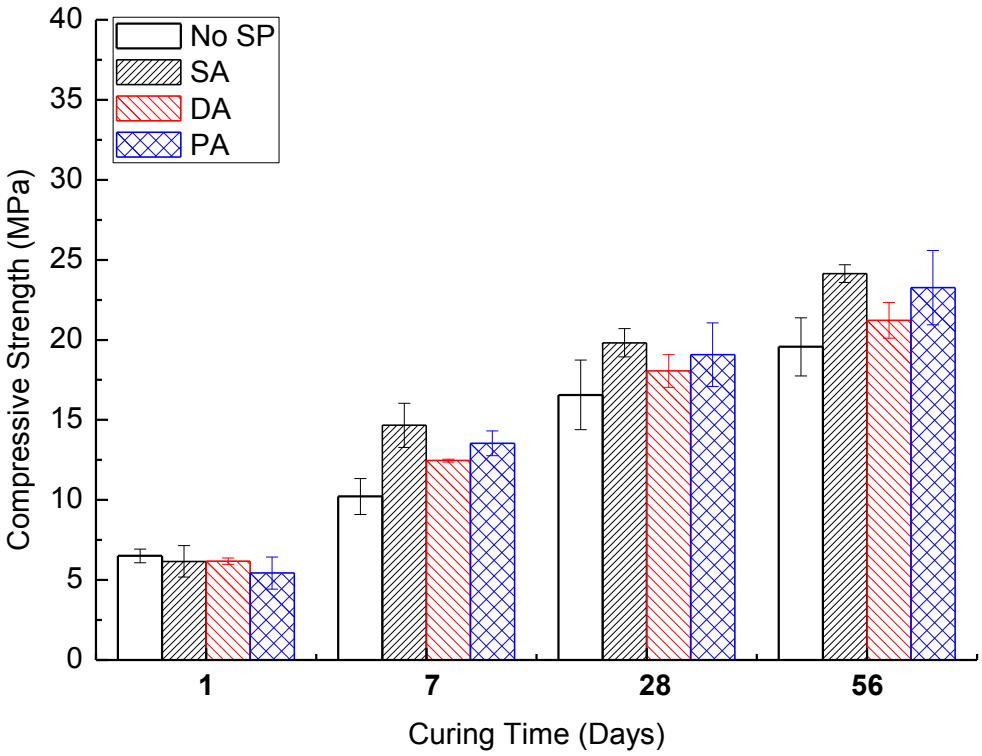

(a) 0.125% NF

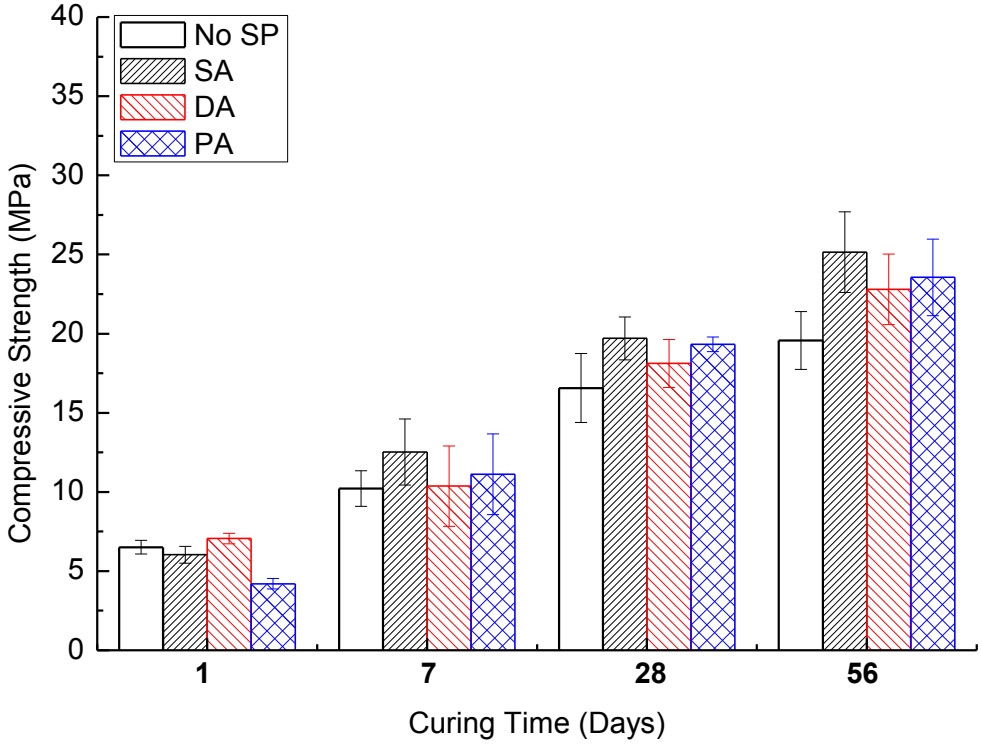

(b) 0.250% NF

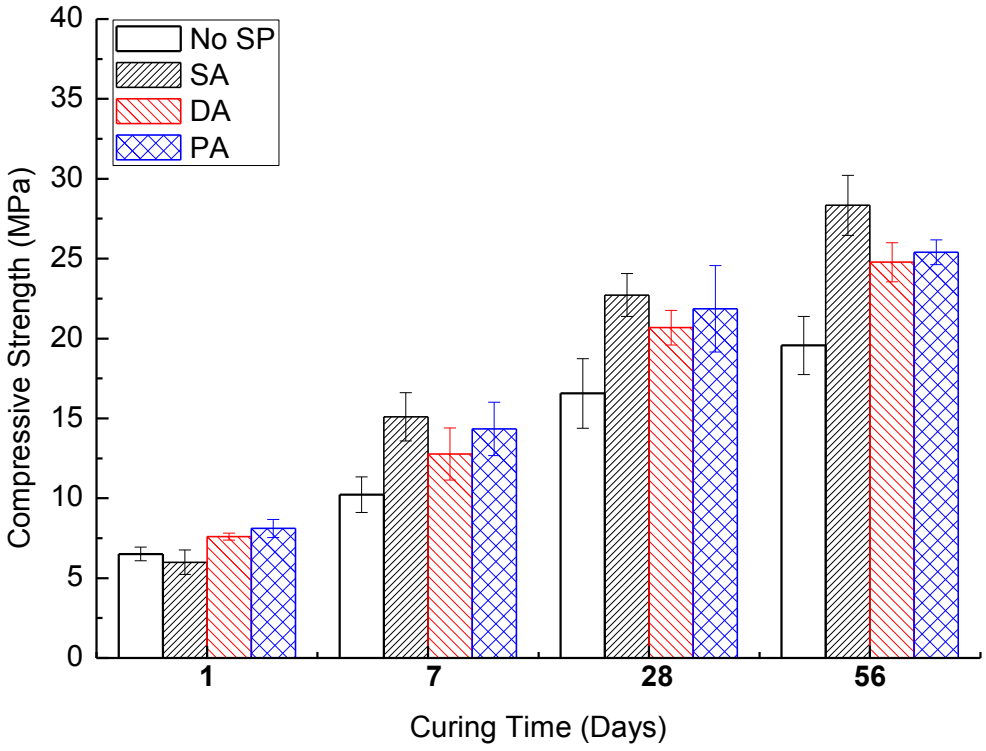

(c) 0.500% NF

Fig 5.20 Effects of different addition methods of NF on compressive strength of NaOH-activated slag paste

5.5.2 Drying shrinkage

The effects of 0.500% LS and NF on the drying shrinkage of hardened NaOH-activated slag paste are presented in ***Fig 5.21 (a)*** and ***Fig 5.21 (b)***, respectively. The addition of SPs showed its influence on the drying shrinkage of hardened NaOH-activated slag. However, the effects depend on the type of SPs and the addition methods, which are discussed in further detail below.

For LS, it can be seen clearly in ***Fig 5.21 (a)*** that the drying shrinkage of NaOH-activated slag progressed rapidly during the first 3 months before reaching a relatively constant level up to 6 months. The same trend applied to both the reference (No SP) prisms and the prisms with SP, while the reference prism exhibited the highest drying shrinkage. It can be noticed that the addition of LS reduced the drying shrinkage of NaOH-activated slag before 3 months. After 3 months, the drying shrinkage of the NaOH-activated slag prism with LS by *SA* was close to that of the reference prism (No SP). However, regardless of the drying period, both the *PA* and

DA methods slightly reduced the drying shrinkage, with less drying shrinkage being observed from *DA*.

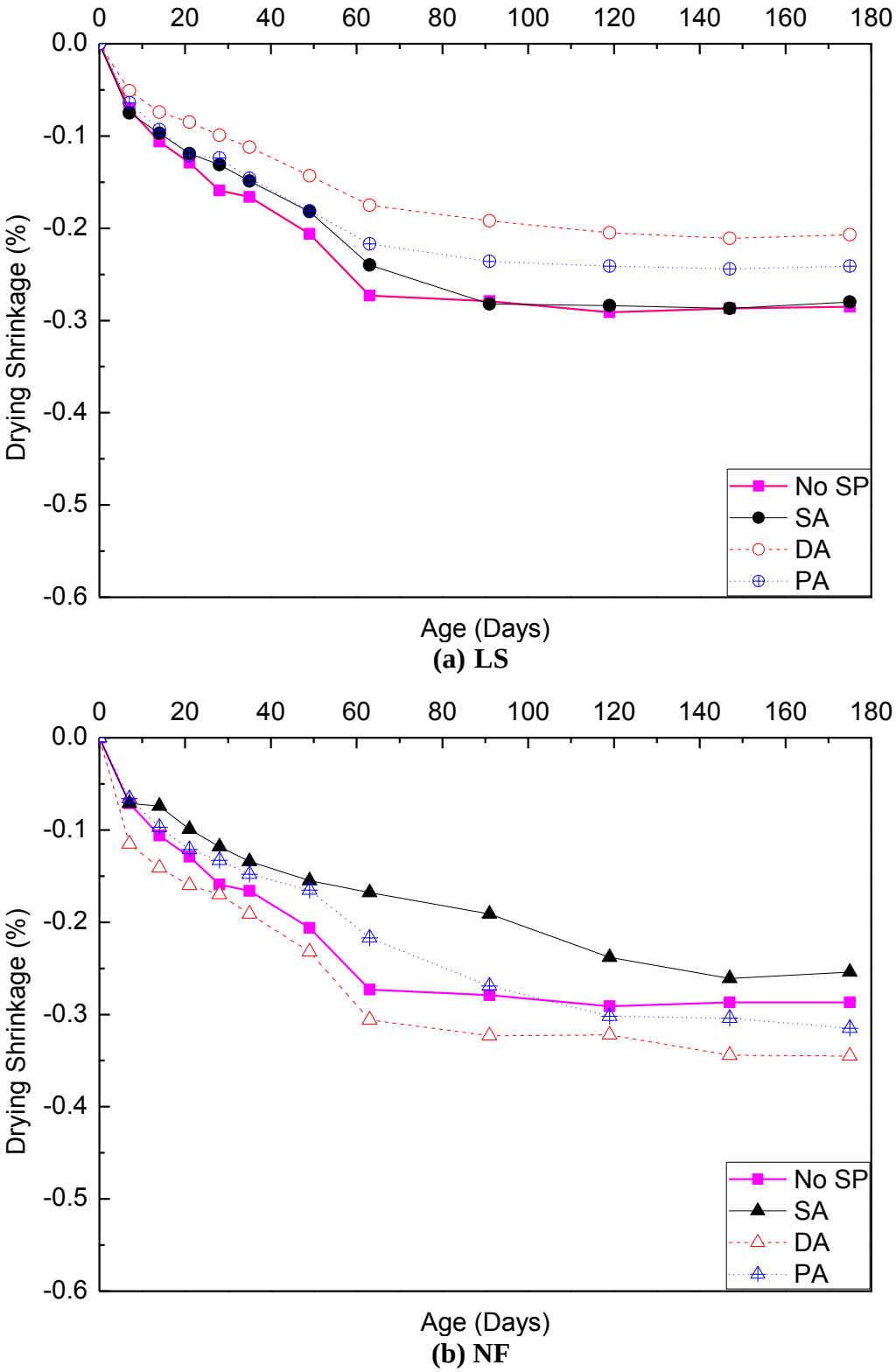

Fig 5.21 Effects of different addition methods of LS on drying shrinkage of NaOH-activated slag paste (at 0.500% dosage): (a) LS and (b) NF

For NF, from ***Fig 5.21 (b)***, it can be seen that different behaviour can be observed. Among all the addition methods, *DA* showed the largest drying shrinkage, while the smallest drying shrinkage was observed in the prism prepared by *SA*. The addition of NF by *PA* reduced the drying shrinkage of NaOH-activated slag before 3 month. However, after 3 months, the drying shrinkage of NaOH-activated slag prism with NF by *PA* increased and was even greater than that of the reference.

The increase of the drying shrinkage in Portland cement system with the addition of SP has been reported in some previous studies in the literature (Ma et al., 2007, Tam et al., 2012). Compared to PC, NaOH-activated slag exhibited larger drying shrinkage. However, the effects of PC-based SPs on the drying shrinkage of NaOH-activated slag have not been reported in the literature. To interpret the effects of PC-based SPs on the drying shrinkage of NaOH-activated slag under different addition methods, a good understanding on the pore distribution of the hardened NaOH-activated slag is essential, which will be discussed in the next section.

5.5.3 Porosity

The pore distribution and accumulative pore volume of the hardened NaOH-activated slag paste with LS are presented in ***Fig 5.22 (a)*** and ***(b)***, respectively, and the characteristics of the pores are summarised in ***Table 5.4***. It is obvious from the results that the addition of LS refined the pore structure of NaOH-activated slag with decreasing porosity and average pore size of the hardened paste. Comparing the different addition methods, lower pore volume and less proportion of micropores were observed in the pastes by separate addition, particularly by *PA*.

The effects of NF on the pore distribution and accumulative pore volume of the hardened NaOH-activated slag paste are presented in ***Fig 5.23 (a)*** and ***(b)***, and the characteristics of the pores are summarised in ***Table 5.4***. Similar to LS, the addition of NF also reduced the porosity volume and average pore diameter. Comparing the different addition methods, the separate addition methods again produced smaller proportion of micropores in the hardened pastes. Noticeably, the highest proportion of micropores was observed in the pastes with *DA*, which is in a good correlation with the drying shrinkage results reported in the previous section.

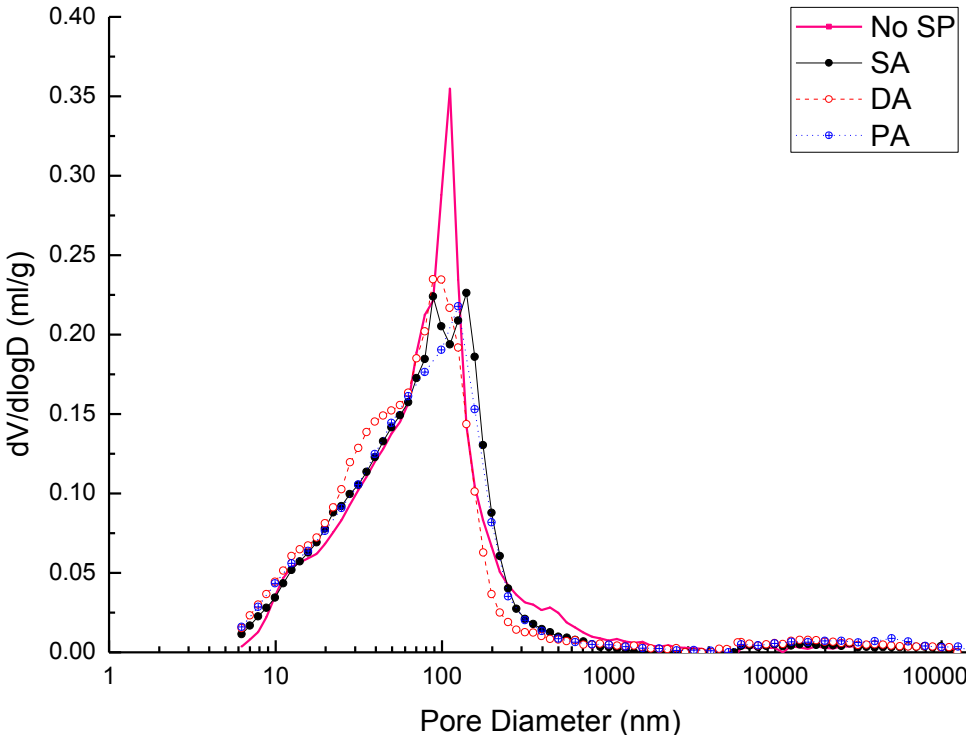

(a) Pore distribution

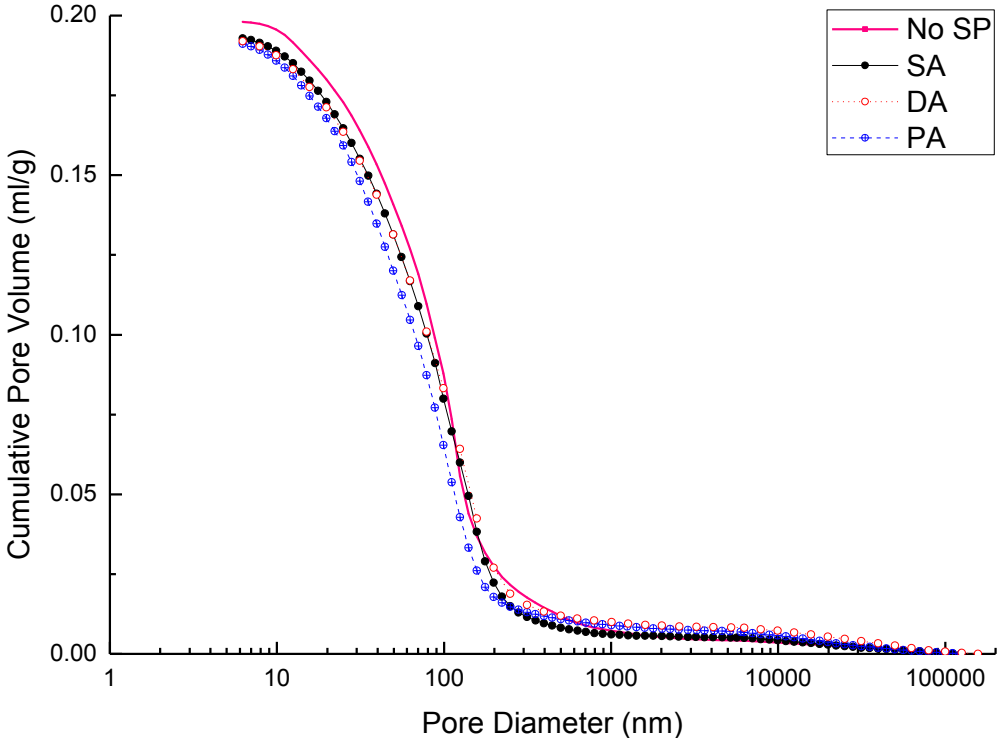

(b) Cumulative pore volume

Fig 5.22 MIP results of hardened NaOH-activated slag paste with LS

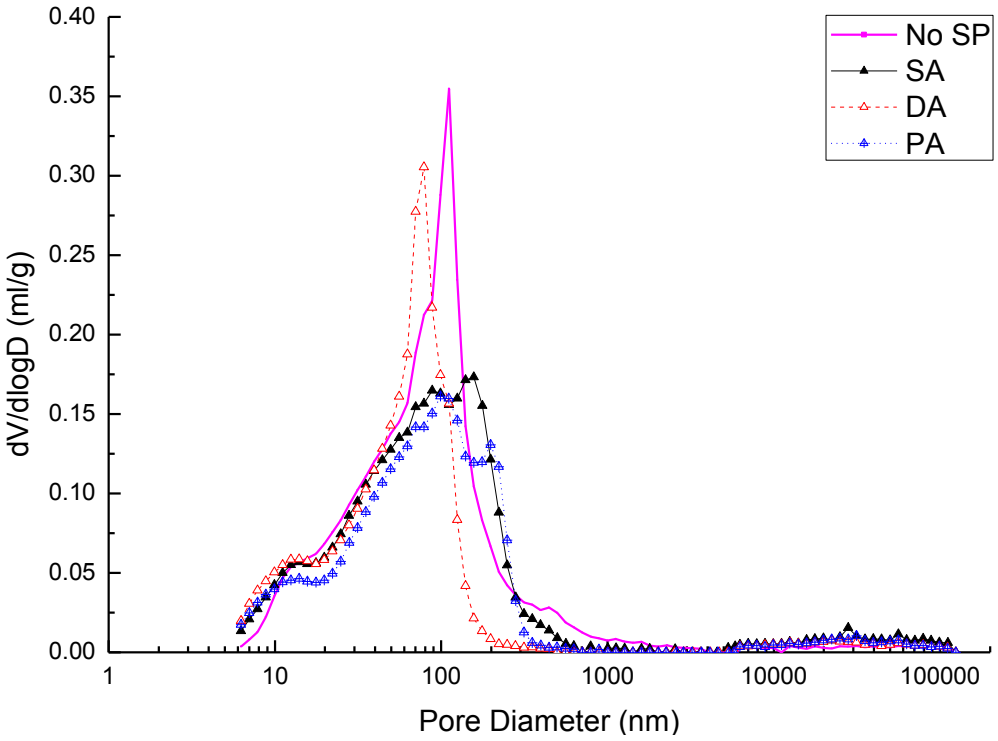

(a) Pore distribution

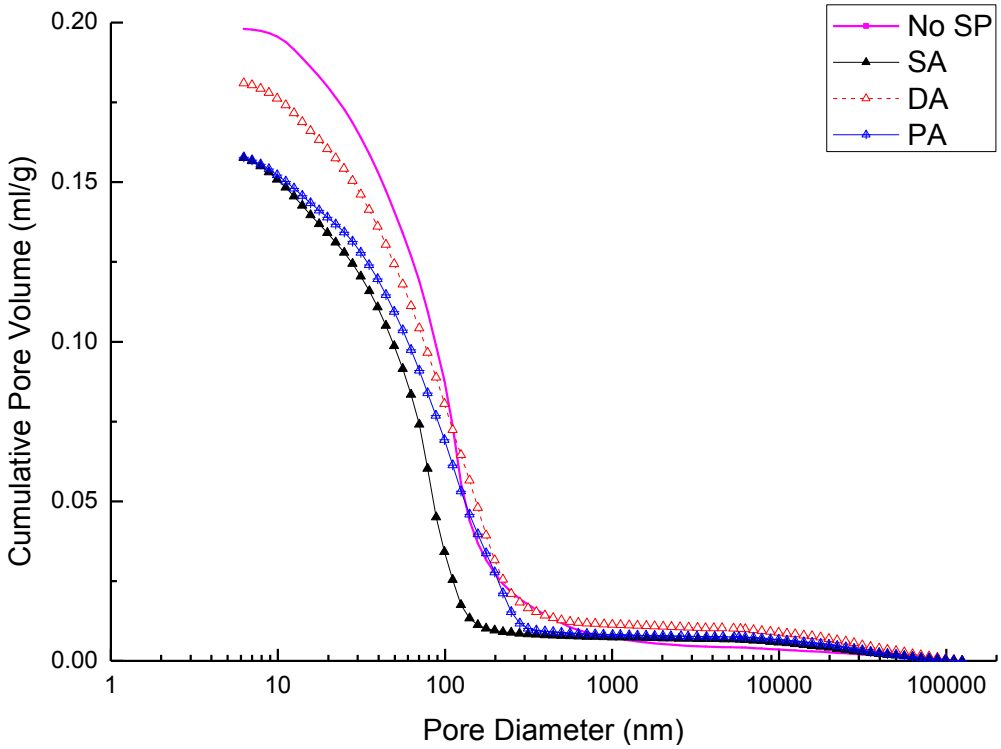

(b) Cumulative pore volume

Fig 5.23 MIP results of hardened NaOH-activated slag paste with NF

Table 5.4 Characteristics of the pores in hardened NaOH-activated slag with PC-based SPs

SP	Addition Methods	Pore Volume (mL/g)	Porosity (%)	Average Pore Size (nm)	Pore Size Distribution/%		
					<10 nm	10 -100 nm	>100 nm
LS	No SP	0.1980	31.94	51.00	2.07	60.83	37.10
	SA	0.1929	31.60	46.09	2.93	60.95	36.12
	DA	0.1920	31.15	46.90	3.91	55.62	40.47
	PA	0.1912	30.62	41.70	4.58	56.32	39.11
NF	No SP	0.1980	31.94	51.00	2.07	60.83	37.10
	SA	0.1576	26.62	37.20	5.21	54.82	39.97
	DA	0.1810	29.69	46.70	7.61	56.28	36.11
	PA	0.1578	26.42	45.00	6.16	55.99	37.85

The gel pores, which are the pores with a pore size smaller than 10 nm, have been reported to be linked to the degree of cement hydration (Zhang and Kong, 2014, Sakai et al., 2006). Therefore, based on the same concept, the increased proportion of the gel pores in the SP modified AAS mixes in Table 5.4 would suggest that the hydration of the NaOH-activated slag was enhanced by the addition of SPs. Compared with SA addition method, both the *DA* and *PA* methods increased the gel pore volume, which indicates that the hydration of NaOH-activated slag was further improved by separate addition method. This could be due to the improved dispersion of the slag particles by separate addition methods.

As discussed in section 2.3.4.2, both compressive strength and drying shrinkage are related to the porosity of hardened pastes. Drying shrinkage mainly happened due to the loss of adsorbed water in the small void in C-S-H hydration product, which could lead to a shrinkage strain (Kawashima and Shah, 2011).

In the case of LS, the average pore diameter and the pore volume of hardened paste were reduced by adding LS. *PA* offered the smallest pore diameter and volume. Therefore, the highest compressive strength of the hardened NaOH-activated slag paste was observed from *PA*. Considering the pore size distribution, both the separate addition methods, namely *PA* and *DA*, produced lower portion of micropores (pore size less than 100 nm). Consequently, lower drying shrinkage was observed in the paste prepared by both *PA* and *DA* methods.

In the case of NF, it can be clearly seen that the addition of NF reduced the average pore diameter and pore volume of the hardened NaOH-activated slag paste, which could be used to illustrate the improved compressive strength of the paste. Among different addition methods, *SA* produced the smallest pore diameter and the lowest pore volume, which could have caused the highest compressive strength.

5.5.4 Summary

The effects of LS and NF on the hardened properties of NaOH-activated slag were investigated. Based on the results, the following conclusion could be drawn.

- The addition of SPs increased the compressive strengths of NaOH-activated slag (with the same w/c ratio) at all ages except 1 day. In the case of LS, the *PA* produced the highest compressive strength among different addition methods, while *SA* provided the highest compressive strength of the paste with NF.
- Simultaneous addition of LS showed no obvious effect on the drying shrinkage of NaOH-activated slag. However, separate LS addition methods reduced the drying shrinkage of NaOH-activated slag and smaller drying shrinkage was observed from *DA*. The addition of NF changed the drying shrinkage of NaOH-activated slag. Among the different addition methods, *DA* produced the largest drying shrinkage, while the lowest drying shrinkage was observed in the prism prepared by *SA*.
- The addition of LS refined the pore structures of NaOH-activated slag by increasing the proportion of micro and mesopores as well as decreasing the average pore size of the NaOH-activated slag. Lower pore volume and larger proportion of micropores were observed in the SP modified pastes by separate addition methods, particularly by *DA*. In the case of NF, the average pore size decreased and the proportion of micropores increased. The change of the microstructure depended on the nature of SPs and the SP addition methods.

5.6 Discussion on the possible mechanism under different addition methods

The adsorption of SP is considered to be based on the electrostatic attraction between the SP and the surface of the particles (Zhang et al., 2015). Thus, the addition of negatively charged chemicals (such as OH^-, $-COO^-$ and $-SO_3^{2-}$) could lead to competitive occupation to the limited positive site on the surface of the particles, in particular so when adding at the same time, which could cause the reduction in the adsorption of SP. When adding SPs and NaOH at different time interval, even a few minutes, could allow them to avoid this competition.

From the results presented in this chapter, the separate addition methods have demonstrated its potential in improving the performance of PC-based SPs in NaOH-activated slag through the reduction in the competitive adsorption between the SP and the NaOH activator. In the perspective of early interaction between SP and activator, the models of three SP addition methods are proposed below with the relevant schematic being presented in ***Fig 5.24***:

1) Simultaneous Addition (adding SP and NaOH at the same time):

In this case, SP dissolves in highly alkaline NaOH solution (pH >14) before being mixed with the slag, the SPs hydrolyse into negatively charged backbone and counter cations. However, some functional groups (such as $-SO_3^-$) are not stable and cleave from the SPs, reducing the charge density of SP.

After mixed with the slag, a large amount of OH^- from the activator (plus some $-SO_3^-$ degrafted from the SPs) tends to be adsorbed on the surface of slag grains, which reduces the surface potential of the slag. Consequently, the zeta potential of NaOH-activated slag becomes negative. The introduced OH^- anions induce the competitive adsorption between the negatively charged SP backbone and the other anions (OH^-, SO_3^-), leading to reduced adsorption of SP, and hence poor dispersion and poor fluidity.

However, as not all the functional groups are cleaved from the SP, the SPs still can be adsorbed onto the slag surface, causing the dispersion of the slag particles and

breakdown of the agglomerates. Consequently, the *SA* still demonstrated its ability in improving the workability of NaOH-activated slag.

2) Delayed Addition (adding NaOH first and then SP):

Under this method, slag firstly reacts with NaOH activator. Compared to the reaction between slag and water, regardless of nature of the slag, the highly alkaline (NaOH) solution accelerates the dissolution and the process not only breaks the Ca-O, Mg-O bond, but also breaks the Si-O-Si and Al-O-Al bonds. As a result, more cations such as Ca^{2+}, Mg^{2+} and Na^{+} are released into the solution (Shi and Day, 1995, Duxson and Provis, 2008). In addition to the dissolved ions, a thin layer colloid phase of hydration product could also be formed on the surface of slag(Wang and Scrivener, 1995).

The above processes not only consume the OH^{-} but also provide new surface sites for SP to adsorb, which can improve the efficiency of the SPs. Compared with *SA*, more cations are released around the slag surface, which are confined within the double layer around the slag under ***DA***. This provides more opportunities for the SPs to be adsorbed by the electrostatic attraction. Moreover, these few minutes time interval between adding the activator and the SP reduces the damage to the SP in highly alkaline media. Thus, compared to *SA*, the adsorption of SP is improved by *DA*.

3) Prior Addition (adding SP first and then NaOH):

Under this method, when the slag first contacts with mixing water, depending on the composition of the slag, various amount of cations, such as Ca^{2+}, K^{+} and Na^{+}, are released into water, forming a positively charged layer near slag surface (Habbaba and Plank, 2010, Habbaba and Plank, 2012). Meantime, the negatively charged functional groups of hydrolysed SPs tend to attach onto the slag surface via electrostatic attraction. The adsorbed SP on the slag surface offers a better dispersion of slag particles and then an improved workability of the slag paste, which also provides a large surface area for further hydration. However, the subsequent addition of the activator (and hence the OH^{-}) could also cause the desorption of SP.

In general, the results obtained from the current study demonstrated that the *PA* provides higher adsorptions of SP than *DA*. The reason could be due to the chemical stability of SPs. For *DA*, before adding SPs, there are large amounts of OH^{-} already

existed in the solution. The existing OH^- could still react with SPs, which could have caused the chemical instability issues of the SP.

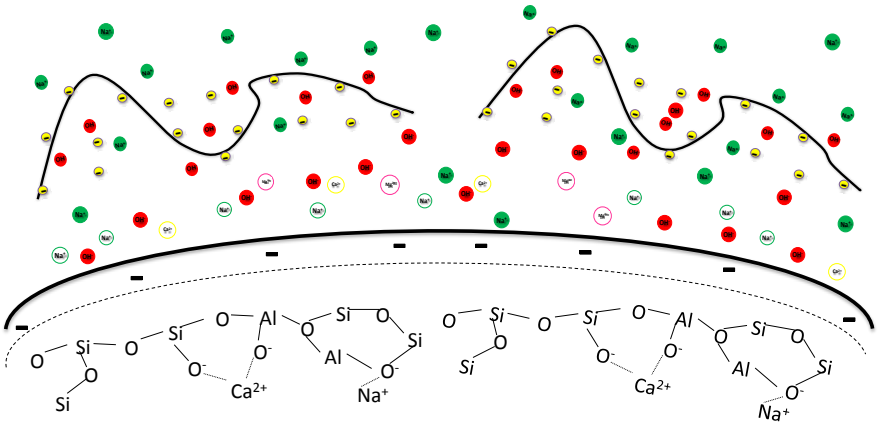

(a) Simultaneous Addition

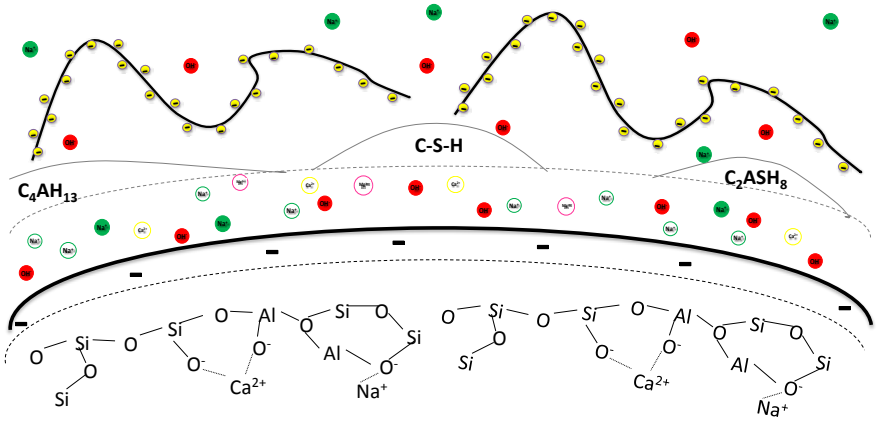

(b) Delayed Addition

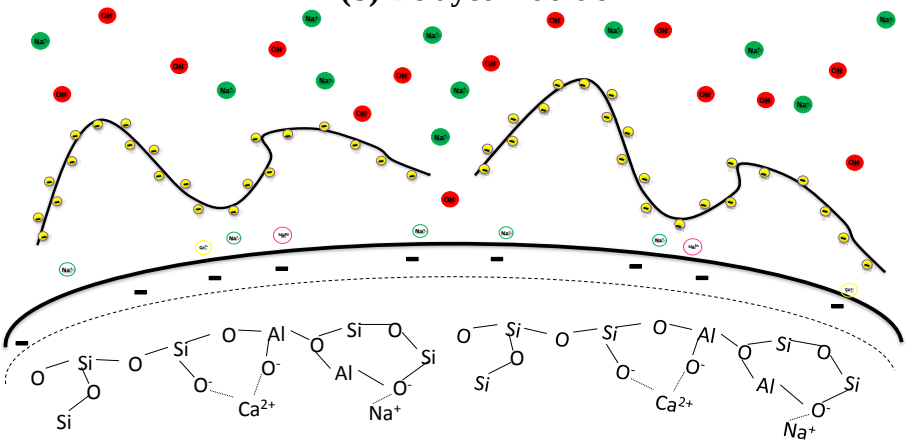

(c) Prior Addition

Fig 5.24 Schematic diagram of the proposed models under different SP addition methods

5.7 Chemical Stability of PC-based superplasticisers in highly alkaline media

As discussed in Chapter 2, the chemical instability of PC-based superplasticiser could cause the reduced performance of PC-based SPs in NaOH-activated slag. Thus, in this section, the chemical structure of LS, NF and PCE, the representatives of the 1st -, 2nd -, and 3rd - generation of superplasticiser, were examined by FTIR in H_2O, and NaOH solution (pH>14), respectively. Their molecular weight and weight distribution were also investigated by HPSEC.

5.7.1 Lignosulfonate superplasticiser

The FTIR spectrum of LS dissolved in different media are presented in ***Fig 5.25*** and the assignments for each peak are summarized in ***Table 5.5***. The structure of LS can be referred to in ***Fig 2.1.*** It can be seen from Fig 5.25 that the chemical structure of LS was changed when it dissolved in NaOH solution. From the FTIR spectrum, one band presenting $-SO_3$ at 662 cm^{-1} disappeared, while new bands corresponding to $-CH_3$ at 1601, 1447 and 880 cm^{-1} were formed. The result suggested that the chemical structure of LS was changed with possible cleavage of the C-S bond and the formation of CH_3 in NaOH solution. Similarly, the disappearance of the peaks at the position around 1600-1650 cm^{-1} suggested that chain breaking happened in LS. Therefore, the above structural changes of LS identified from FTIR spectrum could be attributed to the breakdown of the C-C bond on the backbone of LS and the detachment of $-SO_3$ group.

Table 5.5 FTIR peak assignments for LS

Wavenumber/cm^{-1}	Peak Assignment	Media	
		H_2O	NaOH (pH>14)
3551	O-H stretching	-OH	
3480	O-H stretching	-OH	
3435	O-H stretching		-OH
3415	O-H stretching	-OH	
1637	C-C stretching	-C-C	
1618	C=C stretching	-C=C	
1601	C–H stretching		$-CH_2$, $-CH_3$
1447	C–H bending		$-CH_2$, $-CH_3$
880	C-H bending		$-CH_2$, $-CH_3$
622	S-O deformation	$-SO_3$	

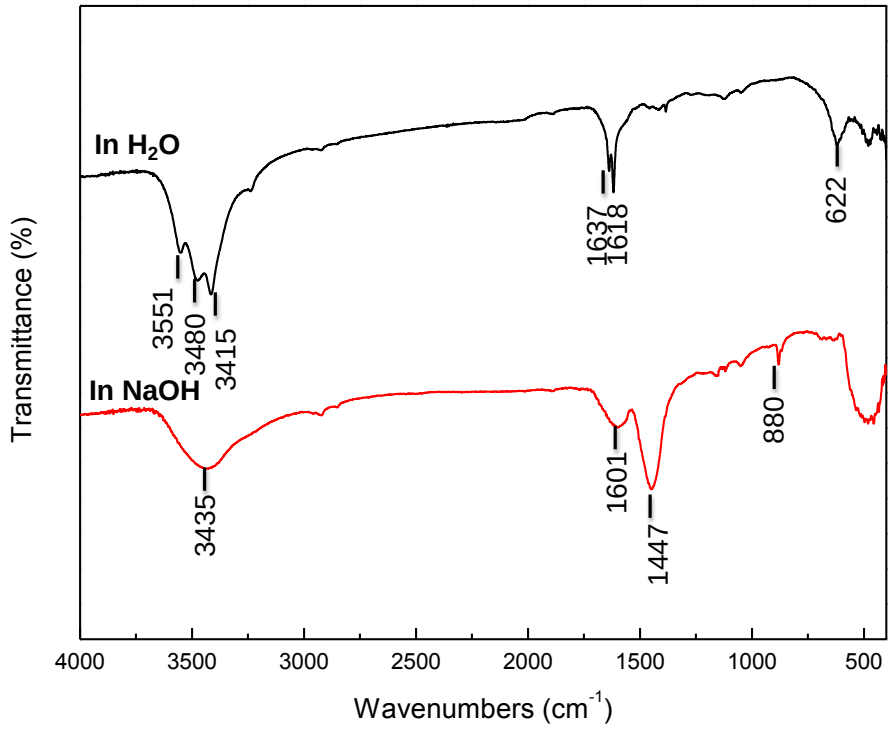

Fig 5.25 FTIR spectra of LS in water and NaOH solution

The molecular weight and the weight distribution of LS in H_2O and NaOH calculated from ***Equations 4.7*** to ***4.9*** are summarised in ***Table 5.6***. Compared with the results of LS dissolved in H_2O, lower molecular weight of LS with slightly narrow molecular weight distribution was observed in NaOH. The reduction of both number-average and mass-average molecular weight of LS indicated that the molecular chain was broken. However, the reduction of the molecular weight was not significant (i.e. less than 400 of M_n and 1500 of M_w). Combining with the FTIR results, although the molecular chain was broken, the hydrolysis of grafted sulfonic group could be the most possible mechanism which has caused the chemical instability of LS in alkaline media.

Table 5.6 Molecular weight and weight distribution of LS

LS	Media	
	H_2O	**NaOH (pH>14)**
M_n	2806	2438
M_w	8641	7173
PDI	3.08	2.94

5.7.2 Naphthalene superplasticiser

The chemical structure of NF in different media is also characterised by FTIR and the results are shown in ***Fig 5.26.*** The schematic diagram of the chemical structure of NF can be referred to in ***Fig 2.4.*** The assignments for each peak of FTIR spectrum are illustrated in ***Table 5.7***. The peak shift can be immediately noticed from the FTIR spectrum in ***Fig 5.26***. For example, the band at 680 cm^{-1} which represents the vibration of the sulfonic groups disappeared in NaOH solution. However, new peaks at 1445 and 880 cm^{-1} which could be attributed to the C-H bending were identified in NaOH solution. These results suggest that the chemical structure of NF was possibly changed with cleavage of the sulfonic group in NaOH solution.

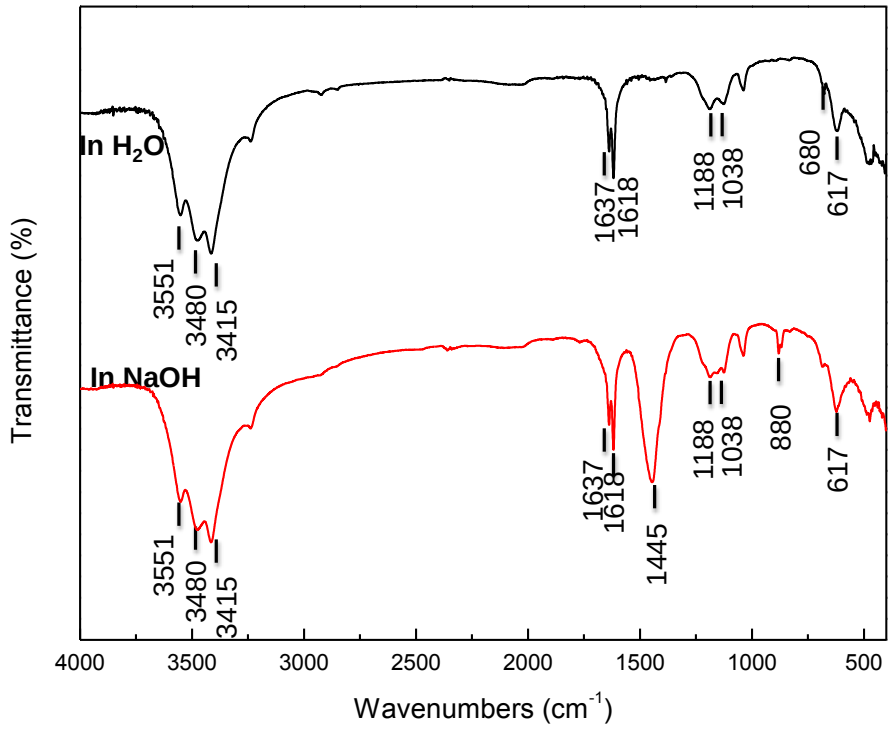

Fig 5.26 FTIR spectra of NF in water and NaOH solution

Table 5.7 FTIR peak assignments for NF

Wavenumber/cm^{-1}	Peak Assignment	Media	
		H_2O	NaOH (pH>14)
3551	O-H stretching	-OH	-OH
3480	O-H stretching	-OH	-OH
3415	O-H stretching	-OH	-OH
1637	C-C stretching	-C-C	-C-C
1618	C=C stretching	-C=C	-C=C
1445	C–H bending		$-CH_2$, $-CH_3$
1188	C-C stretching	-C-C (Aromatic)	-C-C (Aromatic)
1038	C-H bending	$-CH_2$, $-CH_3$	$-CH_2$, $-CH_3$
880	C-H bending		$-CH_2$, $-CH_3$
680	S-O deformation	$-SO_3$	
617	S-O deformation	$-SO_3$	

The molecular weight and the weight distribution of NF in H_2O and NaOH are presented in ***Table 5.8***. Slightly lower molecular weight of NF with similar molecular weight distribution was identified in NaOH solution. These results indicate that the polymer chain of NF did not break down. Therefore, it can be concluded that the degradation of the sulfonic group in NF occurred when it dissolved in NaOH solution, which could have caused the instability issue of the NF in alkaline media.

Table 5.8 Molecular weight and weight distribution of NF

NF	Media	
	H_2O	NaOH (pH>14)
M_n	1902	1898
M_w	3076	3061
PDI	1.62	1.61

5.7.3 Polycarboxylate superplasticiser

The FTIR spectra of the PCE in water and NaOH solution are presented in ***Fig 5.27*** and the assignments for each peak are summarized in ***Table 5.9***. Due to the confidential commercial information which cannot be obtained from the PCE manufacturer, the exact chemical structure of the PCE investigated in the current study is unknown. However, the general chemical structure of the PCE can be referred to in ***Fig 2.6.*** From the FTIR spectrum of the PCE obtained in H_2O in ***Fig***

5.27, the bands at 1727 and 1637 cm^{-1} representing the C=O band in the ester group, the bonds at 1445 cm^{-1} attributed to the carboxylate groups, and the bonds at 1352 and 1250 cm^{-1} due to the C-O-C for poly (ethylene oxide) and the side chain of SP, can all be clearly identified. All these bands are considered as the most important characteristic bands of PCE (Palacios and Puertas, 2004, Yong et al., 2002).

When the PCE was dissolved in NaOH solution, the bands representing the ester groups at 1727 and 1637 cm^{-1} disappeared, while two new bands corresponding to the C-O at 879 cm^{-1}, attributed to alcohol and C=O at 1445 cm^{-1} linked to carboxylic acid, were formed (Bion et al., 2003, Duarte et al., 2004, Palacios and Puertas, 2004). Additionally, the intensity of the peak at 1104 cm^{-1} was significantly increased, indicating more carboxylic groups were formed. Based on the basic principle of chemistry, it is generally accepted that the ester group is prone to hydrolyse into a carboxylic acid and an alcohol, leading to the degradation of the side chain of PCE (Palacios and Puertas, 2004).

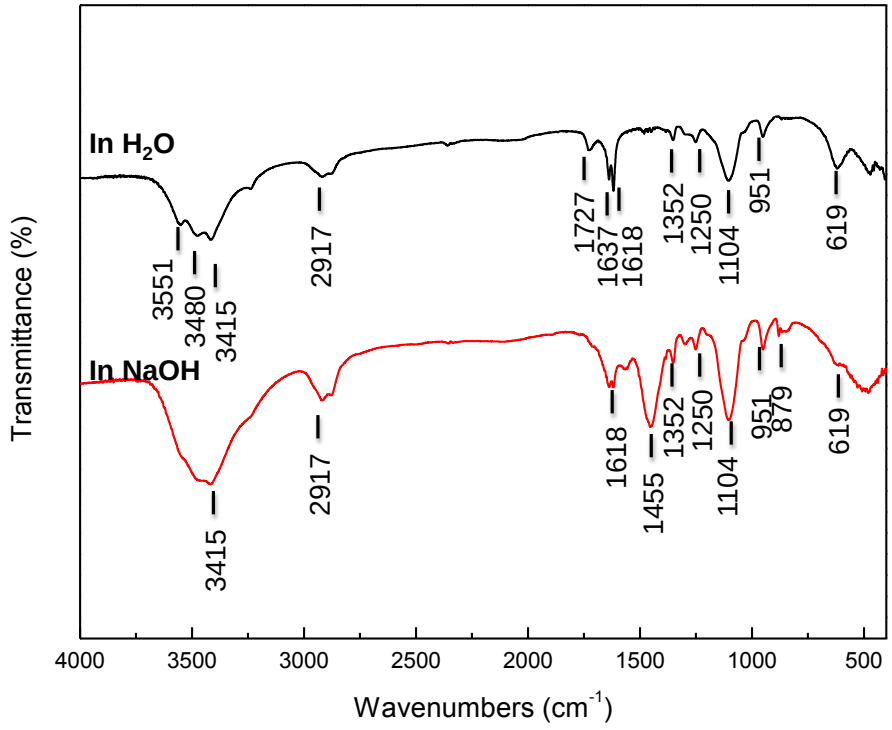

Fig 5.27 FTIR spectra of PCE in water and NaOH solution

Table 5.9 FTIR peak assignments for PCE

Wavenumber/cm^{-1}	Peak Assignment	Media	
		H_2O	NaOH (pH>14)
3551	O-H stretching	-OH	-OH
3480	O-H stretching	-OH	-OH
3415	O-H stretching	-OH	-OH
2917	C-H stretching	$-CH_2$	$-CH_2$
1727	C=O stretching	-C=O (ester)	
1637	C-O stretching	-C-O (ester)	
1618	C–H bending	$-CH_2$, $-CH_3$	$-CH_2$, $-CH_3$
1445	C=O stretching		-COO
1352	C–O stretching	-C-O(PEO)	-C-O(PEO)
1250	-C-O stretching	-C-O(PEO)	-C-O(PEO)
1104	-C-O stretching	-C-O	-C-O
951	C-C stretching	-C-C-	-C-C-
879	C-O stretching		-C-O (alcohol)
619	C-O stretching	-C-O	-C-O

The molecular weight and the weight distribution of PCE in different media are summarised in ***Table 5.10***. Compared to the PCE dissolved in H_2O, both the number average and the mass average molecular weights were significantly decreased in NaOH solution. The molecular weight distribution was also broadened. The reduction of the molecular weight of PCE in NaOH indicates that the molecular chain was broken. Additionally, the FTIR results also revealed that the ester groups of PCE was hydrolysed in NaOH. Therefore, it can be concluded that the main reason caused the instability of the PCE in NaOH solution is because the side chain was degrafted from the backbone.

Table 5.10 Molecular weight and weight distribution of PCE

PCE	Media	
	H_2O	NaOH (pH>14)
M_n	7174	5139
M_w	34863	30647
PDI	4.86	5.96

5.7.4 Summary

The chemical stability of commercially available PC-based superplasticisers, namely, lignosulfonate, naphthalene and polycarboxylate, were examined by FTIR and HPSEC in H_2O and NaOH solution. From the experiments, it can be concluded that the chemical structures of these SPs were changed in NaOH solution: for LS, the cleavage of the grafted sulfonic group and the breakdown of the backbone chain was observed; for NF, its chemical instability in highly alkaline NaOH solution is mainly due to the degradation of the sulfonic group in highly alkaline media; for PCE, its chemical instability in NaOH solution is mainly attributed to the de-graft of the side chain from the backbone. Based on the results obtained from the current study, the chemical stability in NaOH of the above three types of SPs can be ranked in the order: PCE <LS< NF.

5.8 Concluding Remarks

In this chapter, the effects of different addition methods of LS and NF on the properties of NaOH-activated slag were examined. The results demonstrated that, compared to the simultaneous addition (*SA*), the separate addition methods improved the performance of both LS and NF in NaOH-activated slag. Overall, the *Prior Addition* (*PA*) performed better than *Delayed Addition* (*DA*). On the basis of the experimental results obtained in this Chapter, the following specific conclusions can be drawn:

- The separate addition methods of SPs reduced the competitive adsorption between SP and NaOH activator, leading to a higher amount of adsorbed SPs on the slag and a lower value of zeta potential of NaOH-activated slag. *PA* produced the highest adsorption of the SPs on the surface of the slag and the lowest zeta potential of NaOH-activated slag paste.
- The workability of NaOH-activated slag was enhanced due to the increased adsorption of SPs by separate addition methods, which subsequently promoted the dispersion of slag particles. Moreover, the separate addition

reduced both the yield stress and the plastic viscosity of the fresh NaOH-activated slag paste and delayed the setting of the paste.

- Both the compressive strength and the drying shrinkage of the hardened NaOH-activated slag were changed under the separate addition methods of LS and NF. The results were closely related to the porosity result.

However, the chemical instability of the current PC-based SPs is still an issue. Therefore, to further improve the performance of SPs, there is a need to design some alkali-compatible polymers for NaOH-activated slag system.

Chapter 6

Synthesis and Optimisation of Alkali-compatible Polymer for NaOH-activated Slag

6.1 Introduction

As highlighted in Chapters 3 and 5, the chemical stability of SPs in highly alkaline media is one of the main reasons attributed to the reduction of the effectiveness of PC-based SPs in NaOH-activated slag. The 3rd generation of PC-based SP, polycarboxylate ether superplasticisers (PCE), is superior to the 1st and 2nd generation SPs due to the addition of steric repulsion by introducing the side chain. Therefore, its development marks an important milestone for its role in the cement and concrete industry (Andersen et al., 1988, Yamada et al., 2000). However, its application in AAS has been greatly restricted due to its poor alkaline stability (Palacios and Puertas, 2004). As demonstrated in Chapter 5, the chemical structures of all the selected typical PC-based SPs, in terms of LS SP, NF SP and PCE SP, were obviously changed in NaOH solution. Therefore, the synthesis of alkali-compatible superplasticiser (polymer) is essential.

In this chapter, modified polycarboxylate based polymers (MP polymer), which are compatible with the highly alkaline environment, were synthesised, and the optimal synthesis conditions were obtained through response surface method.

The objectives of this chapter are:

- To synthesise alkali-compatible modified polycarboxylate derivation polymers (MP for short hereafter) and to establish the optimal synthesis conditions via response surface method, evaluated by the effect on the rheological properties, namely initial yield stress and initial plastic viscosity of NaOH-activated slag.
- To investigate the chemical stability of synthesised polycarboxylate superplasticisers in highly alkaline media.

6.2 Experimental programme

To achieve those above objectives, the overall research programme is presented in ***Fig 6.1*** and further details are described below. The details of the test are elaborated in Section 4.4.

Stage 1: different types of homopolymers/copolymers with various monomers were investigated by determining their effects on the initial minislump. The suitable polymer with the best performance was then identified.

Stage 2: the optimal synthesis conditions of the selected polymer were obtained and evaluated through the response surface method.

The polymer was synthesised by free radical solution polymerisation. The effects of five factors, including monomer ratio (MR), chain transfer agent concentration (CTA), monomer concentration (MC), initiator concentration (IC) and polymer dosage (PD), were investigated. The performance of alkali-compatible modified polycarboxylate polymer was then optimised by response surface method and evaluated by its effects on the yield stress and the plastic viscosity of NaOH-activated slag paste.

Stage 3: the chemical stability of the selected synthesised modified polycarboxylate polymer samples in highly alkaline media was examined.

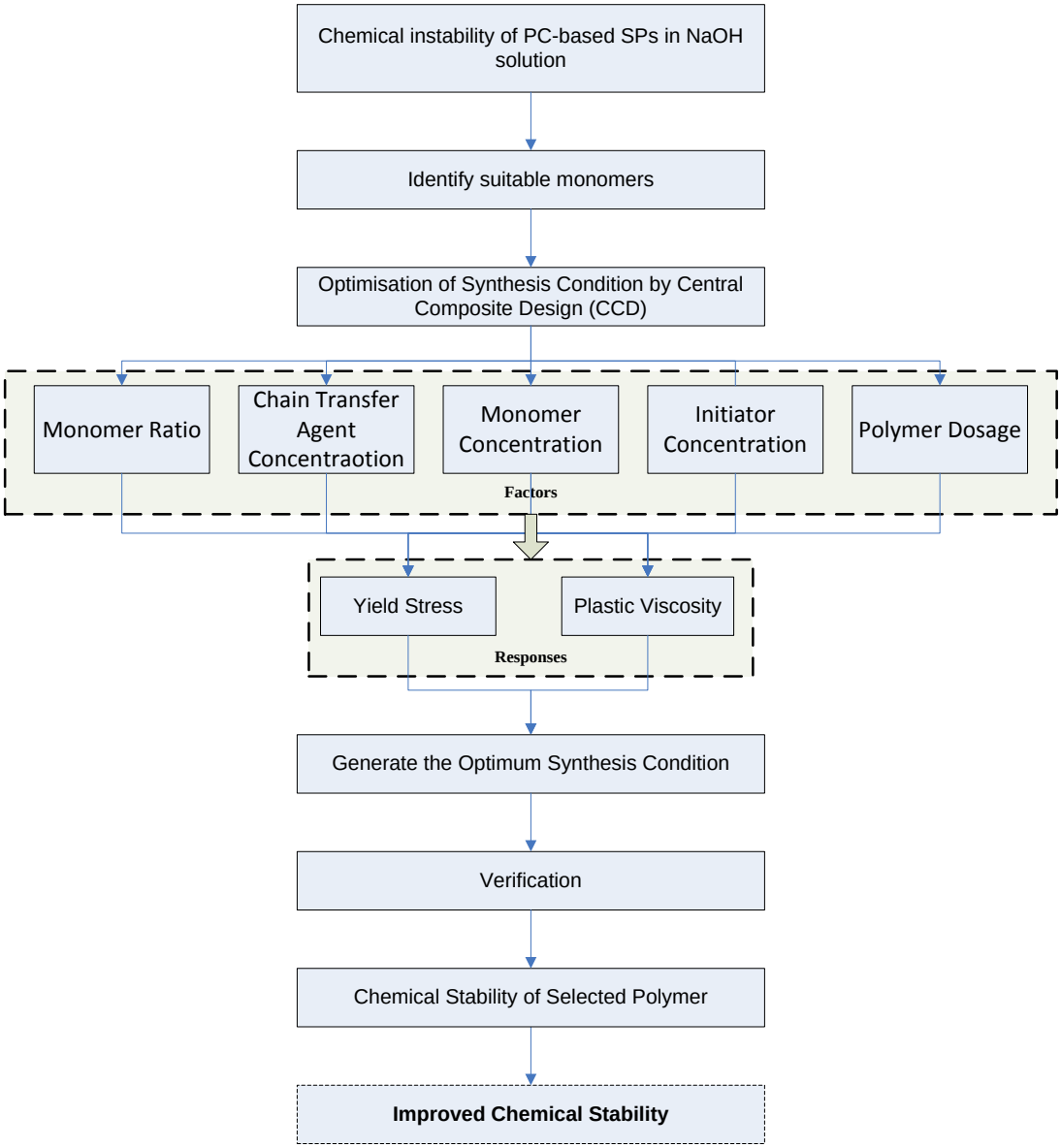

Fig 6.1 Flow chart of the overall research programme of Chapter 6

6.3 Identification of suitable monomers

6.3.1 Introduction

As demonstrated in previous chapters, commercially available PC-based SPs are not stable in highly alkaline NaOH solutions, leading to a reduced efficiency in the performance of NaOH-activated slag. Thus, a reasonable approach is to carefully select and synthesise alkali-compatible superplasticiser. As presented in Chapter 5,

the C-S bond linking $–SO_3^-$ groups from aromatic ring and C-O bond for ester groups for grafting side chain are easy to break down in highly alkaline media and cause the dysfunction of PC-based SPs. Therefore, this synthesis work was conducted to avoid these weak bonds.

Since vinyl polymers exhibit good compatibility to be assembled with different functional anchor groups and are easily polymerised to produce alkali stable polymers with good compatibility to NaOH-activated slag, vinyl based polymers were selected. However, as previously reported, the de-graft of side chains on the link between the backbone and side chain could cause the improper working of PCE SPs; therefore, the chemistry work conducted in this chapter was mainly focused on synthesising a stable backbone of superplasticiser.

In this section, free radical polymerisation (addition polymerisation) was employed to synthesise alkali-compatible polymers. As discussed previously, charge and charge density play important roles in competitive absorption, and vinyl monomers are considered the best candidate to produce alkali-compatible polymer (Winnefeld et al., 2007, Sakai et al., 2003). The investigation was carried out in two stages, as illustrated in ***Fig 6.2***: 1) the effects of different polymer charge and 2) the effects of different anchor groups. The performance of polymers in NaOH-activated slag was examined by measuring the initial minislump.

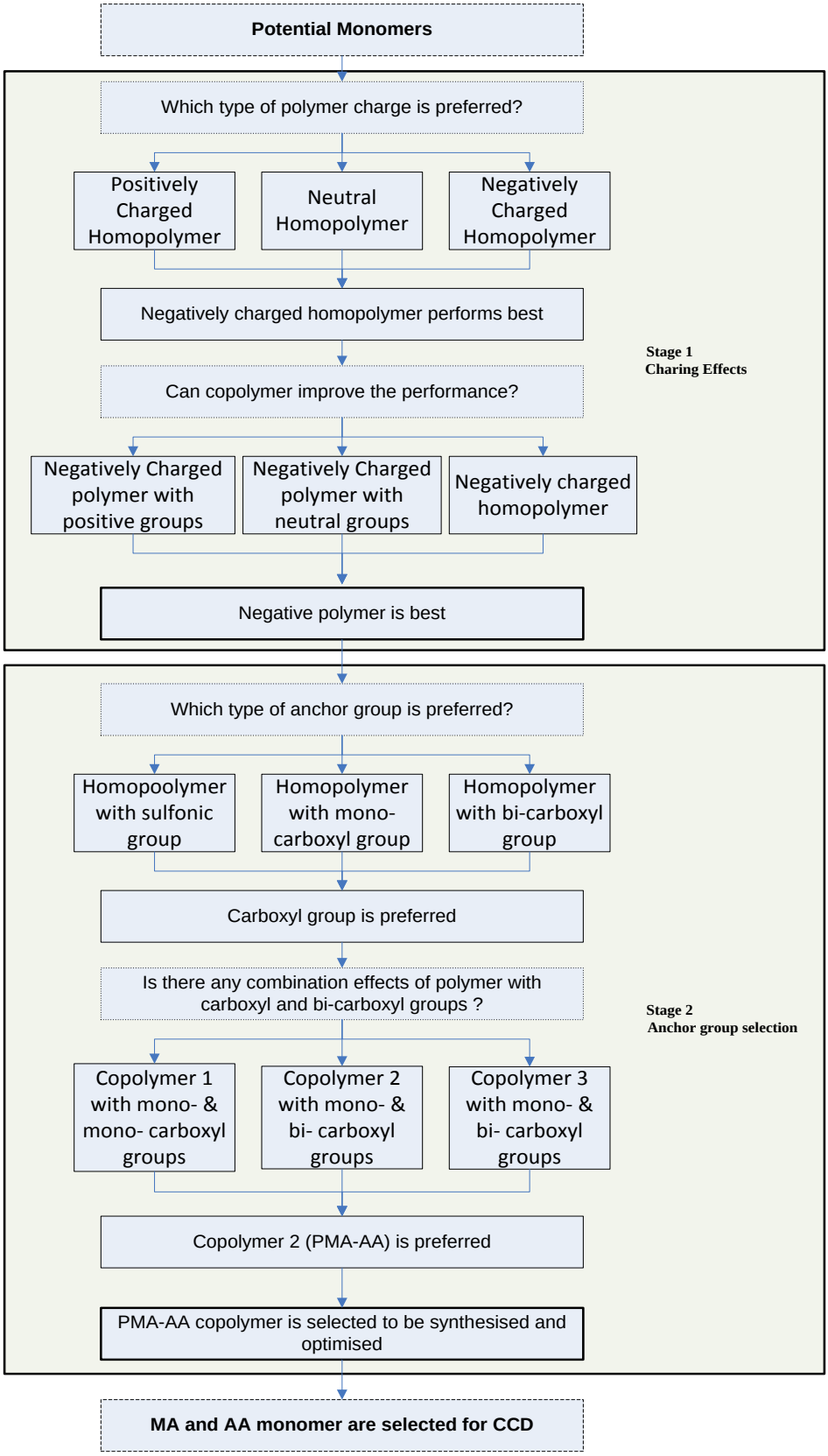

Fig 6.2 Procedure of monomer selection

Based on the literature review and the discussion in section 3.2, the potential monomers used in this synthesis work are listed in ***Table 6.1***, including their charge and anchor groups.

Table 6.1 Potential monomers used in synthesis work

Chemicals	Abbr	Chemical Structure	Charge	Anchor Groups
Diallyldimethyl ammonium chloride	DMDAAC	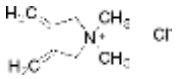	Positive	Ammonium
Acrylamide	AM	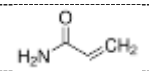	Neutral	Amide
Acrylic acid	AA	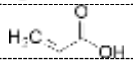	Negative	Mono-carboxyl
Sodium 4-vinylbenzene sulfonate	VBS	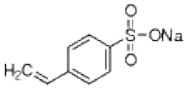	Negative	Sulfonic
2-Acrylamido-2-methyl-1-propanesulfonic acid	AMPS	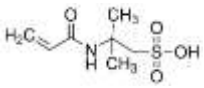	Negative	Sulfonic
Methacrylic acid	MAA	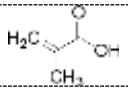	Negative	Mono-carboxyl
Maleic anhydride	MA	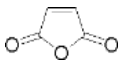	Negative	Bi-carboxyl

6.3.2 Charging effect of Monomer

In order to test the effects of a polymer charge on the performance in NaOH-activated slag, three types of homopolymers were synthesised, namely: Diallyldimethylammonium chloride (short for DMDAAC as positively charged polymer), acrylamide (short for AM as neutral polymer) and acrylic acid (short for AA as negatively charged polymer). Its effects on the initial minislump of NaOH-activated slag were also investigated.

The effects of differently charged polymers on the initial minislump of NaOH-activated slag paste are illustrated in ***Fig 6.3***. It can be clearly demonstrated from that figure that both positively charged and neutrally non-charged polymers showed less improvement on the initial minislump of slag paste. However, when adding negatively charged polymer, the initial minislump value increased from 77mm to 112mm, which suggests that the performance of negatively charged polymer was better than the polymers with positive or neutral charges.

The SPs perform by adsorbing on the surface of particles through the electrostatic attraction and dispersing particles by the residue charge, in particular for those designed based on electrostatic repulsion (Kim et al., 2000a). The neutral polymer PAM cannot be hydrolysed and supplies the charges for adsorption and electrostatic repulsion. Therefore, PAM showed no effect. Although PDMDAAC provides a positive charge after hydrolysation, the hydrolysed positive charge could be shielded due to the steric hindrance by nearby methyl groups (Koetz et al., 1986). Moreover, as discussed previously, the net charge of the particles is important for the dispersion of slag particles (Russel et al., 1992). Although the positive charge could improve the adsorption of SPs, the total net charge of particles with PDMDAAC was reduced. Therefore, the PDMDAAC only showed slight improvement of the initial minislump of NaOH-activated slag. Generally, negative zeta potential is observed in NaOH-activated slag. AA was also negatively charged after hydrolysation, which might reduce the electrostatic attraction due to the competitive adsorption, the formation of Ca-complex between the carboxyl groups of PAA soluble Ca^{2+} promotes the adsorption of SPs (Zingg et al., 2009, Puertas and Vazquez, 2001, Yamada et al., 2000). Therefore, PAA exhibits better performance in NaOH-activated slag.

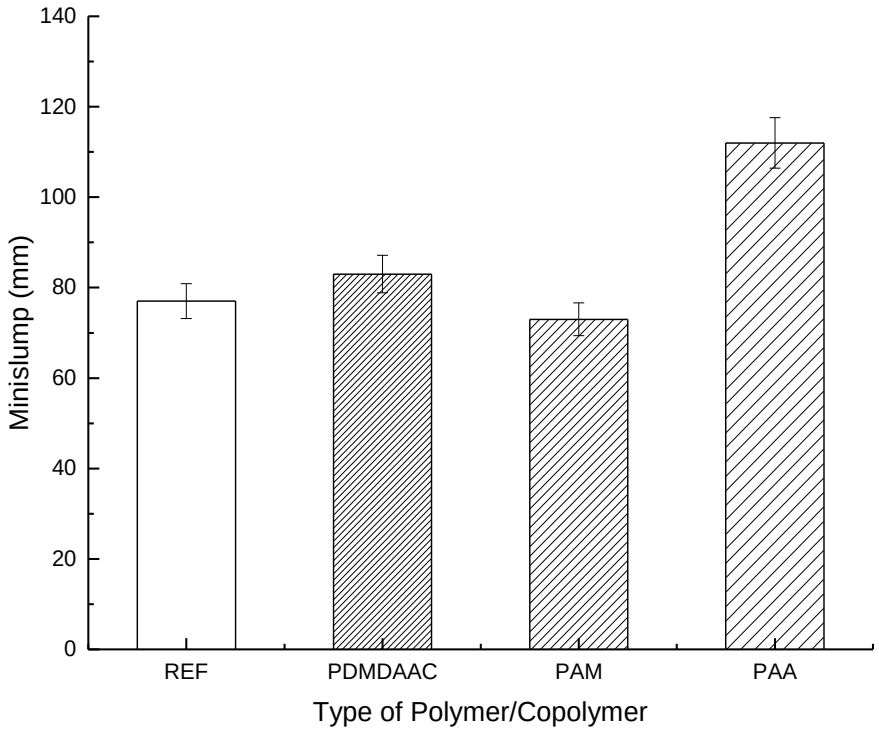

Fig 6.3 Effects of polymer charge on initial minislump of NaOH-activated slag

Following the discovery that the negatively charged PAA exhibited better performance in dispersion of NaOH-activated slag, copolymers based on the PAA with different charged (positive and neutral) groups were synthesised to further investigate the charge effect. The results are presented in ***Fig 6.4***. It can be seen from the figure that the initial minislump of PAA based copolymer was decreased when using positive and neutral anchor groups to form co-polymers. With the proportion of negative groups decreasing, minislump was also decreased. Therefore, the results suggested that the monomer with positive charge or neutral charge does not work in NaOH-activated slag.

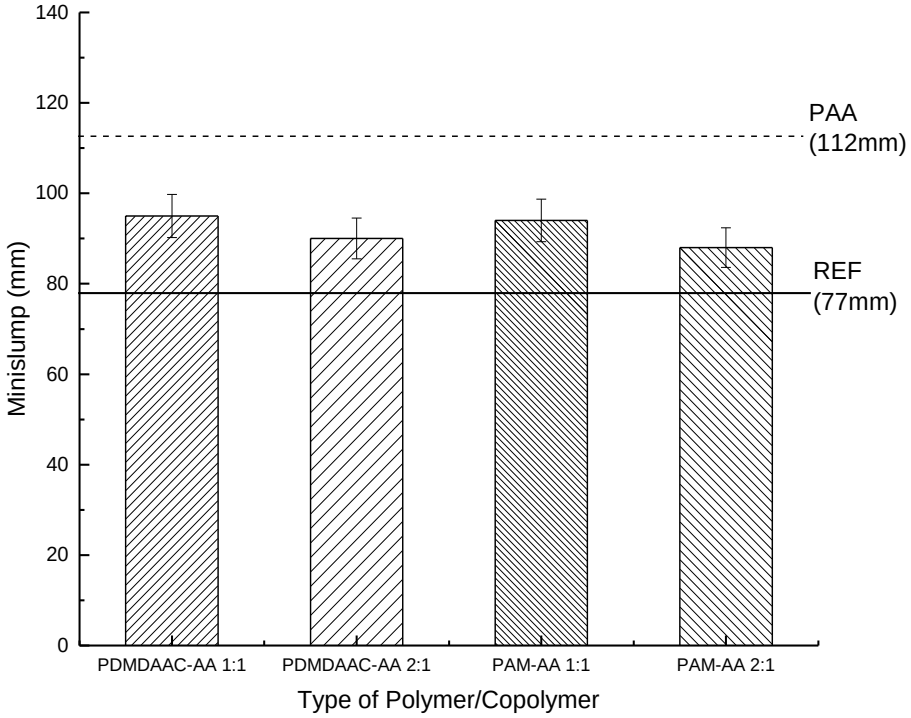

Fig 6.4 Effects of different charged anchor groups of PAA based copolymer on initial minislump of NaOH-activated slag (PDMDAAC-AA 1:1 stands for PDMDAAC and PAA copolymer with monomer ratio of DMDAAC to AA as 1:1; PDMDAAC-AA 2:1 for PDMDAAC and PAA copolymer with monomer ratio of DMDAAC to AA as 2:1; PAM-AA 1:1 for PAM and PAA copolymer with monomer ratio of AM to AA as 1:1; and PAM-AA 2:1 stands for PAM and PAA copolymer with monomer ratio of AM to AA as 2:1)

As discussed previously, the charge density of SPs is one of the most important factors affecting SPs' performance. The copolymerisation with different types of charged monomers reduced the charge density of co-polymers. Therefore, the

improvement of co-polymer on initial minislump was inhibited. Moreover, with an increase of the proportion of DMDAAC or AM, which reduced the charge density of polymer, the initial minislump further decreased. These results confirmed that the charge density is important for the dispersion effect of polymer as stated in other researches in chapter 2 (Winnefeld et al., 2007, Sakai et al., 2003).

To sum up, in terms of charging effect, negative homopolymer performed better than neutral or positively charged homopolymer in NaOH-activated slag. It is also better than co-polymers introduced in either positive or neutral monomers. In the next section, the effect of anchor groups on negatively charged copolymers was investigated.

6.3.3 Effects of anionic anchor groups

Sulphonic and carboxyl groups are most commonly existing in the 3rd generation superplasticisers (Ma et al., 2013, Plank and Yu, 2010, Puertas et al., 2005, Li et al., 2005, Yamada et al., 2000, Ohta et al., 2000). To induce sulfonic groups, sodium 4-vinylbenzenesulfonate (VBS) and 2-Acrylamido-2-methyl-1-propanesulfonic acid (AMPS) monomers were used. To induce carboxyl groups (either vic-$(COO-)_2$ or $-COO^-$ groups), maleic anhydride (MA), acrylic acid (AA), and methacrylic acid (MAA) were employed.

The effects of different negatively charged homopolymers on initial minislump of NaOH-activated slag are shown in ***Fig 6.5***. Obviously, the polymer containing sulfonic groups exhibited less effect on the improvement of minislump of NaOH-activated slag than that containing carboxyl groups. Compared to Poly-VBS, lower minislump spread was observed in the paste added with Poly-AMPS. The reason of lower minislump by poly-AMPS is due to the hydrolysation of amide groups of the AMPS in NaOH solution (Roberts and Caserio, 1977). Compared to PMAA, PAA provided a higher minislump spread. This could be due to the methyl groups of MAA increasing the rigidity of polymers (Wang et al., 2011). PMA provided similar improvement with that of PAA.

The results presented in ***Fig 6.5*** indicated that compared with carboxyl groups, sulfonic groups provided less effect on the improvement of minislump of NaOH-activated slag. The surface affinity of anchor groups on surface could be described

by increasing order as $–SO_3$- < -COO- < vic-(COO-) $_2$. These results match well with Plank's finding (Plank et al. 2007). Therefore, the functional groups of the synthesised polymer are preferred as carboxyl groups.

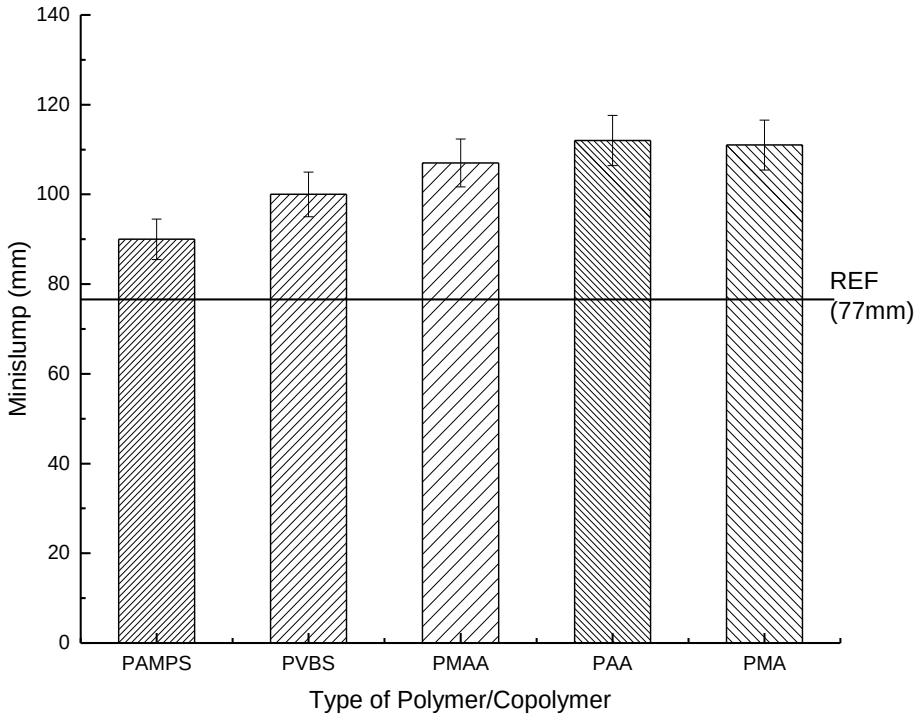

Fig 6.5 Effects of different anchor groups on initial minislump of NaOH-activated slag

The effects of different polycarboxylate copolymer on the initial minislump of NaOH-activated slag are illustrated in ***Fig 6.6.*** From the figure, it is obvious that among different copolymers, PMA-AA provided a higher minislump value of NaOH-activated slag. In addition to inducing the rigidity of polymer by methyl groups of MAA, the charge density of carboxyl based polymer was also reduced by adding methyl groups on the backbone of polymer. Therefore, PMAA-AA and PMAA-MA provided lower minislump of NaOH-activated slag.

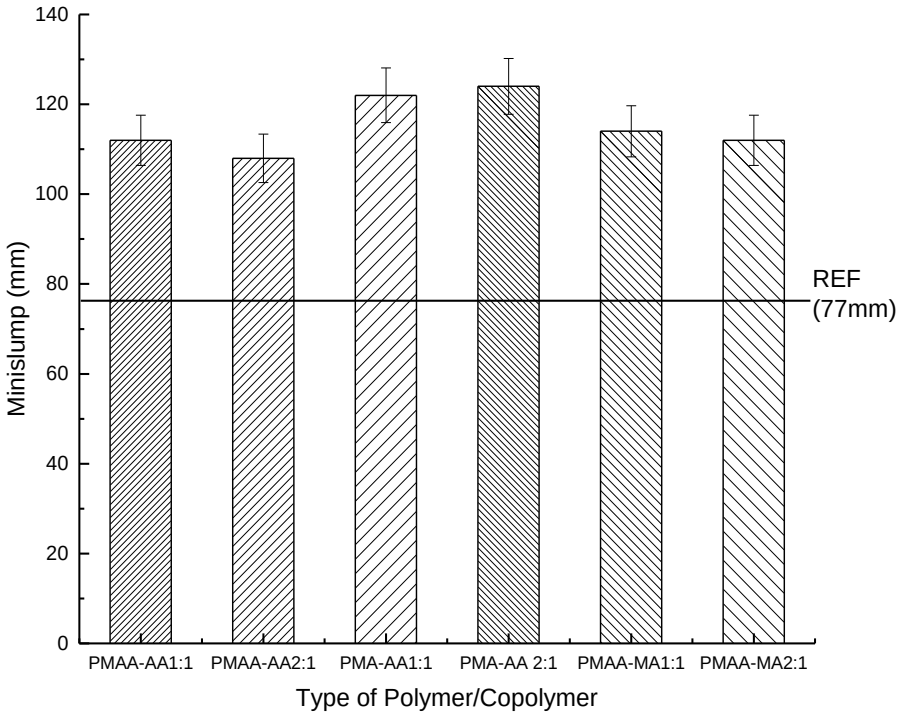

Fig 6.6 Effects of different types of negative anchor groups of PAA based copolymer on initial minislump of NaOH-activated slag

To sum up, the carboxyl groups performed as the most effective functional groups on improving the minislump of NaOH-activated slag. PMA-AA copolymer provided the best performance among various negatively charged monomers. Therefore, the MA and AA monomers were selected to be copolymerised by experimental design in order to achieve the best performance of alkali-compatible polymers.

6.3.4 Summary

In this section, the effects of polymer charge and anchor groups of polymer were investigated by examining their effects on the initial minislump of NaOH-activated slag. Two conclusions can be drawn below:

- The negative polymer performed better than neutral or positive polymer in NaOH-activated slag.
- The carboxyl groups performed as the most effective functional groups on improving the minislump of NaOH-activated slag, while vic- was better than mono COO^- group.

From the trial results, PMA-PAA copolymer showed the highest minislump results of NaOH-activated slag. In next section, the optimising of synthesis of PMA-AA copolymers was conducted.

6.4 Synthesis of alkali-compatible polycarboxylate polymer

6.4.1 Introduction of synthesis work

Optimisation is one of the important procedures to improve the overall performance of a system in order to maximise the benefit from the system. The traditional approach to conducting the optimisation is to monitor one factor each time as the experimental response while keeping other factors as constant. Two main disadvantages of the traditional approach are: 1) the interactive effects among factors are ignored and 2) a large number of experiments must be carried out (Khuri and Mukhopadhyay, 2010). To overcome these issues, the response surface methodology (RSM), which is designed based on mathematical and statistical techniques, is employed. The employment of RSM in experimentation could not only reduce the total number of experiments, which is essential to conduct, but also provide the possibility to evaluate the interaction between the factors on the response (Dean and Voss, 1999).

Generally, three types of designs, namely full three-level factorial design, box-behnken design and central composite design, are most frequently used in RSM. Compared with box-behnken design (BBD) and central composite design (CCD), more experiments will need to be conducted by full three-level factorial design. Therefore, BBD and CCD are preferred (Bezerra et al., 2008, Sun et al., 2010).

The schemes of the experiment based on the study of three variables by box-behnken design and central composite design are presented in ***Fig 6.7.*** It can be clearly seen that compared to BBD, the central composite design provides five effective levels, which allows the experiment to be conducted at the extreme condition of factors (Bezerra et al., 2008). However, for the box-behnken design, all the experiments are confined in the matrix; therefore, the experiment at certain points under extreme conditions could not be conducted.

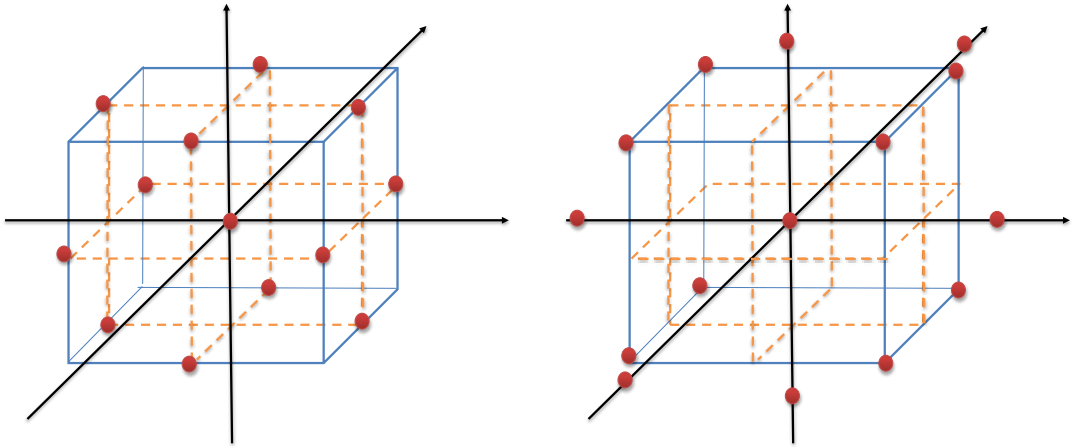

(a) box-behnken design (b) central composite design

Fig 6.7 Schemes of experiment based on the study of three variables: (a) box-behnken design and (b) central composite design (Craney, 2003, Cho and Zoh, 2007, Ferreira et al., 2007)

It has been reported that the central composite design, based on the two-factor design (2^k), is a popular template for experiment design *(Bezerra et al., 2008, Hang et al., 2011, Dalcin et al., 2011, Capella-Peiró et al., 2006, Rigas et al., 2005)*. The general procedure of CCD is described as follows (Bezerra et al., 2008):

(1) Screening test of variables and delimitation of experiment region
(2) Choosing the experimental design and conducting the experiment via selected matrix
(3) Conducting mathematic-statistical treatment of the results
(4) Evaluating the model's fitness
(5) Determining the optimal condition of results
(6) Verifying the optimised condition of the results

In this section, CCD was used to investigate and optimise the synthesis conditions of this modified polycarboxylate polymer. Following the procedure above, the experiments were conducted and the results were analysed by "Design Expert" software.

6.4.2 Central Composite Design (CCD)

6.4.2.1 Screening test of variables and delimitation of experiment

As discussed in section 2.2.3, four factors, which have been identified as the most significant factors controlling the chemical structure of polymers, i.e. *monomer ratio (MR), chain transfer agent concentration (CTA), monomer concentration (MC), initiator concentration (IC)* were selected to investigate and optimise the performance of alkali-compatible polymer (Mandal, 2013). Since *polymer dosage (PD)* is important in affecting the performance of polymer in NaOH-activated slag, it was selected as the fifth factor.

6.4.2.2 Choosing the experimental design and conducting the experiment via selected matrix

For the application of response surface design, it is necessary that the results could be fitted with the following equation (***Equation 6.1***) to generate a response surface.

$$y = \beta_0 + \sum_{i=1}^{k} \beta_i x_i + \epsilon \qquad \textbf{6.1}$$

Where y stands for response, β_0 and β_i for regression coefficients, $\sum_{i=1}^{k} \beta_i x_i$ for linear effect of factor x_i, and ϵ for error from response. In order to determine the critical point, such as maximum, minimum, or saddle point, the polynomial function containing quadratic terms (***Equation 6.2***) is applied in the regression .

$$y = \beta_0 + \sum_{i=1}^{k} \beta_i x_i + \sum_{i=1}^{k} \beta_{ii} x_i^2 + \sum \sum_{i<j} \beta_{ij} x_i x_j + \epsilon \qquad \textbf{6.2}$$

Where y stands for response, β_0, β_i, β_{ii}, and β_{ij} for regression coefficients, $\sum_{i=1}^{k} \beta_i x_i$ for linear effect of factor x_i, $\sum_{i=1}^{k} \beta_{ii} x_i^2$ for quadratic effect of factor x_i, $\sum \sum_{i<j} \beta_{ij} x_i x_j$ for interaction effect between factor x_i and x_j (x_i and x_j were the i and j factor), and ϵ for error from response.

Generally, the CCD consists of three parts: 1) central point, located in the centre of design matrix, which is coded as **0**; 2) factorial point, based on full factorial design (2^k) with two levels coded as **±1** (representing the lower and higher level of each

factor); and 3) axial point, designed in which experimental point at the distance **α** from the central point (Khodadoust and Hadjmohammadi, 2011). The coded values are related to the real value calculated from ***Equation 6.3*** (Kwak, 2005).

$$Z = \frac{(x-\bar{x})}{\Delta X} \qquad \textbf{6.3}$$

Where Z stands for coded value, x for original uncoded value, $\bar{x}$ for mean value of the factor, and Δx for margin increment of x. The α value depended on the variables in the design, which is calculated via ***Equation 6.4***.

$$\alpha = (n_f)^{1/4} \qquad \textbf{6.4}$$

Where n_f stands for the number of factors.

Thus, five levels (-α, -1, 0 +1, + α) for each factor are investigated. Total experimental number required for a CCD is calculated according to ***Equation 6.5*** (Rigas et al., 2005).

$$N = 2^{(n_f)} + 2(n_f) + n_d \qquad \textbf{6.5}$$

Where n_f stands for the number of factors and n_d for replicate number at central point.

As discussed in section 6.3.2.1, in this experiment, five-factor central composite design with 50 experiments was established. The full two level factorial design with five factors (2^5) led to a total of 32 experiments as factorial points (coded as ±1 for each factor). In order to estimate the error (the error term ϵ in **equation 6.1** and **6.2**), 8 additional experiments duplicated at the central point were considered (coded as 0). Besides those three levels, to obtain a polynomial relationship, more experiments were introduced as axial points with code ±α (α=2.378). Thus, totally 10 more mixtures from two axial points of each factor were tested. In the end, a total of 50 mixtures were investigated.

The synthesis process was carried out via free radical polymerisation. The details of the parameters of these factors are shown in ***Table 6.2***. The parameters of the central point (level 0) were selected based on trial experiments carried to select suitable

polymer (section 6.3). Two rheological statistical response models, i.e. initial yield stress and initial plastic viscosity, were quantitatively measured and used for the optimisation. The mixing procedures are referred to Section 4.5.2.2.

Table 6.2 Details of parameters of five factors of experiments

Factors	Parameter	Levels				
		-α (-2.378)	**-1**	**0**	**+1**	**+α (+2.378)**
A	Monomer Ratio (MA:AA)	0.22	1.25	2.00	2.75	3.78
B	CTA concentration,%	0.22	1.25	2.00	2.75	3.78
C	Monomer concentration,%	28.10	35.00	40.00	45.00	51.90
D	Initiator concentration,%	0.40	0.75	1.00	1.25	1.60
E	Polymer Dosage,%	0.00	0.58	1.00	1.42	2.00

The polymerisation reaction is presented in ***Fig 6.8***. The polycarboxylate derivation copolymers were synthesised via free radical solution polymerisation in DI water with a potassium persulphate (KPS) initiator. The polymers were denoted as Poly (MA_x-AA_y), where x is the degree of polymerisation of MA units and y is the degree of polymerisation of AA units. Briefly, a designated quantity of KPS initiator was dissolved in half portion of total water to a 150ml three neck flask with a magnetic stirrer, a thermometer and a condenser (The equipment setup can be referred in ***Fig 4.2***). The temperature was slowly increased to the target temperature through water bath. Then, the desired quantity of the two monomers and chain transfer agent were dissolved in the rest of the Milli-Q water and added into a flask droplet by droplet. The reaction processed for 3 hours under continuous stirring. After polymerisation, the copolymer solution was immediately stored in a fridge to stop further polymerisation.

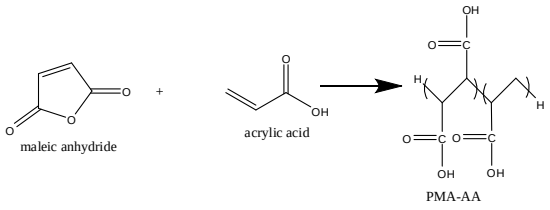

Fig 6.8 polymerisation of PMA-AA copolymer

6.4.2.3 Conducting mathematic-statistical treatment of the results

The analysis of the results was conducted with the Design Expert software (Version 8.0.7, State-Ease Inc. Minneapolis, USA). The results of all experiments for 50 mixtures are presented in ***Table 6.3***. After assessing the best fitting model by the software, quadratic equation of the yield stress (Y_1) and linear equation of the plastic viscosity (Y_2) response surface for the results were generated in ***Equation 6.6*** and ***6.7***. The equation was expressed as functions of monomer ratio (A), chain transfer agent concentration (B), monomer concentration (C), initiator concentration (D) and polymer dosage (E) based as coded unit in ***Table 6.2***.

$$Y_1 = 0.29 - 2.26A - 0.79B + 1.34C - 0.98D - 2.08E + 0.53AB - 0.53AC + 0.79AD + 0.61AE - 0.76BC + 0.97BD + 0.89BE - 1.18CD - 0.47CE + 0.51DE + 1.54A^2 - 0.52B^2 - 0.49C^2 - 0.14D^2 + 1.37E^2 \quad \textbf{6.6}$$

$$Y_2 = 0.55 + 0.037A - 0.031B + 0.035C - 0.061D + 0.021E \quad \textbf{6.7}$$

Table 6.3 Five-factor experiment design layout (in code value)

No.	Code Value					Response	
	Factor A	Factor B	Factor C	Factor D	Factor E	Yield Stress /Pa	Plastic Viscosity/ Pa s
1	-1	-1	-1	-1	-1	1.04	0.48
2	0	0	2.378	0	0	1.71	0.51
3	-1	-1	-1	1	-1	0.58	0.46
4	1	1	-1	-1	-1	-2.43	0.58
5	-1	1	1	-1	1	5.74	0.53
6	0	0	0	0	0	-2.04	0.69
7	-1	-1	1	1	-1	2.04	0.50
8	-2.378	0	0	0	0	23.58	0.50
9	1	-1	1	-1	-1	3.79	0.56
10	-1	1	-1	1	-1	1.11	0.40
11	0	0	0	0	2.378	-2.09	0.53
12	1	1	1	1	-1	0.20	0.51
13	1	1	1	-1	1	0.18	0.63
14	-1	-1	-1	1	1	-0.54	0.44
15	0	0	0	-2.378	0	4.85	0.76
16	1	-1	-1	1	-1	-1.88	0.51
17	-1	1	1	1	1	-0.47	0.46
18	1	1	-1	1	1	-1.58	0.48
19	-1	-1	1	-1	1	3.33	1.00
20	1	1	-1	1	-1	-0.84	0.50
21	-1	-1	-1	-1	1	0.09	0.46
22	0	2.378	0	0	0	-0.31	0.50
23	0	0	0	0	0	-1.94	0.39
24	1	1	1	-1	-1	0.08	0.52

25	0	0	0	0	-2.378	24.22	0.68
26	1	1	1	1	1	0.17	0.53
27	-1	1	-1	-1	1	-1.89	0.38
28	0	0	0	0	0	-2.33	0.52
29	1	1	-1	-1	1	-2.12	0.91
30	1	-1	1	-1	1	1.29	0.69
31	0	0	0	2.378	0	0.11	0.41
32	1	-1	-1	-1	1	-1.94	0.88
33	0	0	0	0	0	3.17	0.47
34	1	-1	-1	1	1	-0.72	0.48
35	-1	-1	1	1	1	0.20	0.48
36	0	-2.378	0	0	0	1.01	0.59
37	-1	1	-1	1	1	0.32	0.40
38	1	-1	1	1	1	-0.07	0.86
39	0	0	0	0	0	-1.94	0.44
40	0	0	-2.378	0	0	-0.69	0.39
41	1	-1	-1	-1	-1	-0.20	0.56
42	-1	-1	1	-1	-1	23.76	0.60
43	-1	1	1	1	-1	1.24	0.48
44	-1	1	-1	-1	-1	0.49	0.46
45	2.378	0	0	0	0	0.43	0.51
46	0	0	0	0	0	2.61	0.49
47	-1	1	1	-1	-1	0.04	0.66
48	0	0	0	0	0	3.39	0.39
49	1	-1	1	1	-1	0.46	0.58
50	0	0	0	0	0	3.93	0.61

6.4.2.4 Evaluating the model's fitness

The evaluation of the mathematic model generated from the results (***Table 6.3)*** was also conducted by using the Design Expert software (Version 8.0.7, State-Ease Inc. Minneapolis, USA).

6.4.2.4.1 Regression analysis of quadratic model of yield stress

The statistical significance of ***Equation 6.6*** was checked by Fisher's F-test for the analysis of variance (ANOVA) and the results were presented in ***Table 6.4***. The value of "Prob > F" less than 0.050 indicates that the regressed model was considered to be significant at 95% confidence level. In ***Table 6.4,*** the Model value of 0.0332 suggested that there is only a 3.32% chance that the error could occur due to noise. In addition, the factor A, E and quadratic factors A^2, E^2 were identified as the significant model term, since values of "Prob > F" of were less than 0.050. This means that monomer ratio (A) and polymer dosage (E) played significant effect on

the yield stress. The coefficient of multiple determinations, R^2, was observed to be 0.5912, which means that the model could explain 59.12% of the total variation in this system. The predict-R^2 value was -0.6142, implying that the predicted model demonstrated better prediction of the response than the current model. The low value of R^2 could be due to the indirect response (yield stress) from the factors. Adequate precision (Adeq Precision) is used for measuring the signal to noise ratio and the value greater than 4 is desirable. The value obtained from the model was 6.998 indicating an adequate signal, suggesting the model can be validly used in the examined range of experiments.

Table 6.4 Analysis of variance (ANOVA) of the fitted models of yield stress response

Source	Sum of Squares	Degree of Freedom	Mean Square	F Value	p-value (Prob>F)
Model	1027.55	20	51.38	2.10	0.0332
A	220.60	1	220.60	9.03	0.0054
B	26.89	1	26.89	1.10	0.3027
C	78.20	1	78.20	3.20	0.0840
D	41.32	1	41.32	1.69	0.2036
E	187.28	1	187.28	7.67	0.0097
AB	8.87	1	8.87	0.36	0.5514
AC	8.89	1	8.89	0.36	0.5509
AD	19.86	1	19.86	0.81	0.3746
AE	11.94	1	11.94	0.49	0.4900
BC	18.38	1	18.38	0.75	0.3929
BD	30.32	1	30.32	1.24	0.2744
BE	25.22	1	25.22	1.03	0.3180
CD	44.77	1	44.77	1.83	0.1863
CE	7.02	1	7.02	0.29	0.5959
DE	8.29	1	8.29	0.34	0.5646
A^2	131.80	1	131.80	5.40	0.0274
B^2	15.04	1	15.04	0.62	0.4390
C^2	13.45	1	13.45	0.55	0.4641
D^2	1.15	1	1.15	0.047	0.8299
E^2	104.90	1	104.90	4.29	0.0472
Residual	708.37	29	24.43		
Lack of Fit	647.82	22	29.45	3.40	0.0508
Pure Error	60.55	7	8.65		
Cor Total	1735.92	49		2.10	0.0332
R^2	0.5912				
Adeq Precision	6.998				

The normal probability and residuals of yield stress fitted model are plotted in ***Fig 6.9 (a)***. The predicted value Vs actual value are plotted in ***Fig 6.9 (b)***. It is clearly seen from both figures that the residual values and predicted/actual values are distributed closely on both sides of the lines, indicating that the experimental data are in a good correlation with the predicted data. All the analysis results indicated the adequacy of a regressed quadratic model is good to present the response of yield stress in the designed range.

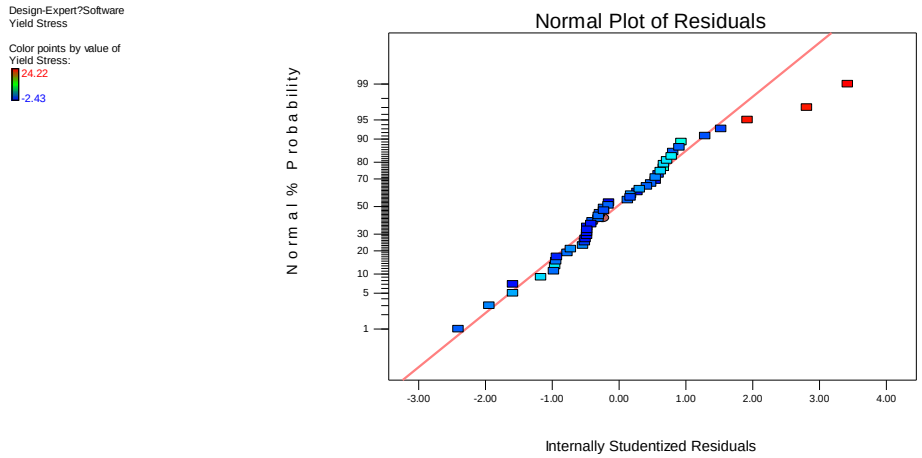

(a) Normal % probability

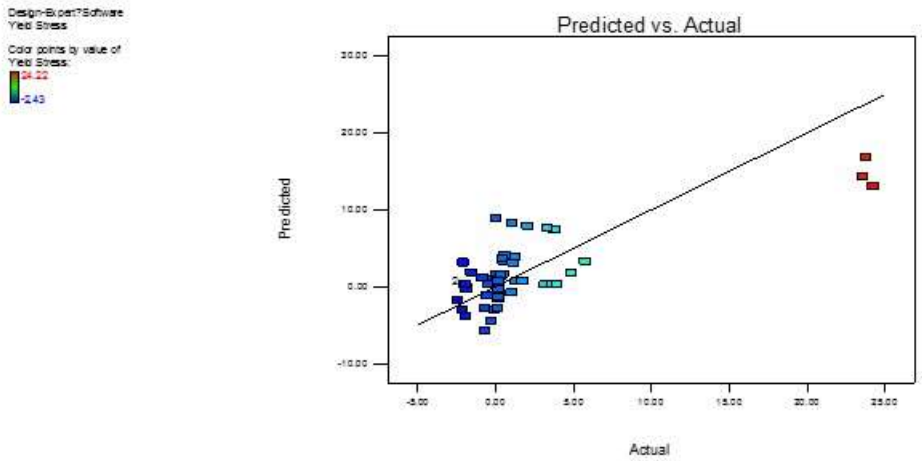

(b) predicted values Vs actual value

Fig 6.9 Diagnostic plot for yield stress

6.4.2.4.2 Regression analysis of linear model of plastic viscosity

The statistical significance of ***Equation 6.7*** was checked by Fisher's F-test for the analysis of variance (ANOVA) and the results were presented in ***Table 6.5***. The value of "Prob > F" less than 0.050 indicates that the regressed model was considered to be significant at 95% confidence level. In ***Table 6.5***, the value of 0.0013 suggested that there is only a 0.13% chance that the error could occur due to noise. The factor D (initiator concentration) was identified as the significant model term, since value of "Prob > F" of is less than 0.050. The coefficient of multiple determinations, R^2, was observed to be 0.3537, which means that the model could only explain 35.37% of the total variation in this system. The analysis results suggested that a correlation exists between the actual and the predicted data. Similar to the analysis of yield stress, adequate precision value (Adeq Precision) obtained from the model of 9.038 indicated an adequate signal, suggesting the model can be used to navigate the design space. The lower value could also be explained by the indirect response from the factors. The results were also confirmed from the plot of normal probability and the plot of predicted value Vs actual value in ***Fig 6.10 (a)*** and ***(b)***.

Table 6.5 Analysis of variance (ANOVA) of the fitted models of plastic viscosity response

Source	Sum of Squares	Degree of Freedom	Mean Square	F Value	p-value (Prob>F)
Model	0.33	5	0.067	4.82	0.0013
A	0.060	1	0.060	4.33	0.0433
B	0.040	1	0.040	2.92	0.0948
C	0.052	1	0.052	3.72	0.0603
D	0.16	1	0.16	11.79	0.0013
E	0.018	1	0.018	1.33	0.2556
Residual	0.61	44	0.014		
Lack of Fit	0.53	37	0.014	1.27	0.3995
Pure Error	0.079	7	0.011		
Cor Total	0.95	49			
R^2	0.3517				
Adeq Precision	9.038				

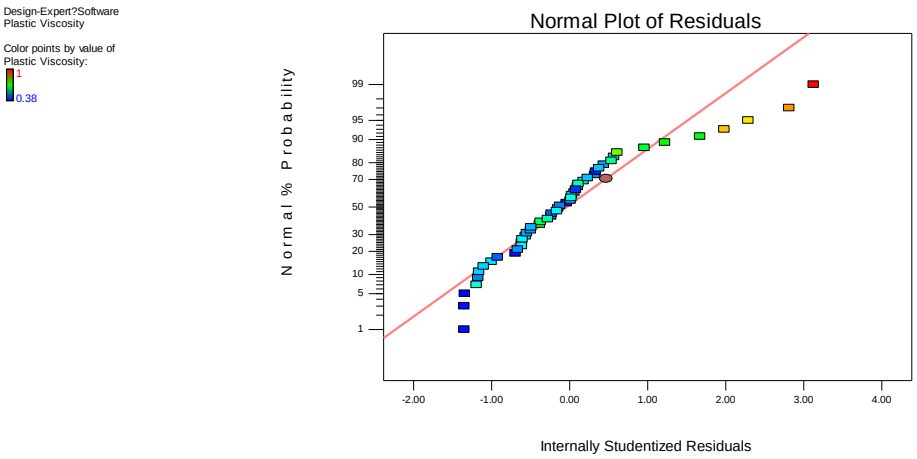

(a) Normal % probability

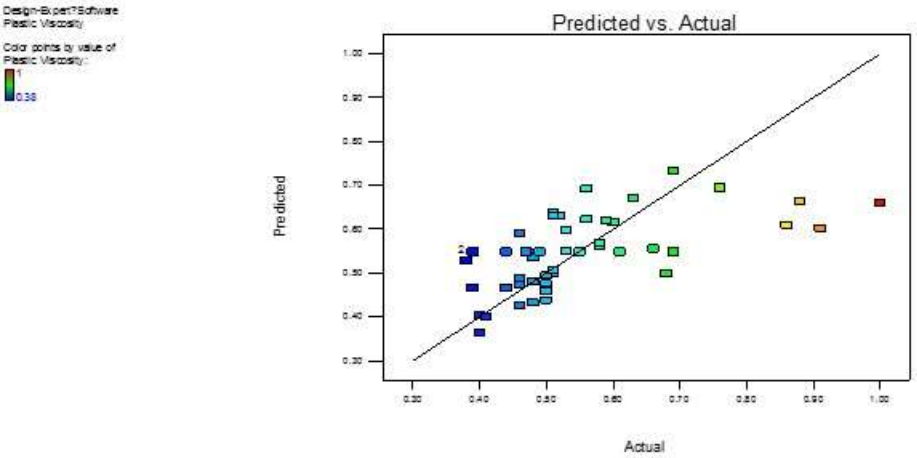

(b) predicted values Vs actual value

Fig 6.10 Diagnostic plot for plastic viscosity

6.4.2.4.3 Response surface plot

The results have been analysed by ANOVA and confirmed that the model we used is valid. Therefore, the response surface can be visually plotted and the effects of various factors are examined in this section.

The coefficients of coded regression models of yield stress and plastic viscosity are presented in ***Table 6.6*** and the effects of factors on the yield stress and plastic viscosity are shown in ***Fig 6.11*** and ***6.12***, respectively. These 3D response surface

plots visualise the relationship between responses and different factors at various levels.

The regression coefficients of the factors represent the change in each response as the change of response by one coded unit of the factor level. The properties of positive and negative coefficients indicate the relationship between the response and the factors. Positive value suggests there is a positive correlation between the response and factors, while negative value indicates a negative relationship between them. From the data presented in the table, it can be seen that yield stress was reduced with the increase of MR, CTA, IC, and PD. However, the increase of MC led to the increment of yield stress. Moreover, MR, MC and PD exhibited a positive correlation to plastic viscosity, while CTA and IC showed a negative one.

Table 6.6 Coefficients of coded regression models of the responses (by coded Value)

Yield Stress		**Plastic Viscosity**	
	Coefficients		**Coefficients**
Intercept	+0.29	Intercept	+0.55
MR (A)	-2.26	MR (A)	+0.037
CTA (B)	-0.79	CTA (B)	-0.031
MC (C)	+1.34	MC (C)	+0.035
IC (D)	-0.98	IC (D)	-0.061
PD (E)	-2.08	PD (E)	+0.021
A ×B	+0.53		
A ×C	-0.53		
A ×D	+0.79		
A ×E	+0.61		
B ×C	-0.76		
B ×D	+0.97		
B ×E	+0.89		
C ×D	-1.18		
C ×E	-0.47		
D ×E	+0.51		
A^2	+1.54		
B^2	-0.52		
C^2	-0.49		
D^2	-0.14		
E^2	+1.37		

For the response equation, the absolute value of the coefficients positively correlates to the change in the response. Thus, a higher coefficient of the factor suggests that a greater change of response is observed when changing one unit of the factor. From the table, it can be clearly seen that regarding yield stress, the coefficients of the factors of MR and PD were higher than others, suggesting that these two factors exhibit more influence on the yield stress of NaOH-activated slag. Although the interaction between the two factors showed effects on the yield stress, compared to MR and PD, less influence (smaller value coefficients) was observed. However, for the plastic viscosity, the influences of each selected factor were quite small and close to each other, suggesting their negligible effects on the plastic viscosity.

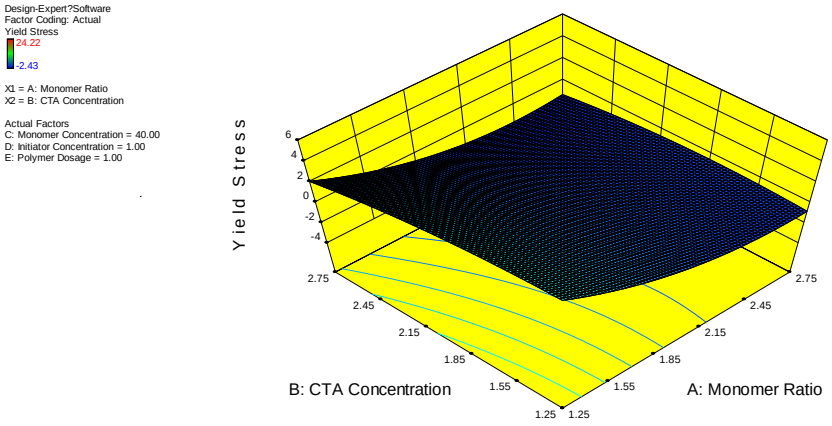

(a) The relationship between MR (-) and CTA (%)

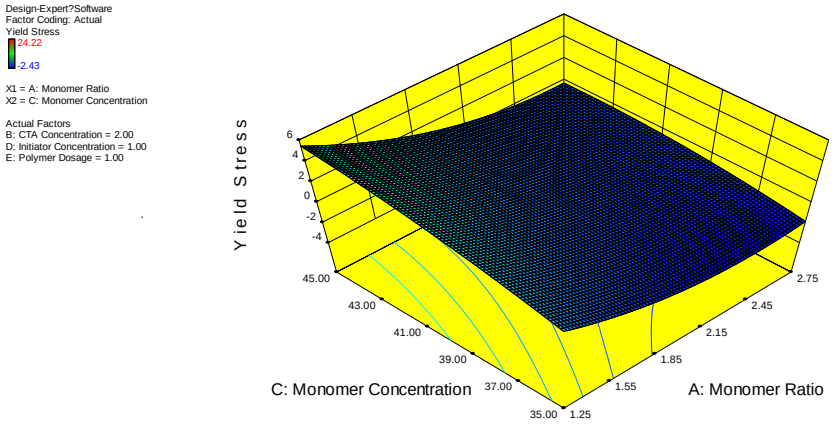

(b) The relationship between MR (-) and MC (%)

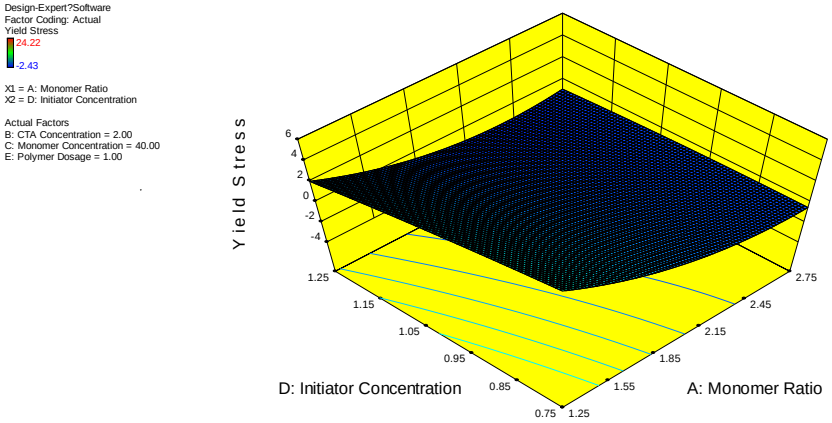

(c) The relationship between MR (-) and IC (%)

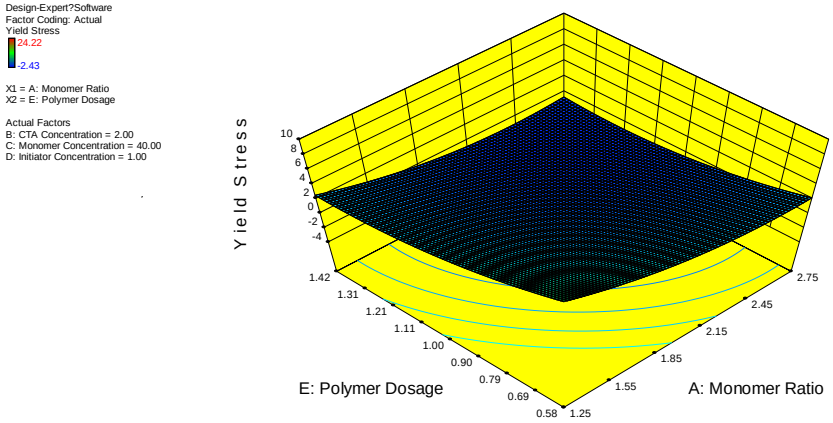

(d) The relationship between MR (-) and PD (%)

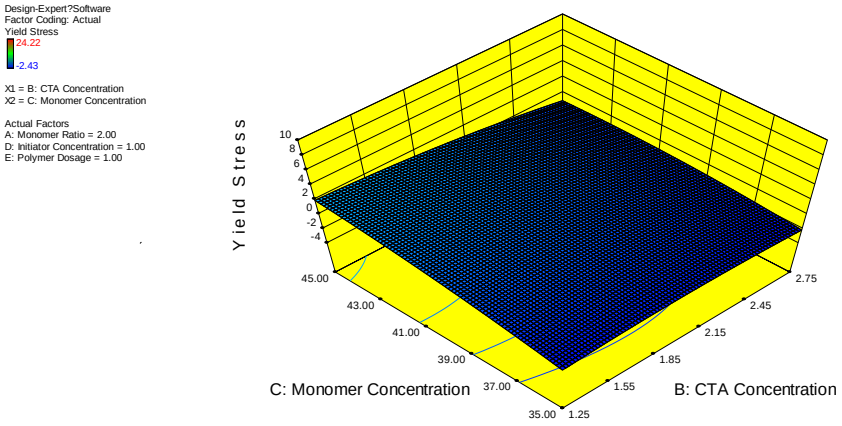

(e) The relationship between CTA (%) and MC (%)

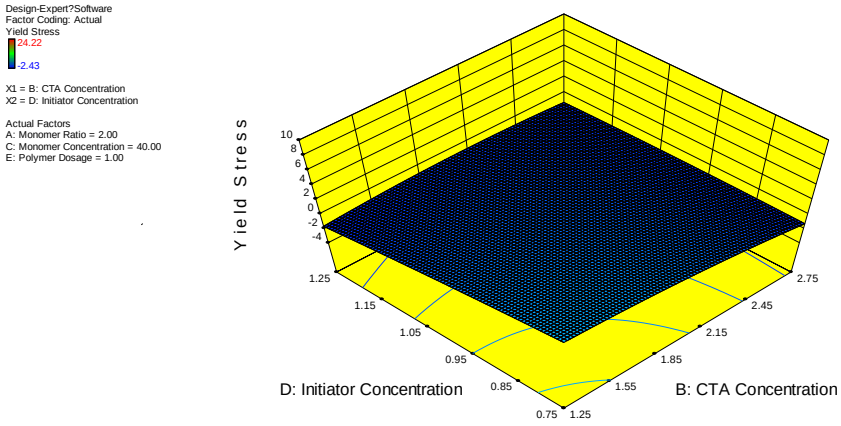

(f) The relationship between CTA (%) and IC (%)

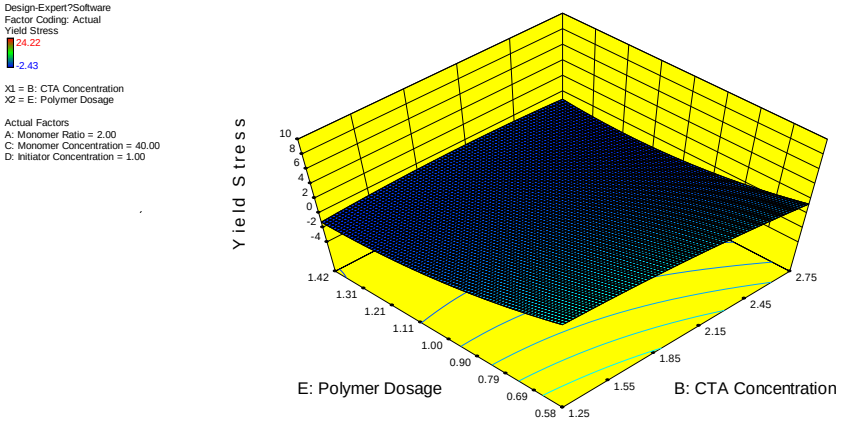

(g) The relationship between CTA (%) and PD (%)

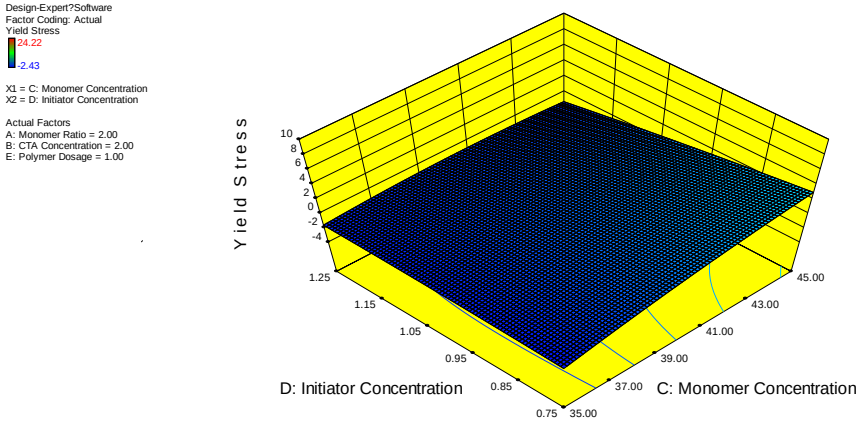

(h) The relationship between MC (%) and IC (%)

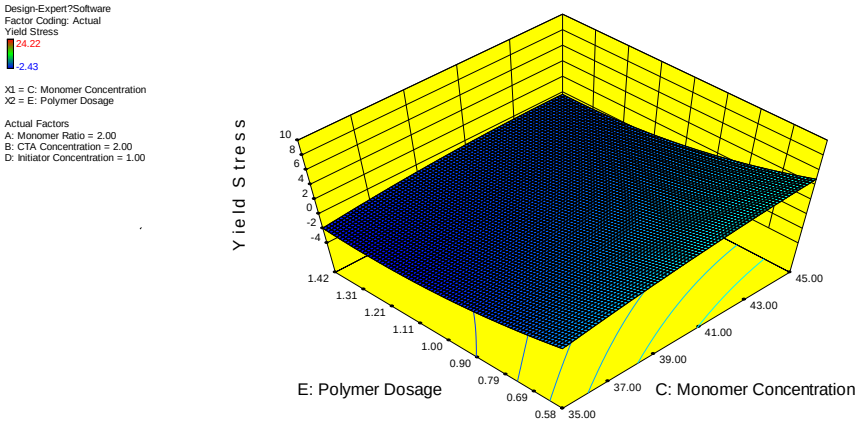

(i) The relationship between MC (%) and PD (%)

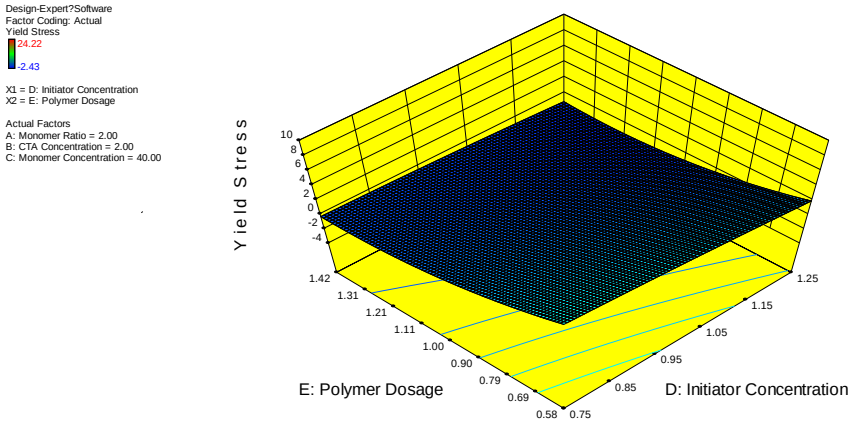

(j) The relationship between IC (%) and PD (%)

Fig 6.11 3D response surface of yield stress in dependence of five factors: A) Monomer ratio (MR); B) Chain transfer agent concentration (CTA); C) Monomer concentration (MC); D) Initiator concentration (IC); and E) Polymer dosage (PD)

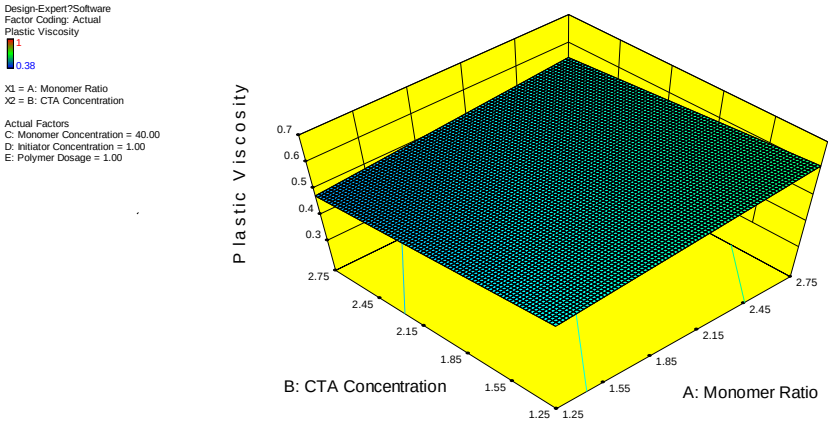

(a) The relationship between MR (-) and CTA (%)

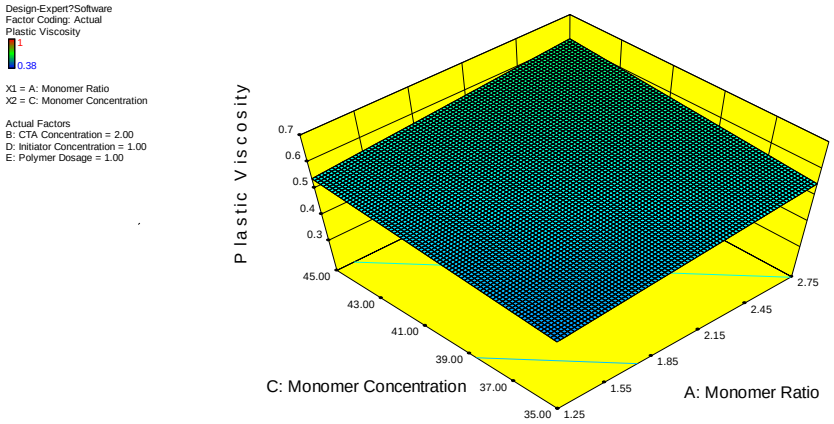

(b) The relationship between MR (-) and MC (%)

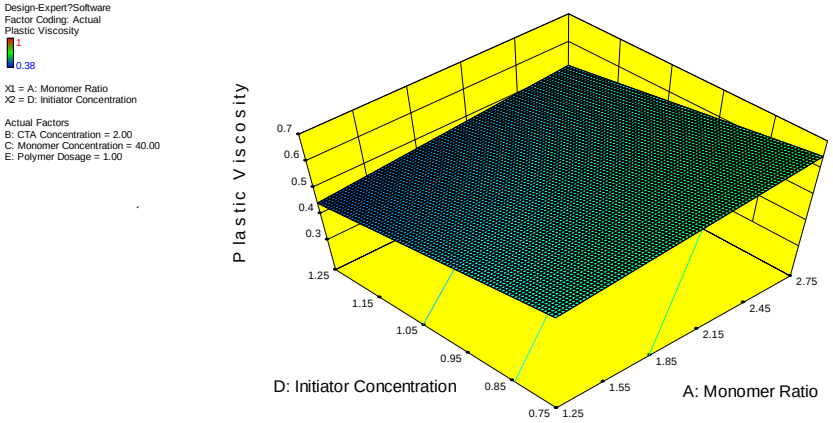

(c) The relationship between MR (-) and IC (%)

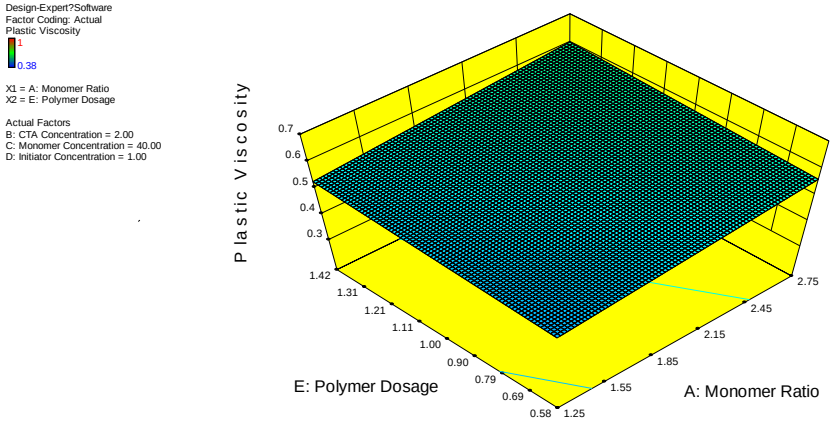

(d) The relationship between MR (-) and PD (%)

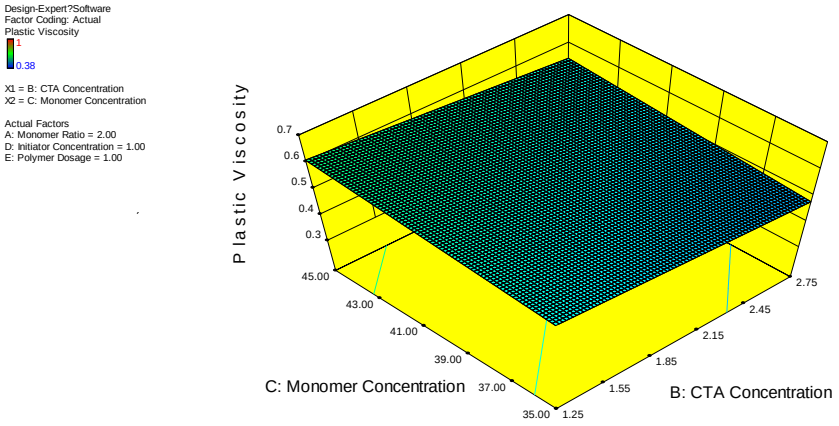

(e) The relationship between CTA (%) and MC (%)

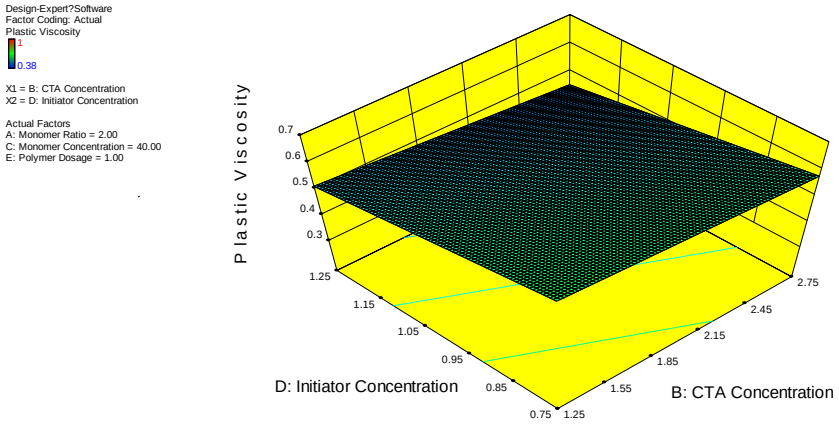

(f) The relationship between CTA (%) and IC (%)

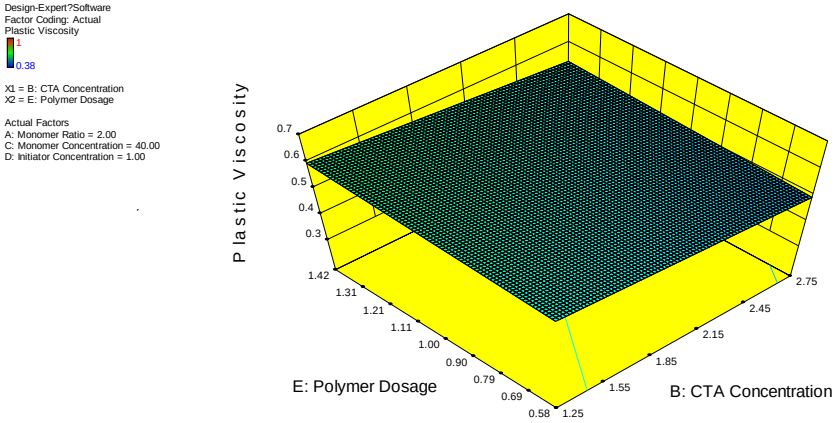

(g) The relationship between CTA (%) and PD (%)

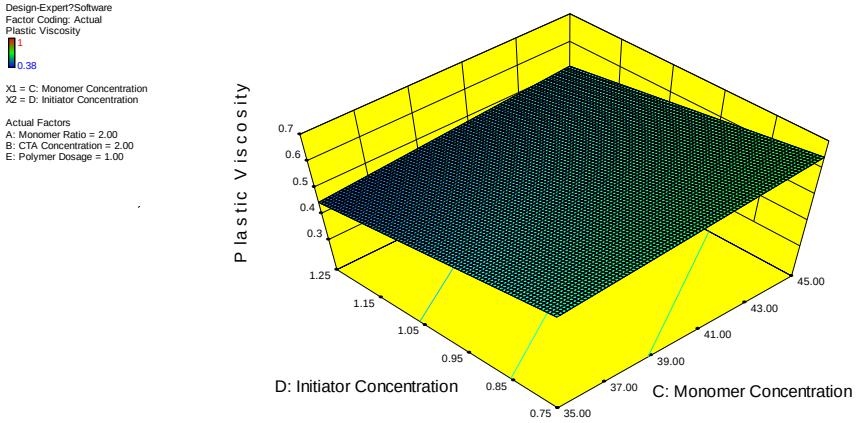

(h) The relationship between MC (%) and IC (%)

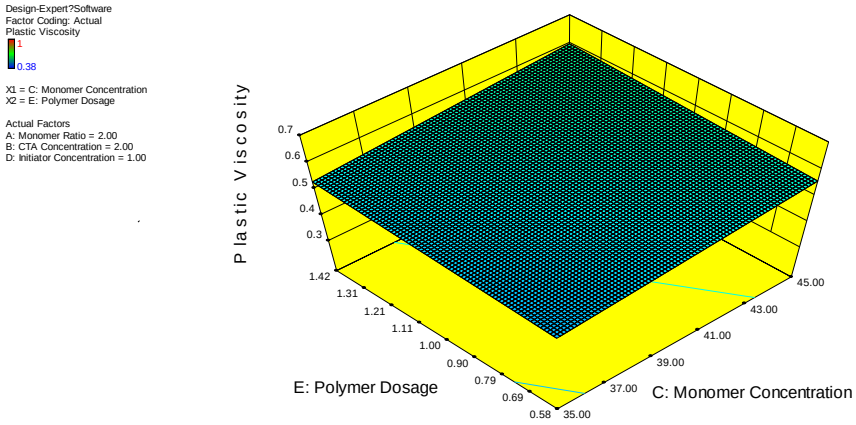

(i) The relationship between MC (%) and PD (%)

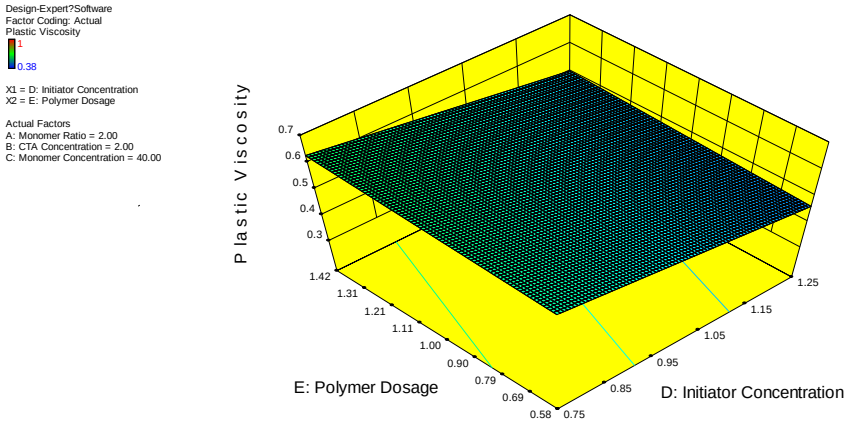

(j) The relationship between IC (%) and PD (%)

Fig 6.12 3D response surface of plastic viscosity in dependence of five factors: A) Monomer ratio (MR); B) Chain transfer agent concentration (CTA); C) Monomer concentration (MC); D) Initiator concentration (IC); and E) Polymer dosage (PD)

6.4.2.5 Determining the optimal condition of results

In the previous section, the effects of selected factors were discussed and the response surface plots were generated. The next step is to identify the optimal conditions for synthesis of the target polymer from the experiment ranges by the design expert software.

6.4.2.5.1 Optimisation procedure

The desirability function (DF) approach was used to establish the optimum criteria based on multi-variables (Jimidar et al., 1996). The general procedure of this approach is to convert each response Y_k into an individual desirability function as $d_k = f(Y_k)$ $(0 \leq d_k \leq 1)$, which can be calculated from ***Equation 6.8-6.11*** (Benyounis et al., 2008, Hassan et al., 1992). If the response (Y_k) meets the target of the optimisation goal, d_k is valued as 1 and if the response is beyond the acceptable limitation, then d_k is 0. The different shape (regression model) of desirability function is controlled by the weight field "w_k". The "weight" is varied in the range between 0.1 and 10, which is used to show the preference to the upper/lower limitation or to a target value during the optimisation process. Value 1 (default) is assigned to the linear pattern of the desirability function (the d_k value varies from zero to one), and value 10 (up to 10) results in a quicker movement towards the goal, showing more emphasis on the goal. On the other side, the value 0.1 makes a slower movement towards the goal. Combined all individual desirability, a single composite response was generated (known as DF), which is defined as the geometric mean of the individual d_k values. Each response is assigned an importance, which is used to express its relation with other response. The importance varies from 1 (+), represented as the least important value, to 5 (+++++) represented as the most important value. The overall function is shown in ***Equation 6.14***.

For maximising process, the desirability functions are defined as

$$d_k = \begin{cases} 0, & \mathbf{Y_k} \leq L_k \\ \left(\frac{\mathbf{Y_k} - L_k}{H_k - L_k}\right)^{w_k}, & L_k < \mathbf{Y_k} < H_k \\ 0, & \mathbf{Y_k} \geq H_k \end{cases} \qquad \textbf{6.8}$$

For minimising process, the desirability function is defined as

$$d_k = \begin{cases} 1, & \mathbf{Y_k} \le L_k \\ \left(\frac{H_k - \mathbf{Y_k}}{H_k - L_k}\right)^{w_k}, & L_k < \mathbf{Y_k} < H_k \\ 0, & \mathbf{Y_k} \ge H_k \end{cases} \quad \textbf{6.9}$$

For setting target goal process, the desirability functions are defined as

$$d_k = \begin{cases} \left(\frac{\mathbf{Y_k} - L_k}{T_k - L_k}\right)^{w_{1k}}, & L_k < \mathbf{Y_k} < T_k \\ \left(\frac{\mathrm{H_k} - \boldsymbol{Y_k}}{H_k - T_k}\right)^{w_{2k}}, & T_k < \mathbf{Y_k} < H_k \\ 0, & Other \end{cases} \quad \textbf{6.10}$$

For setting goal within range, the desirability functions are defined as

$$d_k = \begin{cases} 1, & L_k < \mathbf{Y_k} < H_k \\ 0, & Other \end{cases} \quad \textbf{6.11}$$

For the overall desirability function, the DF is defined as

$$DF = [\prod_1^n {d_k}^{r_k}]^{\frac{1}{\Sigma r_k}} \quad \textbf{6.12}$$

Where d_k stands for individual desirability function of k[th] response, Y_k for optimised value of k[th] response, L_k for lowest value of k[th] response, H_k for highest value of k[th] response, T_k for targeted value of k[th] response, w_k for weight of k[th] response, DF for overall desirability function, n for total number of individual desirability, and r_k for importance of k[th] response. Obviously, it is highly dependent on the individual desirability functions. A DF value equal to 1.0 suggests that all response variations are at their respective optimum or targeted value conditions.

The general steps preceding the numerical optimisation with the software are explained below:

1) Setting the goals for all the parameters including factors and responses, such as minimising, maximising, obtaining a target, selecting a range or none.
2) Evaluating the importance for each chosen goals as the number of '+' (from 1 to 5). One '+' is valued for the least important level, and five '+' for the most importance. Value of 3 is a default setting.
3) Assigning the weights of each goal in order to change the overall desirability function shape (the change only occurs if the operation is chosen as "maximise" and "minimise").

Both the factors and responses can be optimised by a numerical optimisation with any combination of goals provided from the "design expert" software. The goals are set by combining all the desirability as an overall function via maximising function (minimising or selected function value range, defined by the operator's purpose). The numerical operation can generate a better desirability function value through combining all the parameters, and provide useful guidance for further work.

6.4.2.5.2 Optimisation and prediction for the performance of polymers

The aim of optimum synthesis condition and polymer addition dosage was to obtain the best performance of alkali-compatible polymer, providing a low yield stress and a reasonable plastic viscosity when added in NaOH-activated slag. Based on the results and subsequent analysis in previous sections, a quadratic model (***Equation 6.6***) for yield stress and linear model (***Equation 6.7***) for plastic viscosity were utilised to optimise the synthesis conditions and addition dosage. Details of numerical optimisation from the optimisation procedure described in the previous section are shown in ***Table 6.7***. For all the parameters of optimisation, weights of desirability functions were kept at 1 as the default level. One of the purposes of adding SP is to improve the workability of NaOH-activated slag paste by reducing yield stress. Thus, the minimisation of yield stress was defined as importance 5. The optimisation procedure of plastic viscosity was selected as "in range" with importance 3 as default. Among many possible solutions, the highest value of desirability functions was reported as 1 in ***Table 6.7***. Optimised synthesised conditions were: monomer ratio as 2.51, CTA concentration 1.27%, initiator concentration 1.22%, and monomer concentration 35.22%. The optimal polymer dosage is 0.89 (g/100g slag). The software also predicted that under such optimised conditions, the yield stress value would be -2.52 Pa and the plastic viscosity would be 0.51 Pa s^{-1}.

Table 6.7 Characteristics of numerical optimisation

Parameters	Limits		Importance	Weight	Goal	Predict Value
	Lower	Upper				
Monomer Ratio (mole ratio)	1.25	2.75	3	1	In range	2.51
CTA concentration,%	1.25	2.75	3	1	In range	1.27
Monomer concentration,%	35.00	45.00	3	1	In range	35.23
Initiator concentration,%	0.75	1.25	3	1	In range	1.22
Polymer Dosage,%	0.58	1.42	3	1	In range	0.89
Yield Stress/Pa	-2.43	24.22	5	1	Minimise	**-2.52**
Plastic Viscosity/Pa s^{-1}	0.38	1.00	3	1	In range	**0.51**
Desirability			**1.00**			

6.4.2.5.3 Determining the degree of conversion of optimised polymer

In order to determine the degree of conversion for the optimised modified polymer, near infrared spectroscopy measurement was conducted (shown in ***Fig 6.13***). It has been identified that the peak at 6175 cm^{-1} in spectra is attributed to –C=C- bond in acrylate and maleic monomer, and the conversion of polymer, which is reflected from the conversion of these reactive bonds, can be calculated from the absorbance values as ***Equation 6.13*** (Darras et al., 2007). Based on the value obtained from the figure, the degree of conversion of polymer was calculated as 99.15%.

$$p = 1 - \frac{A_p}{A_m} \qquad \textbf{6.13}$$

Where p stands for degree of conversion, A_p for absorbance value of polymer, and A_m for absorbance value of monomer.

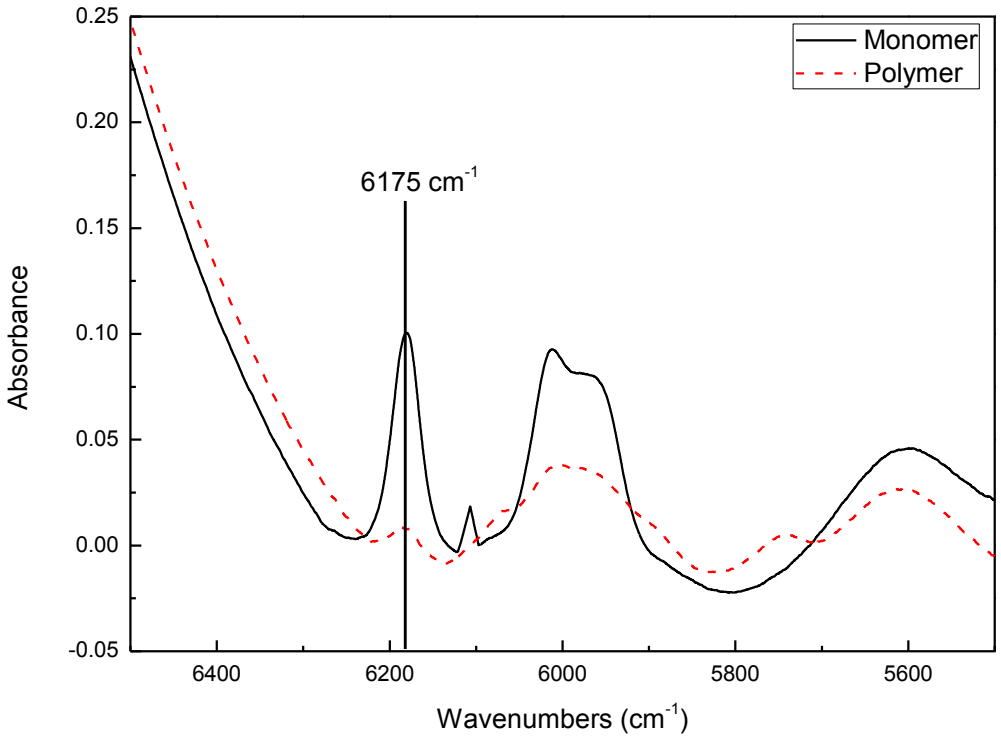

Fig 6.13 Near-infrared spectra of modified polycarboxylate monomers and polymer

6.4.2.6 Verifying the optimised condition of the results

To validate the developed models, three triplicate experiments under the optimum points were conducted to check how close the experimental values and the predicted values were. To evaluate the difference among the rheology test, the yield stress and plastic viscosity of all nine experiments are listed in ***Table 6.8***. From the result, it can be clearly seen that the difference between the tests is not significant. Therefore, the mean value of each batch of polymer could be used for comparison. In addition to comparing the repeatability between the batches, the variation of mean values of each sample among three tests is summarized in ***Table 6.9.***

Table 6.8 Rheological results of validation for the predict model

	Sample 1		Sample 2		Sample 3	
	Yield Stress /Pa	Plastic Viscosity /Pa s	Yield Stress /Pa	Plastic Viscosity /Pa s	Yield Stress /Pa	Plastic Viscosity /Pa s
Test 1	-2.52	0.42	-2.59	0.39	-2.55	0.52
Test 2	-2.48	0.51	-2.38	0.55	-2.53	0.57
Test 3	-2.27	0.46	-2.18	0.52	-2.11	0.48
Average	-2.42	0.46	-2.37	0.49	-2.40	0.52
Standard Deviation	0.13	0.05	0.17	0.09	0.25	0.05
Sample Size	3.00	3.00	3.00	3.00	3.00	3.00
Standard Error	0.08	0.08	0.12	0.05	0.14	0.03
Margin of Error (95%)	0.06	0.07	0.12	0.04	0.13	0.03
Relative Error (%)	6.27	11.01	9.78	19.78	11.73	9.75
Coefficient of variation (%)	5.54	9.73	8.60	17.48	10.37	8.62

Note: The negative value of yield stress does not have physical meaning, further details can be found in Section 2.3.1 and Section 5.4.2.

Table 6.9 Variance of rheological results among different batches of polymer

	Average value of rheological result of different batches of polymer	
	Yield Stress/Pa	Plastic Viscosity/Pa s
Sample 1	-2.42	0.46
Sample 2	-2.37	0.49
Sample 3	-2.40	0.52
Average (μ)	-2.40	0.49
Standard Deviation	0.03	0.03
Sample Size	3.00	3.00
Standard Error	0.02	0.02
Margin of Error (95%)	0.02	0.02
Relative Error (%)	1.19	6.93
Coefficient of variation (%)	1.05	6.12

Note: The negative value of yield stress does not have physical meaning, further details can be found in Section 2.3.1 and Section 5.4.2.

Based on the results listed in ***Table 6.9***, the statistical analysis procedures are shown as follows:

Testing the equality of variance for optimised condition

General procedure is illustrated as follows by ***Equation 6.14*** and ***Equation 6.15***:

Null Hypothesis (H_0): $\mu_1 = \mu_2 = \mu_3$

H_a: $\mu_1 \neq \mu_2 \neq \mu_3$

$$SS_T = SS_{Tr} + SS_E = \sum_{i=1}^{k}\sum_{j-1}^{n_i}(\bar{x}_i - \bar{x})^2 + \sum_{i=1}^{k}\sum_{j-1}^{n_i}(\bar{x}_{ij} - \bar{x}_i)^2 \qquad \textbf{6.14}$$

Where SS_{Tr} is regarded as the sum of squared variations due to the difference in treatment with a degree of freedom "df_{tr}=k-1", SS_E was the sum of squared difference due to experiment error with a degree of freedom "$df_E=\sum_{i=1}^{k}(n_i - 1)$"

$$F = \frac{MS_{tr}}{MS_E} = \frac{SS_{Tr}/df_{Tr}}{SS_E/df_E} \qquad \textbf{6.15}$$

Yield stress:

The analysis was conducted by "Excel" software. And the results are presented in ***Table 6.10***.

Table 6.10 Results for testing the equality of variance for yield stress

Source of Variation	SS	df	MS	F	P-value	F crit
Between Groups	0.002489	2	0.001244	0.03065	0.9700	5.143
Within Groups	0.2436	6	0.04060			
Total	0.2461	8				

For the F-test:

$F = 0.03 < F_{0.05, 2, 6} = 5.14$, which suggests we accept H_0.

For P test:

P=0.97>0.05, which also suggests we accept H_0.

All the F-test and p-value suggested that there the samples are not different in terms of yield stress.

Plastic viscosity:

The analysis was conducted by "Excel" software. And the results are presented in ***Table 6.11***.

Table 6.11 Results for testing the equality of variance for plastic viscosity

Source of Variation	SS	df	MS	F	P-value	F crit
Between Groups	0.005489	2	0.002745	0.7286	0.5209	5.143
Within Groups	0.02260	6	0.003767			
Total	0.02809	8				

For the F-test:

$F = 0.73 < F_{0.05, 2, 6} = 5.14$, which suggests we accept H_0.

For P test:

$P=0.52>0.05$, which also suggests we accept H_0.

All the F-test and p-value suggested that there the samples are not different in terms of plastic viscosity.

It can be concluded that there is no difference in both yield stress and plastic viscosity among verified samples, indicating the verification is valid.

The average values obtained from all samples were **-2.40±0.02 Pa** for yield stress and **0.49±0.02 Pa s** for plastic viscosity. They were 95.24% and 94.23% of predicted values (-2.52 Pa for yield stress and 0.51 Pa s for plastic viscosity). These values were in very good agreement with the values generated from the models.

6.4.3 Summary of synthesis work

In this section, the modified alkali-compatible polycarboxylate polymer was successfully synthesised and the optimal synthesis conditions were obtained via the response surface method, following the procedure detailed in section 6.3.1. Furthermore, the predicted models were statistically verified by experimental values.

The optimal synthesis conditions were identified as monomer ratio (2.51), chain transfer agent concentration (1.27%), monomer concentration (35.23%), initiator concentration (1.22%) and polymer dosage (0.89%), respectively. The average values obtained from all samples were **-2.40±0.02 Pa** for yield stress and **0.49±0.02 Pa s** for plastic viscosity, which were 95.24% and 94.23% of predicted values. The validation tests confirmed that the response model generated from experiment was valid.

6.5 Characterisation of modified polycarboxylate polymer and its stability in alkaline media

In previous section, an alkali-compatible polymer was synthesised under optimal conditions. Further experiments are essential to confirm that it is stable and has a superplasticising effect in NaOH-activated slag system.

Based on the results from designed experiments, five selected samples showing lower yield stress and reasonable plastic viscosity along with the optimised one are used to examine their chemical stability by FTIR and HPSEC. The chemical structure of MP polymer is presented in ***Fig 6.14.*** The FTIR results in NaOH (10.75g NaOH/100g H_2O) compared with that in water are also presented in ***Fig 6.15***; the assignments for each peak are illustrated in ***Table 6.12***.

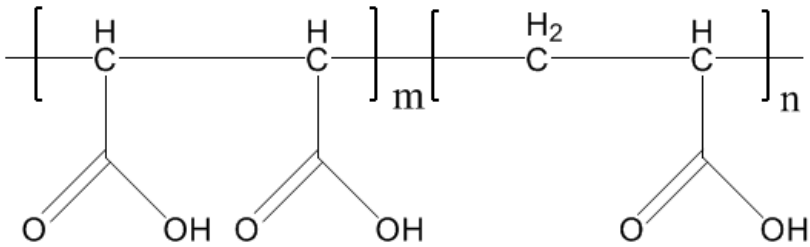

Fig 6.14 Scheme of repeat unit of synthesised MP polymer

The bands observed at 1618 cm^{-1} was represented to the C=O band of bi-carboxyl group, and the band at 1718 cm^{-1} was attributed to the mono-carboxylate groups(Łojewska et al., 2005), which were identified as the most characteristic bands

of carboxylate groups of the acrylic acid and maleic anhydride copolymer. Additionally, the other peaks could be assigned to the carbon backbone of the copolymer (Rivas and Seguel, 1999, Arndt et al., 1999, Mohanty et al., 2013).

Table 6.12 FTIR peaks assignments for MP polymer

Wavenumber/ cm^{-1}	Peak Assignment	Media	
		H_2O	NaOH (pH>14)
3551	O-H stretching	-OH	-OH
3480	O-H stretching	-OH	-OH
3415	O-H stretching	-OH	-OH
1718	C=O stretching	-C=O	-C=O
1637	C-C stretching	-C-C	-C-C
1618	C=O stretching	-C=O	-C=O
1384	C–H bending	$-CH_2$, $-CH_3$	$-CH_2$, $-CH_3$
1240	C-O stretching	-C-O	-C-O
863	C-O stretching	-C-O	-C-O
620	C-O stretching	-C-O	-C-O
478			

As shown in ***Fig 6.15 (a)*** to ***(f)***, similar patterns of FTIR spectrum were observed from different samples in H_2O or in NaOH. Among the samples in water, similar spectra were observed. This could be due to the fact that the change of synthesis condition only affects the polymer configuration, which does not change the functional groups from MA and AA monomers. Moreover, regardless of the samples, it can be seen from the figure that compared to the spectrum in H_2O, there is no peak change in NaOH, which suggested that the MP polymer was stable in NaOH solution.

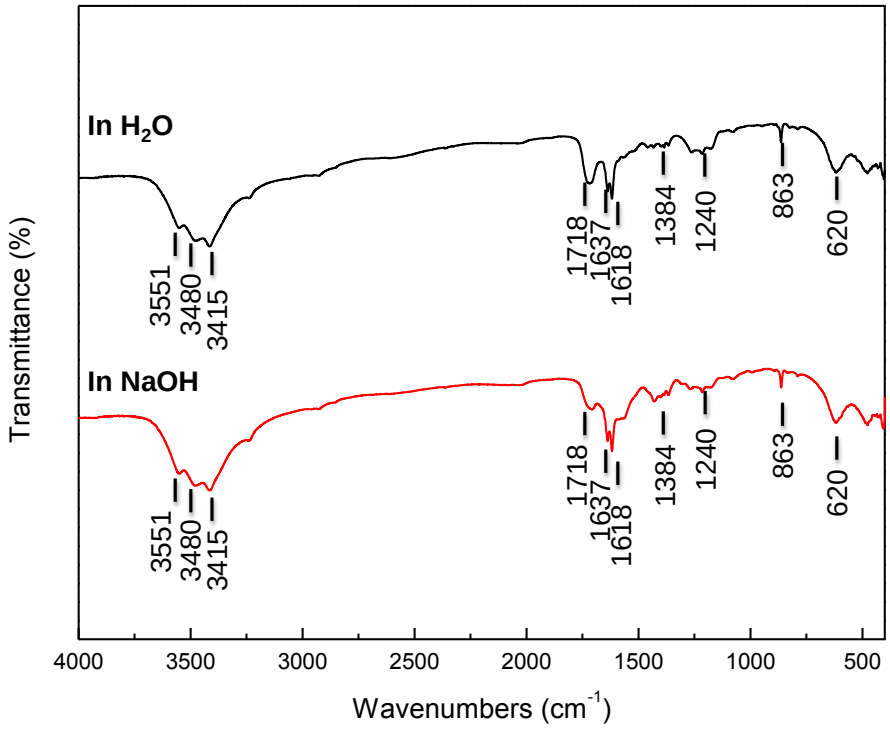

(a) Sample 1

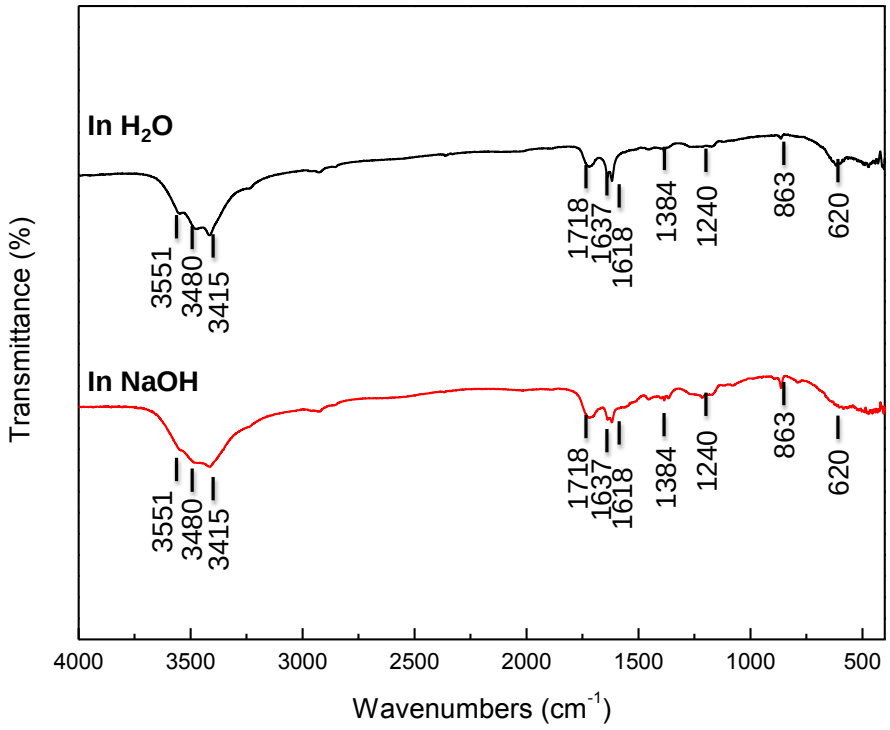

(b) Sample 2

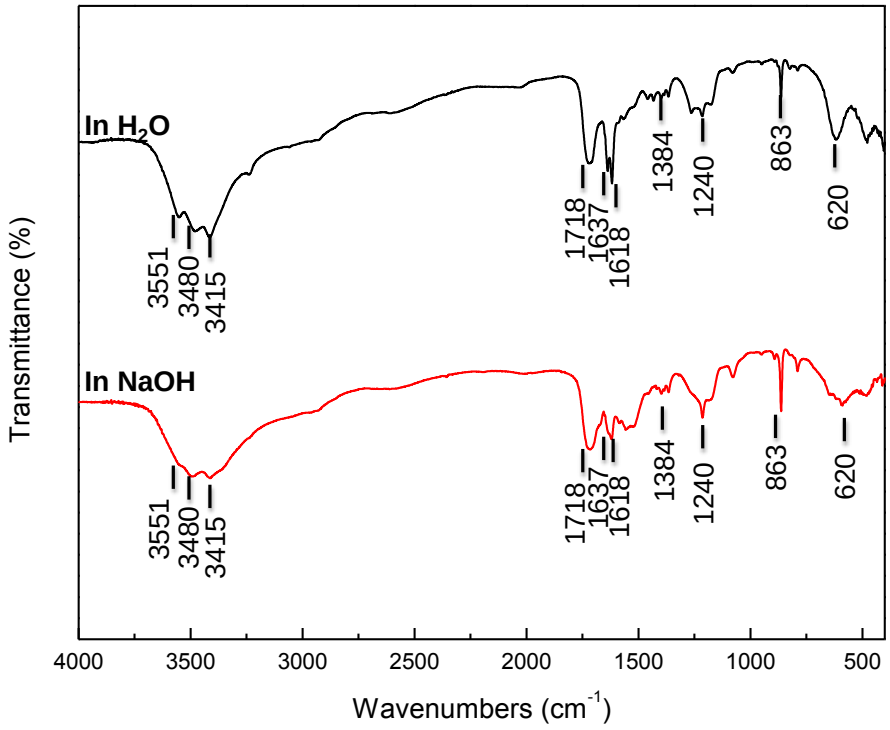

(c) Sample 3

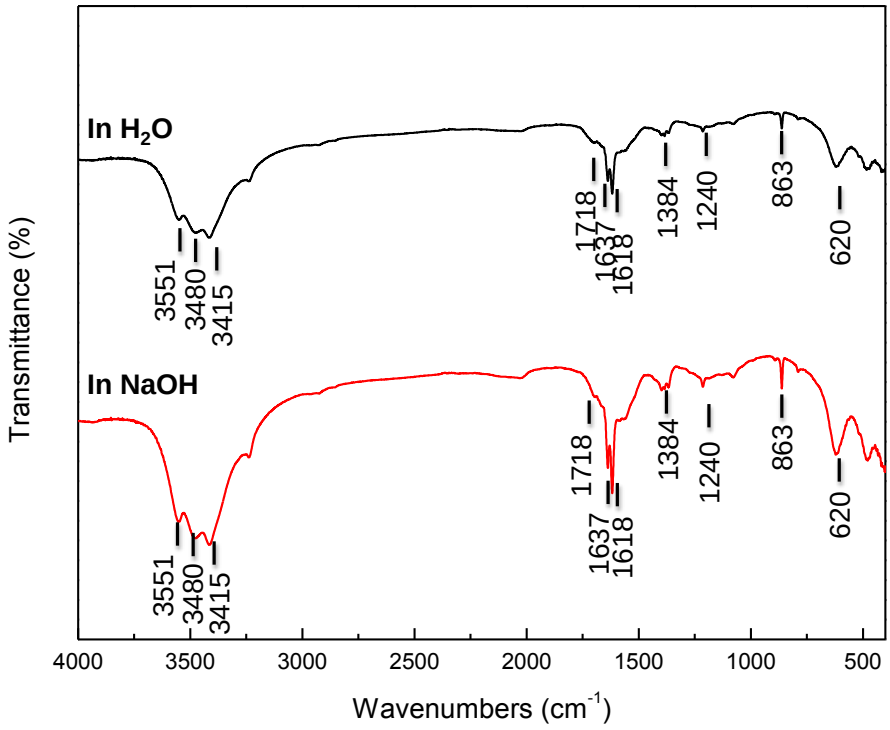

(d) Sample 4

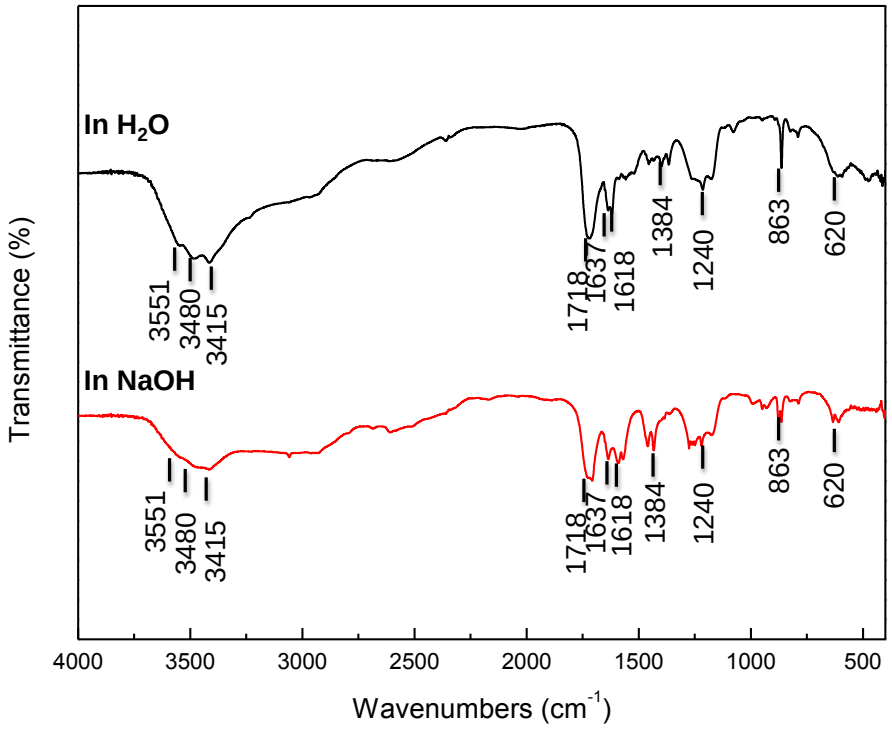

(e) Sample 5

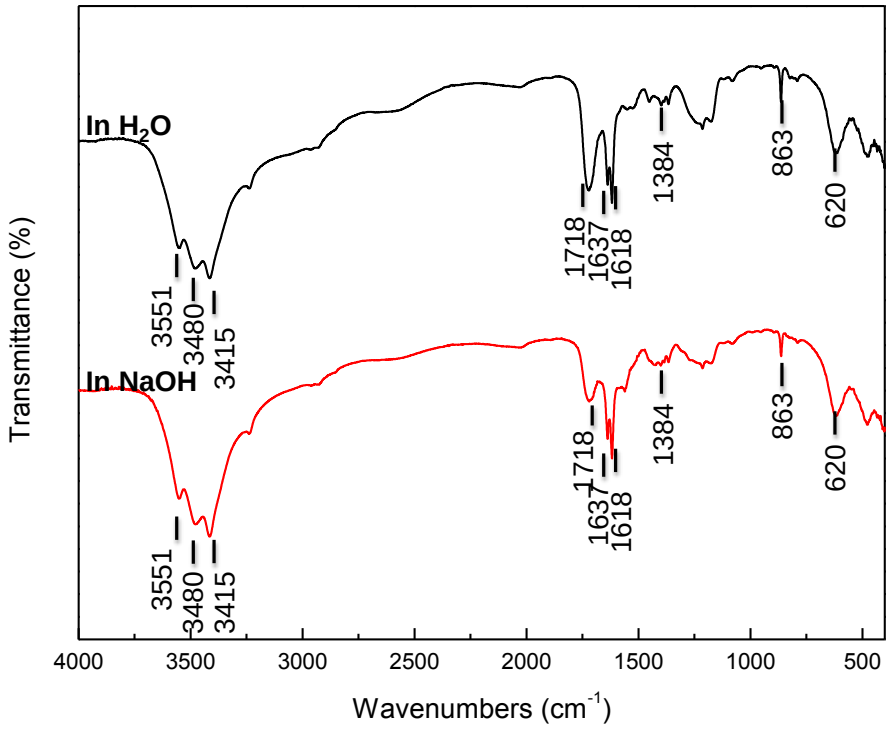

(f) Optimised MP polymer

Fig 6.15 FTIR spectra of selected PMA-AA samples in water and NaOH solution

The molecular weight and weight distribution of selected polymers in different media are summarised in ***Table 6.13***. It can be clearly seen from the figure that, regardless of synthesis, the molecular weight and weight distribution of all the samples did not significantly change when they dissolved in highly alkaline NaOH solution, which suggested that the polymers were stable in NaOH solution. For optimised polymer (MP polymer), obviously, there was no difference in the molecular weight and weight distribution of MP polymer in H_2O and highly alkaline NaOH solution, which indicated that no degradation of polymer happened when the polymer dissolved in NaOH solution.

Combining the FTIR results presented previously, it can be concluded that the modified polycarboxylate polymer is chemically stable in highly alkaline media. As demonstrated in Chapter 3, the chemical instability of PC-based SPs in alkaline media has been identified as one of the issues for its improper work in NaOH-activated slag. Thus, good chemical stability provides a chance for the MP polymer to demonstrate good performance in NaOH-activated slag.

Table 6.13 Molecular weight and weight distribution of selected samples from designed experiment with its yield stress and plastic viscosity

Polymer	Media	Yield Stress /Pa	Plastic Viscosity/ Pa s^{-1}	Molecular weight and weight distribution		
				M_n	M_w	PDI
Sample 1	**H_2O**	-1.58	0.48	3172	6334	2.00
	NaOH			3128	6270	2.00
Sample 2	**H_2O**	-1.88	0.51	3564	6532	1.83
	NaOH			3643	6528	1.79
Sample 3	**H_2O**	-1.94	0.88	3608	6796	1.88
	NaOH			3589	6819	1.90
Sample 4	**H_2O**	-2.12	0.91	3604	6454	1.79
	NaOH			3561	6520	1.83
Sample 5	**H_2O**	-2.43	0.58	3906	6849	1.75
	NaOH			3893	6765	1.74
MP polymer	**H_2O**	-2.40*	0.49*	4063	7044	1.73
	NaOH			4054	7059	1.74

*: This value is the average value from the verification mixes.
Note: The pH value of NaOH iss over 14. The yield stress and plastic viscosity of NaOH-activated were determined based on the higher dosage of polymer samples. M_n stands for number average molecular weight, M_w for weight average molecular weight, and PDI for polydisperse index.

6.6 Discussion

In the experiment, the alkali-compatible polycarboxylate polymers were synthesised by free radical polymerisation; the optimal conditions were identified with the response surface method, and chemical stability of the optimised polymer in both H_2O and NaOH solution were also investigated. In contrast, unlike the PC-based SPs presented in Chapter 5, there was no peak change of MP polymer shown by FTIR spectra, suggesting that the MP polymer was stable in highly alkaline NaOH solution. Similarly, the molecular weight and weight distribution of MP polymer in H_2O and highly alkaline NaOH solution were not altered, which also indicated that no degradation of polymer occurred when the polymer dissolved in NaOH solution. Therefore, it can be concluded that the synthesised alkali-compatible polymers were quite stable in highly alkaline media, which offers a chance to be used as superplasticiser in alkali-activated slag systems.

Free radical polymerisation is one type of addition polymerisation. During free radical polymerisation process, when a free radical generated from initiator contacts to the double bond, one of the covalent bonds is interrupted into two electrons. One of the electrons is attracted to the free radical to form the chemical bond and the one left becomes a new free radical, which is ready to contact another monomer. Therefore, the link bond among monomers of addition polymerisation is a C-C bond. As discussed in Section 3.3.1, the bond dissociation energy is listed in a descending ordered as C-C> C-H> C-O>C-N>C-S. C-H. C-C bonds are more stable than others, and they are stable even in alkaline condition (Darwent, 1970). Therefore, addition polymerisation exhibits its potential to produce alkali-compatible polymer.

From the perspective of polymer chemistry, vinyl based monomers, which contain C=C double bond, are the most favourite monomer type used for the addition polymerisation (Stevens, 1999). Generally, the addition polymerisation could be recognised as the process in which a double bond breaks, and a new single bond is formed. As C=C bond is the double bond contained in vinyl monomer; the product of the addition polymerisation contains a very long hydrocarbon chain. Therefore, it is not surprising that the MP polymers containing C-C and C-H are chemically stable.

Moreover, it has been widely agreed that high charge density of the anionic superplasticisers promotes the adsorption of SPs (Felekoglu and SarIkahya, 2008, Yamada et al., 2000). Vinyl based polymer can offer a good chance to produce high charge density polymers while containing less non-ionic groups and exhibiting good stability (for C-C bond). Therefore, vinyl based polymers are selected to produce alkali-compatible polymers.

From the procedure of monomer selection (section 6.3), the results indicated that the positively charged and neutral polymer exhibited less effect on the improvement or even reduced the performance of NaOH-activated slag. The reason could be explained as: although the positive charge promotes adsorption of polymer on the surface, the net charge of particles was reduced. Therefore, the dispersion effect of positively charged polymer is not good. For neutral polymer, it cannot be hydrolysed and supply the charges for adsorption and electrostatic repulsion. Therefore, the neutral polymer showed no effect. Moreover, the induced positive and neutral anchor groups on PAA based polymers reduce the improvement of minislump of NaOH-activated slag. The reason could be due to less surface affinity of the ammonium group (Zhang et al., 2015). Therefore, the negatively charged polymer is preferred.

Compared with different types of negatively charged groups (i.e. sulfonic and carboxyl groups), the polymers with carboxyl groups provide a better improvement of minislump of NaOH-activated slag than the others. The reason is that carboxyl groups provide the best surface affinity. This matches well with Plank's finding that the surface affinity of anchor groups on surface could be described by an increasing order as $-SO_3$- < -COO- < vic-(COO-) $_2$ (Plank et al. 2007).

In synthesis work, five factors, in terms of *monomer ratio (MR), chain transfer agent concentration (CTA), monomer concentration (MC), initiator concentration (IC)* and *polymer dosage (PD)*, have been identified as the most significant factors affecting the performance of polymers in NaOH-activated slag. Among the five factors, the first four factors were selected to determine the chemical structure of polymers. As discussed previously, each SP has its own range of dosage providing best dispersion effect. Therefore, polymer dosage (PD) was also set as the main factor to be investigated.

As discussed in section 6.4.2, in addition to the single effect of each factor, there exists an interaction between all the factors. Thus, the response surface method was applied to predict the effects of factors. The aim of the optimisation is to produce the polymer with the best improvement on initial rheological properties of NaOH-activated slag. Thus, instead of chemical structure, two indirect responses, the yield stress and plastic viscosity were used to evaluate the effects of factors.

The effects of the single factor on yield stress are listed by an increasing order as: CTA <IC< MC< PD< MR. The yield stress is reduced with the increase of MR, CTA, IC, and PD, while it is reduced with the decrease of MC. As much research has reported, superplasticisers with higher charge density are preferred to exhibit a better dispersion effect. The molecular ratio is the key factor influencing the charge density of polymers. Thus, it showed the most significant effect on the reduction of yield stress.

The synthesised polymer is based on the concept of electrostatic repulsion mechanism. Under this assumption, the negative charged groups (in terms of carboxyl group in this case) were involved in both adsorption and electrostatic repulsion (by residue groups) process (Kim et al., 2000a). Thus, more negative charged groups would afford a better performance of polymer on NaOH-activated slag. Compared with only one carboxyl group from acrylic acid, the anhydride group from maleic anhydride was broken down and formed two carboxyl groups during polymerisation, providing more negative charge. Similarly, as demonstrated by Plank, vic-$(COO^-)_2$ groups offer better surface affinity than $–COO^-$ groups (Plank et al. 2007). Therefore, a higher MA: AA ratio of polymer could supply higher workability and lower yield stress. All samples presented in ***Table 6.8*** are selected mainly on the basis of their reduction effect on the yield stress of NaOH-activated slag. Noticeably, all the samples were synthesised under a higher level monomer ratio (+1), which could partially confirm that the higher monomer ratio of polymer would be preferred.

Moreover, the same monomer ratio guarantees that the polymer is produced with similar charge density. From ***Table 6.8***, despite the effect of NaOH, the polymer samples with high molecular weight exhibited lower yield stress of NaOH-activated slag. As mentioned previously, the synthesis work is mainly designed to improve the

backbone of superplasticiser. Therefore, the effect of lateral chain is neglected. Since there is no lateral chain of synthesised polymer, which would physically hinder the coagulation of particles after the backbone has been encapsulated, the longer chain could somehow minimise this dysfunction by forming a loop structure (Taylor, 1997, Kim et al., 2000b). Thus, polymers with higher molecular weight are preferred to improve the effectiveness of dispersion.

The control of initiator and chain transfer agent concentration is mainly aimed to adjust the molecular weight of polymers. From the perspective of polymer chemistry, theoretically, for the same monomer, the less concentration of initiator and chain transfer agent is used, the longer polymer chain is obtained. Therefore, to produce higher molecular weight polymer, less initiator and chain transfer agent are required. However, the initiator concentration negatively correlated to the yield stress. Similar trend was also found between the chain transfer agent concentration and the yield stress. Based on the previous assumption, higher amount of initiator and chain transfer agent prefer to produce a lower molecular weight polymer. The contradicting results could be attributed to the multiple interactions among those factors.

Moreover, the yield stress of polymer increased with the increase of monomer concentration. The solid content of polymer solution was controlled by the monomer concentration. Generally, the higher monomer concentration is used, the higher solid content of polymer is obtained. However, at the constant initiator concentration, which provided a constant amount of free radical to trigger polymerisation, a higher molecular weight polymer was manufactured with higher monomer concentration. Similarly, the contradicting results could be partially interpreted due to the multiple interactions among those factors. Additionally, in polymer solution with a higher solid content, the polymer chains are prone to entangle with each other. The entanglement could reduce the effectiveness of dispersion effect of polymers. Thus, most commercial PCE SP manufactures do not use a higher solid content, and they control the solid content of their product to around 30-35%.

Obviously, polymer dosage showed significant effects on the improvement of workability of NaOH-activated slag, particularly in the range below the saturated dosage. Thus, a higher polymer dosage provided lower yield stress of NaOH-activated slag.

Different from the effect on yield stress, the effect of factors on the plastic viscosity as listed by an increasing order as: PD <CTA<MC<MR<IC. The plastic viscosity is reduced by increasing CTA, IC and decreasing MR, MC and PD. However, the influences of each selected factors were quite small and close. From this order, it is clearly seen that the polymer structures showed obvious influence on the plastic viscosity of NaOH-activated slag.

The plastic viscosity depends largely on the volume fraction of solid particles and the packing density (Struble and Lei, 1995). As a result, low plastic viscosity might cause the segregation (Feys et al., 2008). In the experiment, the liquid to solid ratio was fixed at 0.48, under which condition the fraction of solid particles was constant, which could be one possible reason for this negligible effect of polymer on viscosity. However, the addition of polymer dispersed the particles and broke the conglomerates of the paste, which also showed some effects on the viscosity. Higher concentration, longer polymer chain and more self-electrostatic properties could increase the plastic viscosity due to the entanglement of the polymer chain. As discussed previously, polymers with higher molecular weight are prone to be synthesised under the condition with lower initiator concentration and less chain transfer agent. The polymer with high molecular weight results in high plastic viscosity of the paste. Similarly, the higher monomer concentration is used, the higher solid content is obtained, which induces more entanglement of polymer chain. The increased number of entanglement increases the plastic viscosity. Although, polymer dosage showed a slightly positive relationship to the plastic viscosity, this influence is too small to be neglected.

Based on the experimental design and taking account of all the interactions of factors, the optimal synthesis condition of MP polymer was clearly identified by numerical optimisation procedure. Additionally, the best performance of MP polymer on rheological properties of NaOH-activated slag was predicted and finally validated by experiments.

Compared with the molecular weight of MP polymer with optimal condition and the selected samples from design matrix, it is clear that the molecular weight of polymers shows a negative relationship to the yield stress of NaOH-activated slag. Since there is only a slight difference of monomer ratio between optimised polymer

and selected polymer, i.e. 2.51 for optimised polymer and 2.75 for selected polymers, respectively, this indicates that the charge density of all the polymers were similar. Therefore, it could be concluded that under similar charge density, linear polymers with long chains are preferred to improve the rheological properties of NaOH-activated slag.

6.7 Concluding Remarks

In this chapter, the alkali-compatible polycarboxylate superplasticiser was synthesised. The polymerisation condition was optimised via the response surface method and its chemical stability was also examined. Based on the results, following conclusion could be drawn below:

- Based on the results of identification procedure of monomers, the negative polymer performed better than neutral or positively charged polymer in NaOH-activated slag. Moreover, the carboxyl groups have been identified as the most effective functional groups on improving the minislump of NaOH-activated slag, while vic- was better than mono COO- group.
- The alkali-compatible modified polycarboxylate polymer (MP polymer) was successfully synthesised and the optimal polymerisation condition was obtained by testing its performance on rheological properties, in terms of yield stress and plastic viscosity, of NaOH-activated slag by the response surface method. The optimal synthesis condition was identified as monomer ratio (2.51), chain transfer agent concentration (1.27%), monomer concentration (35.23%), initiator concentration (1.22%) and polymer dosage (0.89%), respectively. The validation test confirmed that the response model generated from experiment was valid.
- Unlike PC-based SPs, no peak shifts were observed in the FTIR spectrum of MP polymer when it was dissolved in highly alkaline NaOH solution. The molecular weight and weight distribution of MP polymer are not changed when it dissolved in highly alkaline NaOH solution. The results indicated that the MP polymer exhibited better chemical stability in highly alkaline media.

Generally, the synthesised MP polymer demonstrated excellent alkali stability and showed good performance in NaOH-activated slag, which offered a chance to solve the chemical instability issue raised in chapter 3.

As demonstrated that the issue due to the competitive adsorption between SP and NaOH-activated slag has been solved by adding SP at different stages. Moreover, in this chapter, the chemical instability of PC-based superplasticiser has been solved with the new synthesised polymers. However, both approaches were only employed to solve the single issue. Therefore, in order to address two issues together, the effect of different additions of synthesised polymer will be investigated in the following chapter.

Chapter 7

Effect of Different Addition Methods of Synthesised Alkali-compatible Polymer on the Properties of NaOH-activated Slag

7.1 Introduction

As discussed in Chapters 5 and 6, the improper performance of PC-based superplasticiser used in NaOH-activated slag is due to: a) **competitive adsorption** between the SPs and the activators and b) **chemical instability** of PC-based SPs in a highly alkaline media. Chapter 5 demonstrates that the separate SP addition methods can effectively reduce the competitive adsorption and, hence, can improve its performance. Moreover, as reported in Chapter 6, a modified polycarboxylate polymer (MP) is synthesised and its improved chemical stability in NaOH media has been proved. In this chapter, to examine the possibility of combining these two approaches, the synthesised alkali-compatible MP was used in NaOH activated slag system by different addition methods.

The objectives of this chapter are:

- To investigate the interaction and working mechanism of MP in NaOH-activated slag under different SP addition methods;
- To examine the effects of different SP addition methods of MP on the early age properties of NaOH-activated slag, including rheological properties, setting time and early hydration heat;
- To investigate the effects of different SP addition methods of MP on the hardened properties of NaOH-activated slag, in terms of compressive strength, drying shrinkage and porosity.

7.2 Experimental programme

To achieve the above objectives, the overall research programme was developed which is presented in ***Fig 7.1***. All the mixes for investigating the effects of different addition methods of MP are listed in ***Table 7.1***. The test details are described in Section 4.4.

Three aspects of the properties, namely, 1) interaction among SP, activator and slag; 2) early age and 3) hardened properties of NaOH-activated slag were investigated by following the 3 stages as illustrated below:

Stage 1: the adsorption behaviour of MP on the surface of slag particles under different addition methods was investigated. The corresponding zeta potential value was also measured to explore the working mechanism of MP in NaOH-activated slag.

Stage 2: the rheological properties under different addition methods were investigated to examine the effectiveness of MP in fresh NaOH-activated slag. Then, the effects of different SP addition methods on the setting time and 48 hours early age hydration were monitored.

Stage 3: the hardened properties of NaOH-activated slag, in terms of compressive strength and drying shrinkage, were measured. The porosity of the hardened pastes was also examined to explain the influence the MP on the hardened properties so that the possible mechanism related to the effect that the SPs have on the hardened properties of NaOH-activated slag could be identified.

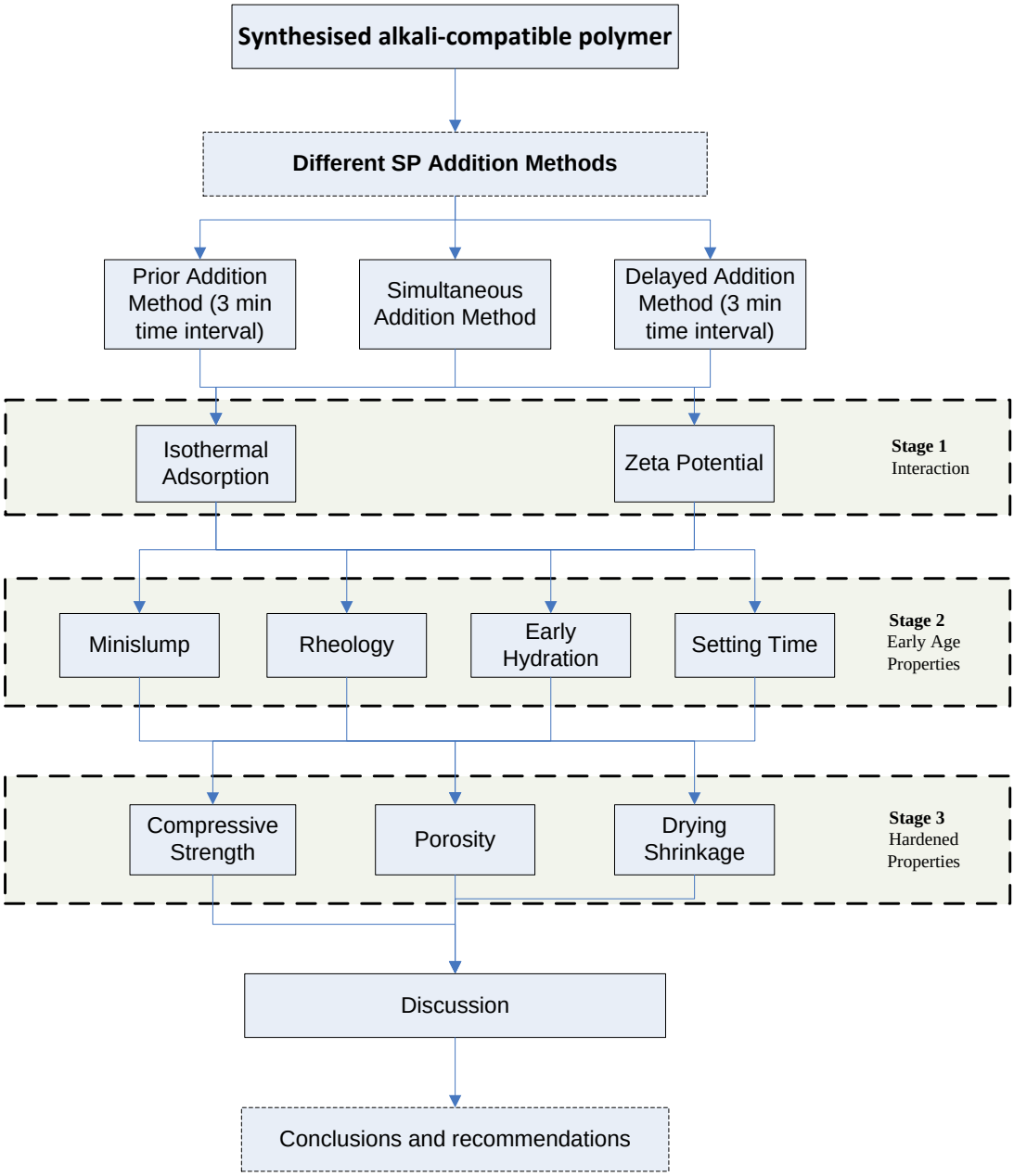

Fig 7.1 Flow chart of the overall research programme of Chapter 7

Table 7.1 Experimental details of MP in NaOH-activated slag

No	Addition Method	Solution	Polymer Dosage (%)	No SP	Modified polycarboxylate polymer		
				Control Test	Interaction	Early Age	Hardened properties
1	N/A	H_2O	0	Zeta			
2		NaOH	0	Zeta, MS, RM, ST,ICC,CS, DS ,MIP			
3		H_2O	0.125		Ads		
4		H_2O	0.250		Ads		
5		H_2O	0.500		Ads		
6		H_2O	0.750		Ads		
7		H_2O	1.000		Ads		
8	SA	NaOH	0.125		Ads		
9		NaOH	0.250		Ads		
10		NaOH	0.500		Ads, Zeta	MS, RM, ST,ICC	CS, DS,MIP
11		NaOH	0.750		Ads, Zeta	MSL, RM	CS
12		NaOH	1.000		Ads, Zeta	MSL, RM	CS
13	DA	NaOH	0.125		Ads		
14		NaOH	0.250		Ads		
15		NaOH	0.500		Ads, Zeta	MSL, RM, ST,ICC	CS, DS,MIP
16		NaOH	0.750		Ads, Zeta	MSL, RM	CS
17		NaOH	1.000		Ads, Zeta	MSL, RM	CS
18	PA	NaOH	0.125		Ads		
19		NaOH	0.250		Ads		
20		NaOH	0.500		Ads, Zeta	MSL, RM, ST,ICC	CS, DS,MIP
21		NaOH	0.750		Ads, Zeta	MSL, RM	CS
22		NaOH	1.000		Ads, Zeta	MSL, RM	CS

Note: **Ads** stands for adsorption; **Zeta** for zeta potential test; **MSL** for minislump test; **RM** for rheology test (by rheometer); **ST** for setting time; **CS** for compressive strength; **DS** for drying shrinkage; **ICC** for Isothermal conduction calorimeter; and **MIP** for Mercury intrusion porosimetry. (The mixing and testing procedures can be referred to in Chapter 4)

7.3 Interactions between MP and alkali activator

In this section, the interactions between MP and slag under different addition methods were studied by the adsorption of the MP polymer on the slag particles as well as the corresponding zeta potential of the slag particles.

7.3.1 Isothermal Adsorption

The effects of different addition methods of MP on the adsorption of NaOH-activated slag are shown in ***Fig 7.2***. It is clear from the figure that compared to the adsorption on pure slag, the adsorption of MP was decreased with the addition of NaOH. This clearly indicates that with SA method, there is still a competitive adsorption between the MP and the activator. The adsorption behaviour is similar to that of LS and NF as reported in Chapter 5. However, the degree of reduction of MP adsorption was much less than that of PC-based SPs in all cases. For example in the presence of NaOH activator, the adsorption of MP at the dosage of 0.500% (by *SA*) was only reduced by 10% from 2.525 mg/g to 2.317 mg/g. For LS and NF (refer to ***Fig 5.2***), at the highest dosage (1.000% of LS and 0.500% of NF), the reduction of the adsorptions of LS and NF were approximately 50% (by *SA*). This is probably due to the improved chemical stability of the MP, allowing more polymer particles available to be adsorbed on the surface of slag.

Comparing the different addition methods, lower adsorption of MP was observed by *PA*, while *SA* provided the highest adsorption. This is different from the result of PC-based SPs as reported in Chapter 5, where *PA* provided the highest adsorption. The possible reason for this phenomenon could be attributed to the different pHs of MP and PC-based polymers. The pH of MP is less than 2 (refer to Chapter 6), while the commercially available PC-based SPs are in the range from 5-9.

Usually, acidic polymer chain is prone to be entangled due to the existing intramolecular hydrogen bond among carboxylic groups, which reduces the “net charge density” of the polymer (Yan, 1998). With the increase of pH value, the configuration of polymer changes from coiled state to stretched state. Thus, the “net

charge density" increases (Hackley, 1997). Therefore, the pH affects the adsorption of the MP due to the change of the configuration of MP.

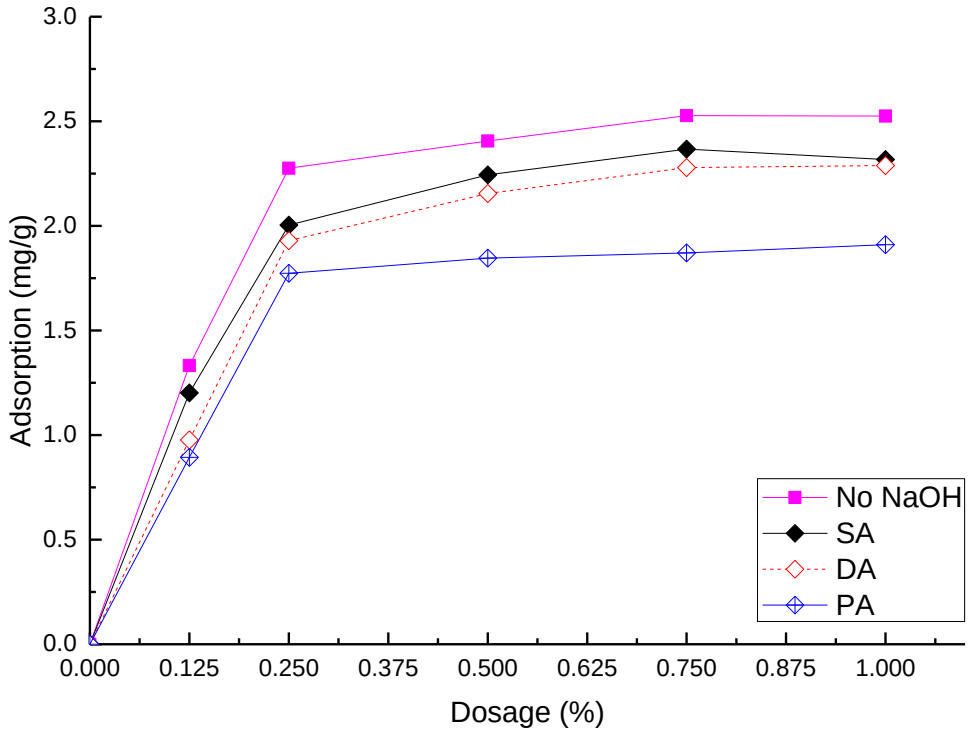

Fig 7.2 Effects of different addition methods of MP on adsorption behaviour of NaOH-activated slag suspension

For *PA*, the acidic MP was added first. The acidic polymer provides less negative charge for adsorbing and dispersing on the surface of slag. Moreover, without NaOH, less Ca^{2+} are dissolved in the solution. Therefore, less Ca-complex, which promotes the adoption of MP, exists between the dissolved Ca^{2+} and carboxylic groups of MP. Consequently, lower adsorption of MP was observed in the case of *PA*.

In the case of *SA* and *DA*, the OH^- ions were simultaneously or prior added. As a result, it released more cations, in particular Ca^{2+}, which promoted the adsorption of MP by forming Ca-complex. Moreover, the neutralisation of acidic polymer changed its configuration by ionising and hydrolysing the intramolecular bond, offering more net charge. Therefore, higher adsorption was observed from both the *SA* and *DA*. It is anticipated that *DA* would have provided higher adsorption of MP due to the reduction of competitive adsorption. However, the adsorbed amount of MP by *DA* was lower than that of *SA*. Therefore, in the case of MP, the competitive adsorption was not a predominant factor to affect the adsorption of MP.

It is also obvious from ***Fig 7.2*** that, when the dosage was less than 0.250%, the adsorption of MP was increased significantly with the increase of MP dosage. However, when adding more MP (>0.250%), the adsorption did not increase significantly, showing the saturated dosage of the MP was around 0.250%.

Table 7.2 Parameters in the Langmuir equation for MP in NaOH-activated slag

Activator	Addition method	R^2	Intercept	Slope	K/ L g^{-1}	As/ mg g^{-1}	ΔG_{ads} /kJ mol^{-1}
H_2O		0.9907	346.1	106.3	3.256	2.890	-2.877
	SA	0.9717	368.3	127.6	2.886	2.715	-2.583
NaOH	DA	0.9709	370.2	134.5	2.752	2.701	-2.467
	PA	0.9883	453.7	151.7	2.991	2.204	-2.267

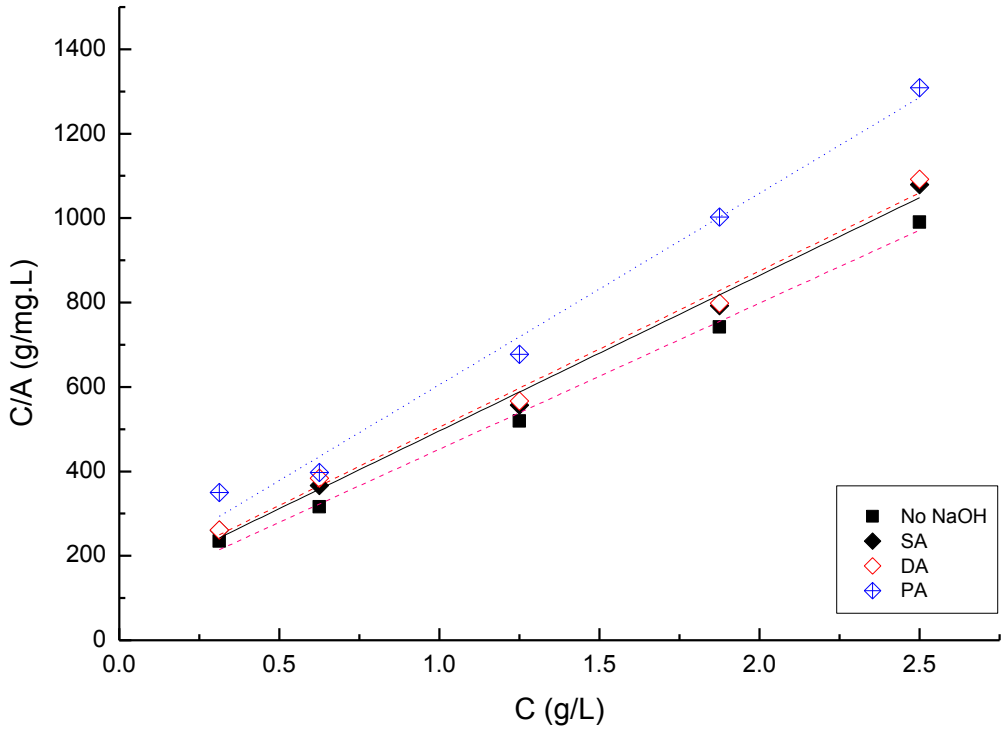

Fig 7.3 Re-plot of adsorption behaviour of MP in NaOH-activated slag by following Langmuir adsorption behaviour model (Where A stands for the adsorbed amount of SP (mg/g) and C for the equilibrium concentration of SP solution (g/L))

Following the procedure mentioned in Section 2.2.4, the quantitative analysis of the adsorption behaviour of MP was conducted and the results are shown in ***Fig 7.3***. The parameters of the equation for this analysis are summarized in ***Table 7.2***. Similar to

the analysis in Chapter 5, the high value of R^2 (>0.95 in all cases) from this analysis suggests that the Langmuir adsorption equation can be used to describe the adsorption behaviour of MP in NaOH-activated slag. The higher values of the characteristics plateau (*As*) by *SA* and *DA* indicates higher electrostatic attraction has been achieved between the slag and the MP polymer. Correspondingly, it can be expected that the higher adsorption by *SA* and *DA* would increase the magnitude of zeta potential and promote the workability of the NaOH-activated slag paste. Moreover, as shown in ***Table 7.2***, the adsorption free energy ΔG_{ads} of MP calculated from the adsorption constant (k) through ***Equation 2.3*** indicates that the adsorption of MP on slag was favourable. The less than 5 kJ·mol^{-1} absolute value of free adsorption energy confirmed that electrostatic adsorption was again the main driving force (Ran et al., 2010).

7.3.2 Zeta potential

Zeta potential is measured to determine the magnitude of the surface charge of the particles, which can be used to detect the electrostatic impact of the adsorbed MP. MP is a type of cationic polymers with negatively charged carboxyl groups. The adsorbed negatively charged MP forms an additional slipping layer, which reduces the zeta potential. Therefore, the adsorption of MP can be indicated from the change of the zeta potential. Based on DLVO theory, the electrostatic repulsion is the dominating dispersion mechanism of the electrolyte; better dispersion can be achieved with higher magnitude of zeta potential.

The effects of different addition methods of MP on the zeta potential of NaOH-activated slag are illustrated in ***Fig 7.4***. Obviously, the addition of MP reduced the zeta potential of NaOH-activated slag from -1.14 mV (without MP) to -4.22 mV at 0.125% dosage, and it further decreased to -5.35 mV at a higher dosage of 0.500%. The reduced zeta potential indicates that the MP polymer was adsorbed on the surface of slag.

Comparing the different addition methods, *SA* and *DA* provide a lower zeta potential of NaOH-activated slag, while *PA* offers a higher zeta potential of NaOH-activated slag. For example, at dosage of 0.500%, the zeta potentials of NaOH-activated slag

by *SA* and *DA* were -5.35 mV and -5.25 mV, respectively, which are lower than that by *PA* (-3.86 mV).

Since MP is negatively charged polymer, the further reduction of the zeta potential indicates that the MP was successfully adsorbed on the surface of slag. The higher magnitude of zeta potential indicates that more SPs are adsorbed onto the surface, which would lead to a higher electrostatic repulsion between the slag particles. Therefore, the dispersion of the slag particles could be improved.

Linking to the adsorption results described in previous section, lower zeta potential was expected from *SA* and *DA* than that from *PA*, as the amount of SP adsorbed by the latter was lower. The higher magnitude of zeta potential by *SA* and *DA* indicates that more MP is adsorbed onto the surface, which would lead to a higher electrostatic repulsion between the slag particles. Hence, it can be predicted that better dispersion of slag particles could be achieved by *SA* and *DA*.

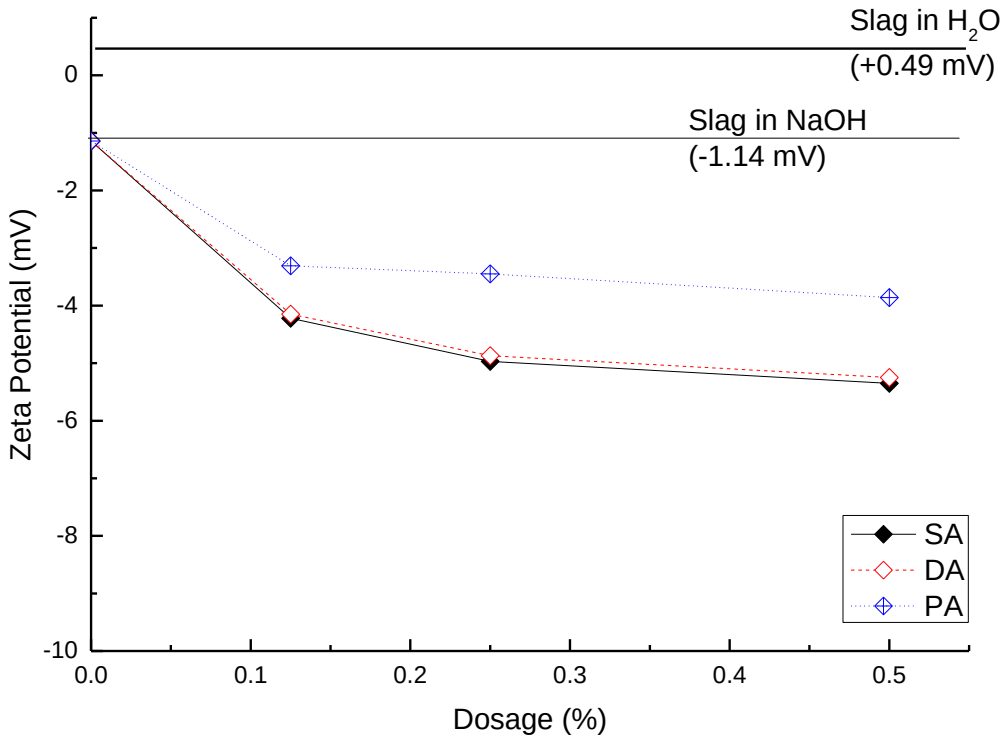

Fig 7.4 Effects of different addition methods of MP on the zeta potential of NaOH-activated slag paste (The zeta potential of slag with water is +0.49 mV)

7.3.3 Summary

The effects of different addition methods of MP on the adsorption and zeta potential of NaOH-activated slag were investigated in this section. On the basis of the results, the following points can be summarised:

- The adsorption of MP on the surface of slag particles followed Langmuir isothermal adsorption behaviour. The electrostatic attraction between the polymer and the slag particles was identified as the main driving force for the adsorption.
- *SA* and *DA* increased the adsorption of the MP on the slag surface. The adsorbed amounts of MP were similar by both *SA* and *DA* methods. *PA* provided the lowest adsorption among three addition methods. In addition to the competitive adsorption, the configuration and charge density played more important roles on dispersion effect of the MP.
- The addition of MP decreased the zeta potential of NaOH-activated slag paste. Lower zeta potential value was observed in the paste prepared by *SA* and *DA*, which correlates well to the adsorption results.

7.4 Effects of different addition methods of MP on early age properties of NaOH-activated slag

The effects of different addition methods on the fresh properties of NaOH-activated slag, in terms of minislump and rheological properties, are reported in this section. Moreover, the setting time of NaOH-activated slag is determined and the early hydration of NaOH-activated slag is also monitored by ICC.

7.4.1 Workability (Minislump)

The initial minislump tests of NaOH-activated slag under different addition methods of MP are illustrated in ***Fig 7.5***. The addition of MP increased the minislump of NaOH-activated slag paste, which indicates that the workability can be improved by adding MP.

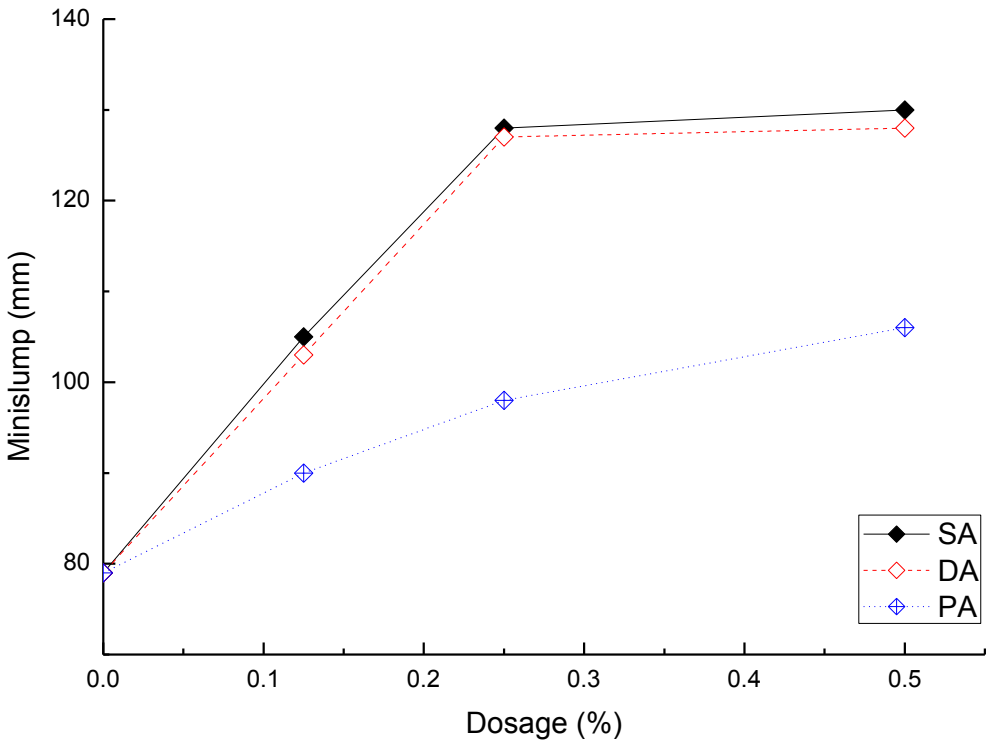

Fig 7.5 Effects of different addition methods of MP on initial minislump of NaOH-activated slag paste

In the case of *SA*, the minislump of the NaOH-activated slag was increased from 79mm (no MP) to over 105mm (at the dosage of 0.125%), and further increased to 130 mm at a higher dosage of 0.500%. The saturation dosage of MP was observed at approximately 0.250%. This is in line with the adsorption results of MP reported in Section 7.3.1.

Comparing the different addition methods, the lowest minislump of NaOH-activated slag was observed from *PA*, while higher minislump spreads were achieved by both *SA* and *DA*, with a slightly higher minislump by *SA*. The minislump spreads of NaOH-activated slag by *SA* and *DA* at the dosage of 0.500% were 130 mm and 129 mm, respectively, which are 22.64% and 21.70% higher than that by *PA* (106 mm).

The change of the minislump was then monitored over time to assess the effects of different addition methods on the workability retention. The results are shown in ***Fig 7.6 (a)*** to ***(c)***. Although the addition of MP improved the initial minislump of NaOH-activated slag, the minislump loss was still significant. This is particularly observed in the NaOH-activated slag with a lower dosage of the MP polymer. For example, as shown in ***Fig 7.6 (a)***, at 0.125% of MP (by *SA*), the minislump quickly decreased

from 105 mm to approximately 70 mm after only 30 minutes, and continually decreased to 60 mm at 60 minutes. Nonetheless, the significant minislump loss was reduced with the increase of MP dosage. In addition to the MP dosage, the addition methods could also affect the workability retention. Comparing the different addition methods, better workability retention was observed in the paste by *SA* and *DA* at higher MP dosages.

The formation of organo-mineral phase (OMP) at the early stages of hydration consumes the SPs, which might cause the workability loss of SPs (Flatt and Houst, 2001). Since the NaOH-activated slag has been identified as a quick setting system (Shi, 1997), the quickly precipitated hydration product of NaOH-activated slag can also accelerate the consumption of MP. Therefore, the slump loss reduced at higher dosage of MP. However, further study is still needed in order to fully understand the relationship between the dosage of MP, addition method and workability retention.

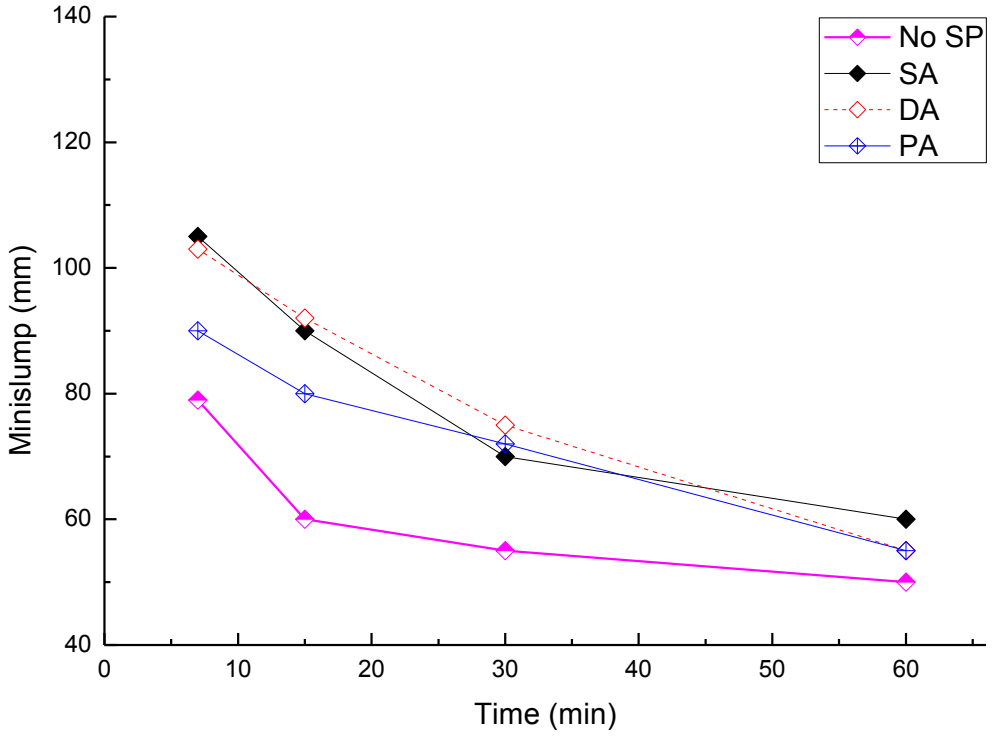

(a) 0.125% MP

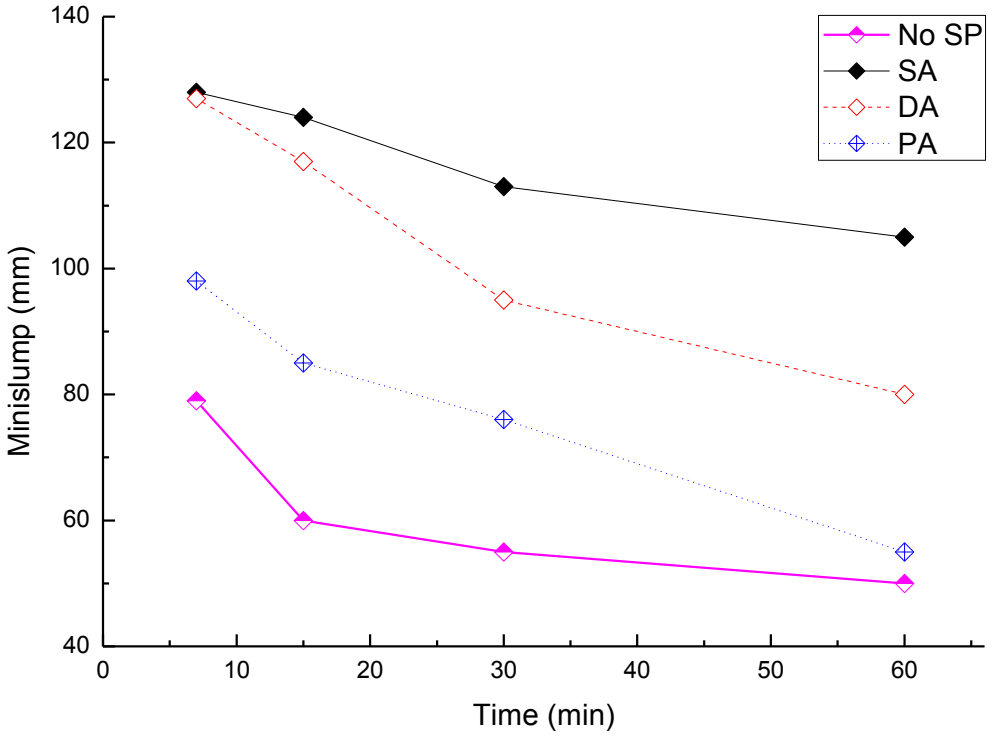

(b) 0.250% MP

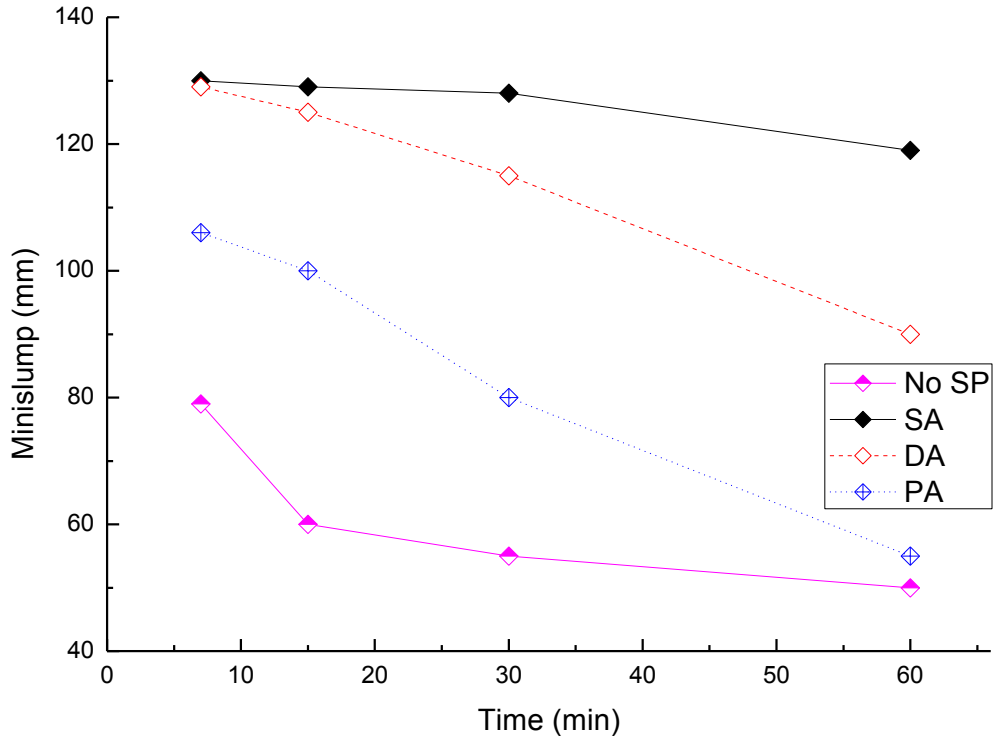

(c) 0.500% MP

Fig 7.6 Effects of MP on minislump loss at different hydration time of NaOH-activated slag paste under different addition methods

7.4.2 Rheological properties

The initial yield stress of NaOH-activated slag pastes calculated from the Bingham model is presented in ***Fig 7.7***. As shown in ***Fig 7.7***, in the case of *SA*, the yield stress of NaOH-activated slag paste with MP was significantly reduced from 20.76 Pa to 3.15 Pa at the dosage of 0.125%, and further decreased to -2.05 Pa at a higher dosage of 0.500%, which corresponded with the minislump results. Similar to the results presented in section 5.4.2, the negative yield stress was observed. The reason for the negative yield stress could be due to the change of the rheological properties from near Bingham to shear thickening. Although the negative yield stress could not be observed in real work, the reduced yield stress indicated that low interparticle force among slag particles and better workability of NaOH-activated slag paste were achieved.

Comparing the different addition methods, *PA* showed the highest yield stress of NaOH-activated slag, suggesting the highest interparticle forces existed in the paste. However, both *SA* and *DA* provided lower yield stress of NaOH-activated slag. Therefore, better workability of NaOH-activated slag is achieved due to less interparticle attraction and less electrostatic repulsions.

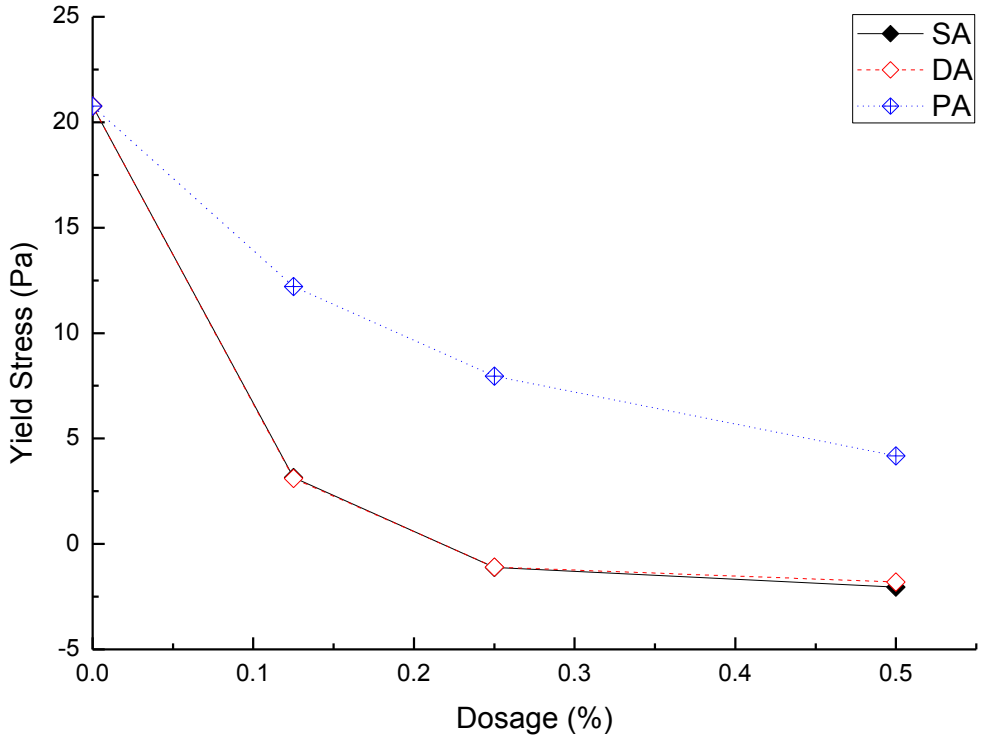

Fig 7.7 Effects of different addition methods of MP on initial yield stress of NaOH-activated slag paste

The effects of MP on the initial plastic viscosity of NaOH-activated slag are presented in ***Fig 7.8***. As plotted in ***Fig 7.8,*** the addition of MP reduced the plastic viscosity of NaOH-activated slag, which indicates that the flocculates in NaOH-activated slag pastes are broken down. Under *SA*, the plastic viscosity of NaOH-activated slag with MP was decreased from 1.92 Pa s to 0.64 Pa s at 0.125% dosage, and further decreased to approximately 0.37 Pa s at a higher dosage of 0.500%.

Compared with *PA*, when adding the SPs by *SA* and *DA*, the plastic viscosity was decreased, with a lower value by *DA* except at 0.125% MP dosage. The reduced plastic viscosity could be due to the modification made to the flocculation, which changed the way that the shear concentrated in the media among the slag grains and/or flocs (Bey et al., 2014). As reported in section 7.3, a higher adsorption and a higher magnitude of zeta potential were observed from the *SA* and *DA*. Consequently, more electrostatic repulsion force was induced, and better dispersion of the slag particles was achieved due to the breakdown of the flocculation.

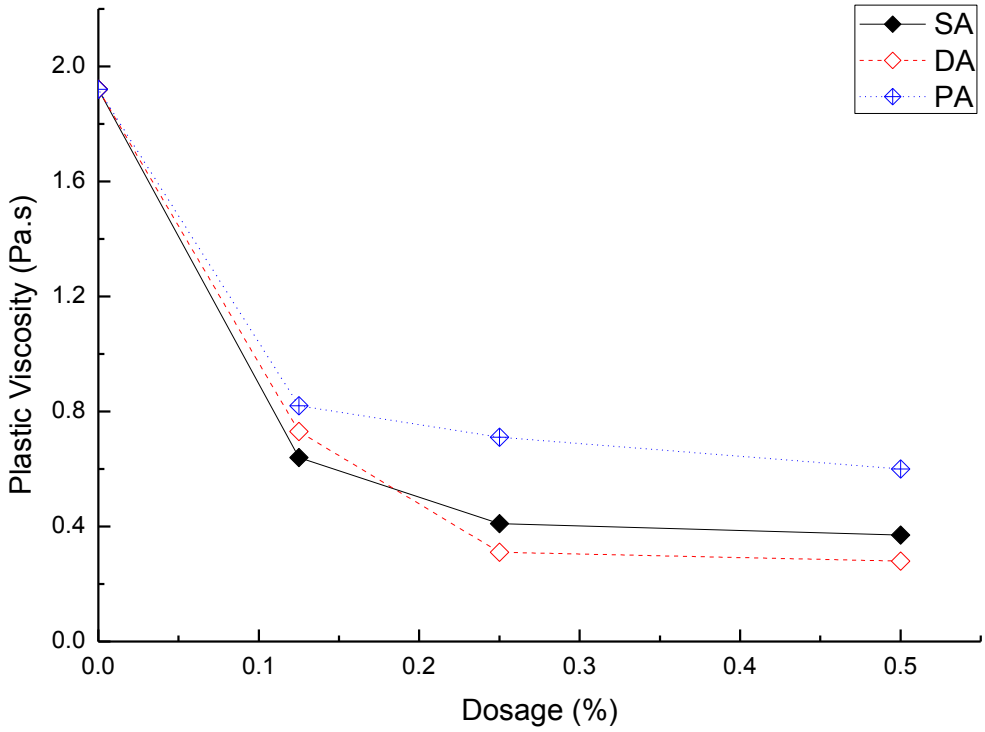

Fig 7.8 Effects of different addition methods of MP on initial plastic viscosity of NaOH-activated slag paste

The effects of MP on the initial yield stress and the initial plastic viscosity under different addition methods are presented by following the vectorised-rheograph approach (Wallevik and Wallevik, 2011) as shown in ***Fig 7.9.*** Both the initial yield stress and the initial plastic viscosity of NaOH-activated slag paste moved toward the lower value, which results in the relocation of the data points to the bottom left of the rheograph. Compared to *PA*, a lower yield stress and a lower plastic viscosity were observed from the *SA* and *DA* except at 0.125% dosage, at which dosage, *DA* showed higher plastic viscosity than that by *SA* and *PA*.

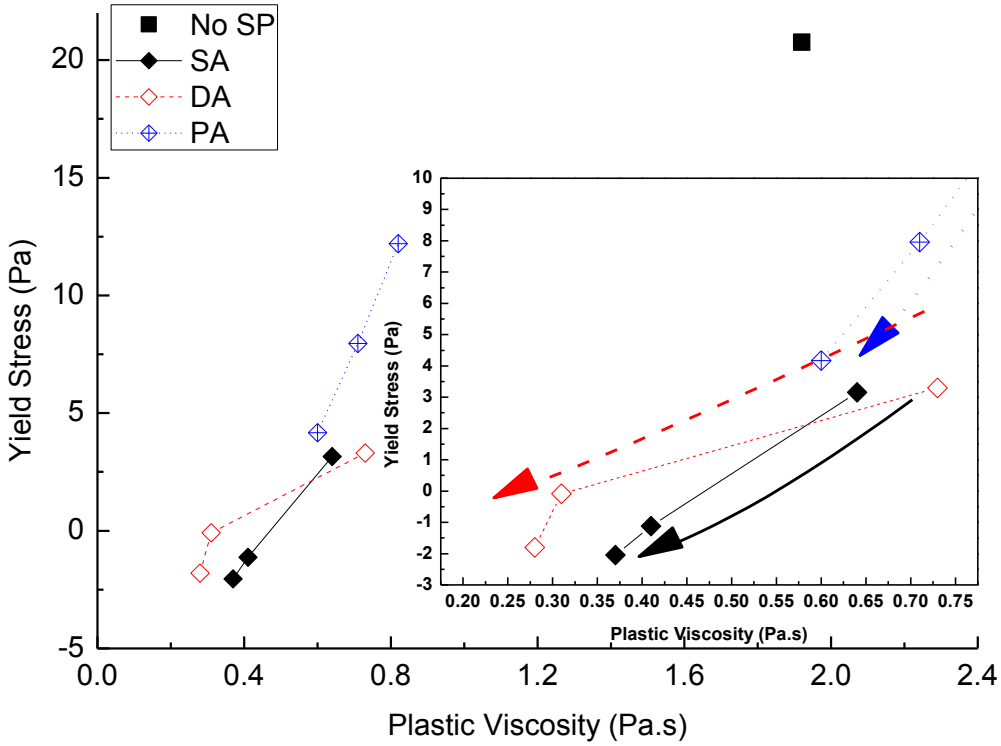

Fig 7.9 Rheograph of NaOH activated slag with MP at 7 minutes (The direction of the arrow indicates the increment of SP dosage)

The effects of MP on the yield stress and the plastic viscosity of NaOH-activated slag at different time interval are presented in ***Fig 7.10*** and ***Fig 7.11***, respectively. Generally, both yield stress and plastic viscosity of NaOH-activated slag were increased over time. It can be seen from the figures that at a lower MP polymer dosage, regardless of the addition methods, both the yield stress and the plastic viscosity obviously increased during the first 30 minutes hydration of NaOH-activated slag. However, when the MP polymer dosage was increased to 0.500%, the increase of yield stress and plastic viscosity by *SA* and *DA* are not obvious. This

could be attributed to the effect of MP addition on the early hydration of NaOH-activated slag, which will be discussed in Section 7.4.4

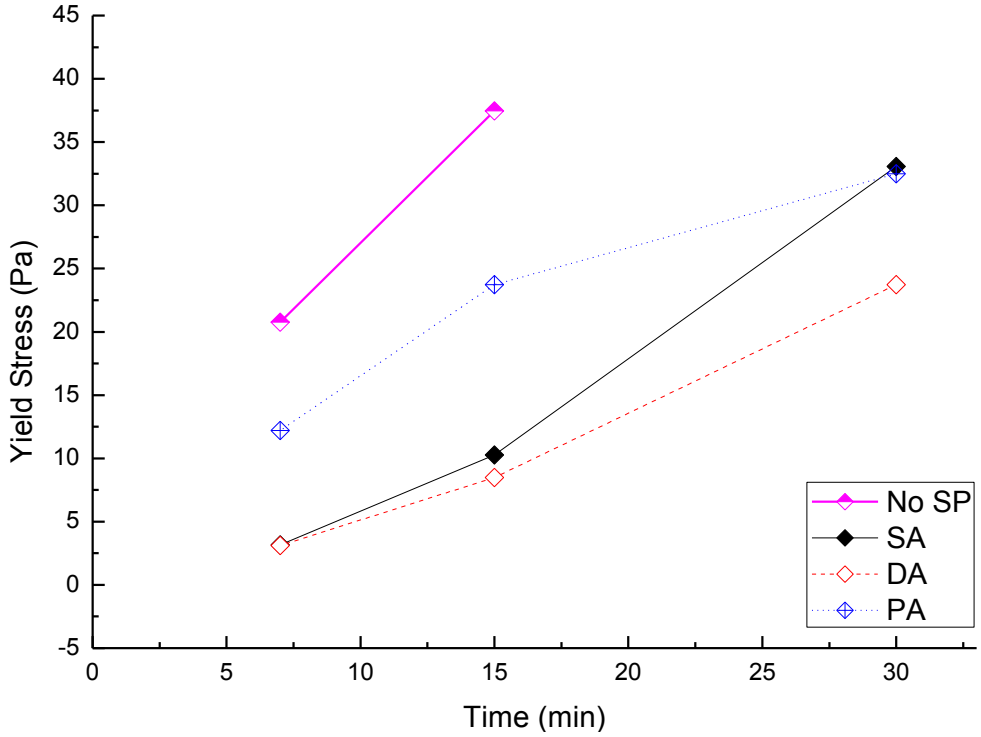

(a) 0.125% MP

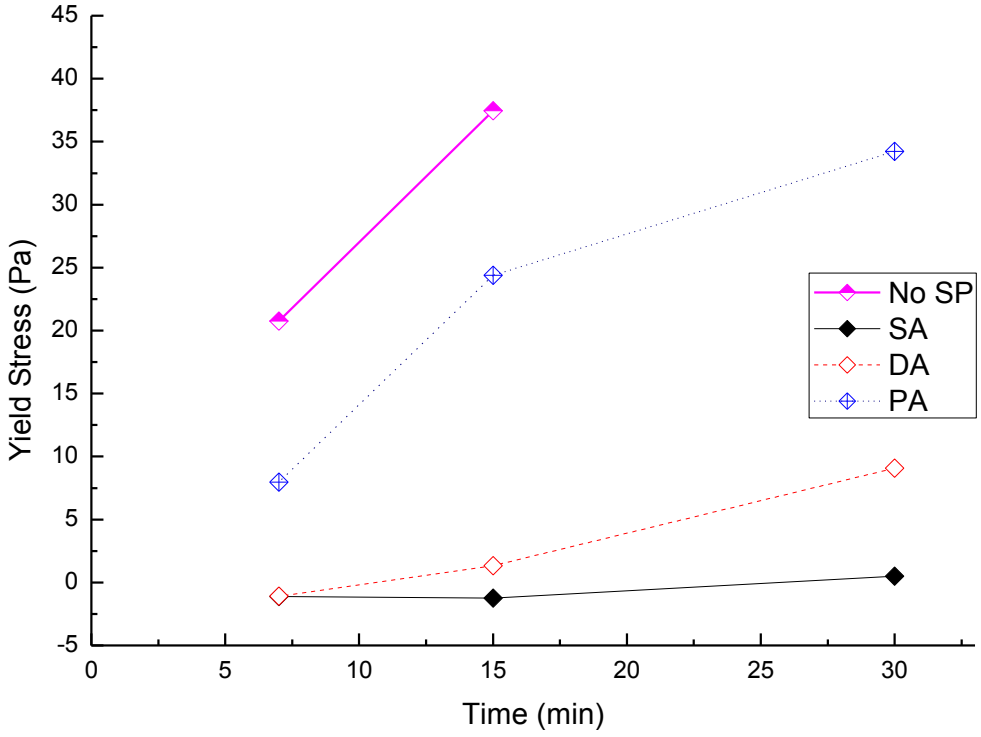

(b) 0.250% MP

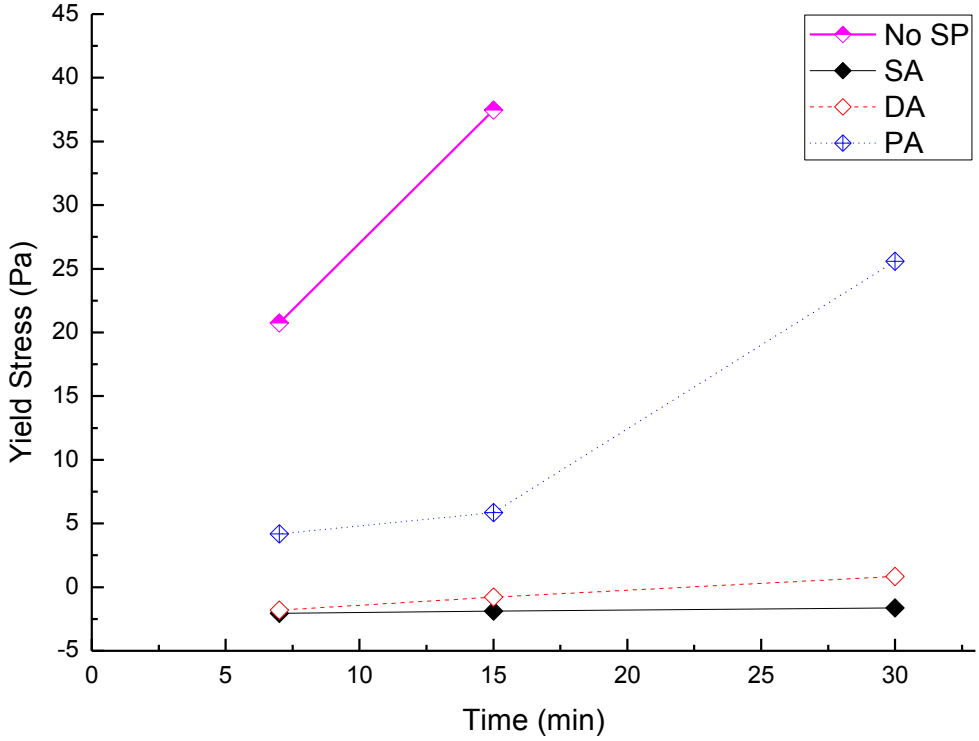

(c) 0.500% MP

Fig 7.10 Effects of MP on yield stress of NaOH-activated slag paste at different hydration time interval under the different addition methods

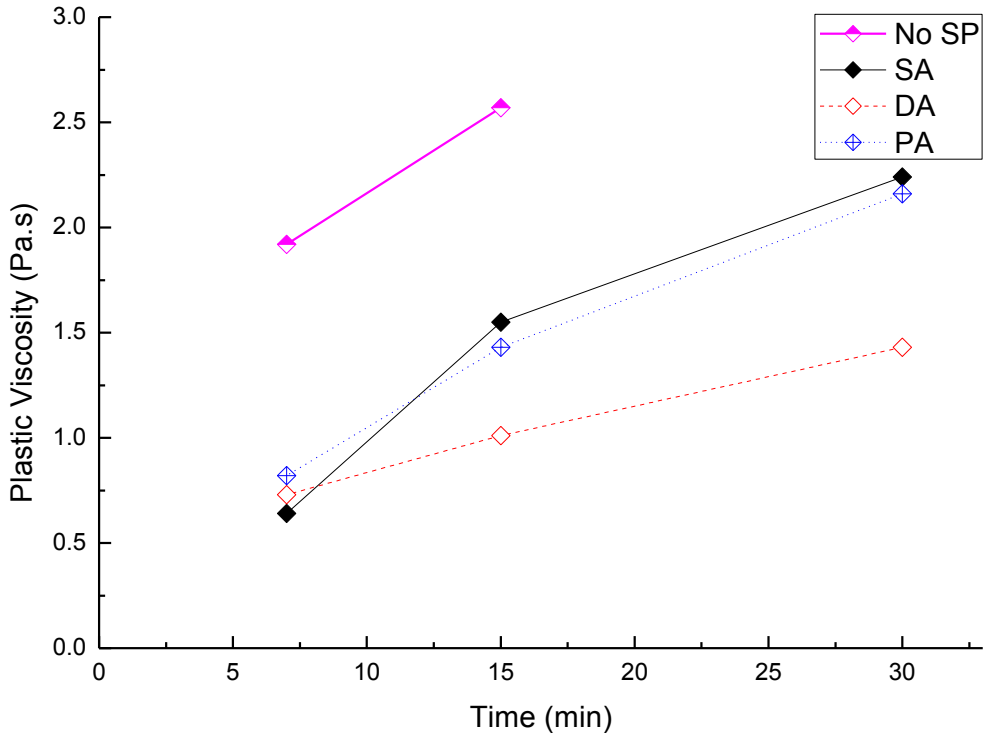

(a) 0.125% MP

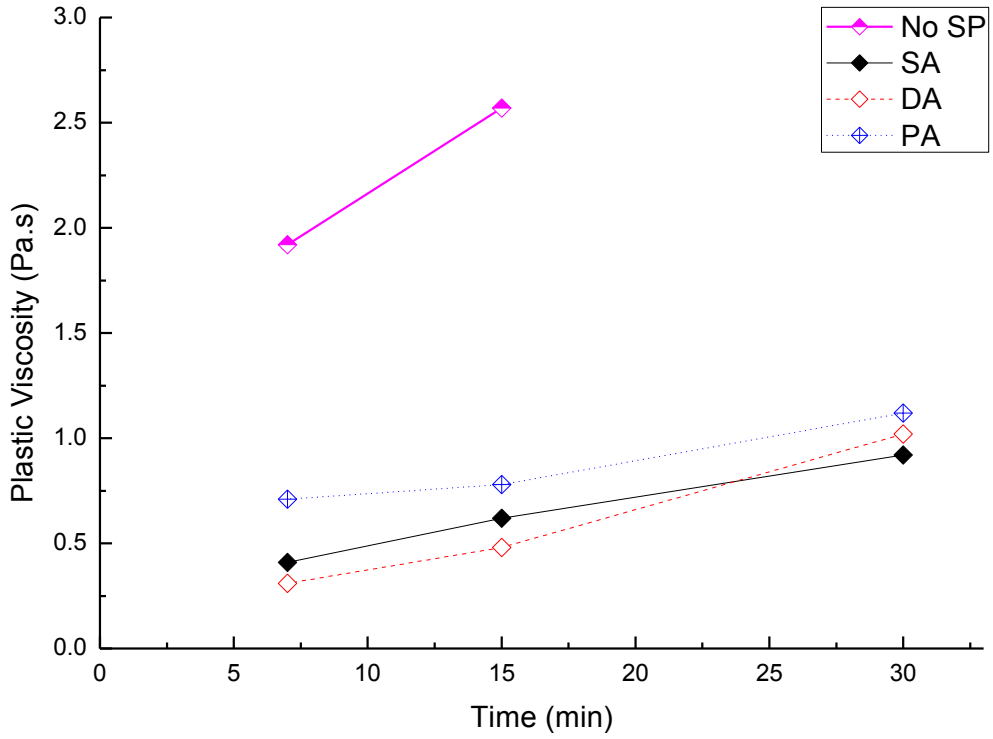

(b) 0.250% MP

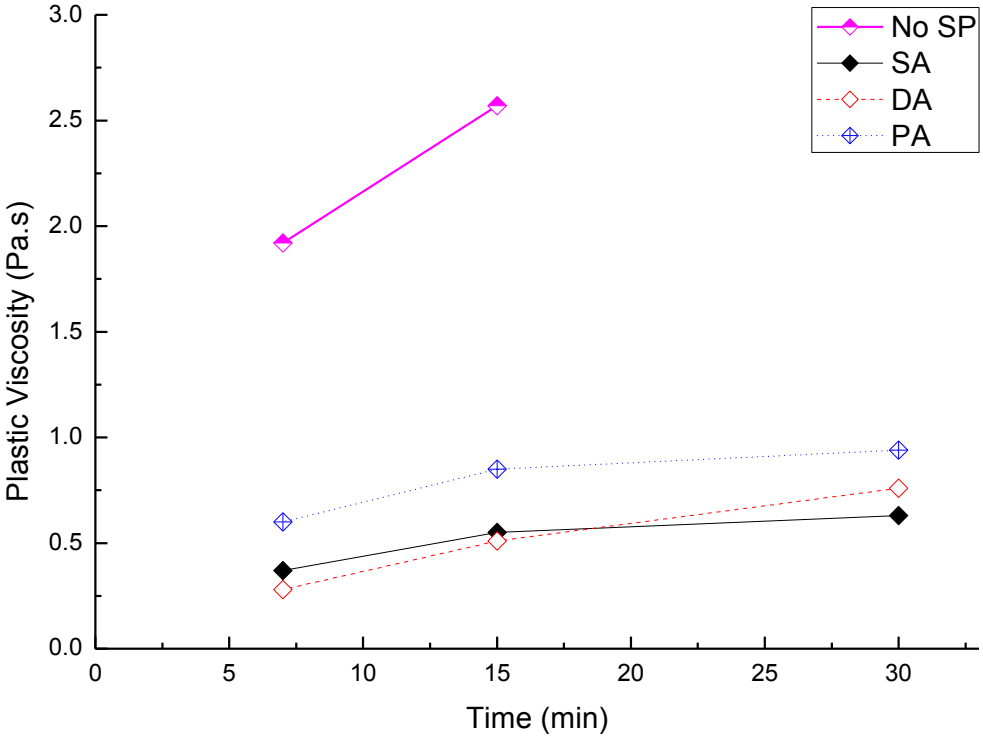

(c) 0.500% MP

Fig 7.11 Effects of MP on plastic viscosity of NaOH-activated slag paste at different hydration time interval under different addition methods

As shown in ***Fig 7.12,*** a relationship between the yield stress and the minislump spread has also been established and an equation of $\tau = -50.65\ln(x) + 242.52$ with the coefficient of 0.9102 was generated. However, similar to previous attempts, it was difficult to establish a relationship between the plastic viscosity and the minislump of NaOH-activated slag with MP (***Fig 7.13***).

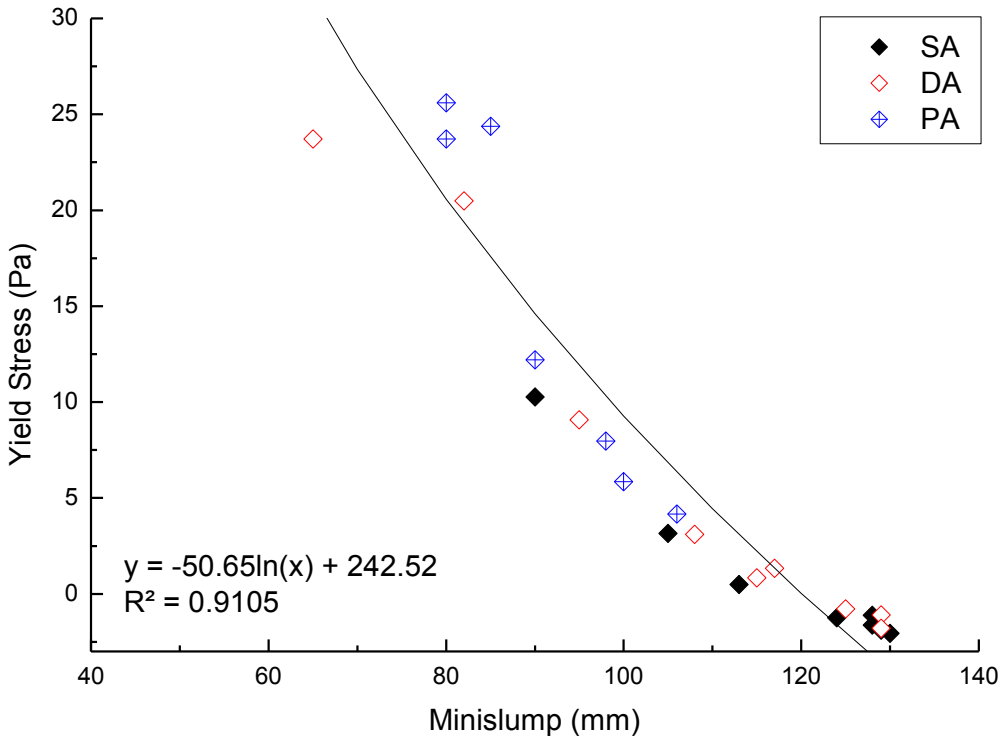

Fig 7.12 Relationship between minislump and yield stress of NaOH-activated slag pastes with MPs

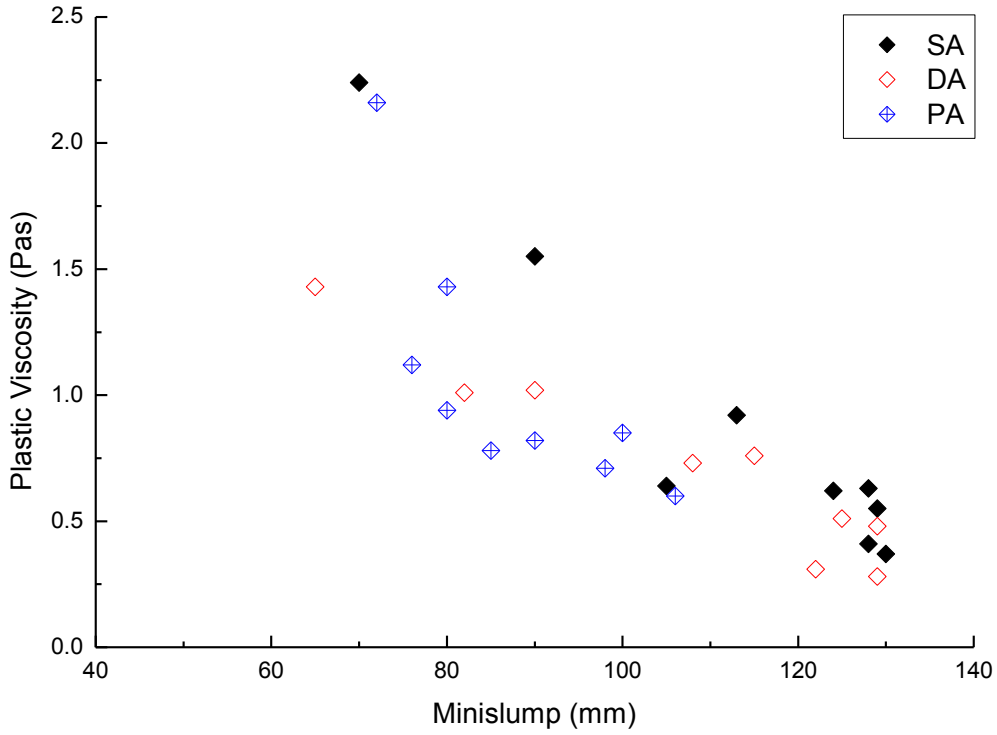

Fig 7.13 Relationship between minislump and plastic viscosity of NaOH-activated slag pastes with MP

7.4.3 Setting time

The effect of MP (at the dosage of 0.500%) on the setting time of NaOH-activated slag is illustrated in ***Fig 7.14***. Regardless of the addition methods utilized, in the presence of MP, both initial and final setting times of NaOH-activated slag were prolonged, and the time interval between the initial setting and the final setting was likewise extended. Comparing the different addition methods, *SA* delayed the initial setting time of NaOH-activated slag from 104 mins to 138 mins, and *DA* prolonged the initial setting to 137 mins. Additionally, *SA* prolonged the final setting time to 208 mins, while *DA* only delayed the final setting time to 158 mins. *PA* demonstrated less effect on the setting time of NaOH-activated slag and the initial and final setting times of which were 110 mins and 130 mins, respectively. As discussed, the setting of NaOH-activated slag is linked to the hydration process, which will be discussed later.

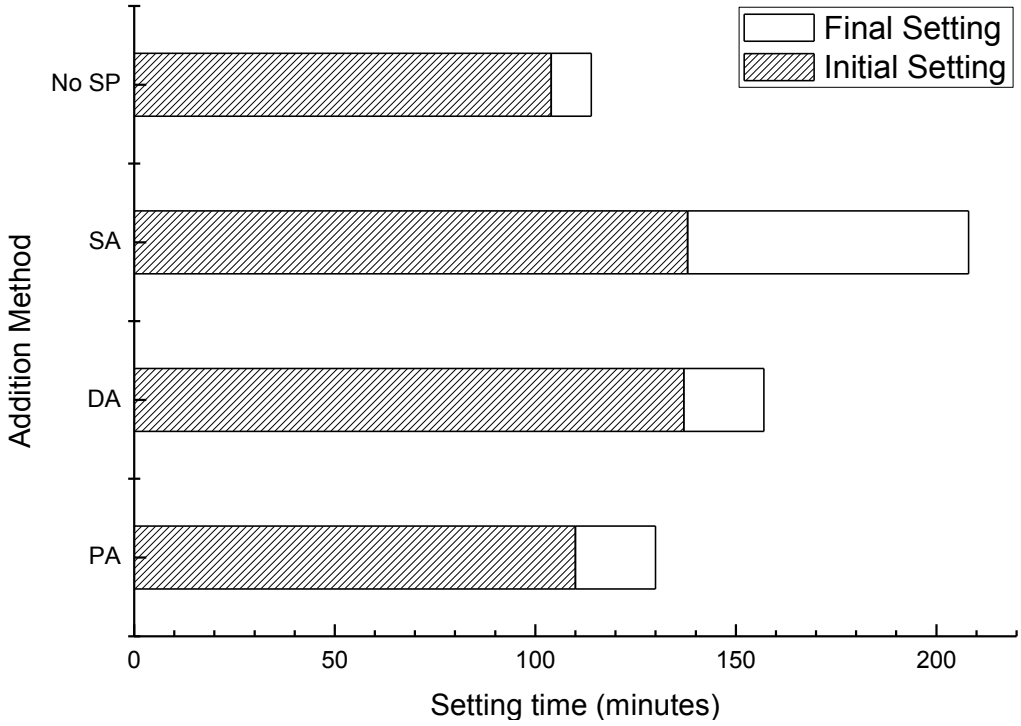

Fig 7.14 Effects of different addition methods of MP on the setting time of NaOH-activated slag paste (0.500% dosage)

7.4.4 Early hydration

The effect of 0.500% MP on the heat flow of NaOH-activated slag paste is presented in ***Fig 7.15.*** From the figure, the addition of MP showed no change to the general heat evolution profile of NaOH-activated slag, which indicates that the overall hydration mechanism did not change. However, the peak time and the intensity of the peak were changed. Apparently, the addition of MP delayed the hydration of the NaOH-activated slag and the accelerating peak has been shifted to longer time.

As displayed in the inset in ***Fig 7.15***, the height of the initial peak, which is attributed to the wetting and dissolution of slag particles, was increased with the addition of MP polymer. Similar to the results reported in Chapter 5, the addition of MP disperses the slag grains and breaks the agglomerates, which increases the total surface area of slag, and hence increases the heat flow of NaOH-activated slag. For *PA*, in order to prepare the activator solution, the same amount of NaOH dissolved in less water (1/3 of which compared to *SA*), and therefore, higher concentration of OH^- are prepared. Hence higher height of initial peak was observed by *PA*. Noticeably,

the magnitude of the initial peaks (14.25 mW/g) was observed with the MP under *PA* method, which is much higher than that with PC-based SPs (it is less than 6 mW/g as reported in section 5.4.4). The reason of the high heat evolution could also be due to the neutralisation of the acidic MP with the high concentration of OH^-, which is usually an exothermal process (Roberts and Caserio, 1977)

Both the *SA* and *DA* methods showed significant retardation effects on the hydration of NaOH-activated slag. From the heat flow, it can be clearly seen that the *SA* provided the longest time before the appearance of an accelerating peak, indicating that longest setting time was observed by *SA*. Therefore, the best minislump retention of NaOH-activated slag by *SA* could also be attributed to the delayed hydration.

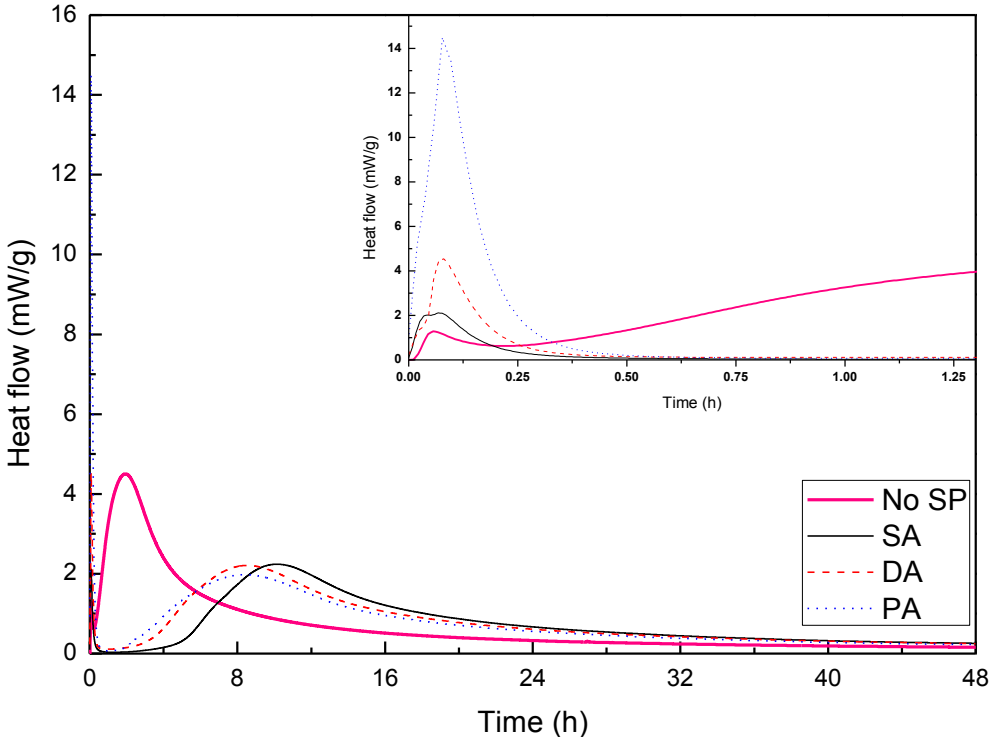

Fig 7.15 Effect of different addition methods of MP on heat flow of NaOH-activated slag paste (at 0.500% dosage)

7.4.5 Summary

The effects of MP on the early age properties of NaOH-activated slag were investigated. The following conclusions could be drawn:

- The initial minislump obtained from the simultaneous and delayed addition methods was higher than that from prior addition method.
- The addition of MP reduced the minislump loss of NaOH-activated slag paste during the first one hour, especially at higher dosage. Comparing the different addition methods, *SA* and *DA* showed better minislump retention. The poorest minislump retention was observed from *PA*.
- Lower yield stress and plastic viscosity of NaOH-activated slag pastes were observed by *SA* and *DA*.
- Both the yield stress and the plastic viscosity of NaOH-activated slag paste under different addition methods were increased over time. A correlation between minislump and yield stress was observed in the experiment.
- The addition of MP delayed the setting time of NaOH-activated slag. *SA* showed the best retardation effect on the setting time of NaOH-activated slag, while *PA* showed the shortest initial setting.
- The addition of MP did not change the general shape of hydration heat flow, which suggests that the hydration mechanism was not altered. However, the addition of MP delayed the appearance of the accelerating peaks of NaOH-activated slag.

7.5 Effects of different addition methods of MP on hardened properties of NaOH-activated slag

In this section, the effects of the different addition methods of MP on the hardened properties, in terms of compressive strength and drying shrinkage, were investigated. The pore structure of hardened NaOH-activated slag was also determined.

7.5.1 Compressive strength

The effect of different addition methods of MP on the compressive strength of NaOH-activated slag is shown in ***Fig 7.16 (a)*** *to* ***(c)***. Generally, the addition of MP increased the compressive strengths of the hardened NaOH-activated slag pastes except the dosage of 0.125% at 1 day. The improvement of one day compressive strength by adding MP was not obvious. The compressive strength was reduced by separate addition at polymer dosage of 0.125%. Compared to the reference, only 94.49% and 89.10% of 1 day compressive strength were achieved by *DA* and *PA*, respectively. However, with the development of hydration time, higher values of compressive strength were observed in the hardened paste with MP. With increasing polymer dosage, the compressive strengths of NaOH-activated slag were also increased. The reason for the increase of compressive strength by adding MP could be similarly attributed to the change of the microstructure of hardened paste by breaking the flocculation of NaOH-activated slag at its fresh state, which will be discussed in section 7.5.3.

Comparing the different addition methods, it was found that *SA* provided the highest compressive strength at all curing ages, while *PA* offered the lowest compressive strength. The change of compressive strength of NaOH-activated slag pastes is again related to the modification of the pore structure of the hardened NaOH-activated slag paste, which will be discussed in section 7.5.3.

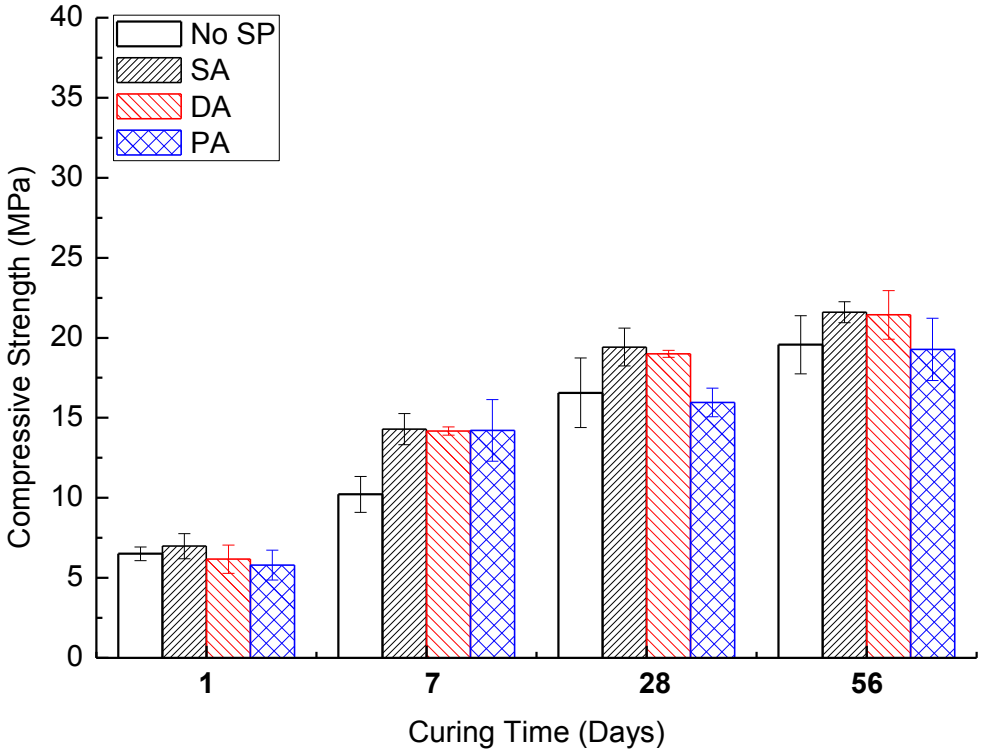

(a) 0.125% MP

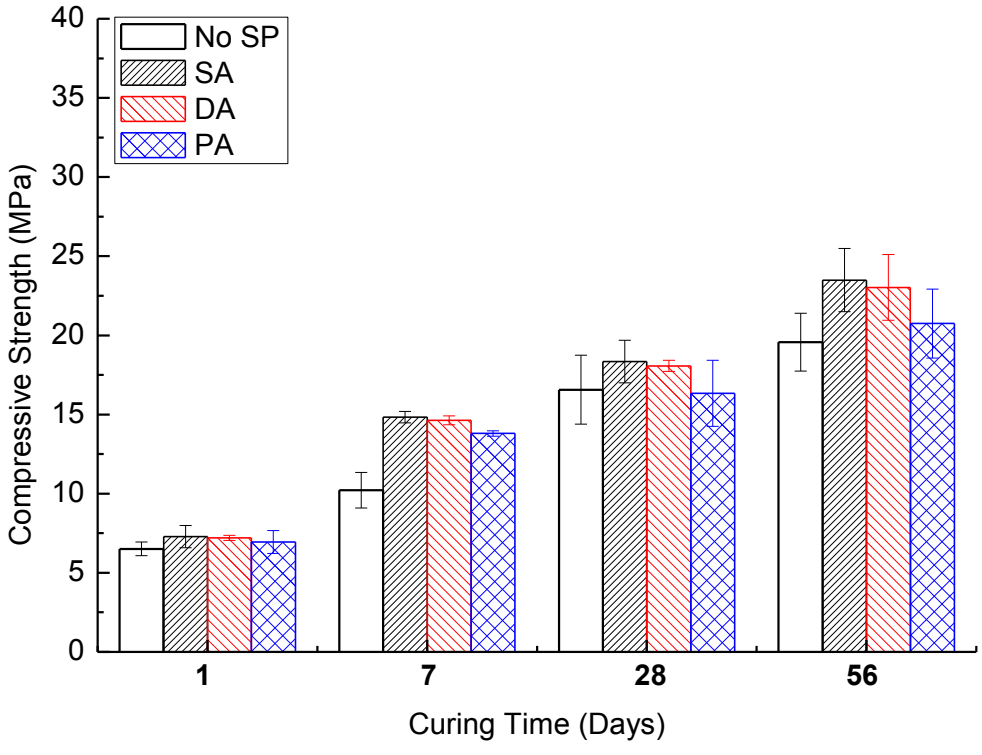

(b) 0.250% MP

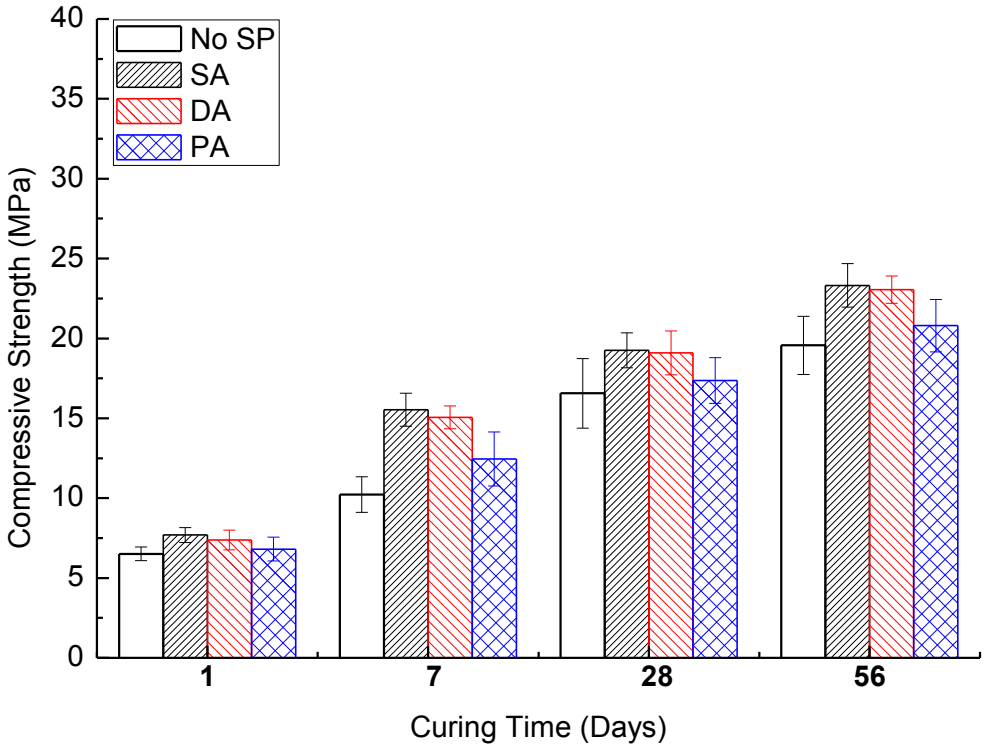

(c) 0.500% MP

Fig 7.16 Effects of different addition methods of MP on the compressive strength of NaOH-activated slag paste

7.5.2 Drying shrinkage

The effects of 0.500% MP on the drying shrinkage of hardened NaOH-activated slag paste are presented in ***Fig 7.17***. The addition of SPs showed slight influence on the drying shrinkage of hardened NaOH-activated slag prism, which was related to the change of porosity of hardened paste in section 7.5.3.

It can be seen clearly in ***Fig 7.17*** that the drying shrinkage of NaOH-activated slag prism progressed rapid during the first 3 months before reaching a relatively constant level (up to 6 months). The addition of MP by *PA* slightly reduced the early stage drying shrinkage of NaOH-activated slag. After 3 months drying, the drying shrinkage by *PA* was similar to that of reference. However, compared to the reference, slightly lower drying shrinkage was observed from both *SA* and *DA* at early stage of drying. After 3 months, the drying shrinkages of NaOH-activated slag prisms prepared by *SA* and *DA* were increased and even higher than that of reference.

It has been accepted that the drying shrinkage of hardened paste is highly related to its pore structure (Bentur et al., 2001). To interpret the effects of MP on the drying shrinkage of NaOH-activated slag under different addition methods, the understanding of the effects of the MP polymer on the pore distribution of the hardened NaOH-activated slag is essential, which is to be discussed in the next section.

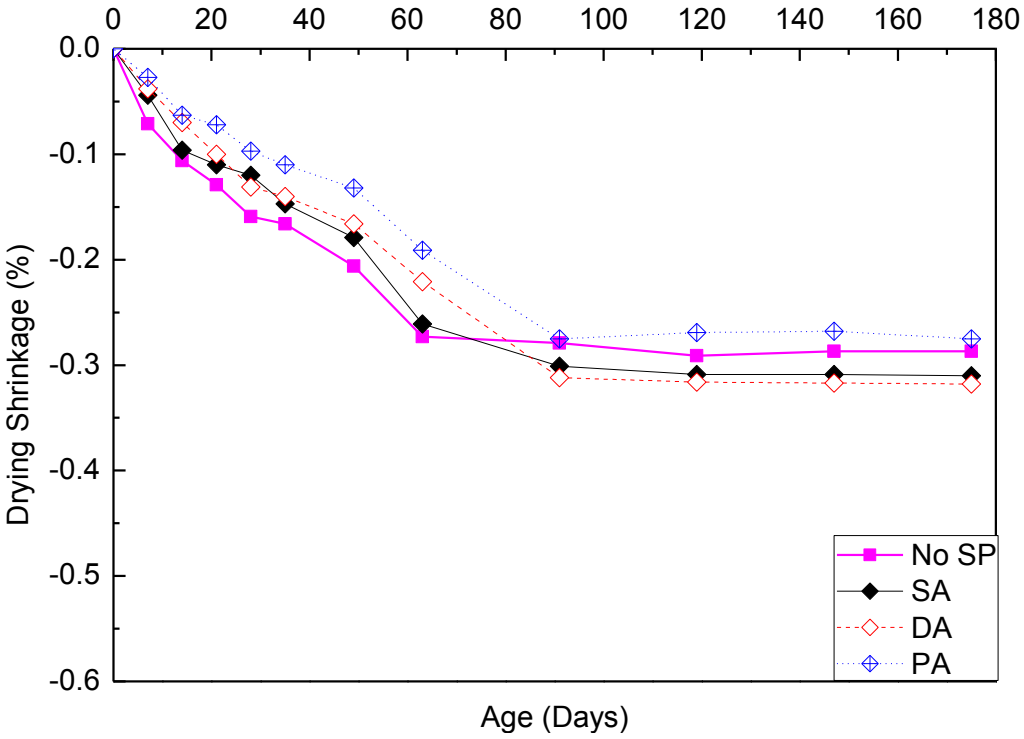

Fig 7.17 Effects of different addition methods of MP on drying shrinkage of NaOH-activated slag paste (at 0.500% dosage)

7.5.3 Porosity

The pore distribution and cumulative pore volume of the hardened NaOH-activated slag paste with MP are presented in ***Fig 7.18***, and the characteristics of the pores are summarised in ***Table 7.3***. The addition of MP refined the pore structures of NaOH-activated slag with decreasing average pore size of the hardened paste. Among different addition methods, larger pore volume and higher porosity were observed in the pastes by *PA*. Both *SA* and *DA* provided larger proportion of micropores (< 100 nm), which is related to the drying shrinkage.

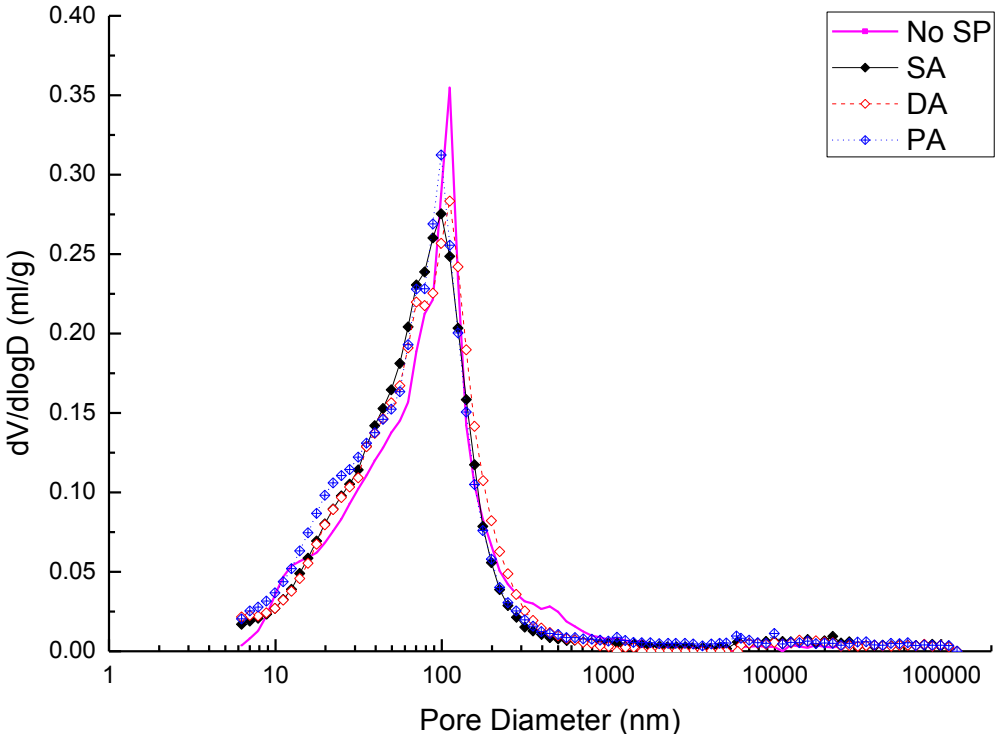

(a) Pore distribution

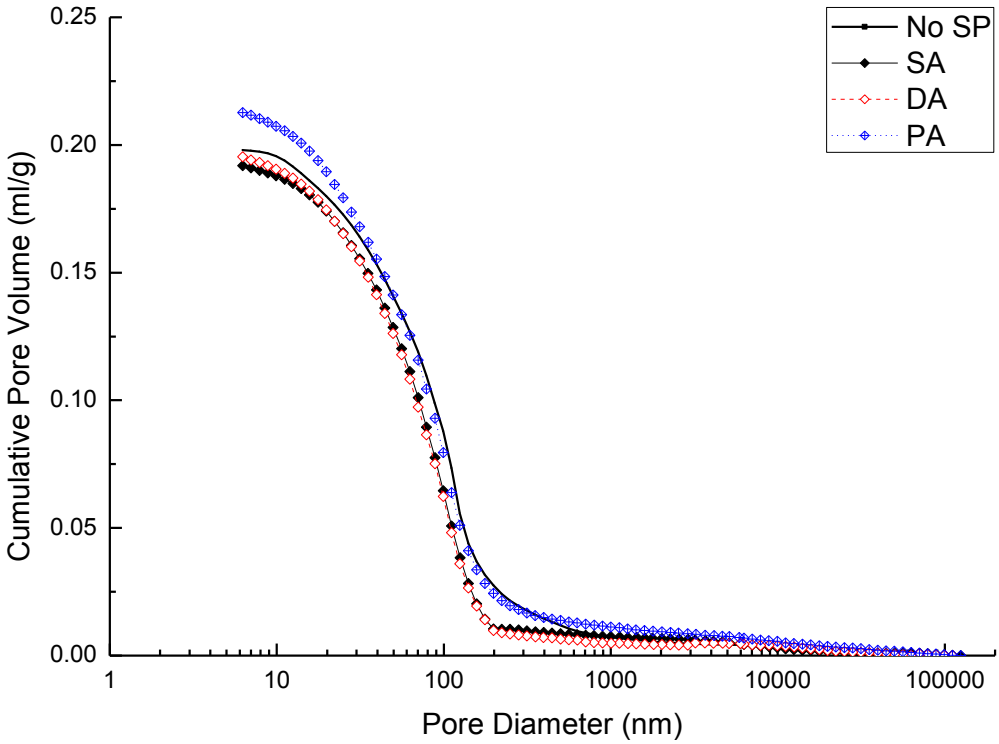

(b) Cumulative pore volume

Fig 7.18 MIP results of hardened NaOH-activated slag paste with MP

The gel pores (pore size < 10 nm) have been reported to be linked to cement hydration degree (Zhang and Kong, 2014, Sakai et al., 2006). Therefore, the increased proportion of gel pores by adding MP indicates that the hydration of the hardened NaOH-activated slag paste was enhanced. Comparing the different addition methods, both *SA* and *DA* methods increased the gel pore volume, which suggests the hydration of NaOH-activated slag was further improved. The reason could be due to the improved dispersion of slag particles and, hence, improved hydration.

Table 7.3 Characteristics of pores in hardened NaOH-activated slag

Samples	Pore Volume (mL/g)	Porosity (%)	Average Pore Size (nm)	Pore Size Distribution/%		
				<10 nm	10 -100 nm	>100 nm
No SP	0.1980	31.94	51.00	2.07	60.83	37.10
SA	0.1919	31.43	47.70	3.80	62.56	33.64
DA	0.1964	31.92	48.70	3.29	64.81	31.90
PA	0.2126	32.21	49.60	2.34	61.27	36.39

7.5.4 Summary

The effects of MP on the hardened properties of NaOH-activated slag were investigated. Based on the results, the following conclusions could be drawn:

- The addition of MP increased the compressive strength of NaOH-activated slag at a given w/c ratio. Comparing the addition methods, the *SA* provided the highest compressive strength among the different addition methods, while *PA* provided the lowest compressive strength of the AAS paste.
- The addition of MP affected the drying shrinkage of NaOH-activated prisms. The larger drying shrinkage was observed in the hardened NaOH-activated slag prism prepared by *SA* and *DA*, while smaller drying shrinkage was observed in the prism prepared by *PA*.
- The addition of MP refined the pore structure of NaOH-activated slag except by *PA*. Smaller average pore size was observed in the hardened NaOH-activated slag pastes by *SA* and *DA*. *PA* provided a smaller proportion of micropores in the hardened NaOH-activated slag pastes.

7.6 Discussion on the function mechanisms of MP in NaOH activated slag

Compared to the PC-based SPs reported in section 5.3.1, the reduction in the adsorption of MP on the surface of slag by NaOH activator is minimised. The reason for this improved adsorption of MP could be due to the enhanced chemical stability of MP. As discussed previously, the chemical instability of SPs has been identified as one of the main issues causing the dysfunction of SPs in AAS. Therefore, the enhanced chemical stability benefits the performance of SPs.

The results in section 5.7 demonstrated that the cleavage of negatively charged anchor groups of LS and NF in high concentration NaOH solution reduced the efficiency of the LS and the NF. Since the adsorption of SPs is due to the electrostatic attraction between the negatively charged anchor groups and the positively charged particle surface, the charge density of SPs is one of the important factors affecting the adsorption of SPs (Plank et al., 2007, Zingg et al., 2008). The higher the charge density of SPs, the higher the adsorption. As reported in section 5.7, the cleavage of anchor groups reduces the charge density of the LS and the NF. Consequently, the adsorption of the LS and the NF is reduced. Section 6.4 demonstrated that the MP exhibits an excellent chemical stability in NaOH solution, which means the quantity of anchor groups is not reduced. Therefore, it is supposed that the adsorption ability of MP in NaOH remains the same as that in water.

In addition to the decrease of charge density, the cleaved 'molecules', for example, sulfonic ions can also induce the competitive adsorption, which further influence the performance of SPs. However, in the case of MP, there is no cleavage of the anchor groups. Therefore, the induced competition due to the de-graft of SPs can be ignored.

The MP is a copolymer with mono- and bi-carboxylic groups as anchor groups, which is polymerised from acidic monomers, kept at pH below 2. Under the acid condition, the MP could be entangled due to the existing intramolecular hydrogen bond among carboxylic groups, which reduces the total number of available carboxylic groups, and consequently decreases the charge density of polymer (Kawaguchi et al., 1990, Katono et al., 1991). Therefore, the reduced available carboxylic groups could decrease the effectiveness of polymer.

Among the three addition methods, *PA* exhibits poorest improvement of the performance of MP, which is probably due to the lowest adsorption amount by *PA*. Two reasons could be attributed to the low adsorption of MP by *PA*: 1) less dissolved Ca^{2+} cations which lead to insufficient sites for adsorption and 2) the charge density of polymer is reduced in the low-pH environment.

For *PA*, the un-neutralised polymers with fewer available carboxylic groups contact the slag before adding large amount of OH^-. Therefore, the adsorption is decreased due to the reduced charge density of acidic MP. In addition, without the presence of NaOH, less Ca^{2+} dissolved near the slag surface when in contact with water, which offers less chance to form a Ca-complex. Therefore, less SPs are absorbed on the surface of slag.

Compared to the *PA*, both *SA* and *DA* methods provide higher adsorption of MP on NaOH-activated slag. The reason can be attributed to the activation of slag by the NaOH-activator, which increases the pH of solution and releases a large amount of cations, such as Ca^{2+} and Mg^{2+} from slag. Additionally, the reaction with NaOH also changes the configuration of MP, providing more carboxyl groups from the MP to interact with slag. Therefore, higher adsorption of MP is observed by *SA* and *DA*.

Moreover, compared to *DA*, the MPs are mixed in NaOH solution by *SA*, providing enough time for the dissociation of the intramolecular hydrogen bonds and the disentanglement of the polymer chain. Consequently, more carboxylic groups are released and then the performance of MP is improved. Therefore, higher adsorption is observed by *SA*.

7.7 Concluding Remarks

In this chapter, the effects of different addition methods of MP on NaOH-activated slag paste were examined. Comparing different addition methods, *SA* provided the best performance on enhancing both fresh and hardened properties of NaOH-activated slag, while *PA* displayed the least improvement in NaOH-activated slag. Based on the experimental results, the following specific conclusions could be drawn:

- The decrease of the adsorption induced by the competitive adsorption between MP and NaOH activator was reduced. Comparing different addition methods, the *SA* offered the highest amount of adsorbed MP on the slag and the lowest value of zeta potential of NaOH-activated slag, while *PA* provided the lowest adsorption of MP and the highest zeta potential of NaOH-activated slag paste.
- The workability of NaOH-activated slag with MP was enhanced due to the increased adsorption of MP by simultaneous addition methods, which increased the workability of NaOH-activated slag. Comparing the different addition methods, the *SA* reduced both yield stress and plastic viscosity of the fresh NaOH-activated slag paste and delayed the setting of the paste.
- Higher compressive strength and drying shrinkage was observed in the hardened NaOH-activated slag paste with MP prepared by *SA*. The porosity results supported the investigation on hardened NaOH-activated slag.

The different trends obtained in this chapter could be attributed to formation of intramolecular hydrogen bonds within the polymer chain by the un-neutralisation of polymers after polymerisation. Therefore, the effects of different treatment of the MP on the performance of NaOH-activated slag must be considered in the future.

Chapter 8

Conclusion and recommendation

8.1 Conclusions

Effects of different addition methods of PC-based SPs in NaOH-activated slag

The separate addition methods improved the efficiency of lignosulfonate (LS) and naphthalene (NF) superplasticiser in NaOH-activated slag by avoiding competitive adsorption between the SPs and the NaOH activator. In general, the *Prior Addition* (PA) performed better than the *Delayed Addition* (DA). Some specific conclusions can be drawn as follows:

- The separate addition methods reduced the competitive adsorption between the SPs and the NaOH activator, leading to a higher adsorption of the SPs on the slag and a lower value of zeta potential of NaOH-activated slag. *PA* provided the greatest adsorption amount of SPs and lowest zeta potential of NaOH-activated slag paste.
- The workability (in terms of minislump spread) of NaOH-activated slag was enhanced by separate addition methods. Moreover, the separate addition reduced both the yield stress and the plastic viscosity of the fresh NaOH-activated slag paste. Comparing the different addition methods, *PA* provided longest setting time. Consequently, best workability retention was observed from *PA*.
- Both compressive strength and drying shrinkage of hardened NaOH-activated slag were changed under the separate addition methods of LS and NF. The addition of the SPs did not induce the reduction of the compressive strength of NaOH-activated slag. However, the drying shrinkage varies, which depended on the type of SPs and the addition methods. The results were in good correlation with the porosity results.

Overall, all the PC-based SPs investigated in this thesis, namely LS, NF and PCE, were not stable in the NaOH solution. Even though by adopting separate addition method, they have demonstrated their potential to be used in NaOH-activated slag system, the chemical instability of these SPs in highly alkaline media is still not ideal which should be addressed by synthesizing alkaline-stable SPs.

Synthesis of alkali-compatible polymer

The modified polycarboxylate based (MP) polymer with carboxylic anchor groups was synthesised and its optimal conditions were generated by central composite design. The MP polymer showed good chemical stability in NaOH solution. Some specific conclusions can be drawn as follows:

- The negatively charged polymer showed better performance in NaOH-activated slag than that of neutral or positively charged polymer. The carboxyl groups were demonstrated as the most effective functional groups on improving minislump of NaOH-activated slag. The vic- COO^- groups exhibited better improvement in NaOH-activated slag than mono- COO^- group.
- The alkali-compatible MP polymer was successfully synthesised and the optimal polymerisation conditions were obtained by testing its performance in rheological properties, in terms of yield stress and plastic viscosity, of NaOH-activated slag by response surface method. The optimal synthesis conditions were identified as: 1) monomer ratio (**2.51**), 2) chain transfer agent concentration (**1.27%**), 3) monomer concentration (**35.23%**), 4) initiator concentration (**1.22%**) and 5) polymer dosage (**0.89%**). The average values obtained from the samples polymerised under the optimised formulation were **-2.40±0.02 Pa** for yield stress and **0.49±0.02 Pa s** for plastic viscosity, which were 95.24% and 94.23% of predicted value from the model generated from respond surface. The validation test confirmed that the response model generated from experiment was valid.
- When it dissolved in highly alkaline NaOH solution, different to the PC-based SPs, no peak shifts were observed in the FTIR spectrum of MP polymer. Moreover, the molecular weight and weight distribution of MP polymer did not change in highly alkaline NaOH solution. The results indicated that the MP polymer exhibited better chemical stability in highly alkaline NaOH solution.

Effects of different addition methods of synthesised polymer

Overall, *SA* and *DA* provided better performance on enhancing both fresh and hardened properties of NaOH-activated slag, while *PA* displayed worst improvement in NaOH-activated slag. Some specific conclusions can be drawn as follows:

- The reduction of adsorption of MP induced by NaOH activator is minimised due to the enhanced chemical stability of the MP in alkaline media. The *SA* provided the greatest amount of adsorbed MP polymer on the slag and the lowest value of zeta potential of NaOH-activated slag, while *PA* provided the lowest adsorption of MP polymer and the highest zeta potential of NaOH-activated slag paste.
- The workability of NaOH-activated slag was enhanced due to the increased adsorption of MP polymer by SA. Correspondingly, the *SA* reduced both yield stress and plastic viscosity of the fresh NaOH-activated slag paste and delayed the setting of the paste. Comparing the two separate addition methods, *DA* performed better than *PA*.
- Higher compressive strength and larger drying shrinkage of hardened NaOH-activated slag were observed under *SA* and *DA*. The results were in good correlation with the porosity results.

8.2 Recommendation and future work

Effects on the different parameters of alkali-activated slag system

The effects of different addition methods of two PC-based SPs, namely, lignosulfonate and naphthalene, in NaOH-activated slag were studied in Chapter 5. It is known that the separate addition of SPs reduces the competitive adsorption between SPs and NaOH activator. However, the work is only a start point with fixed Na_2O% of NaOH activator. Due to the complexity of AAS system, its effects in AAS with different type of activator (i.e. waterglass, Na_2SO_4 and combined activator) and different dosage of activator should be investigated systematically. Additionally, the nature of the slag is also important. Therefore, the effects of slag composition and particle size distribution should also be investigated.

Effects in AAS mortar and concrete

The work conducted in the thesis was only focused on the NaOH-activated slag paste. Its effect on the mortar and concrete has not been studied yet. Therefore, it is recommended to carry out a systematic study to investigate the performance of different addition methods of PC-based SPs and/or synthesised alkali-compatible MP on the properties of NaOH-activated slag mortar and concrete. This is considered as the most important step towards the eventual application of PC-based SPs and MP in practice.

Effects of SPs based on water-reducing effect

All the experiments conducted in this thesis were based on the plasticising effect of SPs, under which condition the water slag ratio was fixed. In practice, the SPs also can be used to reduce the water content and improve the hardened properties of concrete. Therefore, the water-reducing effects of PC-based SPs and synthesized MP in AAS system should be further investigated.

Mechanism of SPs in AAS

Although the work conducted in this thesis has investigated the effect of SPs in NaOH-activated slag paste, the mechanism of SPs on the hydration of AAS, is not fully understood. In addition, the interaction between the fresh properties and the

hardened properties of NaOH-activated slag is still not fully interpreted. Therefore, it is recommended to systematically investigate the mechanism of different addition methods of PC-based SPs and/or synthesised alkali-compatible SPs in NaOH-activated slag mortar and concrete.

Effects of chemical structure of alkali-compatible polymer

The alkali-compatible polymer was successfully synthesised and its optimal synthesis condition was also identified in Chapter 6. However, the polymer was designed based only on the modification of the backbone of SPs. As demonstrated, in addition to electrostatic repulsion, the improved efficiency of the 3rd generation superplasticiser can be attributed to the steric repulsion from the side chain. Therefore, in next stage, the alkali-compatible MPs with strongly grafted side chain should be produced and the effects of chemical structures of the polymer also need to be fully investigated.

Effects of combination with other chemical admixtures and the compatibility with other chemical admixture

The work conducted in this thesis improved the performance of superplasticiser on the workability and rheological properties of AAS. However, compared to its effects on PC, the workability retention was still unsatisfactory, which could be attributed to the quick setting of AAS. Thus, the retarder is considered to be essential for improving the efficiency of SPs in AAS. On the other hand, in practice, various chemical admixtures are normally added into concrete to enhance different properties. The work carried out in this thesis was only investigated the effects of SPs. Therefore, the combination of SPs with other chemicals and its compatibility with other chemical admixture should be investigated in the future.

Commercialisation of the alkali-compatible polymer

Current synthesis work was conducted in laboratory scale. To commercialise the product, the synthesis work in pilot industrial scale and even industrial scale should be considered.

References

ADJOUDJ, M. H., EZZIANE, K., KADRI, E. H., NGO, T.-T. & KACI, A. 2014. Evaluation of rheological parameters of mortar containing various amounts of mineral addition with polycarboxylate superplasticizer. *Construction and Building Materials,* 70**,** 549-559.

AIAD, I. 2003. Influence of time addition of superplasticizers on the rheological properties of fresh cement pastes. *Cement and Concrete Research,* 33**,** 1229-1234.

AIAD, I., ABD EL-ALEEM, S. & EL-DIDAMONY, H. 2002. Effect of delaying addition of some concrete admixtures on the rheological properties of cement pastes. *Cement and Concrete Research,* 32**,** 1839-1843.

AIAD, I., EL-DIDAMONY, H., HEIKAL, M. & AL-MASRY, S. 2013. Effect of delayed addition time of synthesized SSPF condensate on the durability of sulphate resisting cement pastes incorporating micro-silica. *Construction and Building Materials,* 48**,** 1092-1103.

AïTCIN, P. C. 2000. Cements of yesterday and today: Concrete of tomorrow. *Cement and Concrete Research,* 30**,** 1349-1359.

ALI, M. B., SAIDUR, R. & HOSSAIN, M. S. 2011. A review on emission analysis in cement industries. *Renewable and Sustainable Energy Reviews,* 15**,** 2252-2261.

ALONSO, M. M., PALACIOS, M. & PUERTAS, F. 2013. Compatibility between polycarboxylate-based admixtures and blended-cement pastes. *Cement and Concrete Composites,* 35**,** 151-162.

ALONSO, M. M., PALACIOS, M., PUERTAS, F., DE LA TORRE, A. G. & ARANDA, M. A. G. 2007. Effect of polycarboxylate admixture structure on cement paste rheology. *Materiales De Construccion,* 57**,** 65-81.

ALONSO, M. V., OLIET, M., RODRíGUEZ, F., GARCIA, E., GILARRANZ, M. A. & RODRíGUEZ, J. J. 2005. Modification of ammonium lignosulfonate by phenolation for use in phenolic resins. *Bioresource Technology,* 96**,** 1013-1018.

ALONSO, M. V., RODRÍGUEZ, J. J., OLIET, M., RODRÍGUEZ, F., GARCÍA, J. & GILARRANZ, M. A. 2001. Characterization and structural modification of

ammonic lignosulfonate by methylolation. *Journal of Applied Polymer Science,* 82**,** 2661-2668.

AMBROISE, J., GEORGIN, J. F., PEYSSON, S. & PÉRA, J. 2009. Influence of polyether polyol on the hydration and engineering properties of calcium sulfoaluminate cement. *Cement and Concrete Composites,* 31**,** 474-482.

ANDERSEN, P. J., KUMAR, A., ROY, D. M. & WOLFE-CONFER, D. 1986. The effect of calcium sulphate concentration on the adsorption of a superplasticizer on a cement: Methods, zeta potential and adsorption studies. *Cement and Concrete Research,* 16**,** 255-259.

ANDERSEN, P. J., ROY, D. M. & GAIDIS, J. M. 1988. The effect of superplasticizer molecular weight on its adsorption on, and dispersion of, cement. *Cement and Concrete Research,* 18**,** 980-986.

ARNDT, K. F., RICHTER, A., LUDWIG, S., ZIMMERMANN, J., KRESSLER, J., KUCKLING, D. & ADLER, H. J. 1999. Poly(vinyl alcohol)/poly(acrylic acid) hydrogels: FT-IR spectroscopic characterization of crosslinking reaction and work at transition point. *Acta Polymerica,* 50**,** 383-390.

ARTELT, C. & GARCIA, E. 2008. Impact of superplasticizer concentration and of ultra-fine particles on the rheological behaviour of dense mortar suspensions. *Cement and Concrete Research,* 38**,** 633-642.

ASTM C490: 2000. Standard Practice for Use of Apparatus for the Determination of Length Change of Hardened Cement Paste, Mortar, and Concrete. *ASTM International. West Conshohocken.*

AYDıN, S. & BARADAN, B. 2012. Mechanical and microstructural properties of heat cured alkali-activated slag mortars. *Materials and Design,* 35**,** 374-383.

AYDıN, S. & BARADAN, B. 2014. Effect of activator type and content on properties of alkali-activated slag mortars. *Composites Part B: Engineering,* 57**,** 166-172.

BAGHABRA AL-AMOUDI, O. S., ABIOLA, T. O. & MASLEHUDDIN, M. 2006. Effect of superplasticizer on plastic shrinkage of plain and silica fume cement concretes. *Construction and Building Materials,* 20**,** 642-647.

BAKHAREV, T., SANJAYAN, J. G. & CHENG, Y.-B. 1999. Alkali activation of Australian slag cements. *Cement and Concrete Research,* 29**,** 113-120.

BAKHAREV, T., SANJAYAN, J. G. & CHENG, Y. B. 2000. Effect of admixtures on properties of alkali-activated slag concrete. *Cement and Concrete Research,* 30**,** 1367-1374.

BANFILL, P. F. G. 1994. Rheological methods for assessing the flow properties of mortar and related materials. *Construction and Building Materials,* 8**,** 43-50.

BANFILL, P. F. G. 2006. Rheology of fresh cement and concrete. *Rheology Reviews,* 2006**,**. 61-130.

BARNES, H. A. & WALTERS, K. 1985. The yield stress myth? *Rheologica Acta,* 24**,** 323-326.

BARR, B., HOSEINIAN, S. B. & BEYGI, M. A. 2003. Shrinkage of concrete stored in natural environments. *Cement and Concrete Composites,* 25**,** 19-29.

BEN HAHA, M., LE SAOUT, G., WINNEFELD, F. & LOTHENBACH, B. 2011. Influence of activator type on hydration kinetics, hydrate assemblage and microstructural development of alkali activated blast-furnace slags. *Cement and Concrete Research,* 41**,** 301-310.

BENAICHA, M., ROGUIEZ, X., JALBAUD, O., BURTSCHELL, Y. & ALAOUI, A. H. 2015. Influence of silica fume and viscosity modifying agent on the mechanical and rheological behavior of self compacting concrete. *Construction and Building Materials,* 84**,** 103-110.

BENTUR, A., IGARASHI, S. & KOVLER, K. 2001. Prevention of autogenous shrinkage in high-strength concrete by internal curing using wet lightweight aggregates. *Cement and Concrete Research,* 31**,** 1587-1591.

BENYAHIA, B., LATIFI, M. A., FONTEIX, C., PLA, F. & NACEF, S. 2010. Emulsion copolymerization of styrene and butyl acrylate in the presence of a chain transfer agent.: Part 1: Modelling and experimentation of batch and fedbatch processes. *Chemical Engineering Science,* 65**,** 850-869.

BENYOUNIS, K. Y., OLABI, A. G. & HASHMI, M. S. J. 2008. Multi-response optimization of CO_2 laser-welding process of austenitic stainless steel. *Optics & Laser Technology,* 40**,** 76-87.

BERNAL, S. A., SAN NICOLAS, R., MYERS, R. J., MEJ A DE GUTI RREZ, R., PUERTAS, F., VAN DEVENTER, J. S. J. & PROVIS, J. L. 2014. MgO content of slag controls phase evolution and structural changes induced by accelerated carbonation in alkali-activated binders. *Cement and Concrete Research,* 57**,** 33-43.

BEY, H. B., HOT, J., BAUMANN, R. & ROUSSEL, N. 2014. Consequences of competitive adsorption between polymers on the rheological behaviour of cement pastes. *Cement and Concrete Composites,* 54**,** 17-20.

BEZERRA, M. A., SANTELLI, R. E., OLIVEIRA, E. P., VILLAR, L. S. & ESCALEIRA, L. A. 2008. Response surface methodology (RSM) as a tool for optimization in analytical chemistry. *Talanta,* 76**,** 965-977.

BION, N., SAUSSEY, J., HANEDA, M. & DATURI, M. 2003. Study by in situ FTIR spectroscopy of the SCR of NOx by ethanol on Ag/Al_2O_3—Evidence of the role of isocyanate species. *Journal of Catalysis,* 217**,** 47-58.

BJORNSTROM, J. & CHANDRA, S. 2003. Effect of superplasticizers on the rheological properties of cements. *Materials and Structures,* 36**,** 685-692.

BORGET, P., GALMICHE, L., LE MEINS, J. F. & LAFUMA, F. 2005. Microstructural characterisation and behaviour in different salt solutions of sodium polymethacrylate-g-PEO comb copolymers. *Colloids and Surfaces A: Physicochemical and Engineering Aspects,* 260**,** 173-182.

BOUHAMED, H., BOUFI, S. & MAGNIN, A. 2007. Dispersion of alumina suspension using comb-like and diblock copolymers produced by RAFT polymerization of AMPS and MPEG. *Journal of Colloid and Interface Science,* 312**,** 279-291.

BS EN 12305-2:2009. Testing fresh concrete. Slump-test. *British Standards Institution,* London.

BS EN 12305-3:2009. Testing fresh concrete. Vebe test. *British Standards Institution.*

BS EN 12305-4:2009. Testing fresh concrete. Degree of compactability. *British Standards Institution,* London.

BS EN 12305-5:2009. Testing fresh concrete. Flow table test. *British Standards Institution,* London.

BS EN 12305-8:2010. Testing fresh concrete. Self-compacting concrete. Slump-flow test. *British Standards Institution,* London.

BS EN 12305-9:2010. Testing fresh concrete. Self-compacting concrete. V-funnel test. *British Standards Institution,* London.

BS EN 12305-10:2010. Testing fresh concrete. Self-compacting concrete. L box test. *British Standards Institution,* London.

BS EN 12305-11:2009. Testing fresh concrete. Self-compacting concrete. Sieve segregation test. *British Standards Institution,* London.

BS EN 12305-12:2009. Testing fresh concrete. Self-compacting concrete. J-ring test. *British Standards Institution,* London.

BS EN 196-3:2005. Methods of testing cement. Determination of setting times and soundness. *British Standards Institution,* London.

BS EN 197-1:2011. Cement. Composition, specifications and conformity criteria for common cements. *British Standards Institution,* London.

BS EN 934-2:2009. Admixtures for concrete, mortar and grout . Concrete admixtures. Definitions, requirements, conformity, marking and labelling. *British Standards Institution,* London.

BS ISO 16014-2:2012. Plastics. Determination of average molecular mass and molecular mass distribution of polymers using size-exclusion chromatography. Universal calibration method. *British Standards Institution,* London.

BS ISO 16014-3:2012. Plastics. Determination of average molecular mass and molecular mass distribution of polymers using size-exclusion chromatography. Low-temperature method. *British Standards Institution,* London.

BULLARD, J. W., JENNINGS, H. M., LIVINGSTON, R. A., NONAT, A., SCHERER, G. W., SCHWEITZER, J. S., SCRIVENER, K. L. & THOMAS, J. J. 2011. Mechanisms of cement hydration. *Cement and Concrete Research,* 41**,** 1208-1223.

BURGOS-MONTES, O., PALACIOS, M., RIVILLA, P. & PUERTAS, F. 2012. Compatibility between superplasticizer admixtures and cements with mineral additions. *Construction and Building Materials,* 31**,** 300-309.

BÜYÜKYAĞCı, A., TUZCU, G. & ARAS, L. 2009. Synthesis of copolymers of methoxy polyethylene glycol acrylate and 2-acrylamido-2-methyl-1-propanesulfonic acid: Its characterization and application as superplasticizer in concrete. *Cement and Concrete Research,* 39**,** 629-635.

CARTUXO, F., DE BRITO, J., EVANGELISTA, L., JIM NEZ, J. R. & LEDESMA, E. F. 2015. Rheological behaviour of concrete made with fine recycled concrete aggregates – Influence of the superplasticizer. *Construction and Building Materials,* 89**,** 36-47.

CAPELLA-PEIRÓ, M. E., BOSE, D., RUBERT, M. L. F. & ESTEVE-ROMERO, J. 2006. Optimization of a capillary zone electrophoresis method by using a central composite factorial design for the determination of codeine and paracetamol in pharmaceuticals. *Journal of Chromatography B,* 839**,** 95-101.

CESTARI, A. R., VIEIRA, E. F. S., SILVA, E. C. S., ALVES, F. J. & ANDRADE JR, M. A. S. 2013. Synthesis, characterization and hydration analysis of a novel epoxy/superplasticizer oilwell cement slurry – Some mechanistic features by solution microcalorimetry. *Journal of Colloid and Interface Science,* 392**,** 359-368.

CHANDRA, S. & BJÖRNSTRÖM, J. 2002. Influence of superplasticizer type and dosage on the slump loss of Portland cement mortars—Part II. *Cement and Concrete Research,* 32**,** 1613-1619.

CHENG, L. Q. & WANG, W. P. 2010. Synthesis of Polycarboxylic Acid-Based Superplasticizer via ATRP in Aqueous Media [J]. *Polymer Materials Science & Engineering,* 2**,** 011.

CHO, H. Y. & SUH, J. M. 2005. Effects of the synthetic conditions of poly{carboxylate-g-(ethylene glycol) methyl ether} on the dispersibility in cement paste. *Cement and Concrete Research,* 35**,** 891-899.

CHO, I. H. & ZOH, K. D. 2007. Photocatalytic degradation of azo dye (Reactive Red 120) in TiO_2/UV system: Optimization and modeling using a response

surface methodology (RSM) based on the central composite design. *Dyes and Pigments,* 75**,** 533-543.

ÇOLAK, A. 2005. Properties of plain and latex modified Portland cement pastes and concretes with and without superplasticizer. *Cement and Concrete Research,* 35**,** 1510-1521.

COLLEPARDI, M. 1998. Admixtures used to enhance placing characteristics of concrete. *Cement and Concrete Composites,* 20**,** 103-112.

COLLINS, F. & SANJAYAN, J. 2001. Early age strength and workability of slag pastes activated by sodium silicates. *Magazine of Concrete Research,* 53**,** 321-326.

COLLINS, F. & SANJAYAN, J. G. 1999. Strength and shrinkage properties of alkali-activated slag concrete placed into a large column. *Cement and Concrete Research,* 29**,** 659-666.

CRANEY, T. A. 2003. Probabilistic engineering design. *Reliability Review, The R&M Engineering Journal,* 23**,** 1-6.

CUNNINGHAM, J. C., DURY, B. L. & GREGORY, T. 1989. Adsorption characteristics of sulphonated melamine formaldehyde condensates by high performance size exclusion chromatography. *Cement and Concrete Research,* 19**,** 919-928.

CYR, M., LEGRAND, C. & MOURET, M. 2000. Study of the shear thickening effect of superplasticizers on the rheological behaviour of cement pastes containing or not mineral additives. *Cement and Concrete Research,* 30**,** 1477-1483.

DALCIN, M. G., PIRETE, M. M., LEMOS, D. A., RIBEIRO, E. J., CARDOSO, V. L. & DE RESENDE, M. M. 2011. Evaluation of hexavalent chromium removal in a continuous biological filter with the use of central composite design (CCD). *Journal of Environmental Management,* 92**,** 1165-1173.

DARRAS, V., FICHET, O., PERROT, F., BOILEAU, S. & TEYSSIÉ, D. 2007. Polysiloxane–poly(fluorinated acrylate) interpenetrating polymer networks: Synthesis and characterization. *Polymer,* 48**,** 687-695.

DARWENT, B. D. 1970. Bond dissociation energies in simple molecules. *NSRDS-NBS NO. 31, U. S. DEPT. COMMERCE, WASHINGTON, D. C. JAN. 1970, P 48*.

DE LARRARD, F., HU, C., SEDRAN, T., SZITKAR, J. C., JOLY, M., CLAUX, F. & DERKX, F. 1997. A new rheometer for soft-to-fluid fresh concrete. *ACI Materials Journal,* 94**,** 234-243.

DE SCHUTTER, G., BARTOS, P. J. M., DOMONE, P. & GIBBS, J. 2008. *Self-compacting concrete*, WHITTLES PUBLISHING, Dunbeath.

DEAN, A. & VOSS, D. 1999. Response surface methodology. *Design and analysis of experiments***,** 547-86.

DEAN, J. A. 1999. *Lange's handbook of chemistry*, McGRAW-HILL, INC, New York

DIAMOND, S. 2006. The patch microstructure in concrete: The effect of superplasticizer. *Cement and Concrete Research,* 36**,** 776-779.

DOUGLAS, E., BILODEAU, A. & MALHOTRA, V. M. 1992. Properties and durability of alkali-activated slag concrete. *ACI Materials Journal,* 89**,** 509-516.

DOUGLAS, E. & BRANDSTETR, J. 1990. A preliminary study on the alkali activation of ground granulated blast-furnace slag. *Cement and Concrete Research,* 20**,** 746-756.

DUARTE, L. F., BARROS, A., ALMEIDA, C., SPRAUL, M. & GIL, A. M. 2004. Multivariate Analysis of NMR and FTIR Data as a Potential Tool for the Quality Control of Beer. *Journal of Agricultural and Food Chemistry,* 52**,** 1031-1038.

DURAN ATIŞ, C., BILIM, C., ÇELIK, Ö. & KARAHAN, O. 2009. Influence of activator on the strength and drying shrinkage of alkali-activated slag mortar. *Construction and Building Materials,* 23**,** 548-555.

DUREKOVIC, A. & TKALCIC-CIBOCI, B. 1991. Cement pastes of low water to solid ratio: An investigation of the polymerization of silicate anions in the presence of a superplasticizer and silica fume. *Cement and Concrete Research,* 21**,** 1015-1022.

DUXSON, P. & PROVIS, J. L. 2008. Designing Precursors for Geopolymer Cements. *Journal of the American Ceramic Society,* 91**,** 3864-3869.

EL-DIDAMONY, H., AIAD, I., HEIKAL, M. & AL-MASRY, S. 2014. Impact of delayed addition time of SNF condensate on the fire resistance and durability of SRC–SF composite cement pastes. *Construction and Building Materials,* 50**,** 281-290.

EL-DIDAMONY, H., HEIKAL, M. & ABD EL ALEEM, S. 2012. Influence of delayed addition time of sodium sulfanilate phenol formaldehyde condensate on the hydration characteristics of sulfate resisting cement pastes containing silica fume. *Construction and Building Materials,* 37**,** 269-276.

EL-GAMAL, S. M. A., AL-NOWAISER, F. M. & AL-BAITY, A. O. 2012. Effect of superplasticizers on the hydration kinetic and mechanical properties of Portland cement pastes. *Journal of Advanced Research,* 3**,** 119-124.

EL GAMAL, S. M. & BIN SALMAN, H. M. 2012. Effect of addition of Sikament-R superplasticizer on the hydration characteristics of portland cement pastes. *HBRC Journal,* 8**,** 75-80.

ELAKNESWARAN, Y., NAWA, T. & KURUMISAWA, K. 2009. Zeta potential study of paste blends with slag. *Cement and Concrete Composites,* 31**,** 72-76.

ERDOGDU, S. 2005. Effect of retempering with superplasticizer admixtures on slump loss and compressive strength of concrete subjected to prolonged mixing. *Cement and Concrete Research,* 35**,** 907-912.

ERDOĞDU, Ş., ARSLANTÜRK, C. & KURBETCI, Ş. 2011. Influence of fly ash and silica fume on the consistency retention and compressive strength of concrete subjected to prolonged agitating. *Construction and Building Materials,* 25**,** 1277-1281.

ESCALANTE-GARC ÍA, J. I., FUENTES, A. F., GOROKHOVSKY, A., FRAIRE-LUNA, P. E. & MENDOZA-SUAREZ, G. 2003. Hydration Products and Reactivity of Blast-Furnace Slag Activated by Various Alkalis. *Journal of the American Ceramic Society,* 86**,** 2148-2153.

FAN, W., STOFFELBACH, F., RIEGER, J., REGNAUD, L., VICHOT, A., BRESSON, B. & LEQUEUX, N. 2012. A new class of organosilane-

modified polycarboxylate superplasticizers with low sulfate sensitivity. *Cement and Concrete Research,* 42**,** 166-172.

FANTINEL, F., RIEGER, J., MOLNAR, F. & HÜBLER, P. 2004. Complexation of polyacrylates by Ca^{2+} ions. Time-resolved studies using attenuated total reflectance Fourier transform infrared dialysis spectroscopy. *Langmuir,* 20**,** 2539-2542.

FELEKOGLU, B. & SARIKAHYA, H. 2008. Effect of chemical structure of polycarboxylate-based superplasticizers on workability retention of self-compacting concrete. *Construction and Building Materials,* 22**,** 1972-1980.

FELEKOĞLU, B., TOSUN, K. & BARADAN, B. 2011. Compatibility of a polycarboxylate-based superplasticiser with different set-controlling admixtures. *Construction and Building Materials,* 25**,** 1466-1473.

FERNÀNDEZ-ALTABLE, V. & CASANOVA, I. 2006. Influence of mixing sequence and superplasticiser dosage on the rheological response of cement pastes at different temperatures. *Cement and Concrete Research,* 36**,** 1222-1230.

FERNANDEZ-JIMENEZ, A. & PUERTAS, F. 2001. Setting of alkali-activated slag cement. Influence of activator nature. *Advances in Cement Research,* 13**,** 115-121.

FERNANDEZ-JIMENEZ, A. & PUERTAS, F. 2003. Effect of activator mix on the hydration and strength behaviour of alkali-activated slag cements. *Advances in Cement Research,* 15**,** 129-136.

FERNÁNDEZ, J. M., DURAN, A., NAVARRO-BLASCO, I., LANAS, J., SIRERA, R. & ALVAREZ, J. I. 2013. Influence of nanosilica and a polycarboxylate ether superplasticizer on the performance of lime mortars. *Cement and Concrete Research,* 43**,** 12-24.

FERRARI, G., CERULLI, T., CLEMENTE, P., DRAGONI, M., GAMBA, M. & SURICO, F. 2000. Influence of Carboxylic Acid-Carboxylic Ester Ratio of Carboxylic Acid Ester Superplasticizer on Characteristics of Cement Mixtures. *Special Publication,* 195**,** 505-520, Tallahassee.

FERRARI, L., BERNARD, L., DESCHNER, F., KAUFMANN, J., WINNEFELD, F. & PLANK, J. 2012. Characterization of Polycarboxylate-Ether Based Superplasticizer on Cement Clinker Surfaces. *Journal of the American Ceramic Society,* 95**,** 2189-2195.

FERRARI, L., KAUFMANN, J., WINNEFELD, F. & PLANK, J. 2010. Interaction of cement model systems with superplasticizers investigated by atomic force microscopy, zeta potential, and adsorption measurements. *Journal of Colloid and Interface Science,* 347**,** 15-24.

FERRARI, L., KAUFMANN, J., WINNEFELD, F. & PLANK, J. 2011. Multi-method approach to study influence of superplasticizers on cement suspensions. *Cement and Concrete Research,* 41**,** 1058-1066.

FERRARIS, C. F., OBLA, K. H. & HILL, R. 2001. The influence of mineral admixtures on the rheology of cement paste and concrete. *Cement and Concrete Research,* 31**,** 245-255.

FERREIRA, S. L. C., BRUNS, R. E., FERREIRA, H. S., MATOS, G. D., DAVID, J. M., BRANDÃO, G. C., DA SILVA, E. G. P., PORTUGAL, L. A., DOS REIS, P. S., SOUZA, A. S. & DOS SANTOS, W. N. L. 2007. Box-Behnken design: An alternative for the optimization of analytical methods. *Analytica Chimica Acta,* 597**,** 179-186.

FEYS, D., VERHOEVEN, R. & DE SCHUTTER, G. 2008. Fresh self compacting concrete, a shear thickening material. *Cement and Concrete Research,* 38**,** 920-929.

FEYS, D., VERHOEVEN, R. & DE SCHUTTER, G. 2009. Why is fresh self-compacting concrete shear thickening? *Cement and Concrete Research,* 39**,** 510-523.

FLATT, R. J. 2004. Towards a prediction of superplasticized concrete rheology. *Materials and Structures,* 37**,** 289-300.

FLATT, R. J. & HOUST, Y. F. 2001. A simplified view on chemical effects perturbing the action of superplasticizers. *Cement and Concrete Research,* 31**,** 1169-1176.

GAIDIS, J. M. & ROSENBERG, A. M. 1984. Multicomponent concrete superplasticizer. Google Patents, US US4460720 A

GAO, P. W., DENG, M. & FENG, N. Q. 2001. The influence of superplasticizer and superfine mineral powder on the flexibility, strength and durability of HPC. *Cement and Concrete Research,* 31**,** 703-706.

GAO, P. W., LU, X. L., YANG, C. X., LI, X. Y., SHI, N. N. & JIN, S. C. 2008. Microstructure and pore structure of concrete mixed with superfine phosphorous slag and superplasticizer. *Construction and Building Materials,* 22**,** 837-840.

GARBALIŃSKA, H. & WYGOCKA, A. 2014. Microstructure modification of cement mortars: Effect on capillarity and frost-resistance. *Construction and Building Materials,* 51**,** 258-266.

GIFFORD, P. M. & GILLOTT, J. E. 1997. Behaviour of mortar and concrete made with activated blast furnace slag cement. *Canadian Journal of Civil Engineering,* 24**,** 237-249.

GIRAUDEAU, C., D'ESPINOSE DE LACAILLERIE, J.-B., SOUGUIR, Z., NONAT, A. & FLATT, R. J. 2009. Surface and Intercalation Chemistry of Polycarboxylate Copolymers in Cementitious Systems. *Journal of the American Ceramic Society,* 92**,** 2471-2488.

GLUKHOVSKY, V. D., ROSTONVSKAJA, G. S. & RUMYNA, G. V. High strength slag alkaline cement. The seventh international congress on the chemistry of cement, 1980 Paris, France. 164-168.

GOŁASZEWSKI, J. 2012. Influence of cement properties on new generation superplasticizers performance. *Construction and Building Materials,* 35**,** 586-596.

GRABIEC, A. M. 1999. Contribution to the knowledge of melamine superplasticizer effect on some characteristics of concrete after long periods of hardening. *Cement and Concrete Research,* 29**,** 699-704.

GRIGG, R. B. & BAI, B. J. 2004. Calcium lignosulfonate adsorption and desorption on Berea sandstone. *Journal of Colloid and Interface Science,* 279**,** 36-45.

GUÉRANDEL, C., VERNEX-LOSET, L., KRIER, G., DE LANÈVE, M., GUILLOT, X., PIERRE, C. & MULLER, J. F. 2011. A new method to analyze copolymer based superplasticizer traces in cement leachates. *Talanta,* 84**,** 133-140.

GUO, W. J., SUN, N., QIN, J. J., ZHANG, J., PEI, M. S., WANG, Y. & WANG, S. N. 2012. Synthesis and properties of an amphoteric polycarboxylic acid-based superplasticizer used in sulfoaluminate cement. *Journal of Applied Polymer Science,* 125**,** 283-290.

HABBABA, A. & PLANK, J. 2010. Interaction Between Polycarboxylate Superplasticizers and Amorphous Ground Granulated Blast Furnace Slag. *Journal of the American Ceramic Society,* 93**,** 2857-2863.

HABBABA, A. & PLANK, J. 2012. Surface Chemistry of Ground Granulated Blast Furnace Slag in Cement Pore Solution and Its Impact on the Effectiveness of Polycarboxylate Superplasticizers. *Journal of the American Ceramic Society,* 95**,** 768-775.

HACKLEY, V. A. 1997. Colloidal Processing of Silicon Nitride with Poly(acrylic acid): I, Adsorption and Electrostatic Interactions. *Journal of the American Ceramic Society,* 80**,** 2315-2325.

HANG, Y., QU, M. & UKKUSURI, S. 2011. Optimizing the design of a solar cooling system using central composite design techniques. *Energy and Buildings,* 43**,** 988-994.

HASSAN, E. E., PARISH, R. C. & GALLO, J. M. 1992. Optimized Formulation of Magnetic Chitosan Microspheres Containing the Anticancer Agent, Oxantrazole. *Pharmaceutical Research,* 9**,** 390-397.

HEIKAL, M., MORSY, M. S. & AIAD, I. 2005. Effect of treatment temperature on the early hydration characteristics of superplasticized silica fume blended cement pastes. *Cement and Concrete Research,* 35**,** 680-687.

HEWLETT, P. C. 2004. *Lea's chemistry of cement and concrete*, Butterworth-Heinemann, Oxford

HIRATA, T., ITO, H., KOBAYASHI, H., TAHARA, H. & TSUBAKIMOTO, T. 1989. Cement dispersant. Google Patents, US4870120 A.

HODNE, H. & SAASEN, A. 2000. The effect of the cement zeta potential and slurry conductivity on the consistency of oil-well cement slurries. *Cement and Concrete Research,* 30**,** 1767-1772.

HONG, S. Y., KIM, J. C. & KIM, J. K. 1993. Studies on the hydration of alkali activated slag. 3rd Beijing International Symposium on Cement and Concrete, 1993 Beijing, China. 1059-1063.

HSU, K. C., CHEN, S. D. & SU, N. 2000. Water-soluble sulfonated phenolic resins. III. Effects of degree of sulfonation and molecular weight on concrete workability. *Journal of Applied Polymer Science,* 76**,** 1762-1766.

HSU, K. C., CHIU, J. J., CHEN, S. D. & TSENG, Y. C. 1999. Effect of addition time of a superplasticizer on cement adsorption and on concrete workability. *Cement and Concrete Composites,* 21**,** 425-430.

ISMAIL, I., BERNAL, S. A., PROVIS, J. L., SAN NICOLAS, R., HAMDAN, S. & VAN DEVENTER, J. S. J. 2014. Modification of phase evolution in alkali-activated blast furnace slag by the incorporation of fly ash. *Cement and Concrete Composites,* 45**,** 125-135.

ISOZAKI, K. 1986. Some properties of alkali-activated slag cements. *CAJ Review***,** 4, 120-123.

JANSEN, D., GOETZ-NEUNHOEFFER, F., NEUBAUER, J., HAERZSCHEL, R. & HERGETH, W. D. 2013. Effect of polymers on cement hydration: A case study using substituted PDADMA. *Cement and Concrete Composites,* 35**,** 71-77.

JANSEN, D., NEUBAUER, J., GOETZ-NEUNHOEFFER, F., HAERZSCHEL, R. & HERGETH, W. D. 2012. Change in reaction kinetics of a Portland cement caused by a superplasticizer — Calculation of heat flow curves from XRD data. *Cement and Concrete Research,* 42**,** 327-332.

JAU, W. C. & YANG, C. T. 2010. Development of a modified concrete rheometer to measure the rheological behavior of conventional and self-consolidating concretes. *Cement and Concrete Composites,* 32**,** 450-460.

JIANG, L. F., KONG, X. M., LU, Z. C. & HOU, S. S. 2015. Preparation of amphoteric polycarboxylate superplasticizers and their performances in cementitious system. *Journal of Applied Polymer Science,* 132**,** 41348, 1-8.

JIANG, S., KIM, B.-G. & AïTCIN, P.-C. 1999. Importance of adequate soluble alkali content to ensure cement/superplasticizer compatibility. *Cement and Concrete Research,* 29**,** 71-78.

JIANG, W. 1997. *Alkali-activated Cementitious Materials: Mechanisms, Microstructure and Properties.* PhD. The Pennsylvania State University.

JIMIDAR, M., BOURGUIGNON, B. & MASSART, D. L. 1996. Application of Derringer's desirability function for the selection of optimum separation conditions in capillary zone electrophoresis. *Journal of Chromatography A,* 740**,** 109-117.

JIN, J. H. 2002. *Properties of Mortar for Self-Compacting Concrete.* PhD. University College London.

JOLICOEUR, C., SIMARD, M., TO, T., SHARMAN, J., ZAMOJSKA, R., DUPUIS, M., SPIRATOS, N., DOUGLAS, E. & MALHOTRA, V. 1992. Chemical activation of blast-furnace slag: an overview and systematic experimental investigations. *Advances in Concrete Technology***,** 94-1.

JUILLAND, P., GALLUCCI, E., FLATT, R. J. & SCRIVENER, K. 2010. Dissolution theory applied to the induction period in alite hydration. *Cement and Concrete Research,* 40**,** 831-844.

KASHANI, A., PROVIS, J. L., QIAO, G. G. & VAN DEVENTER, J. S. J. 2014a. The interrelationship between surface chemistry and rheology in alkali activated slag paste. *Construction and Building Materials,* 65**,** 583-591.

KASHANI, A., PROVIS, J. L., XU, J. T., KILCULLEN, A. R., QIAO, G. G. & VAN DEVENTER, J. S. J. 2014b. Effect of molecular architecture of polycarboxylate ethers on plasticizing performance in alkali-activated slag paste. *Journal of Materials Science,* 49**,** 2761-2772.

KASZUBA, M., CORBETT, J., WATSON, F. M. & JONES, A. 2010. *High-concentration zeta potential measurements using light-scattering techniques*.

Philosophical Transactions of the Royal Society of London A: Mathematical, Physical and Engineering Sciences, 368, 4439-4451.

KATONO, H., MARUYAMA, A., SANUI, K., OGATA, N., OKANO, T. & SAKURAI, Y. 1991. Thermo-responsive swelling and drug release switching of interpenetrating polymer networks composed of poly(acrylamide-co-butyl methacrylate) and poly (acrylic acid). *Journal of Controlled Release,* 16**,** 215-227.

KAWAGUCHI, S., KITANO, T., ITO, K. & MINAKATA, A. 1990. Dissociation behavior of poly(fumaric acid) and poly(maleic acid). II. Model calculation. *Macromolecules,* 23**,** 731-738.

KAWASHIMA, S. & SHAH, S. P. 2011. Early-age autogenous and drying shrinkage behavior of cellulose fiber-reinforced cementitious materials. *Cement and Concrete Composites,* 33**,** 201-208.

KHATIB, J. M. & MANGAT, P. S. 1999. Influence of superplasticizer and curing on porosity and pore structure of cement paste. *Cement and Concrete Composites,* 21**,** 431-437.

KHODADOUST, S. & HADJMOHAMMADI, M. 2011. Determination of N-methylcarbamate insecticides in water samples using dispersive liquid–liquid microextraction and HPLC with the aid of experimental design and desirability function. *Analytica Chimica Acta,* 699**,** 113-119.

KHURI, A. I. & MUKHOPADHYAY, S. 2010. Response surface methodology. *Wiley Interdisciplinary Reviews: Computational Statistics,* 2**,** 128-149.

KIM, B. G., JIANG, S. P. & A ÏTCIN, P. C. 2000a. Slump improvement mechanism of alkalies in PNS superplasticized cement pastes. *Materials and Structures,* 33**,** 363-369.

KIM, B. G., JIANG, S. P., JOLICOEUR, C. & AïTCIN, P. C. 2000b. The adsorption behavior of PNS superplasticizer and its relation to fluidity of cement paste. *Cement and Concrete Research,* 30**,** 887-893.

KNAUS, S. & BAUER-HEIM, B. 2003. Synthesis and properties of anionic cellulose ethers: influence of functional groups and molecular weight on flowability of concrete. *Carbohydrate Polymers,* 53**,** 383-394.

KOETZ, J., LINOW, K. J., PHILIPP, B., HU, L. P. & VOGL, O. 1986. Effects of charge density and structure of side-chain branching on the composition of polyanion-polycation complexes. *Polymer,* 27**,** 1574-1580.

KONG, X. M., SHI, Z. H. & LU, Z. C. 2014. Synthesis of novel polymer nano-particles and their interaction with cement. *Construction and Building Materials,* 68**,** 434-443.

KRIVENKO, P. V. Alkaline cements. Proceeding of 9th International Congress on the Chemistry of Cement, 1992 New Delhi. 482-488.

KRIVENKO, P. V. Alkaline cements. *In:* KRIVENKO, P. V., ed. 1st International Conference on Alkaline Cements and Concretes,, 1994 Kiev, Ukraine. 1, 11-129.

KWAK, J. S. 2005. Application of Taguchi and response surface methodologies for geometric error in surface grinding process. *International Journal of Machine Tools and Manufacture,* 45**,** 327-334.

LAI, R., GUO, H. D. & KAMACHI, M. 2009. Synthesis of a graft polymer PVAc-g-[P(AN-r-BVE)-b-PCHO] in "one-step" by radical/cationic transformation polymerization and coupling reaction. *Polymer,* 50**,** 3582-3586.

LARRARD, F., FERRARIS, C. F. & SEDRAN, T. 1998. Fresh concrete: A Herschel-Bulkley material. *Materials and Structures,* 31**,** 494-498.

LEI, L. & PLANK, J. 2012. Synthesis, working mechanism and effectiveness of a novel cycloaliphatic superplasticizer for concrete. *Cement and Concrete Research,* 42**,** 118-123.

LEI, L. & PLANK, J. 2014. A study on the impact of different clay minerals on the dispersing force of conventional and modified vinyl ether based polycarboxylate superplasticizers. *Cement and Concrete Research,* 60**,** 1-10.

LEWIS, J. A., MATSUYAMA, H., KIRBY, G., MORISSETTE, S. & YOUNG, J. F. 2000. Polyelectrolyte Effects on the Rheological Properties of Concentrated Cement Suspensions. *Journal of the American Ceramic Society,* 83**,** 1905-1913.

LI, C., FENG, N., LI, Y. & CHEN, R. 2005. Effects of polyethlene oxide chains on the performance of polycarboxylate-type water-reducers. *Cement and Concrete Research,* 35**,** 867-873.

LI, H. Q., HUANG, G. H., AN, C. J. & ZHANG, W. X. 2012. Kinetic and equilibrium studies on the adsorption of calcium lignosulfonate from aqueous solution by coal fly ash. *Chemical Engineering Journal,* 200–202**,** 275-282.

LIM, G. G., HONG, S. S., KIM, D. S., LEE, B. J. & RHO, J. S. 1999. Slump loss control of cement paste by adding polycarboxylic type slump-releasing dispersant. *Cement and Concrete Research,* 29**,** 223-229.

LIU, X. H. 2010. *Removal of Humic Substances from Water Using Solar Irradiation and Granular Activated Carbon Adsorption.* PhD, University College London.

LIU, X. M., WANG, Z. M., ZHU, J., ZHENG, Y. S., CUI, S. P., LAN, M. Z. & LI, H. Q. 2014. Synthesis, characterization and performance of a polycarboxylate superplasticizer with amide structure. *Colloids and Surfaces A: Physicochemical and Engineering Aspects,* 448**,** 119-129.

ŁOJEWSKA, J., MIŚKOWIEC, P., ŁOJEWSKI, T. & PRONIEWICZ, L. M. 2005. Cellulose oxidative and hydrolytic degradation: In situ FTIR approach. *Polymer Degradation and Stability,* 88**,** 512-520.

LOU, H. M., JI, K. B., LIN, H. K., PANG, Y. X., DENG, Y. H., QIU, X. Q., ZHANG, H. B. & XIE, Z. G. 2012. Effect of molecular weight of sulphonated acetone-formaldehyde condensate on its adsorption and dispersion properties in cementitious system. *Cement and Concrete Research,* 42**,** 1043-1048.

LUO, Y. R. & KERR, J. A. 2007. Bond dissociation energies. *CRC Handbook of Chemistry and Physics,* 90, Boca Raton.

LV, S. H., GAO, R. J., CAO, Q., LI, D. & DUAN, J. P. 2012. Preparation and characterization of poly-carboxymethyl-β-cyclodextrin superplasticizer. *Cement and Concrete Research,* 42**,** 1356-1361.

MA, B. G., WANG, X. G., LIANG, W. Q., LI, X. G. & HE, Z. 2007. Study on early-age cracking of cement-based materials with superplasticizers. *Construction and Building Materials,* 21**,** 2017-2022.

MA, Q. M. 2013. *Chloride Transport and Chloride induced Corrosion of Steel Reinforcement in Sodium Silicate Solution Activated Slag Concrete.* PhD. Queen's University Belfast.

MA, S. D., ZHAO, P., GUO, Y., ZHONG, L. S. & WANG, Y. 2013. Synthesis, characterization and application of polycarboxylate additive for coal water slurry. *Fuel,* 111**,** 648-652.

MA, Z. H., LI, Q., YUE, Q., GAO, B., XU, X. & ZHONG, Q. Q. 2011. Synthesis and characterization of a novel super-absorbent based on wheat straw. *Bioresource Technology,* 102**,** 2853-2858.

MANDAL, B. M. 2013. *Fundamentals of Polymerization*, World Scientific, London.

MARCHON, D., SULSER, U., EBERHARDT, A. & FLATT, R. J. 2013. Molecular design of comb-shaped polycarboxylate dispersants for environmentally friendly concrete. *Soft Matter,* 9**,** 10719-10728.

MARKETSANDMARKETS 2014. Concrete Superplasticizer Market by Types (SNF, PC, SMF & MLS), Application (Ready-Mix, Precast, Self-Compacting, High Performance, Shotcrete & Others), Forms (Liquid & Powder) & Geography - Regional Trends & Forecast to 2018. MarketsandMarkets.

MATIAS, D., DE BRITO, J., ROSA, A. & PEDRO, D. 2013. Mechanical properties of concrete produced with recycled coarse aggregates – Influence of the use of superplasticizers. *Construction and Building Materials,* 44**,** 101-109.

MATSUSHITA, Y. & YASUDA, S. 2005. Preparation and evaluation of lignosulfonates as a dispersant for gypsum paste from acid hydrolysis lignin. *Bioresource Technology,* 96**,** 465-470.

MCCARTER, W. J., CHRISP, T. M. & STARRS, G. 1999. The early hydration of alkali-activated slag: developments in monitoring techniques. *Cement & Concrete Composites,* 21**,** 277-283.

MEDDAH, M. S., ZITOUNI, S. & BELÂABES, S. 2010. Effect of content and particle size distribution of coarse aggregate on the compressive strength of concrete. *Construction and Building Materials,* 24**,** 505-512.

MEHTA, P. K. & MONTEIRO, P. J. M. 2006. *Concrete: Microstructure, Properties, and Materials*, The McGraw-Hill Companies, New York.

MIKANOVIC, N. & JOLICOEUR, C. 2008. Influence of superplasticizers on the rheology and stability of limestone and cement pastes. *Cement and Concrete Research,* 38**,** 907-919.

MIYAKE, N., ANDO, T. & SAKAI, E. 1985. Superplasticized concrete using refined lignosulfonate and its action mechanism. *Cement and Concrete Research,* 15**,** 295-302.

MOHANTY, S., DAS, B. & DHARA, S. 2013. Poly(maleic acid) – A novel dispersant for aqueous alumina slurry. *Journal of Asian Ceramic Societies,* 1**,** 184-190.

MOLLAH, M. Y. A., ADAMS, W. J., SCHENNACH, R. & COCKE, D. L. 2000. A review of cement–superplasticizer interactions and their models. *Advances in Cement Research,* 12**,** 153-161.

MORRIS, G. E., FORNASIERO, D. & RALSTON, J. 2002. Polymer depressants at the talc–water interface: adsorption isotherm, microflotation and electrokinetic studies. *International Journal of Mineral Processing,* 67**,** 211-227.

MOZGAWA, W. & DEJA, J. 2009. Spectroscopic studies of alkaline activated slag geopolymers. *Journal of Molecular Structure,* 924–926**,** 434-441.

MPOFU, P., ADDAI-MENSAH, J. & RALSTON, J. 2003. Investigation of the effect of polymer structure type on flocculation, rheology and dewatering behaviour of kaolinite dispersions. *International Journal of Mineral Processing,* 71**,** 247-268.

MURATA, J. & KIKUKAWA, H. 1992. Viscosity equation for fresh concrete. *ACI Materials Journal,* 89**,** 230-237.

NADIF, A., HUNKELER, D. & KÄUPER, P. 2002. Sulfur-free lignins from alkaline pulping tested in mortar for use as mortar additives. *Bioresource Technology,* 84**,** 49-55.

NÄGELE, E. & SCHNEIDER, U. 1989a. From cement to hardened paste — an elektrokinetic study. *Cement and Concrete Research,* 19**,** 978-986.

NÄGELE, E. & SCHNEIDER, U. 1989b. The zeta-potential of blast furnace slag and fly ash. *Cement and Concrete Research,* 19**,** 811-820.

NEUBAUER, C. M., YANG, M. & JENNINGS, H. M. 1998. Interparticle Potential and Sedimentation Behavior of Cement Suspensions: Effects of Admixtures. *Advanced Cement Based Materials,* 8**,** 17-27.

NGUYEN, V. H., REMOND, S. & GALLIAS, J. L. 2011. Influence of cement grouts composition on the rheological behaviour. *Cement and Concrete Research,* 41**,** 292-300.

NOWAK, A. 2015. Influence of Superplasticizer on Porosity Structures in Hardened Concretes. *Procedia Engineering,* 108**,** 262-269.

NONAT, A. 2004. The structure and stoichiometry of C-S-H. *Cement and Concrete Research,* 34**,** 1521-1528.

OHTA, A., SUGIYAMA, T. & UOMOTO, T. 2000. Study of dispersing effects of polycarboxylate-based dispersant on fine particles. *ACI SPECIAL PUBLICATIONS,* 195**,** 211-228.

OKADA, E. & SAKAGAMI, K. 1982. Process for preparation of AE concrete or AE mortar. Google Patents, US4325736 A.

OKAFOR, F. O. 1991. An investigation on the use of superplasticizer in palm kernel shell aggregate concrete. *Cement and Concrete Research,* 21**,** 551-557.

OUYANG, X. P., QIU, X. Q. & CHEN, P. 2006. Physicochemical characterization of calcium lignosulfonate—A potentially useful water reducer. *Colloids and Surfaces A: Physicochemical and Engineering Aspects,* 282-283**,** 489-497.

PACHECO-TORGAL, F., CASTRO-GOMES, J. & JALALI, S. 2008. Alkali-activated binders: A review - Part 1. Historical background, terminology,

reaction mechanisms and hydration products. *Construction and Building Materials,* 22**,** 1305-1314.

PALACIOS, M., BANFILL, P. F. G. & PUERTAS, F. 2008. Rheology and setting of alkali-activated slag pastes and mortars: Effect of organic admixture. *ACI Materials Journal,* 105**,** 140-148.

PALACIOS, M., HOUST, Y. F., BOWEN, P. & PUERTAS, F. 2009a. Adsorption of superplasticizer admixtures on alkali-activated slag pastes. *Cement and Concrete Research,* 39**,** 670-677.

PALACIOS, M. & PUERTAS, F. 2004. Stability of superplasticizer and shrikage reducing admixtures in high basic media. *Materiales De Construccion,* 54**,** 65-86.

PALACIOS, M. & PUERTAS, F. 2005. Effect of superplasticizer and shrinkage-reducing admixtures on alkali-activated slag pastes and mortars. *Cement and Concrete Research,* 35**,** 1358-1367.

PALACIOS, M., PUERTAS, F., BOWEN, P. & HOUST, Y. F. 2009b. Effect of PCs superplasticizers on the rheological properties and hydration process of slag-blended cement pastes. *Journal of Materials Science,* 44**,** 2714-2723.

PAN, Q., SHI, C. L. & ZHU, B. 2014. Effect of Aminosulphonate Based Superplasticizer on the Properties of Slag Pastes. *Advanced Materials Research,* 864**,** 755-758.

PANG, Y. X., GAO, W., LOU, H. M., ZHOU, M. S. & QIU, X. Q. 2014. Influence of modified lignosulfonate GCL4-1 with different molecular weight on the stability of dimethomorph water based suspension. *Colloids and Surfaces A: Physicochemical and Engineering Aspects,* 441**,** 664-668.

PANG, Y. X., QIU, X. Q., YANG, D. J. & LOU, H. M. 2008. Influence of oxidation, hydroxymethylation and sulfomethylation on the physicochemical properties of calcium lignosulfonate. *Colloids and Surfaces A: Physicochemical and Engineering Aspects,* 312**,** 154-159.

PARK, C. K., NOH, M. H. & PARK, T. H. 2005. Rheological properties of cementitious materials containing mineral admixtures. *Cement and Concrete Research,* 35**,** 842-849.

PEI, M. S., WANG, D. J., HU, X. B. & XU, D. F. 2000. Synthesis of sodium sulfanilate-phenol-formaldehyde condensate and its application as a superplasticizer in concrete. *Cement and Concrete Research,* 30**,** 1841-1845.

PEI, M. S., YANG, Y. Q., ZHANG, X. Z., ZHANG, J. & DONG, J. J. 2004. Synthesis and the effects of water-soluble sulfonated acetone–formaldehyde resin on the properties of concrete. *Cement and Concrete Research,* 34**,** 1417-1420.

PENG, G., XU, S. M., PENG, Y., WANG, J. D. & ZHENG, L. C. 2008. A new amphoteric superabsorbent hydrogel based on sodium starch sulfate. *Bioresource Technology,* 99**,** 444-447.

PENG, J. H., QU, J. D., ZHANG, J. X., CHEN, M. F. & WAN, T. Z. 2005. Adsorption characteristics of water-reducing agents on gypsum surface and its effect on the rheology of gypsum plaster. *Cement and Concrete Research,* 35**,** 527-531.

PICKELMANN, J. & PLANK, J. 2012. A mechanistic study explaining the synergistic viscosity increase obtained from polyethylene oxide (PEO) and β-naphthalene sulfonate (BNS) in shotcrete. *Cement and Concrete Research,* 42**,** 1409-1416.

PLANK, J., BRANDL, A. & LUMMER, N. R. 2007. Effect of different anchor groups on adsorption behavior and effectiveness of poly(N,N-dimethylacrylamide-co-Ca 2-acrylamido-2-methylpropanesulfonate) as cement fluid loss additive in presence of acetone–formaldehyde–sulfite dispersant. *Journal of Applied Polymer Science,* 106**,** 3889-3894.

PLANK, J., DAI, Z. & ANDRES, P. R. 2006. Preparation and characterization of new Ca–Al–polycarboxylate layered double hydroxides. *Materials Letters,* 60**,** 3614-3617.

PLANK, J. & GRETZ, M. 2008. Study on the interaction between anionic and cationic latex particles and Portland cement. *Colloids and Surfaces A: Physicochemical and Engineering Aspects,* 330**,** 227-233.

PLANK, J. & HIRSCH, C. 2007. Impact of zeta potential of early cement hydration phases on superplasticizer adsorption. *Cement and Concrete Research,* 37**,** 537-542.

PLANK, J., PÖLLMANN, K., ZOUAOUI, N., ANDRES, P. R. & SCHAEFER, C. 2008. Synthesis and performance of methacrylic ester based polycarboxylate superplasticizers possessing hydroxy terminated poly(ethylene glycol) side chains. *Cement and Concrete Research,* 38**,** 1210-1216.

PLANK, J. & SACHSENHAUSER, B. 2009. Experimental determination of the effective anionic charge density of polycarboxylate superplasticizers in cement pore solution. *Cement and Concrete Research,* 39**,** 1-5.

PLANK, J., SACHSENHAUSER, B. & DE REESE, J. 2010. Experimental determination of the thermodynamic parameters affecting the adsorption behaviour and dispersion effectiveness of PCE superplasticizers. *Cement and Concrete Research,* 40**,** 699-709.

PLANK, J., SCHROEFL, C., GRUBER, M., LESTI, M. & SIEBER, R. 2009. Effectiveness of polycarboxylate superplasticizers in ultra-high strength concrete: The importance of PCE compatibility with silica fume. *Journal of Advanced Concrete Technology,* 7**,** 5-12.

PLANK, J., VLAD, D., BRANDL, A. & CHATZIAGORASTOU, P. 2005. Colloidal chemistry examination of the steric effect of polycarboxylate superplasticizers. *Cem. Int,* 3**,** 100-110.

PLANK, J. & WINTER, C. 2008. Competitive adsorption between superplasticizer and retarder molecules on mineral binder surface. *Cement and Concrete Research,* 38**,** 599-605.

PLANK, J. & YU, B. 2010. Preparation of hydrocalumite-based nanocomposites using polycarboxylate comb polymers possessing high grafting density as interlayer spacers. *Applied Clay Science,* 47**,** 378-383.

PU, X. C. 2010. *Alkali-activated slag cement and concrete,* Science Press, Beijing

PUERTAS, F., FERNÁNDEZ-JIMÉNEZ, A. & BLANCO-VARELA, M. T. 2004. Pore solution in alkali-activated slag cement pastes. Relation to the

composition and structure of calcium silicate hydrate. *Cement and Concrete Research*, 34**,** 139-148.

PUERTAS, F., PALOMO, A., FERNANDEZ-JIMENEZ, A., IZQUIERDO, J. D. & GRANIZO, M. L. 2003. Effect of superplasticisers on the behaviour and properties of alkaline cements. *Advances in Cement Research*, 15**,** 23-28.

PUERTAS, F., SANTOS, H., PALACIOS, M. & MARTINEZ-RAMIREZ, S. 2005. Polycarboxylate superplasticiser admixtures: effect on hydration, microstructure and rheological behaviour in cement pastes. *Advances in Cement Research*, 17**,** 77-89.

PUERTAS, F., VARGA, C. & ALONSO, M. M. 2014. Rheology of alkali-activated slag pastes. Effect of the nature and concentration of the activating solution. *Cement and Concrete Composites*.

PUERTAS, F. & VAZQUEZ, T. 2001. Early hydration cement. Effect of admixtures superplasticizers. *Materiales De Construccion*, 51**,** 53-61.

QIAN, G. R., SUN, D. D. & TAY, J. H. 2003. Immobilization of mercury and zinc in an alkali-activated slag matrix. *Journal of Hazardous Materials*, 101**,** 65-77.

RAJAOKARIVONY-ANDRIAMBOLOLONA, Z., THOMASSIN, J. H., BAILLIF, P. & TOURAY, J. C. 1990. Experimental hydration of two synthetic glassy blast furnace slags in water and alkaline solutions (NaOH and KOH 0.1 N) at 40 ° C: structure, composition and origin of the hydrated layer. *Journal of Materials Science*, 25**,** 2399-2410.

RAMACHANDRAN, V. S. Absorption and Hydration Behavior of Tricalcium Aluminate-Water and Tricalcium Aluminate-Gypsum-Water Systems in the Presence of Superplasticizers. ACI Journal Proceedings, 1983 (May-June). ACI, 235-241.

RAMACHANDRAN, V. S. 1996. *Concrete admixtures handbook: properties, science and technology*, Cambridge University Press, Cambridge.

RAN, Q. P., LIU, J. P., MIAO, C. W. & YAN, S. 2012. Effect of Linkage Bond between Backbone and Side Chain in Comb-Like Copolymer Dispersants on Early Properties of Concentrated Cement Suspensions. *Procedia Engineering*, 27**,** 223-230.

RAN, Q. P., SOMASUNDARAN, P., MIAO, C. W., LIU, J. P., WU, S. S. & SHEN, J. 2009. Effect of the length of the side chains of comb-like copolymer dispersants on dispersion and rheological properties of concentrated cement suspensions. *Journal of Colloid and Interface Science,* 336**,** 624-633.

RAN, Q. P., SOMASUNDARAN, P., MIAO, C. W., LIU, J. P., WU, S. S. & SHEN, J. 2010. Adsorption Mechanism of Comb Polymer Dispersants at the Cement/Water Interface. *Journal of Dispersion Science and Technology,* 31**,** 790-798.

RASHAD, A. M. 2013. A comprehensive overview about the influence of different additives on the properties of alkali-activated slag – A guide for Civil Engineer. *Construction and Building Materials,* 47**,** 29-55.

RATINAC, K. R., STANDARD, O. C. & BRYANT, P. J. 2004. Lignosulfonate adsorption on and stabilization of lead zirconate titanate in aqueous suspension. *Journal of Colloid and Interface Science,* 273**,** 442-454.

RAY, I., GUPTA, A. P. & BISWAS, M. 1996. Physicochemical studies on single and combined effects of latex and superplasticiser on portland cement mortar. *Cement and Concrete Composites,* 18**,** 343-355.

RECALDE LUMMER, N. & PLANK, J. 2012. Combination of lignosulfonate and AMPS®-co-NNDMA water retention agent—An example for dual synergistic interaction between admixtures in cement. *Cement and Concrete Research,* 42**,** 728-735.

REN, J., BAI, Y., EARLE, M. J. & YANG, C. H. A preliminary study on the effect of separate addition of lignosulfonate superplasticiser and waterglass on the rheological behaviour of alkali-activated slags. Third International Conference on Sustainable Construction Materials & Technologies (SCMT3), 2013 Kyoto, T4-4 3, 1-11.

RIGAS, F., DRITSA, V., MARCHANT, R., PAPADOPOULOU, K., AVRAMIDES, E. J. & HATZIANESTIS, I. 2005. Biodegradation of lindane by Pleurotus ostreatus via central composite design. *Environment International,* 31**,** 191-196.

RIVAS, B. L. & SEGUEL, G. V. 1999. Poly(acrylic acid-co-maleic acid)–metal complexes with copper(II), cobalt(II), and nickel(II): Synthesis, characterization and structure of its metal chelates. *Polyhedron,* 18**,** 2511-2518.

RIXOM, M. R. & MAILVAGANAM, N. P. 1999. *Chemical admixtures for concrete*, Taylor & Francis.

RIXOM, M. R. & WADDICOR, J. 1981. Role of lignosulfonates as superplasticizers. *ACI Special Publication,* 68.

ROBERTS, J. D. & CASERIO, M. C. 1977. *Basic principles of organic chemistry*, WA Benjamin, Inc.

RODRIGUEZ, E., BERNAL, S., DE GUTIERREZ, R. M. & PUERTAS, F. 2008. Alternative concrete based on alkali-activated slag. *Materiales De Construccion,* 58**,** 53-67.

ROY, A., SCHILLING, P. J., EATON, H. C., MALONE, P. G., BRABSTON, W. N. & WAKELEY, L. D. 1992. Activation of Ground Blast-Furnace Slag by Alkali-Metal and Alkaline-Earth Hydroxides. *Journal of the American Ceramic Society,* 75**,** 3233-3240.

ROY, D. M. 1999. Alkali-activated cements Opportunities and challenges. *Cement and Concrete Research,* 29**,** 249-254.

RUSSEL, W. B., SAVILLE, D. A. & SCHOWALTER, W. R. 1992. *Colloidal dispersions*, Cambridge university press.

ŞAHMARAN, M., CHRISTIANTO, H. A. & YAMAN, İ. Ö. 2006. The effect of chemical admixtures and mineral additives on the properties of self-compacting mortars. *Cement and Concrete Composites,* 28**,** 432-440.

SAKAI, E., KASUGA, T., SUGIYAMA, T., ASAGA, K. & DAIMON, M. 2006. Influence of superplasticizers on the hydration of cement and the pore structure of hardened cement. *Cement and Concrete Research,* 36**,** 2049-2053.

SAKAI, E., YAMADA, K. & OHTA, A. 2003. Molecular structure and dispersion-adsorption mechanisms of comb-type superplasticizers used in Japan. *Journal of Advanced Concrete Technology,* 1**,** 16-25.

SCHILLING, P. J., ROY, A., EATON, H. C., MALONE, P. G. & BRABSTON, W. N. 1994. Microstructure, strength, and reaction products of ground granulated blast-furnace slag activated by highly concentrated NaOH solution. *Journal of Materials Research-Ibero-American Journal of Materials,* 9**,** 188-197.

SHI, C. Early hydration and microstructure development of alkali-activated slag pastes. 10th International Congress on the Chemistry of Cement, 1997 Gothenburg, Sweden,3ii099,1- 8.

SHI, C., KRIVENKO, P. V. & ROY, D. 2006. *Alkali-activated cements and concretes,* Taylor&Francis Group, London.

SHI, C. J. 1996. Strength, pore structure and permeability of alkali-activated slag mortars. *Cement and Concrete Research,* 26**,** 1789-1799.

SHI, C. J. & DAY, R. L. 1995. A calorimetric study of early hydration of alkali-slag cements. *Cement and Concrete Research,* 25**,** 1333-1346.

SHI, C. J. & DAY, R. L. 1996. Some factors affecting early hydration of alkali-slag cements. *Cement and Concrete Research,* 26**,** 439-447.

SIMMONS, M. R., YAMASAKI, E. N. & PATRICKIOS, C. S. 2000. Cationic homopolymer model networks and star polymers: synthesis by group transfer polymerization and characterization of the aqueous degree of swelling. *Polymer,* 41**,** 8523-8529.

SINGH, N. B., SARVAHI, R. & SINGH, N. P. 1992. Effect of superplasticizers on the hydration of cement. *Cement and Concrete Research,* 22**,** 725-735.

SINGH, N. B., SINGH, V. D., RAI, S. & CHATURVEDI, S. 2002. Effect of lignosulfonate, calcium chloride and their mixture on the hydration of RHA-blended portland cement. *Cement and Concrete Research,* 32**,** 387-392.

SONG, S., SOHN, D., JENNINGS, H. M. & MASON, T. O. 2000. Hydration of alkali-activated ground granulated blast furnace slag. *Journal of Materials Science,* 35**,** 249-257.

SONG, S. J. & JENNINGS, H. M. 1999. Pore solution chemistry of alkali-activated ground granulated blast-furnace slag. *Cement and Concrete Research,* 29**,** 159-170.

SRINIVASAN, S., BARBHUIYA, S. A., CHARAN, D. & PANDEY, S. P. 2010. Characterising cement-superplasticiser interaction using zeta potential measurements. *Construction and Building Materials,* 24**,** 2517-2521.

STEVENS, M. P. 1999. *Polymer chemistry*, Oxford university press New York.

STRÁNÏL, O. & SEBÖK, T. 1999. Relationships between the properties of ligninsulphonates and parameters of modified samples with cement binders: Part III. Determination of sulphonated compounds content, characteristic of sulphonation, sorption studies. *Cement and Concrete Research,* 29**,** 1769-1772.

STREITWIESER, A., HEATHCOCK, C. H., KOSOWER, E. M. & CORFIELD, P. J. 1992. *Introduction to organic chemistry*, Macmillan New York.

STRUBLE, L. J. & LEI, W. G. 1995. Rheological changes associated with setting of cement paste. *Advanced Cement Based Materials,* 2**,** 224-230.

STUART, K. D., ANDERSON, D. A. & CADY, P. D. 1980. Compressive strength studies on portland cement mortars containing fly ash and superplasticizer. *Cement and Concrete Research,* 10**,** 823-832.

SUN, Y. X., LIU, J. C. & KENNEDY, J. F. 2010. Application of response surface methodology for optimization of polysaccharides production parameters from the roots of Codonopsis pilosula by a central composite design. *Carbohydrate Polymers,* 80**,** 949-953.

TAM, C. M., TAM, V. W. Y. & NG, K. M. 2012. Assessing drying shrinkage and water permeability of reactive powder concrete produced in Hong Kong. *Construction and Building Materials,* 26**,** 79-89.

TATTERSALL, G. H. & BANFILL, P. 1983. *The rheology of fresh concrete*, Pitman Books Ltd., London.

TAYLOR, H. F. 1997. *Cement chemistry*, Thomas Telford Services Ltd, London.

TELYSHEVA, G., DIZHBITE, T., PAEGLE, E., SHAPATIN, A. & DEMIDOV, I. 2001. Surface-active properties of hydrophobized derivatives of lignosulfonates: Effect of structure of organosilicon modifier. *Journal of Applied Polymer Science,* 82**,** 1013-1020.

TERMKHAJORNKIT, P. & NAWA, T. 2004. The fluidity of fly ash-cement paste containing naphthalene sulfonate superplasticizer. *Cement and Concrete Research,* 34**,** 1017-1024.

TORN, L. H., DE KEIZER, A., KOOPAL, L. K. & LYKLEMA, J. 2003. Mixed adsorption of poly(vinylpyrrolidone) and sodium dodecylbenzenesulfonate on kaolinite. *Journal of Colloid and Interface Science,* 260**,** 1-8.

UCHIKAWA, H., HANEHARA, S. & SAWAKI, D. 1997. The role of steric repulsive force in the dispersion of cement particles in fresh paste prepared with organic admixture. *Cement and Concrete Research,* 27**,** 37-50.

UCHIKAWA, H., HANEHARA, S., SHIRASAKA, T. & SAWAKI, D. 1992. Effect of admixture on hydration of cement, adsorptive behavior of admixture and fluidity and setting of fresh cement paste. *Cement and Concrete Research,* 22**,** 1115-1129.

UCHIKAWA, H., SAWAKI, D. & HANEHARA, S. 1995. Influence of kind and added timing of organic admixture on the composition, structure and property of fresh cement paste. *Cement and Concrete Research,* 25**,** 353-364.

UCHIKAWA, H., UCHIDA, S., OGAWA, K. & HANEHARA, S. 1984. Influence of $CaSO_4 \cdot 2H_2O$, $CaSO_4 \cdot 12H_2O$ and $CaSO_4$ on the initial hydration of clinker having different burning degree. *Cement and Concrete Research,* 14**,** 645-656.

VIALLIS-TERRISSE, H., NONAT, A. & PETIT, J.-C. 2001. Zeta-Potential Study of Calcium Silicate Hydrates Interacting with Alkaline Cations. *Journal of Colloid and Interface Science,* 244**,** 58-65.

VIKAN, H. & JUSTNES, H. 2007. Rheology of cementitious paste with silica fume or limestone. *Cement and Concrete Research,* 37**,** 1512-1517.

WALLEVIK, J. E. 2006. Relationship between the Bingham parameters and slump. *Cement and Concrete Research,* 36**,** 1214-1221.

WALLEVIK, O. H. & WALLEVIK, J. E. 2011. Rheology as a tool in concrete science: The use of rheographs and workability boxes. *Cement and Concrete Research,* 41**,** 1279-1288.

WANG, C. E., YAN, Q., LIU, H. B., ZHOU, X. H. & XIAO, S. J. 2011. Different EDC/NHS Activation Mechanisms between PAA and PMAA Brushes and the Following Amidation Reactions. *Langmuir,* 27**,** 12058-12068.

WANG, S.-D., PU, X.-C., SCRIVENER, K. & PRATT, P. 1995. Alkali-activated slag cement and concrete: a review of properties and problems. *Advances in Cement Research,* 7**,** 93-102.

WANG, S. D. & SCRIVENER, K. L. 1995. Hydration products of alkali activated slag cement. *Cement and Concrete Research,* 25**,** 561-571.

WANG, S. D. & SCRIVENER, K. L. 2003. 29Si and 27Al NMR study of alkali-activated slag. *Cement and Concrete Research,* 33**,** 769-774.

WANG, S. D., SCRIVENER, K. L. & PRATT, P. L. 1994. Factors affecting the strength of alkali-activated slag. *Cement and Concrete Research,* 24**,** 1033-1043.

WASHBURN, E. W. 1921. The Dynamics of Capillary Flow. *Physical Review,* 17**,** 273-283.

WENG, W.-H., HSU, K.-C. & SHEEN, Y.-N. 2010. A water-soluble amphoteric copolymer: Synthesis and its dispersion properties on cement particles. *Journal of Applied Polymer Science,* 118**,** 1313-1319.

WILKINSON, M. C. 1972. Surface properties of mercury. *Chemical Reviews,* 72**,** 575-625.

WINNEFELD, F., BECKER, S., PAKUSCH, J. & GÖTZ, T. 2007. Effects of the molecular architecture of comb-shaped superplasticizers on their performance in cementitious systems. *Cement and Concrete Composites,* 29**,** 251-262.

YAMADA, K., OGAWA, S. & HANEHARA, S. 2001. Controlling of the adsorption and dispersing force of polycarboxylate-type superplasticizer by sulfate ion concentration in aqueous phase. *Cement and Concrete Research,* 31**,** 375-383.

YAMADA, K., TAKAHASHI, T., HANEHARA, S. & MATSUHISA, M. 2000. Effects of the chemical structure on the properties of polycarboxylate-type superplasticizer. *Cement and Concrete Research,* 30**,** 197-207.

YAN, M. F., YANG, D. J., DENG, Y. H., CHEN, P., ZHOU, H. F. & QIU, X. Q. 2010. Influence of pH on the behavior of lignosulfonate macromolecules in aqueous solution. *Colloids and Surfaces A: Physicochemical and Engineering Aspects,* 371**,** 50-58.

YAN, R. X. 1998. *Water Soluble Polymer,* Beijing, Chemical Industry Press.

YANG, C. H., PAN, Q. & ZHOU, H. 2013. Adsorption of Calcium Lignosulphonate Water Reducer on Alkali-Activated Slag Cement Pastes. *Advanced Materials Research,* 681**,** 7-10.

YANG, C. H., SONG, Y., CHEN, K., YE, J. X. & JIANG, A. 2009. Adsorption characteristics of surfactant in alkali- activated slag cement systems. *Concrete***,** 42-45.

YILMAZ, V. T., ODABA¢OĞLU, M., İÇBUDAK, H. & ÖLMEZ, H. 1993. The degradation of cement superplasticizers in a highly alkaline solution. *Cement and Concrete Research,* 23**,** 152-156.

YONG, S. H., LI, Q. M. & QUAN, Y. Z. 2002. Effect of modification by poly (ethylene oxide) on the reversibility of insertion/extraction of Li^+ ion in V_2O_5 xerogel films. *Journal of Materials Chemistry,* 12**,** 1926-1929.

YOSHIOKA, K., TAZAWA, E. I., KAWAI, K. & ENOHATA, T. 2002. Adsorption characteristics of superplasticizers on cement component minerals. *Cement and Concrete Research,* 32**,** 1507-1513.

YOUSUF, M., MOLLAH, A., PALTA, P., HESS, T. R., VEMPATI, R. K. & COCKE, D. L. 1995. Chemical and physical effects of sodium lignosulfonate superplasticizer on the hydration of portland cement and solidification/stabilization consequences. *Cement and Concrete Research,* 25**,** 671-682.

YUAN, X. H., CHEN, W. & YANG, M. 2014. Effect of superplasticizers on the early age hydration of sulfoaluminate cement. *Journal of Wuhan University of Technology-Mater. Sci. Ed.,* 29**,** 757-762.

ZHANG, M. H., SISOMPHON, K., NG, T. S. & SUN, D. J. 2010. Effect of superplasticizers on workability retention and initial setting time of cement pastes. *Construction and Building Materials,* 24**,** 1700-1707.

ZHANG, R., GUO, H., LEI, J., ZHANG, A. & GU, H. 2007. Effect of molecular structure on the performance of polyacrylic acid superplasticizer. *Journal of Wuhan University of Technology-Materials Science Edition,* 22**,** 245-249.

ZHANG, R. G., LI, Q., ZHANG, A. F., LIU, Y. & LEI, J. H. 2008. The Synthesis Technique of Polyacrylic Acid Superplasticizer. *Journal of Wuhan University of Technology-Materials Science Edition,* 23**,** 830-833.

ZHANG, T., SHANG, S., YIN, F., AISHAH, A., SALMIAH, A. & OOI, T. L. 2001. Adsorptive behavior of surfactants on surface of Portland cement. *Cement and Concrete Research,* 31**,** 1009-1015.

ZHANG, Y. R. & KONG, X. M. 2014. Influences of superplasticizer, polymer latexes and asphalt emulsions on the pore structure and impermeability of hardened cementitious materials. *Construction and Building Materials,* 53**,** 392-402.

ZHANG, Y. R., KONG, X. M., LU, Z. B., LU, Z. C. & HOU, S. S. 2015. Effects of the charge characteristics of polycarboxylate superplasticizers on the adsorption and the retardation in cement pastes. *Cement and Concrete Research,* 67**,** 184-196.

ZHOR, J., BREMNER, T., CABRERA, J. & RIVERA-VILLARREAL, R. Role of lignosulfonates in high performance concrete. International RILEM Conference on the Role of Admixtures in High Performance Concrete, 1999. RILEM Publications SARL, 143-165.

ZHU, X. R., SONG, D. S., WANG, S. B. & QI, W. L. 2001. Research and application of high performance retarder for alkali-slag cement. *Cement***,** 1-3.

ZINGG, A., WINNEFELD, F., HOLZER, L., PAKUSCH, J., BECKER, S., FIGI, R. & GAUCKLER, L. 2009. Interaction of polycarboxylate-based superplasticizers with cements containing different C_3A amounts. *Cement & Concrete Composites,* 31**,** 153-162.

ZINGG, A., WINNEFELD, F., HOLZER, L., PAKUSCH, J., BECKER, S. & GAUCKLER, L. 2008. Adsorption of polyelectrolytes and its influence on the rheology, zeta potential, and microstructure of various cement and hydrate phases. *Journal of Colloid and Interface Science,* 323**,** 301-312.

ZIVICA, V. 2007. Effects of type and dosage of alkaline activator and temperature on the properties of alkali-activated slag mixtures. *Construction and Building Materials,* 21**,** 1463-1469.

Appendix

Appendix A the operation procedure of UV-spectrometer

Preparation

1. Turn on spectrophotometer by pressing the power switch (IO) at the back of the instrument. The instrument will initiate checking, wait for 15 minutes until the Warm up is done.
2. System calibration (once a month)
3. Start the UV-analyst software installed in the computer by double clicking the icon on the desktop. The instrument is automatically controlled by the software.

Operation

Wavelength Scanning

1. Selecting Wavelength Scan Mode
    a. On the **File** menu, click **New**. Select **Wavelength Scan Measurement** from a dialog box and click **OK**
    b. Click T or **A** on the tool bar to select Data Acquisition Mode
    c. Click "**Spanner**" icon on the toolbar
    d. Key in the lower limit of scan range in the **From** box. Acceptable entries range from 190-1100 nm
    e. Key in upper limit of scan range in the **To** box. Acceptable entries range from 190-1100 nm
    f. Click the arrow next to **Step**, and select a scan interval. Six scan intervals can be selected from 0.1-5.0nm
    g. Select a smoothing filter value
    h. Click **OK** return to the wavelength scan sub-menu

2. Collecting a Spectrum in Wavelength Scan
    a. Close the cover of the sample compartment. On the **UV-Photometer** menu, click **Background** or **B** on the toolbar. The instrument will run background correction automatically, then the status bar will show **Ready**

b. Place sample cuvettes which contain a reference or blank solutions in both the reference and sample holders. On the **UV-Photometer** menu, click **Automatic Black Calibration** or click **Z** on the toolbar to zero the instrument
c. Place a sample in the sample cuvette holder. Close the cover of the sample compartment
d. Click (**Start**) on the toolbar. The instrument will start scanning automatically
e. The real time spectrum will be displayed on the screen during the scanning

Single Wavelength Measurement

The UV-Vis Analyst provides a convenient method to measure photometric value at a fixed wavelength

1. Click G icon on the toolbar
2. Key in the desired wavelength position and select Abs or T%, then click **Go**
3. Place a reference in the sample compartment and click Zero
4. Place a sample in the same compartment. The wavelength position and photometric value will be displaced in the readout box

Spectrum Displaying

1. Rescale
    a. On the **Setting** menu, click **Display Range**
    b. Key in the display range variables for X-axis from 190 to 1100 and Y-axis from -1 to 3.
    c. You can also set display intervals on both X and Y axes. To do this, first tick the box of **Manual Settings** and then key in the intervals
    a. Click **OK**
2. Zoom
    a. Click the "**Zoom**" on the toolbar
    b. Position the cursor in the upper-left corner of the area you want to select

c. Hold the left mouse button to drag the cursor to outline the spectrum area you want to enlarge
d. Release the mouse button. The part of the spectrum which is displayed within the outlined area will be enlarged. Click to undo scale. To zoom again, click twice (once to cancel and once to re-active)

3. Peaks and Valleys
   a. On the **View** menu, click **Peaks**, all peaks detected will be listed in a table format beside the spectrum
   b. On the **View**, click **Valleys**, all valleys displayed will be listed

Saving and Reloading

1. Position the cursor in the spectrum, click the right mouse button. In the **File** menu you will be able to **Save as** or **Load** a saved file in **My Documents/Downloads**. Then you can transfer to your own USB.
2. To open saved file in Excel, open Excel from Microsoft Office. Find the saved file form My Documents, and then open with fixed width.

Shutting down

1. Turn off the instrument and the computer. It is important to turn off the instrument once analysis is completed as this will save/extend the lifetime of the light sources.
2. Fill the log book, record any error and report to technical staff.

Appendix B the DT 300 operation procedure

Preparation

1. Turn on the Electronic Box by depressing the power button on the front panel firstly. **It is important that the Electronics Unit be turned on first.**
2. Start the DTI software by double click the icon on the left top corner of windows. The instrument will automatic controlled by software.
3. A combination of 3 windows appearing on the screen. (Top one is DTI software Home Page and the other two are message asking you to wait till installation finished and Instrument Status)
4. When the start-up tests are complete, the Home page will appear. "Ready for measurements!" will appear on the status bar at the bottom of the window.

Calibration

pH Calibration

1. Click on the menu item Calibrate- pH on the Home page.
2. The Buffer Temperature form will appear. Typically enter this temperature in the box, and click OK. (If the temperature probe is also in the buffer solution, you can simply click Cancel and the measured temperature will be used instead of your manual input).
3. After the Buffer Temperature form closes, the pH calibration form appears. Three commonly used buffers are pre-selected.
4. To start calibration, click on the row containing the buffer you want to use first. Dip the pH probe in this buffer with pH=4.0. Make sure the buffer is stirred, one way or the other, while you measure the pH. Depress the Measure pH button to measure the pH. Press again every few seconds until the value is no longer changing.
5. When a stable value has been reached for one buffer, move on to the next. Click on the row containing the buffer as pH=7.0 and pH= 10.0. Repeat step 4
6. Click on the "Calibrate" button.

7. Click on the Save button to permanently save these calibration constants.

Zeta Calibration

1. Put Ludox silica standard solution into a small container and disperse the particle by ultrasonic mixing for 1 min.
2. Click on Calibrate Zeta potential on the home page. The Zeta Calibration form will appear. The measured value will normally be fairly close to the calibration value if the probe has not been replaced.
3. Click on the Calculate calibration button to compute the new calibration constants. If the calibration is successful, the Save button will appear. Click on the Save button to permanently save the new constants and exit this calibration form

Test Operation

1. Empty any sample from the chamber.
2. Fill the chamber with new sample.
3. On the Home page, click on each type measurement that you want to perform.
4. Select the name of the media from list of materials.
5. Select whether your disperse phase is a solid or liquid.
6. Select the name of the disperse phase from list of materials.
7. Enter the weight fraction of your sample and click calculates.
8. Press the Run button. And wait till the measurement is complete, and the analysis of results appears.
9. On Analysis report, click on File- Print report if needed. (Or record by hand).

Finishing

1. Clean the CVI, pH and temperature probes carefully.
2. Close the DTI software
3. Shut down the computer
4. Turn of the electronics Unit
5. Shut down the power from the socket.

Appendix C the Rheometer operation procedure:

Before Test:

1. Switch on computer, rheometer (from control unit).
2. From desktop, open excel file named as “water trial”.
3. **Save** the file **as** your experiment name on your folder (It would be suggested to setup your folder in disk D).
4. Click the **DAS Wizard** tool bar (a small box appears in the upper left corner of the xcel windows).
5. A dialog box will then appear (Please **DONOT** change any paremeter from DAS winzard window)

During Test:

1. Fill the sample into container (approximately 700 ml).
2. Place the container to fixed mould of viscometer and setup the helical impeller. Then lock the impeller by pulling down the locker.
3. Adjusting the recorder to “zero” by rotating the knob on control unit.
4. Then click “**Run Task”** button on the dialog box and **“Start”** button on chart recorder **at the SAME time.**
5. When the test finished and the programme finished running, click **“OK”** on the dialog box

After Test:

1. Copy the recorded two columns (in sheet 1) into another sheet (in sheet 2) and save the file.
2. For up-curve, it is suggested to select the data from row **100** to **300** (in sheet 1).
3. For down-curve, it is suggested to select the data from row **380** to **580** (in sheet 1).
4. Obtain the results (Yield stress and plastic viscosity) from sheet 2.
5. Record the data by hand and save the file again.